PAT and Beyond

ACADEMISCH PROEFSCHRIFT

ter verkrijging van de graad van doctor
aan de Universiteit van Amsterdam
op gezag van de Rector Magnificus

prof. mr. P.F. van der Heijden

ten overstaan van een door het college voor promoties ingestelde commissie, in het openbaar te verdedigen in de Aula der Universiteit

op dinsdag 6 december 2005, te 10:00 uur

door **Erik Türon Smidstrup Skibsted**

geboren te Bogense, Denemarken

Promotiecommissie:

Promotor:	prof. dr. A.K. Smilde
Co-promotor:	dr. J.A. Westerhuis
Overige leden:	prof. dr. L.M.C. Buydens
	prof. dr. R.J.M.M. Does
	prof. dr. H.W. Frijlink
	dr. W. Th. Kok
	dr. D.T. Witte

Faculteit der Natuurwetenschappen, Wiskunde en Informatica

“Aut inveniam viam aut faciam”

(I will find a way or make one)

To Maya, William and Johanna

LIST OF ABBREVIATIONS

The most commonly used abbreviations in this thesis are listed In Table 1.

Table 1. Abbreviations.

API	Active Pharmaceutical Ingredient
ATR	Attenuated Total Reflectance
D	*D* statistic
DoE	Design of Experiments
EMEA	European Medicine Evaluation Agency
FDA	Food and Drug Administration
FT-IR	Fourier-Transform Infrared
FT-NIR	Fourier-Transform Near-infrared
GMP	Good Manufacturing Practice
LOO CV	Leave-One-Out Cross Validation
MSPC	Multivariate Statistical Process Control
MIR	Mid-Infrared
NAS	Net Analyte Signal
NDA	New Drug Application
NIR	Near Infrared
PAT	Process Analytical Technology
PC	Principal Component
PCA	Principal Component Analysis
PLS	Partial Least Squares
PSD	Particle Size Distribution
Q	Q statistic
RES	Residuals
RFT	Right First Time
RTR	Real Time Release
RMSEC	Root Mean Squared Error of Calibration
RMSECV	Root Mean Squared Error of Cross Validation
RMSEP	Root Mean Squared Error of Prediction
SDF	Solid Dosage Form
SE indicator	Signal to Error indicator
SEC	Standard Error of Calibration
SEP	Standard Error of Prediction
SPC	Statistical Process Control

SPE	Squared Prediction Error
SQC	Statistical Quality Control
T2	Hotelling T^2 statistic

NOTATION

Throughout the thesis and papers the following notation will be used. Boldface capital characters denote matrices, boldface lower-case characters denote vectors and lower case italic characters denote scalars, superscript T denotes the transposed matrix or vector and the superscript + denotes the Moore-Penrose generalised inverse of a matrix[1]. The matrix $\mathbf{I}_J$ is the $J \times J$ identity matrix.

INTRODUCTION

This thesis will present the research performed during the PhD project which started in January 2001. The project has been a joint project between Novo Nordisk A/S in Denmark (www.novonordisk.com) and The University of Amsterdam (UvA) in The Netherlands (www.uva.nl). The project was financed by Novo Nordisk A/S, CoOperate Research Affairs (CORA). Eric Witte, who at that time was manager for Analytical Development at Novo, formulated the project together with Professor Age Smilde (UvA). Novo was interested in the possibilities of spectroscopy and chemometrics in tablet development and manufacturing and the group headed by Prof. Smilde was at that time deeply involved in spectroscopy, process analysis and chemometrics, so Novo sort of *had the problems* and UvA *the solutions*. In the joint project, the experimental work has been conducted at Novo while periods of writing took place at UvA.

Almost simultaneously to the initiation of the PhD project did the American food and drug administration (FDA) started to promote process analytical technology (PAT) to the pharmaceutical industry[2] and in this thesis work are multiple examples of PAT.

The pharmaceutical industry is a highly regulated industry and in many cases innovation is first initiated when there are external requirements. Today's quality systems in pharmaceutical industries are gigantic organizations that are operated under the requirements of Good Manufacturing Practice (GMP), which can be a 'straight jacket' for innovation. The FDA PAT initiative is therefore very important when it comes to innovation and introduction of PAT. For now, PAT is not mandatory but the 'carrot' from the FDA is that future inspections of the companies will be based on risk assessment. This means that if a company uses PAT and proves a high level of process understanding, their products are considered of less risk to the public safety compared to pharmaceutical products manufactured in the traditional way. Companies that do not prove process understanding will then be of more concern to the FDA. Besides the regulatory aspect of PAT other benefits are improved process understanding, improved quality control, less batch rejections and higher throughput which all adds to the favours. Though PAT is not mandatory, the situation could certainly change when a large number of successful applications have been approved by the authorities. PAT is the road to low cost and high quality drugs which benefits the pharmaceutical companies and the public healthcare systems. Even the public has started to pay attention to the way pharmaceutical manufacturing is conducted. In September 2003 The Wall Street Journal published an article[3] with the following introduction text "*The pharmaceutical industry has a little secret: Even as it invents futuristic new drugs, its manufacturing techniques lag far behind those of potato-chip and laundry soap makers".* The article described the FDA PAT initiative and the general status of drug manufacturing. The public healthcare system is demanding safer and cheaper innovative drugs, which adds to the insensitive for the drug manufactures to start to develop their manufacturing systems.

The timing of this PhD project is excellent and it is the hope of the author that the research can help 'paving' the road. In the first chapter the reader will be

introduced to some of the regulatory initiatives that facilitate the transition that is starting to take place in the pharmaceutical industry.

Pharmaceutical drugs can roughly be divided into biotechnological drugs e.g. injectables of protein based drugs manufactured with fermentation processes and solid dosage form drugs e.g. tablets and capsules prepared with drugs from chemical synthesis. Though Novo is mostly recognized for biotech drugs i.e. insulin and protein based drugs for haemostatis, there are several tablet products in the product portfolio and in the research pipeline. The pharmaceutical manufacturing area where most PAT examples come from is the manufacturing of tablets which in more wide terms is called solid dosage form manufacturing (SDF). Especially two distinct SDF manufacturing processes are used at Novo and in the industry as general. These two processes will be explained in Chapter 3. For both of the two manufacturing processes, several examples of near-infrared (NIR) spectroscopy based quality measurements are shown in the literature. Therefore, it was decided that NIR should be the general tool for quality measurements in the investigated processes. Chapter 2 provides a short description of the NIR theory.

During the project five original papers have been produced. Four papers are inserted in the end of the thesis in their submitted/accepted form[4-7] and one paper[8] is integrated in the thesis as chapter four in an extended version. The papers will be introduced in the following chapters. Finally, concluding remarks and suggestions for future research are dealt with in Chapter 5.

The thesis title ‘PAT and Beyond’ is selected because a great deal of the research presented in the thesis can be applied to a wide selection of process analyzers and monitoring systems in general. Also the ideas for process models laided down in chapter 4 are applicable for many different PAT systems. Finally, PAT is in focus when presenting future research ideas.

CHAPTER 1. THE FDA PAT INITIATIVE AND OTHER REGULATORY INITIATIVES

In this chapter, the FDA PAT initiative and other major regulatory initiatives will shortly be described because they are the key drivers for the current interest and implementation of NIR and chemometrics in the pharmaceutical industry. In September 2004, the FDA published the PAT guidance document[2]. Together with this guidance document FDA has trained a set of inspectors in PAT. This team of inspectors performs operational visits at pharmaceutical sites and approves PAT applications throughout the world.

The definition of PAT (from: www.fda.gov/cder/OPS/PAT.htm):

> *A system for designing, analyzing, and controlling manufacturing through timely measurements (i.e., during processing) of critical quality and performance attributes of raw and in-process materials and processes with the goal of ensuring final product quality.*

The PAT tools are categorized into four areas:

- Multivariate data acquisition and analysis tools
- Modern process analyzers or process analytical chemistry tools
- Process and endpoint monitoring and control tools
- Continuous improvement and knowledge management tools

One thing that should be noticed is the use of the words *timely measurements* in the definition. With the PAT initiative, FDA promotes the use of the information that is collected during processing and usage of in-line process analyzers, which is in contrast to the extensive end-off-line quality testing performed in pharmaceutical manufacturing today. This thesis contributes to the first three bullets in the list of PAT tools.

Alongside the FDA PAT initiative, The European Medicine Evaluation Agency (EMEA) also launched a PAT team in November 2003 (www.emea.eu.int/Inspections/PAThome.html). The International Conference on Harmonization (ICH) that works on world wide harmonization of quality of technical requirements for registration of human medicines for US, European and Japanese regulatory authorities, has also started to promote PAT. In their document[9] on quality risk management, PAT is being seen as an integrated tool. Finally, numerous interested groups e.g. International Society of Pharmaceutical Engineering (www.ispe.org) and American Society for Testing and Materials (www.astm.org) are currently working on the development of guidance documents for PAT tools, in order to educate and facilitate the implementation of PAT in the industry.

One of the most interesting possibilities that PAT offers is release of the product to the market at the moment it exit the last manufacturing step i.e. real time release. In today's manufacturing the actual process time compared to the time spend on quality testing after manufacturing is very low, so real time release offers some significant benefits for the manufacture. In 2001 a presentation was given to the FDA Science Board by G. K. Raju from Massachusetts Institute of Technology (MIT) Pharmaceutical Manufacturing Initiative (PHARMI). This presentation demonstrated how a significant amount of the overall cycle time for drug manufacturing was occupied with quality testing and waiting for test results before the drug products could be released[10]. This presentation also sparked the FDA PAT initiative and some highlights deserve presentation here. For example, the development time for a blend process could in average be reduced by a factor 10 to 15. Six different types of pharmaceutical manufacturing processes were scrutinized, from tablet processes with few unit operations to complex liquid drug product manufacturing processes. Six typical and different manufacturing processes were evaluated (A-F in Figure 1). The actual process time and the quality control (QC) testing time for each of the process types are illustrated in Figure 1. Process A was a tablet manufacturing process compromised of the

following steps: weighting of the constituents – granulation – drying – tabletting. No information about process B and C. Process D was also a tablet manufacturing process compromised of the following steps: weighting of the constituents – granulation – drying – tabletting – film coating – packaging. Process E appears to be a manufacturing process where the final drug product is granules contained in a capsule container and is compromised of the following steps: two step granulation – coating – blending – encapsulation. Process F was a manufacturing process where the final drug product was a solution but no processing details were provided. It was highlighted at the end of the presentation that some data have been disguised for reasons of sensitivity and confidentiality. To the best of the authors knowledge no other studies are available that separates the overall manufacturing time into different components. One reason is that this type of information is maybe considered highly sensitive information for most pharmaceutical companies.

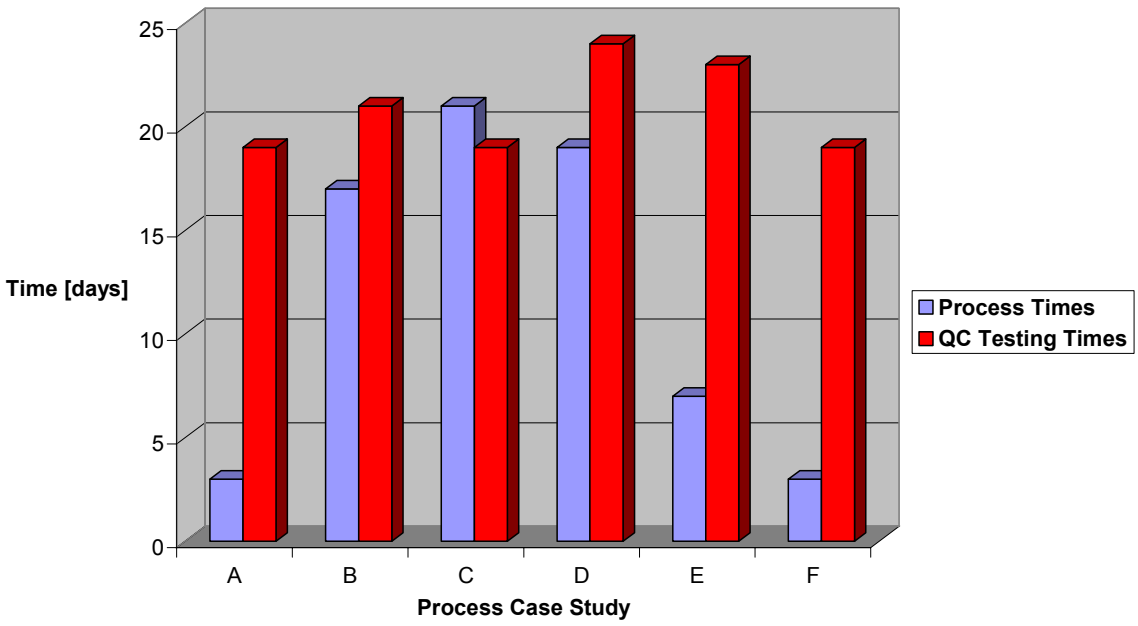

Figure 1. Process and QC testing times for different types of manufacturing processes[10].

The numbers shows that there exist a big opportunity for time and cost savings in most types of pharmaceutical manufacturing processes. Periods where drugs are stored and wait for QC test results can be minimized and potentially removed. This can increase the efficiency of the manufacturing plant. By implementing the QC tests on-line during manufacturing the overall cycle time will be decreased dramatically. For some drug manufactures the long QC testing time may not be their major concern, but for them PAT offers numerous other advantages i.e. less batch rejections, decreased number of out-of-specification situations and higher product quality. A special topic within PAT is real time release. Real time release is quality control during manufacturing instead of when the product is finalized. In this thesis is a theoretical framework for real time release and real examples will be presented in Chapter 4 and Chapter 5.

CHAPTER 2. VIBRATIONAL SPECTROSCOPY

One of the PAT tools is modern process analyzers. A great deal of these analyzers is based on the principles of vibrational spectroscopy. Vibrational spectroscopy techniques are becoming very popular options for a wide range of applications in solid dosage forms manufacturing and has also been the analysis tool in this project.

Vibrational spectroscopy

The most common way of presenting the electromagnetic spectrum is shown in Figure 2. The wavelength is presented in either nanometres or reciprocal centimetres also called wavenumber. Fourier-transform instruments use reciprocal centimetres and filter instruments, array instruments and grating instruments uses nanometres.

Most analytical chemist is familiar with mid-infrared or simply MIR which is the wavelength region from 4000 to 200 cm^{-1}. MIR is primarily used for chemical identification. Different molecular bonds absorbs at specific wave numbers in the MIR region which also is referred to as the “fingerprint region”. When the bonds absorb electromagnetic radiation, the bond will begin to vibrate. There are $3N$-6 normal modes of vibration (known as fundamentals) of a molecule ($3N$-5 for linear molecules), where N is the number of atoms. Two of these modes are called stretching and bending (Figure 3). As an example a three atom molecule is depicted (Figure 3). The centre atom is stationary and the different vibrations are explained by the motions of the two attached atoms. When the bond length between the two atoms and the centre atom simultaneously is increasing or decreasing (in the plane of the paper) it is called symmetric stretch. If one of the bonds is stretching while the other is decreasing in length (still in the plane) the stretch is asymmetric. The bonds can also bend while maintaining the distance to the centre atom. The bending can be symmetric or asymmetric in the plane and also symmetric or asymmetric out of the plane.

The absorption in the MIR region is primarily due to fundamental vibrations. NIR spectral absorption bands exists because the vibration is not a simple harmonic motion and weaker overtones of bond vibrations occur at about two, three, four or five times the wavenumber in MIR. It is actually these overtones that are recognized in the NIR region. The overtones of stretching vibration are usually stronger than bending or rocking modes. In the upper part (5200 – 4000cm-1) of the NIR region in close proximity to the MIR is the combination band region found. These bands appear at frequencies that represent the sum of the two vibrations. The NIR region used to be called the “spectroscopic garbage can” because these were not fundamental absorption bands but weaker overtones. Interpretation was difficult compared to MIR but due to the development of multivariate statistics and increased computer power, the NIR region has become “accessible” to the spectroscopist.

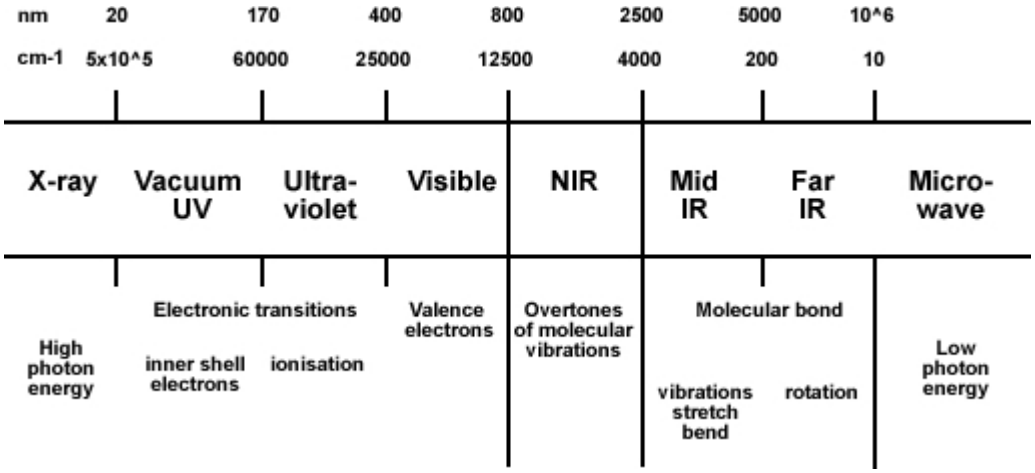

Figure 2. The electromagnetic spectrum.

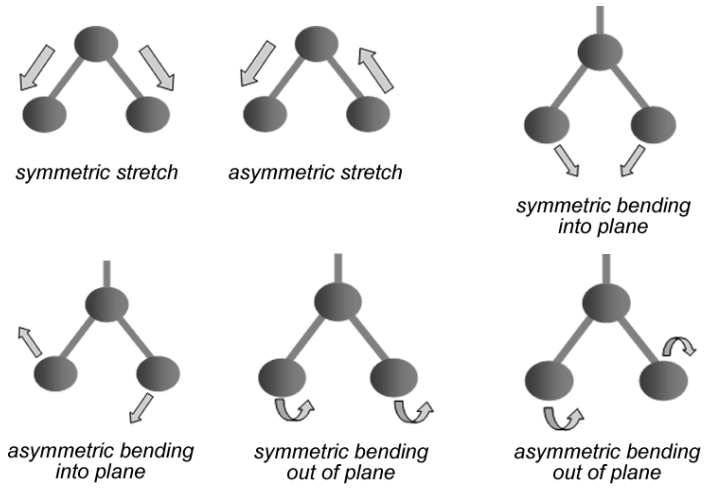

Figure 3. Stretching and bending vibrational modes.

Spectra – structure correlations

Some of the most common groups that are measured with NIR are hydrocarbons, amines and amides, hydroxyls, water, carbonyl compounds and generally just X-H (X=O,N,C) i.e. if a hydrogen bond is present in the molecule it can be detected with NIR. This versatile range of functional groups is one of reasons for the wide range of NIR applications presented in the industry today. Some typical group NIR absorption bands are listed below. If the values are scrutinized it is evident that the peaks are broad and overlap exists. This can in some instances be solved by derivatization of the spectra or the use of chemometrics.

Table 2. List of typical absorption bands (in cm^{-1}) for functional groups in NIR.

Group	Combinations	First overtone region	Second overtone region	Third overtone region
CH	4098-4405	5618-5917	8130-8547	10695-11050
CH2	4149-4444	5714-5988	8264-8696	10811-11111
CH3	4167-4545	5848-6135	8368-8929	10989-11494
H2O	5208-5405	6920-7117	10101-10471	13072-13514
RNH2	4535-4637	6623-6711	9542-9852	12195-12821
ArCH		6061-6211	9091-9259	11494-11765
ROH	4785-4854	6757-7092	10638-10811	13369-13793

Sample presentation in near-infrared

One of the key advantages with NIR, compared to MIR is that no sample preparation is usually needed. Also almost any physical state of a sample can be measured e.g. solid, liquid or gas. Depending on the sample properties it can be measured either in reflectance, transmittance or trans-reflectance mode. In a reflectance measurement (Figure 4.a) the NIR light is radiated on the sample surface and part of the diffuse reflected light is collected by the detector. This measurement type is used for solids e.g. powders. The NIR radiation can also pass through the sample and then be collected by the detector; this is called transmittance (Figure 4.b). Whole tablets can be assed with transmittance spectroscopy and liquid samples are also measured in transmittance. The trans-reflectance measurement (Figure 4.c) is a combination of the two previous. The NIR radiation is passed through the sample and reflected on a mirror, passing through the sample again and to the detector. When measuring liquids and liquids with suspended solids, trans-reflectance has proven to be useful. It is difficult to give a rule of thumb for what type of sample presentation that provides the best results. This has to be tested on a case-to-case basis.

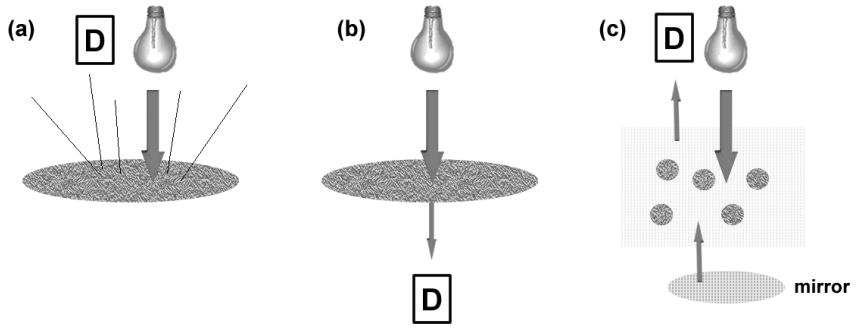

Figure 4. The three main sample presentations. Reflectance (a), transmittance (b) and trans-reflectance (c). The detector is symbolized as a box with letter D.

Factors effecting near-infrared measurements

NIR spectra are influenced by many physical factors[11] e.g. particle size, density, temperature. Figure 5 shows reflectance spectra of three different lactose batches. The difference between the chemically identical batches is the mean particle size. This is identified as a clear offset between the spectra.

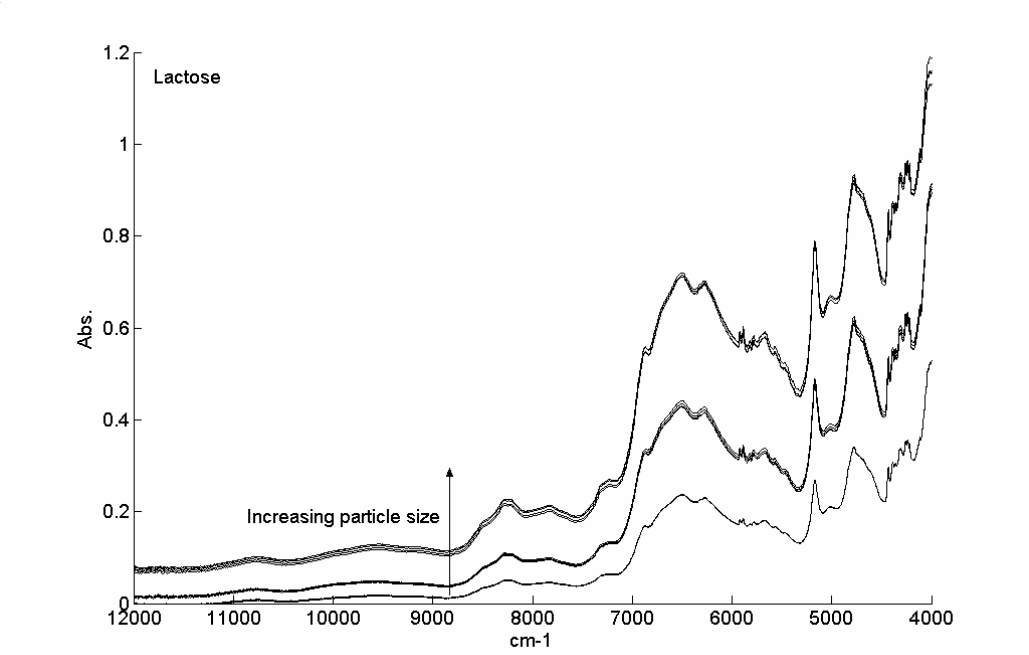

Figure 5. Reflectance spectra of three different Lactose qualities with three different mean particle sizes.

When quantitative models are made, the non-wanted spectral variation sometimes needs to be minimized in order to get a good predictive model. This can be done by various pre-processing methods[12-17]. Secondly, if the relevant spectral variation is only taking part in isolated regions of the spectrum model improvements can be made by performing wavelength selection[18-21].

The most common way of evaluating the effectiveness of different pre-processing methods and choices of wavelength selection is to compute the prediction uncertainty of an independent test set i.e. the root mean square error of

prediction (RMSEP) or root mean square error of prediction cross-validation (RMSECV) if only a smaller dataset is available. The pre-processing method or selected wavelength region that provides the lowest prediction error is then selected. This requires that a calibration set have been produced and measured with NIR and reference analysis has been performed. If the reference analysis is erroneous or a calibration set is not available, other evaluation criteria have to be used.

Calibration methods based on the calculation of the Net Analyte Signal (NAS) have proven successful. Net analyte signal is defined as the part of a signal that is unique for the analyte of interest. Lorber[22] demonstrated how figures of merit e.g. multivariate sensitivity, signal-to-noise ratio, selectivity and limit of detection could be computed from the net analyte signal of the analyte. These figures of merit can be used to judge whether a pre-processing method is beneficial for the analytical performance and they can also be used for wavelength selection. Faber[23] used the inverse multivariate sensitivity of the analyte to judge whether a certain pre-processing method e.g. derivative would improve the predictive ability of the calibration model or not. Xu and Schechter[24] developed an error indicator for wavelength selection. Boelens et al.[25] have also demonstrated the usability of NAS for improving detection limit for a spectroscopic process analysis by tuning Savitzky-Golay filters.

We introduced a new error indicator called the signal-to-error indicator (SE)[26]. A signal-to-error (SE) value is computed for the analyte using various pre-processing methods and wavelength selections applied to the spectra. The highest SE value indicates the optimal pre-processing and wavelength interval. The indicator was used to find the optimal pre-processing method and wavelength regions for two quantitative NIR methods i.e. a method using reflectance spectra of pharmaceutical powder mixtures and a model using transmission spectra of pharmaceutical tablets. The SE indicator was compared

to the inverse sensitivity indicator and the error indicator and was superior in both cases.

CHAPTER 3. SOLID DOSAGE FORM MANUFACTURING

Solid dosage forms (SDF) manufacturing is the production of tablets and capsules. When the formulation scientist is starting to develop a new dosage form, SDF is the first option to consider. Some of the advantages with SDF are[27];

- High accuracy of API dosage
- Few problems with drug stability compared to other drug types
- Mass production is economic compared to other drug types
- The final drugs are easy to pack and distribute to customers
- Little inconvenience for the patients when using the drug

A tablet in its most simple form is a mixture of API and supporting excipients which is compressed into a tablet. In most cases the API and excipients are crystalline powders. These compounds can in some cases just be mixed and compressed directly into a tablet (direct compression). In cases where that is not possible, they are blended with some kind of adhesive liquid (granulation fluid) to form granules (wet granulation) which adds technical qualities to the formulation e.g. flowability, homogeneity and compressibility. The wet granules are dried, mixed with other compounds that prevent the granules from sticking in the tablet press and finally the granules are compressed into tablets.

When the tablet is administrated into the body it disintegrates and breaks down first into granules and then primary particles. From the granules and primary particles the API is dissolved (called dissolution) and is being absorbed into the blood stream and transported to the intended parts of the body. Another SDF is a capsule. The excipients and API are placed in a gelatine capsule either in the form of a powder mixture or granules. The gelatine capsule dissolves when administrated in the body and dissolution from the granules and primary particles

takes place. Because there are no capsule based drugs currently in Novo portfolio or research pipeline, all work in this thesis has been focused on tablet based drugs. This however does not mean that this research cannot improve capsule manufacturing, as it is only the last physical form that differ capsules and tablets. Until the point where the tablets are compressed or the capsules filled, the manufacturing processes are similar.

Manufacturing processes and quality control

In this paper the different manufacturing processes and quality control will be explained in more detail. Quality control is divided into in-process quality control which is control performed during processing and final quality control, which concerns the final drug product. Especially the use of NIR as a quality control tool will be dealt with. In Table 3 is a list of terms that explain how the sample is presented to NIR analysis. These terms are commonly used in the literature and this thesis.

Table 3. Overview of measurement modes in NIR spectroscopy.

Mode	Description
Off-line	The sample is removed from the process and send to NIR analysis in a laboratory.
At-line	The sample is removed from the process and analyzed with NIR on an instrument placed in close proximity to the process.
On-line	The sample is automatically removed from the process e.g. a flow stream, and measured in the NIR instrument and returned to the process or discarded.
In-line	A fibre optic probe or optical window is interfaced between the NIR instrument and the process.

The two most common solid dosage forms manufacturing processes are direct compression and wet granulation (Figure 6). Both these processes are used at Novo and a lot of research has been performed on these[28-30]. Both types of processes have been investigated in this project. Figure 6 depicts direct compression and wet granulation. Each of the processes consists of several unit operations which will be described hereafter.

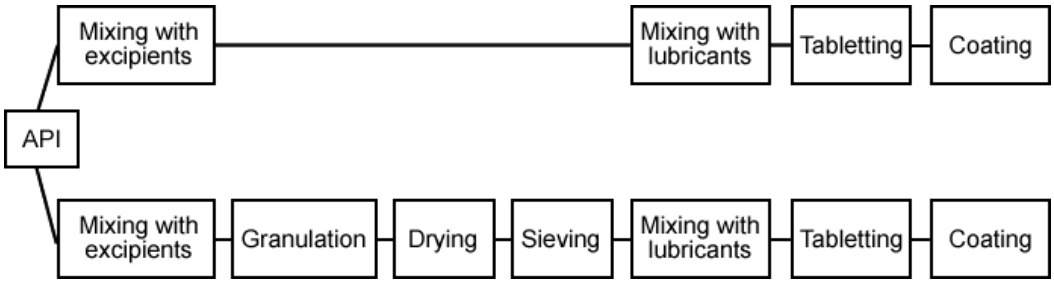

Figure 6. Schematic overview of the two major manufacturing routes for tablets. Direct compression (top) and wet granulation (low).

API SYNTHESIS

For both process types the starting point is the manufacturing of the active pharmaceutical ingredient (API). This is usually done by chemical synthesis followed by crystallization, drying and milling. The synthesis process is in many cases run according to a recipe with some form of monitoring e.g. temperature, pH and conductivity etc. but little or no process control. Without process control, the API yield and quality are likely to vary because of variation in the raw materials, environment and equipment. The traditional monitoring tools provide a thermodynamically process view and can be used for process control, but the introduction of process analyzers adds more chemical information about the synthesis process. Raman spectroscopy has proven feasible for monitoring synthesis processes[31]. Also infrared spectroscopy has proven successful for synthesis monitoring[32;33]. FT-IR provides high quality spectra which are easy to interpret and equipped with ATR crystal probes many different complex samples e.g. liquids with suspended crystals can be measured. But IR has a few drawbacks. Some FT-IR instruments require nitrogen cooling which makes them stationary. Secondly, the probe is connected to the instrument with a mechanical arm wherein the IR beam is transported, using optical mirrors in the joints of the arm. A NIR probe has an advantage over a FT-IR probe because it is connected to the instrument with fibre optics which can bend and transport NIR light over a long distance. This provides some operational benefits in a synthesis plant, because the instrument can be apart from the synthesis unit in a protected room and the instrument does not require cooling. NIR probes can be inserted directly into the reaction vessel and depending on the optical properties of the solution reflectance, transmittance or trans-reflectance probes can be used. Stordrange et al.[34] demonstrated how a reactant and intermediate component could be monitored with a NIR trans-reflectance probe during the chemical reaction. An alternative to using a probe is to pump the sample out of the reaction vessel for analysis. Blanco et al.[35] demonstrated an on-line setup where a sample flow was pumped from the reactor through a flowcell in the NIR instrument and back to the reactor.

After synthesis, the API is in most cases removed from the solution with a crystallization step. Crystallization can be a difficult process to control, and if the API can have several polymorphic forms, this process step can cause big quality problems. The polymorphic form can have a significant influence on solubility and the biological efficiency of the final drug. In other cases the level of impurities or the particle morphology and size are mainly depending on the crystallization process. In the recent years more analyzers are used for monitoring and control of crystallization processes. On of the most promising techniques is a focused beam reflectance measurement (FBRM) with a probe directly in the crystallization slurry[36]. A laser beam is sent into the slurry of liquid and particles through a lens rotating at high velocity e.g. 4500 rpm. The beam is focused in a point in front of the probe window and when the beam hits a particle the instruments detects the backscattered light. Depending on the size of the particle the duration of backscattered light will vary and the average chord length of the crystal can be calculated[37;38]. The technique has proven rugged, precise and easy to install and will presumably be one of the most widely used and successful PAT tools. But FBRM is only providing physical information about the crystals. Spectroscopic measurements on the contrary can provide both physical and chemical information. Most of the applications in the literature are based on MIR[39] or Raman analyzers[40;41], but NIR based solutions have also been reported. Févotte et al.[42] for example used a NIR reflectance probe to monitor polymorphic transition of an API in suspension and also later during filtering of the crystals from the suspension. Vaccari et al.[43] showed how a crystallization process could be monitored and controlled by NIR. The FDA actually participated in an excellent white paper on PAT and crystallization processes[44].

Direct compression process

Direct compression is a tablet manufacturing process with few process steps. The API is mixed with excipients and the formulation is poured directly into the tablet machine and compressed. After tabletting the tablets are film coated and

finally packed (Figure 6). It is a practical and economic advantageous process type which can be performed with a minimum requirement for production facilities and equipment. For APIs that are sensitive to heat and moist, the process does also provide better stability then wet granulation processes where contact with moisture and drying steps are required. Key for the direct compression is that mixtures have good flowability and good compression properties.

MIXING

After the materials are weighed they are poured into a mixer and mixed according to a predefined time interval. The most critical quality aspect of the powder mixing processes is to ensure blend uniformity. When the final tablets are compressed each tablet should contain the same amount of API. If the prior mixing is not performed optimally the API is not homogeneously spread in the powder blend and large variation in the API content of the final tablets will be likely to appear. The in-process quality control of blend uniformity is traditionally done by removing a small set of powder samples from the blend. The samples are analyzed in distant laboratories using time consuming methods. This means that the analysis results are first available days/weeks after the entire manufacturing has ended, leaving no opportunity for improving the blend quality. A great deal of the demonstrated NIR applications in SDF has actually been monitoring and control of blend uniformity. Popo et al.[45] demonstrated how powder samples could be removed from the mixing process and the API content quantified. Ufret et al.[46] measured the powder mixing process though a glass window in the mixer and evaluated the mixing process in real-time. Hailey et al.[47] developed an automated system where a NIR probe was inserted through the bearings of a V-blender for end-point control of the mixing process.

On of the key differences between the suggested NIR methods is sampling. In some methods the NIR measurements are always performed at the same spot in the mixer over time[48]. The problem is that the spectra lack spatial information about overall homogeneity and “dead spots” cannot be detected. Other examples

include the mounting of six optical windows on the surface of the blender from where the monitoring is performed[49]. With this approach information is only gathered from the surface regions of the blender.

In this project a novel method was developed, using a NIR probe and control charts to monitor the quality of mixing[5]. A hand held NIR probe was inserted at various positions in the mixer at different time points during mixing. Different model types were developed to predict the API concentration in each measurement spot. The variance and mean of the API concentration predictions, were compared statistically to a “golden batch” (batch with perfect mixing) in two control charts. One control chart for the variance and one control chart for the mean. The ‘golden batch’ was used to set the control limits in the two charts. With this method a mixing process was investigated. At different time points the mixer was stopped and fifty spectra were recorded. The variance and mean of the fifty API predictions were calculated and plotted in the two control charts. The optimal blend uniformity was achieved after 25 minutes and after that the mixing quality worsened. This is called segregation or de-mixing and usually these phenomena are known to exist but difficult to identify using traditional blend uniformity analysis. After thirty minutes of mixing, the variance exceeded the limits in the control charts (Figure 7). This was indicating that the homogeneity (expressed as analyte variance) was getting worse i.e. higher compared to the golden batch. In a real life application the operator would terminate the mixing process when the limits are exceeded and not continue de-mixing as the example illustrates.

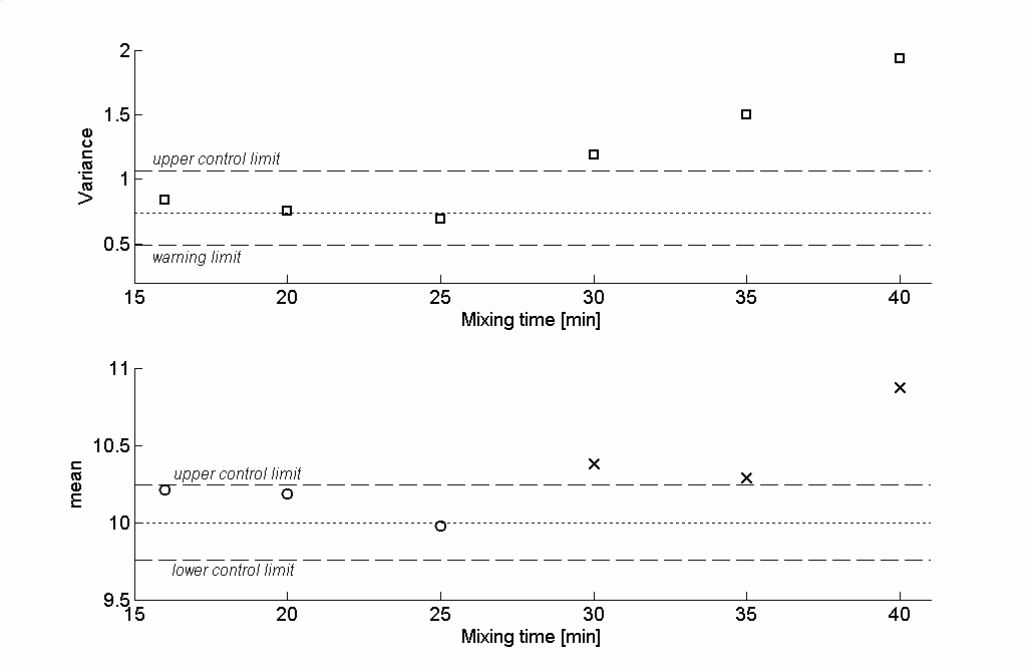

Figure 7. The de-mixing phenomenon was detected after thirty minutes of mixing[5]. At time points where the variance was different from the golden batch the mean could not be compared statistically to the golden batch (marked with x in mean chart).

The method offers several advantages over other NIR methods. It was flexible in the way that it could be used as a qualitative method, and also as a quantitative method with a few extra calibration batches. The control charts were based on F and T statistics and finally the sampling procedure is comparable to common industry practice. This allows a full characterization of the blend quality in all parts of the mixer. The method is simple and a strong tool for performing in-process quality control of the mixing process. The analysis is applied at-line and only takes minutes. With the method, blend uniformity can be assured before the powder blend is compressed into tablets.

TABLETTING

The compressed tablet is subjected to a series of quality tests e.g. hardness, water content, dissolution, disintegration time, microbiology test, quantification of impurities and content uniformity tests[27]. Many of these tests are time consuming, are performed in distant quality control laboratories and only a few

number of samples are analyzed which in return provides weak statistical certainty of the entire batch quality. Also for quality control of whole tablets NIR has been proven successful. Chen et al.[50] demonstrated how both the API content and also the hardness could be quantified with NIR. In a recent work by Donoso et al. [51] even the tablet porosity could be quantified using reflectance NIR.

Tablets can be measured both in reflectance[52] and transmission mode[53]. When measuring in reflectance mode the whole NIR spectrum is available but when using transmission spectroscopy usually only the second and third overtone region is successfully measured. The reason is that the penetration depth of NIR radiation decreases when moving from higher to lower wavenumber i.e. the absorption increases. This is also the reason why reflectance spectra is showing an upward moving curvature, when going from higher to lower wavenumbers. In many cases it is not a problem for transmission spectroscopy of tablets to only use the 2nd and 3rd overtones as the molecular information is present in the entire NIR region. Figure 8 shows the reflectance spectrum of a tablet and the transmittance spectrum of the same tablet. In the transmittance spectrum the region from 7000 cm^{-1} to 4000 cm^{-1} is not useful because of complete absorption. Also the absorption values below 7000 cm^{-1} are high and only 10 % to 0.1 % of the light exits the tablet, nevertheless this is sufficient to make a good calibration model.

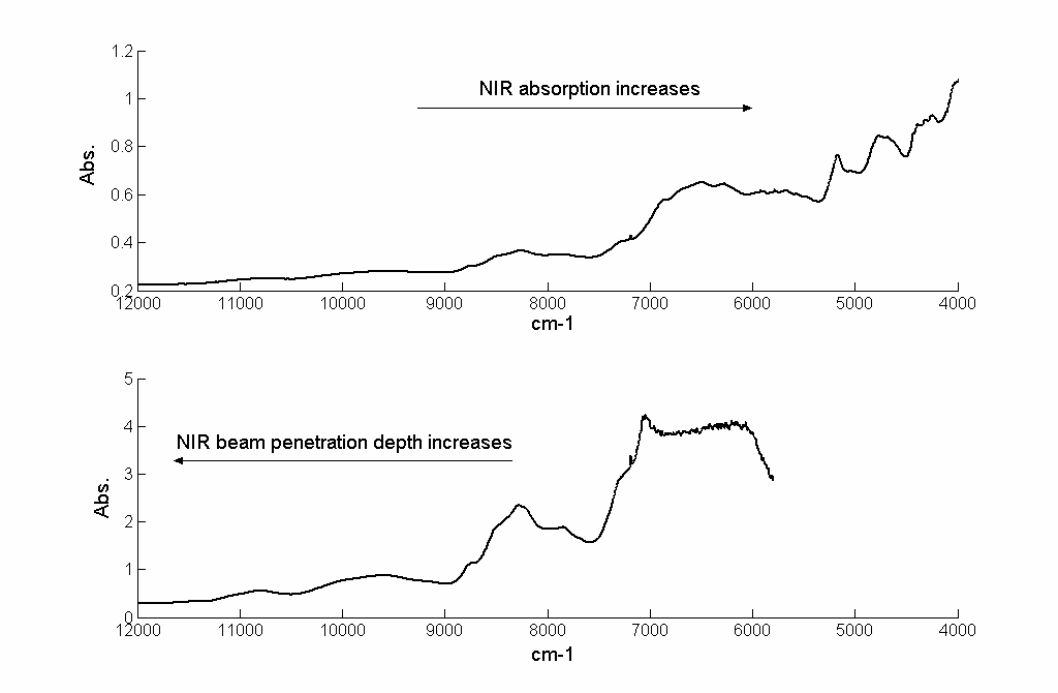

Figure 8. Reflectance spectrum of tablet (top) and transmittance of the same tablet (bottom).

One of the advantages with NIR is that no sample preparation is needed and the measurement is non-destructive. This also means that everything that has NIR absorption in the sample matrix, contributes to the final spectrum. In normal quantitative calibration the objective is to correlate the spectral variance to one particular analyte or property of interest disregarding the information of the other components in the sample matrix.

In the project a new methodology was developed called net analyte signal based statistical quality control (NAS-SQC)[6] where all components could be monitored simultaneously . The method was demonstrated with transmission NIR spectra measured on a commercial available anti-inflammatory solid dosage product (Feldene) produced by Pfizer, who kindly delivered data for the paper.

The measured spectral vector is the sum of the spectra of the analyte of interest, the excipients, and other physical phenomena (called interferents), this is

referred to as Beer's law[54]. With NAS-SQC, the idea is that the measured spectral vector is split into three independent vectors. One vector is called net analyte signal (NAS) vector and is unique for the analyte. The other vector is called interference (INT) vector and is unique for the excipients and the interferents. The NAS and INT vectors describe the systematic part of the spectroscopic variation. The last vector is describing the non-systematic or residual variation and this vector is called the residual (RES) vector. In Figure 9 is an example of a 1st derivative tablet transmission spectrum, which has been split up into the NAS, INT and RES vector.

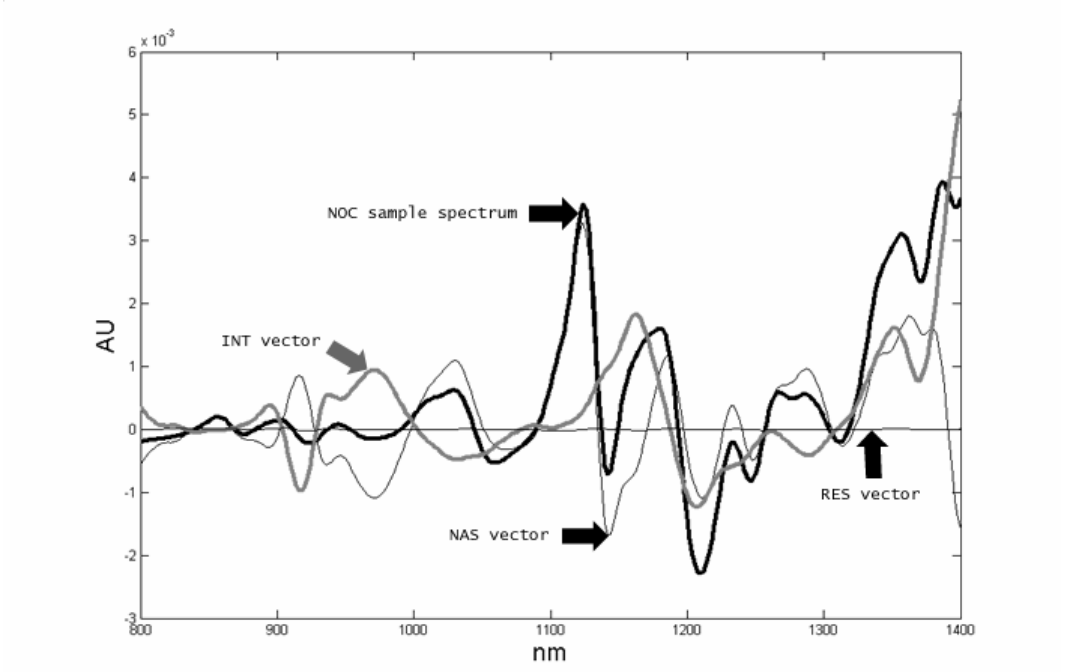

Figure 9. The spectral vector (NOC sample spectrum) is split into three vectors; NAS vector, INT vector and RES vector[6].

For each of the three vectors a separate control charts was developed with statistical limits. The control charts were developed with a set of good quality sample spectra. The samples should be having the analyte concentration and the composition of the interferents within a desired range. These in-control samples are named normal operating condition (NOC) samples. The NOC spectra are

split into the NAS, INT and RES vector parts and for each part statistical limits are calculated for their respective control charts. The control charts are called NAS, INT and RES chart. In the corresponding paper[6] we also demonstrated how the limits in the NAS chart could be either statistical limits or concentration limits depending on the user requirements. When the control charts were developed, future samples could then be monitored. In Figure 10 are examples of fifty four 'future' samples. For the NAS chart concentration limits were calculated and the two horizontal lines equal the range 85% to 115% (desired range) of the target analyte content in the tablets. The samples symbolized with plus-signs were somehow out-of-control and the samples symbolized with squares were in-control samples. Samples # 1-10 had API content slightly below 85 % and these samples were below the lower NAS control limit. Samples # 11-20 had API content above 115 % and were above the upper NAS control limit. Samples # 21-22 were special samples with API within the desired range but elevated moisture content; these samples were flagged in the INT chart but within the limits in the NAS chart. Samples # 23-34 were special samples where the composition of the interferents were out of the desired range while the analyte was within the desired range; these samples were also flagged in the INT chart and within the control limits of the NAS chart except for samples # 23-25, but some explanations for that unexpected result was given. Finally, samples # 35-44 were NOC production samples within the desired ranges and samples # 45-54 contained analyte slightly below the upper NAS control limit, but still in-control. This is clearly represented by the specific charts. Some of the residuals for samples # 45-54 were also slight above the limit in the RES chart. An explanation could be that these were special laboratory samples that with a sample composition that was deliberate different from production samples that were used to develop the chart limits. These differences might account for the high residual values.

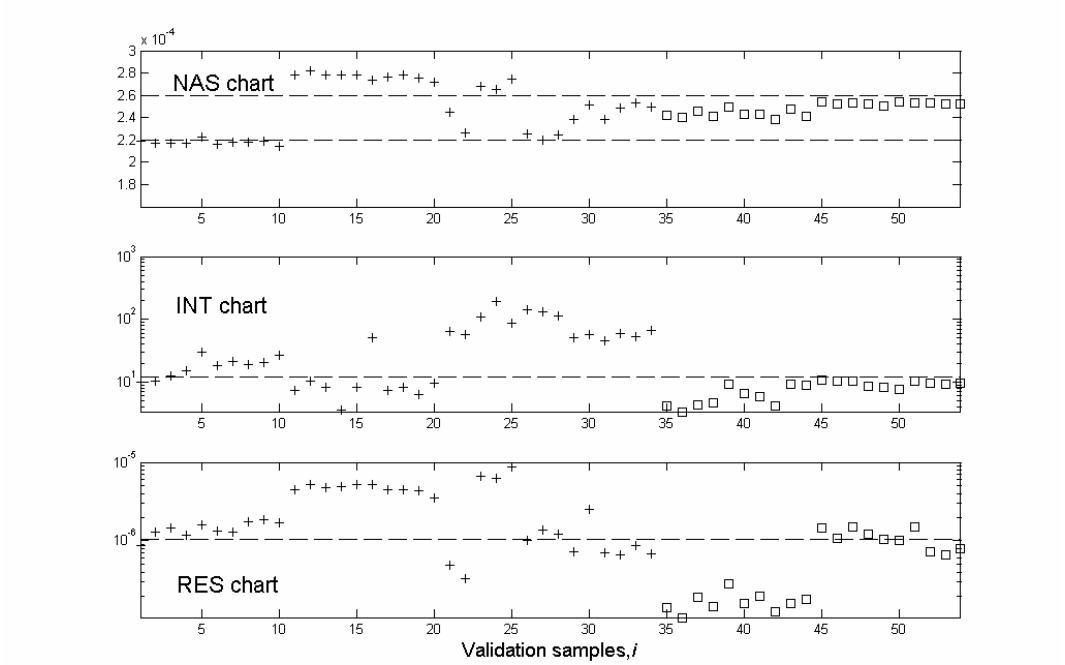

Figure 10. The validation samples plotted in the NAS-SQC control charts[6]. The samples out-of-control is symbolized with plus-signs and the samples in-control is symbolized with squares.

The NAS-SQC method provides some new and improved possibilities of ensuring multiple quality characteristics. Also diagnostics is improved which makes trouble shooting easier in case of out-of-control situations.

COATING

After tabletting, a film coating is often applied to the tablets. The film coating is sprayed upon the tablets in either larger drum or pan coaters or the coating is performed in a fluidized bed system. The purpose of the film coating is to e.g. add mechanical strength, colour, improve taste or protect the API from degradation imposed by moisture or oxygen. The amount of coating applied to the tablets are usual not determined despite it in some cases is influencing the final drug product quality. Andersson et al.[55] showed how the coating could be determined with reflectance NIR both on single tablets and also in-line during coating[56].

PACKAGING

After coating the tablets are packed. In multi-product facilities or during of manufacturing of placebo and tablets with API for clinical trials, it is of vital importance that the different tablets are not mixed together. Also here NIR has been useful, because the measurement can be performed non-destructively through the packaging material and the tablets can be identified, even in-line as the packed tablet pass on a conveyer belt[57-59].

Wet granulation process

In case of a cohesive API or a formulation with poor flowability wet granulation can be advantages. After mixing of the API and excipients a granulation liquid is mixed into the powders and larger granules are built. The granulation liquid is typically a mixture of a binder and water.

GRANULATION

Granulation is typically performed in a high shear mixer or a fluid bed reactor[29]. In fluid bed granulation, the powder mix is fluidized by a flow of air injected upwards through the bottom of the reactor. The granulation liquid is dispersed from a spraying unit above the powder bed. When granulation is finished the air flow is kept and the granules dried in the fluid bed reactor. In high-shear granulation, an impeller maintains the powder in agitation in a closed vessel, and here also a granulation liquid is sprayed from the top. As the granulation liquid droplets disperse in the powder, granulation starts. During granulation, another smaller wing (chopper), mounted in the side of the vessel, rotates thereby reducing larger agglomerates. When the granulation is finished, the granules are in most cases moved to another process unit and dried. Usually the granulation process is simply controlled by time and no or few in-process measurements are used in order to obtain consistent high quality granules. This, in spite that many properties of the granules and final drug are controlled by granulation variables[60-62].

Some in-process measurements have been used e.g. power consumption has been demonstrated as a useful monitoring tool[63] and also torque measurements[64]. Also some more sophisticated examples of process monitoring and control of the granulation process have appeared. Watano et al.[65] demonstrated a very sophisticated setup. With an image probe inserted in a high shear mixer they recorded images of the granules with a CCD camera. The images were applied to a model and used for an automated feed back control and control of granule growth. Another emerging technique in pharmaceutical industry is acoustic sensing that can be used to monitor boiling processes, gas evolution, mixing, grinding and fluidization processes[66]. If the material has density and compressibility changes during the processing the sound velocity through the material will also change, which can be measured with piezoelectric acoustic emission sensors somewhere on the process vessel. The recorded power spectra can then be used to provide a process 'fingerprint'. Whitaker et al.[66] demonstrated end-point monitoring of a granulation process with acoustic monitoring and PLS prediction of future tablet crushing strength with the acoustic data measured during granulation. One of the advantages with acoustic monitoring is that it is a truly non-invasive technique, not very expensive and easy to install. The sensors are literally glued onto the process equipment. Some drawbacks are that the power spectra are difficult or impossible to interpret. Secondly it will be difficult to transfer a model to another process unit as the 'sound' of the individual process equipment is part of the model data. Acoustic monitoring is still in its infancy in the pharmaceutical industry but is has some appealing advantages and might become a popular technique after maturation.

Because NIR measurements are affected by both physical and chemical properties of the granule sample it is very useful for monitoring granulation. Otsuka et al.[67] measured granules from wet granulation with reflectance NIR probe and made calibration models between NIR spectra and median particle size of the final granules. Also fluid bed granulation has been monitored with NIR.

Rantanen et al.[68] demonstrated how the moisture content could be monitored in real-time during granulation and drying in a fluid bed reactor using in-line NIR measurements with a reflectance probe. In another paper by Rantanen et al.[69] in-line NIR was used to define end-points for different phases in a fluid bed granulation process.

In this project a tablet manufacturing process was examined including high shear granulation. Using a hand-held NIR probe directly into the high-shear granulator unit, batches with particle size quality defects were identified. The results are presented in detail at page 45 in this thesis.

DRYING

Wet granulation is followed by drying of the wet mass granules. If the preceding granulation has been performed in a fluid bed reactor the drying is simply continued in the fluid bed reactor by fluidization of the wet granules with hot air. When granulation has been performed in e.g. high shear granulators the wet granules are dried in other process equipment e.g. fluid bed reactor. Alternatively some high shear mixers have build-in drying capability based on microwaves.

During drying a series of complex physical and chemical processes take place within the granules. Evaporation of water from the surface is taking place; water is diffusing from the core of the granules to the surface and solidification of crystal bridges within the granules. If the drying is performed in a fluid bed there is also destruction of larger agglomerates by shear forces when the particles are fluidized. Water has a large contribution in the MIR and NIR spectral region and can easily be monitored during the drying process with these techniques. With NIR it is also possible to discriminate between the different states water can be e.g. free water and crystal water[70]. Dziki et al.[71] showed how NIR could be used to discriminate between acceptable and unacceptable batches of sarafloxacin for formulation purposes based on the evaluation of water mobility within the crystal lattice.

Multiple phenomena are on-going during drying and distinct drying phases appear over the entire period of drying. Therefore, in-line NIR monitoring is a valuable tool in order to monitor, understand and apply process control. A few papers have described in-line drying monitoring in fluid bed reactors by NIR. Morris et al.[72] measured NIR non-invasive through a lower positioned inspection window in the fluid bed reactor. This is an easy way to perform NIR monitoring but in the authors experience fouling of inspection windows happens frequently, which could blind the measurements. Frake et al.[73] mounted a reflectance probe directly into the fluid bed reactor near the bottom of the rector. The probe window was positioned near the reactor wall in the downward flow (to ensure the probe was kept clean), at a point of high product density. No detailed instructions of how to make the NIR probe port were provided.

It was decided to use the approach demonstrated by Frake et al.[73] and a probe port and a customized reflectance probe were designed. Though it is fairly easy to install a NIR probe into a fluid bed reactor, a few design considerations need to be taken into consideration. Some of the main design considerations were:

- Prevent intrusion of air alongside the probe which can disturb material flow and the measurements in front of the probe
- Easy cleaning
- Removable probe and replaceable by plug
- Maintenance free optical probe window, with minimal risk of material fouling
- Adjustable penetration depth for the probe in order to optimize measurements
- Easy to perform background measurement with reflectance standard

The solution was a probe port in stainless steel and a probe adaptor with an inner cylinder in Teflon (Figure 11 and Figure 12). First the position of the probe

port was selected in close proximity to a sampling port so representative reference measurements could be taken. Also downward material flow and a high product density were present at that position which would improve the likelihood of good spectra. Secondly, this position in the mixer will always be covered with moving material regardless of the batch sizes that are practice in the Novo laboratory. By installing a Teflon cylinder in the adaptor, a tight fit was achieved and there was no air intrusion along the probe. The mounting screw could add pressure to the probe and maintain it in-position during operation and the penetration depth could vary and be optimized. It was discovered that a good measurement was obtained when the face of the probe was approximately 2 mm off the reactor wall. After the probe was fit in the adaptor, the adaptor was inserted into the NIR probe port until the mounting collars of the NIR probe port and the adaptor meet. The adaptor was locked to the NIR probe port with a standard wing screw (Figure 12). A metal plug with a collar and inner dimensions of the probe port was also manufactured which could replace the NIR probe when this was not in operation. The reflectance probe was custom build by Bruker Optics Scandinavia. A special electro polished optical window was used at the end of the probe and no material fouling was ever experienced, either in the granulation or in the drying process. Finally, if a reference measurement was needed before material was poured into the reactor, the adaptor with probe could easily be removed and a reference measurement could be performed. If this procedure was not remembered it was also possible to gently remove the NIR probe from the adaptor, perform the reference measurement and place the probe back into position in the adaptor, without wet material pouring out.

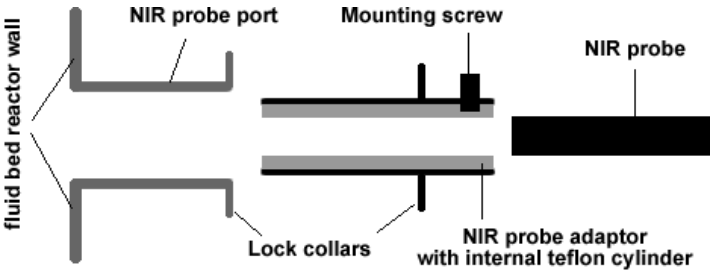

Figure 11. Cross section view of NIR probe port, adaptor and reflectance probe.

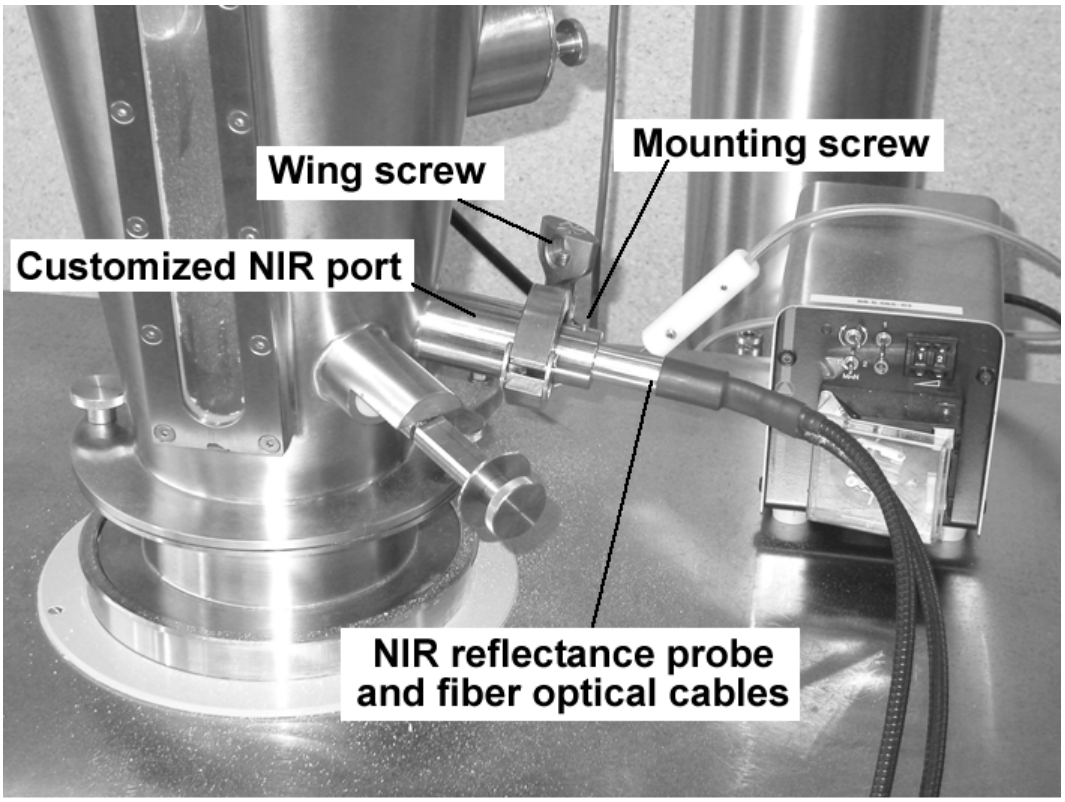

Figure 12. Picture of NIR reflectance probe and probe port in laboratory fluid bed reactor at Novo.

The probe interface was used for monitoring drying processes with in-line NIR in this thesis. At page 51 it is demonstrated how calibration models were built between in-line NIR reflectance spectra and loss-on-drying and drying curves were predicted for a set of DoE batches.

Tabletting, film coating and packaging are similar for granulated drugs and will not be further described.

CHAPTER 4: A THEORETICAL FRAMEWORK FOR REAL TIME RELEASE OF PHARMACEUTICAL PRODUCTS.

The introduction of the FDA's Process Analytical Technology (PAT) Initiative [http://www.fda.gov/cder/OPS/PAT.htm] has shed new light on Real Time Release (RTR) or the Parametric Release concept [Box 1]. In this paper we use Parametric Release and Real Time Release interchangeable. In 2001 Parametric Release was presented by the European Medicine Evaluation Agency (EMEA) as a method for ensuring product sterility[74] without performing the actual microbial analysis. The guidance document also stated that the concept was applicable to any manufacturing process considered. This was a dramatic suggestion considering the extensive end-of-line quality testing performed today in pharmaceutical manufacturing.

Box 1. Definition of Parametric Release[74]

"Parametric release is a system of release that gives assurance that the product is of the intended quality based on the information collected during the manufacturing process and on the compliance with specific GMP requirements related to Parametric release."

General questions to be addressed.

An RTR system is a system that ensures that when the last manufacturing step is passed all the final release criteria are met. Three basic questions have to be addressed for such a system:

1. Do we have a (preferably early) warning system if something is going wrong during manufacturing? – monitoring capability
2. Do we have an idea how to adjust the process, and whether it is possible? – control capability
3. If we monitor and control our processes, will the final product meet its quality criteria? - RTR capability

The overall purpose of this discussion is to provide a theoretical framework for RTR. This is done first by discussing two types of monitoring, their distinctions and potential associated process control (Box 2). Suggestions for how the monitoring and control tools can be applied to the manufacturing process are presented.

For reasons of simplicity this discussion concerns only batch processes with the natural characteristics of these. Typically in batch process manufacturing a product undergoes a series of individual process steps or unit operations. Each unit operation is normally operated by a recipe with fixed process variables e.g. defined processing time. During processing or after finalization of a unit operation step, measurements can be applied e.g. temperature, humidity, flow and spectroscopy. The measured variables are named quality variables while fixed and controlled settings are named controlled variables.

Box 2. Definition of Process Control[75].

Process Control is the active changing of the process based on the results of process monitoring. Two types of intervention (process control) are possible. The first is based on engineering judgment while the other is automated.

Once the process monitoring tools have detected an out-of-control situation, the person responsible for the process makes a change to bring the process back into control. *Out-of-control Action Plans* (OCAPS) detail the action to be taken once an out-of-control situation is detected. A specific flowchart, that leads the process engineer through the corrective procedure, may be provided for each unique process.

Advanced Process Control Loops are automated changes to the process that are programmed to correct for the size of the out-of-control measurement. A classical example of automated process control is the control of base addition in a fermentation process based upon the response from a pH electrode submerged in the fermentation tank; this is an example of feed backward control.

Monitoring and control.

We present two classes of monitoring, statistical monitoring (A) and monitoring based on regression models (B). The two classes are listed in Table 4. The regression models are divided into three models depending whether the intermediate or final quality parameters are predicted and depending on how much of the entire manufacturing process has been completed when prediction is performed. For convenience each class is provided with a symbol which will be used in the text.

Table 4. Model classes.

Class	Model symbol	Description
A. Statistical model	A	Statistical model comparing current process observations with historical process observations e.g. multivariate statistical process control (MSPC) models.
B. Regression models	B.1	Intermediate quality predictions. A regression model between predictors and intermediate quality parameters. For example, used for feedback control.
	B.2	Final quality predictions. A regression model between predictors and final quality parameters at a point where the entire manufacturing process has not been completed. For example, used for feed forward control.

	B.3	Final quality predictions. A regression model between predictors and final quality parameters when the entire manufacturing process has been completed. Used for RTR.

Figure 13 illustrates how the various model types can be applied and how process control can be associated with the models in a manufacturing process constructed of individual unit processes (P1, P2 and P3). Each process step can be evaluated based on measurements during and after finalization of the process step called intermediate quality characteristics (e.g. Q_2). The entire manufacturing process is evaluated on the final quality characteristics (Q_{final})

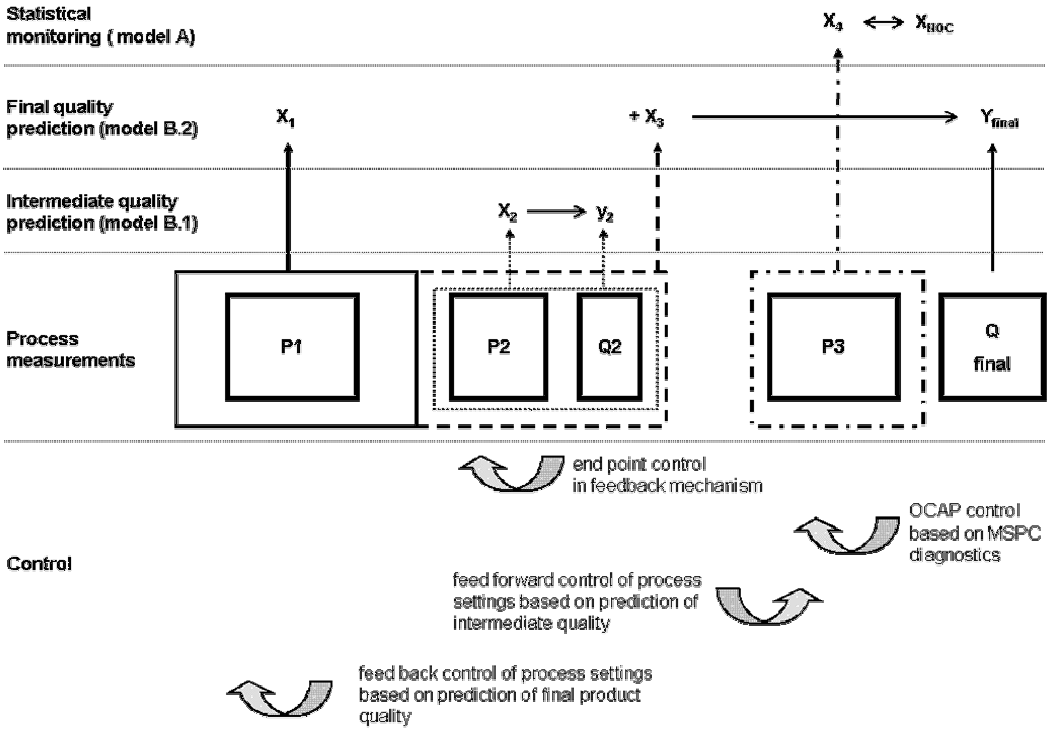

Figure 13. Graphic presentation of the models, applications and control over the entire manufacturing process. P_{index} symbolize different unit operations. The X_{index} symbolize measurements from a unit operation. Q_{index} symbolize quality characteristics. One sided arrow ($\rightarrow$) symbolize a regression model and double sided arrow ($\leftrightarrow$) a statistical model.

Statistical monitoring.

The purpose of the statistical monitoring is to provide the operator with a monitoring tool to observe the "state of the process". There is no direct link between the observations and the final product quality. There is only a link between the observations and the historical observations which are selected by evidence of providing an acceptable summary of intermediate and final product quality characteristics.

Based on a historical dataset, statistical control limits can be derived for each of the individual unit operations using quality variables from that particular step. Using the statistical monitoring strategy it can be verified up to the point of monitoring whether the process is within the normal operating conditions (NOC) or whether it is out of control. In case of an out-of-control situation the operator inspects a contribution chart. The contribution chart shows what variable or variables that causes the out-of-control situation and the operator can react and try to get the process back to NOC state.

The methodology does not provide the operator with a forward predicting capability of final product quality parameters. It allows the operator to compare the process at a given point in time with a historical dataset. In case of an *out-of-control* situation the operator can identify the process variables causing the upset by exploring contribution plots[76]. Using that information in combination with mechanistic process knowledge obtained from designed experiments during the process development phase the operator can choose a strategy to force the batch back into an NOC state i.e. a process control tool.

A classical method which can be used for the statistical monitoring strategy is multivariate statistical process control based on developing a Principal Component Analysis (PCA) model[77] on NOC batches and two control charts for the operator based on *D* and *SPE* statistics. In case that an observation is

exceeding the limits in the control charts the operator can switch to the contribution plot and identify what caused the process disturbance.

Monitoring using regression models.

There is a two-fold purpose when using regression models. The first is to predict the outcome of the process (stage) i.e. intermediate or final quality characteristics. The second is to provide a tool for process control.

Using multivariate regression models it is possible to predict intermediate and final product quality characteristics. A calibration stage is needed for developing regression models between data blocks (predictors) and quality parameters. It is possible to use controlled variables, quality variables and combinations thereof as predictors. In Table 4 the difference between the three types of regression models was presented. An example of intermediate quality prediction (B.1) is to monitor the evolution of a quality parameter during processing and use the prediction to control the duration of the process this is called end-point monitoring e.g. water content during drying. When a regression model is used for prediction of final quality two different approaches can be viewed. In the first approach final product quality characteristics are predicted at a given point during the process chain with the measured data available up to that time point as predictors (B.2). With this approach the final quality is estimated prior to process finalization giving the answer to the question - *are we on the right track*? This approach was already demonstrated by Nomikos and MacGregor[78].

The last approach (B.3) is an extreme of class (B.2). When the last process step is finalized all data blocks can be used for prediction of the product quality characteristics (B.3) i.e. substitution of time consuming end product quality control (QC) tests. If the product meets release specifications it can be shipped immediately without storage during time consuming QC tests.

In case predictions indicate that final product quality will not be of an intended quality intervention with the process should be initiated i.e. process control. The process control could be performed by the operator according to an *Out-of-control Action Plans* (OCAPS) or an automated control.

The control could be feed back[79] or feed forward. Most typically the feed back control includes adjustments of process variables in real-time based on in-line measurements or end-point control. An example of feed forward control could be that based on the measurements of the raw materials or intermediate quality different selections of process settings can be chosen for the process steps ahead. This type of process control has not been investigated in depth by the chemometric society but recent examples are Jørgensen and Næs[80] and Gustafsson et al.[81]. In both examples infrared spectroscopic assessment of raw materials were used as predictors. Westerhuis et al.[82] demonstrated how in-process measurements during tablet manufacturing could be used to predict settings of the final tabletting step in order to achieve a certain quality characteristic of the tablet. What type of process control strategy to apply is case dependent and no general recommendations are hard to give. But what can be said is that forward control is desirable because usually more opportunities exists for changing quality characteristics of the product while feed backward control often is more strict in the sense that the product has gone through some processing before the feedback control is initiated and less opportunities for changing quality characteristics exists. The drawback of feed forward control is that designed experiments are needed and more batches compared to a simpler feed back control.

Multivariate regression methods e.g. PLS[83], multi-block PLS[84], N-way PLS[85] and other regression techniques can be used to develop models for predicting intermediate and final product quality parameters.

The pros and cons for both components are summarized in Table 5.

Table 5. Summary of statistical monitoring and monitoring based on regression models.

Strategy	Pros	Cons
Statistical monitoring	Algorithms are known. Statistics are well understood. Diagnostics are easy. *Out-of-control* situations can be early detected and actions can be initiated based on the diagnostics of the contribution plot i.e. *Out-of-control Action Plans* (OCAPS).	Not possible to predict final product quality characteristics. Requires numerous NOC batches with known and acceptable quality profile. Also batches that have quality defects needs to be used in order to validate an out-of-normal batch are identified.
Monitoring with regression models	A direct link between the process and the product is established.	Requires a calibration step and designed experiments. This might be very time and resource consuming if all process variables have to be spanned independently. To develop feed forward control strategies detailed knowledge is required about the process equipment capability.

No general rule is derived for a RTR system. Such a system is product and process specific. Generically viewed, an RTR system begins with risk assessment and designed experiments for each unit operations individually and/or several unit operations in conjunction, and an assessment of how they contribute to the final quality characteristics.

By identification, monitoring and control of the variation in the process stream, consistent quality is achieved and the need for final quality tests removed i.e. a complete RTR system is implemented.

CHAPTER 5. EXAMPLES OF REAL TIME RELEASE

In the previous chapter was a theoretical framework for RTR presented. Four models were explained and in this chapter examples will be presented.

Tablet manufacturing process and reference analysis

The manufacturing process consisted of several unit operations which are symbolized in Figure 14. First all compounds (Table 6) were weighed (wei). Then the active pharmaceutical ingredient (API), lactose, microcrystalline cellulose, polyvinylpyrrolidone and crosscarmellose were mixed (mix_1) in a high shear mixer. A granulation liquid of polyvinylpyrrolidone and water was added to the high shear mixer and the granulation was performed (gra). The wet granules were removed and put through a sieve (s) before added into a fluid bed reactor where the granules were dried (dry). The dried granules were removed and put again through a sieve (s) and placed in a drum mixer. Glidants were added and mixed with the granules (mix_2). The finalized granules were compressed into tablets (tab). During drying samples were removed from the fluid bed reactor and loss on drying analysis was performed. After drying, a sample was subjected to particle size analysis. The disintegration time was also determined on finalized tablets from each batch.

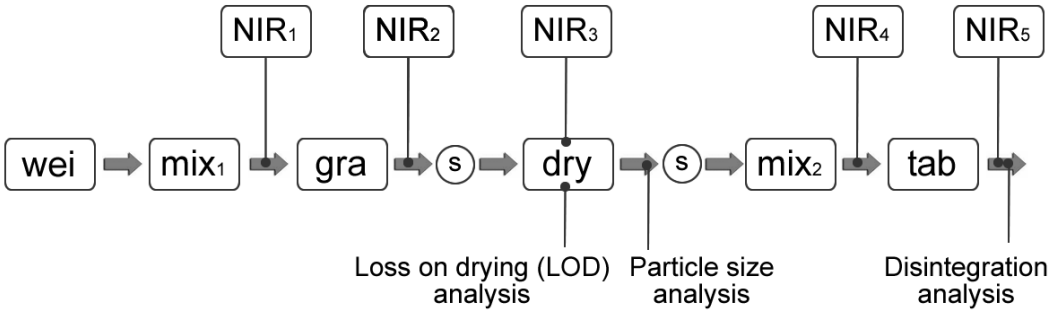

Figure 14. Overview of unit operations, NIR measurements and reference analysis points.

Table 6. Formulation of tablet (100% API label claim), granulation liquid and glitter compounds.

	Compound	g
Main compounds	API	175
	Lactose	966
	Microcrystalline cellulose	221
	Polyvinylpyrrolidone	84
	Crosscarmellose	97
Granulation liquid	Polyvinylpyrrolidone	37
	Purified water	372
Glitter compounds	Magnesium stearate	8
	Talc	16

BATCH OVERVIEW

Six calibration batches with varying amount of API e.g. 0% (placebo), 75%, 85%, 100%, 115% and 125% of API label claim. In the calibration batches with API amount different from 100% label claim the API was interchanged with lactose and microcrystalline cellulose keeping the ratio between those two components constant. Also a set of designed batches (DoE batches, all with 100% API label claim) were manufactured (Table 8). In the DoE batches three process variables; dry mixing time, granulation liquid flow and drying temperature were varied according to a full factorial design in total eleven batches plus an extra training batch (#1), and three centre points (#10-12).

Table 7. Batch overview.

Batch	*Description*		
Placebo batch	a batch without API (also used for calibration)		
Calibration batches	Five batches with 75%, 85%, 100%, 115% and 125% of API label claim		
DoE batches	Mixing time [min.]	Gran. liquid flow [ml/min.]	Drying temp. [C]
# 1	1	30	60
# 2	1	30	50
# 3	4	30	50
# 4	1	90	50
# 5	4	90	50
# 6	1	30	70
# 7	4	90	70
# 8	1	90	70
# 9	4	30	70
# 10	2.5	60	60
# 11	2.5	60	60
# 12	2.5	60	60

NIR ANALYZER AND MEASUREMENT DETAILS

All NIR measurements were performed with a new versatile FT-NIR Bruker Multi Purpose Analyzer (MPA) (Bruker Optics, Ettlingen, Germany). With this NIR analyzer the manufacturing process was investigated at several points (Figure 14). In Figure 14, the NIR measurement points symbolized with boxes with NIR_i inside. NIR_3 is an online measurement, obtained during the drying step, while the other NIR measurements are obtained after the process step was finished. Table 8 contains details for the NIR measurements.

Table 8. NIR measurement details.

NIR_1, NIR_2 and NIR_4	Reflectance measurement with handheld probe. 16 scans/spectrum. The region from 4000-12500 cm-1 was scanned. Resolution 8cm-1.
NIR_3	Reflectance measurement with process probe. 64 scans/spectrum. The region from 4400-12500 cm-1 was scanned. Resolution 8 cm-1.
NIR_5	Transmission measurement. 32 scans/spectrum. The region from 5800-12500 cm-1 was scanned. Resolution 8 cm-1.

MSPC model A

The quality problem

During the production of the DoE batches powder samples were removed after drying in the fluid bed reactor (Figure 15).

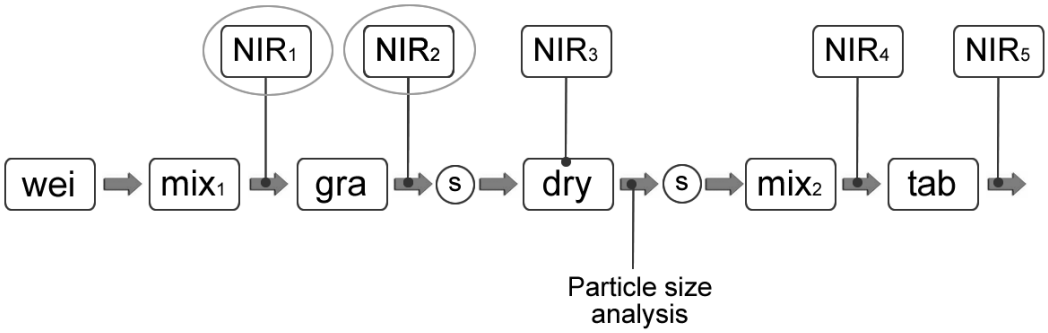

Figure 15. Overview of process steps. The point of sampling for particle size analysis after the drying step is marked. The two points of NIR measurements are highlighted by circles around the NIR symbol boxes.

The powder samples were subject to particle size analysis using a Mastersizer S-series Long Bench particle size analyzer (Malvern, Worcestershire, UK). The particle size distribution (PSD) of the granules is an important in-process quality parameter. Large differences in the particle sizes can cause segregation and a too narrow distribution would lack desired tabletting properties[86]. The PSD analysis provides six values i.e. the fractiles (10%, 50% and 90%) of the particles size, the volume weighted mean, the surface weighted mean and the specific surface area. The results from the PSD analysis of twelve DOE batches were collected in a 12×6 matrix. In order to get an overview of the PSD results, a PCA model with two PCs was fitted to the data. A scatter plot of the score values of PC1 vs. PC2 is displayed below (Figure 16). Two batches were distinctly different i.e. a batch with fine particles and a batch with coarse particles. These batches had particle size quality problems and were easily identified in the score plot.

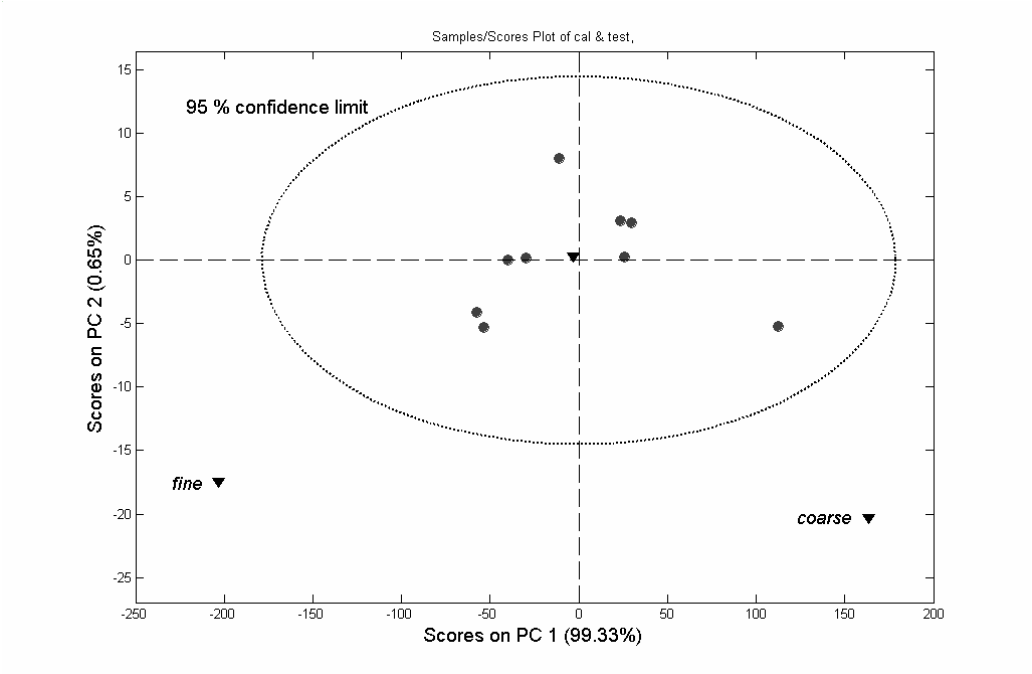

Figure 16. Scatter plot of score values of PC1 vs. PC2. The 95 % confidence limit for the normal operating condition (NOC) batches is symbolized with a dotted ellipse. Two batches were distinctly different from the other batches. In the lower left quadrant was a batch with very fine particles and in the lower right quadrant was a batch with coarse particles.

A desirable RTR monitoring system would be able to identify and forecast these events and ultimately provide information for a process control system which could prevent non-wanted PSD. We wanted to see whether an MSPC model could provide an early warning of these manufacturing problems and identify the good batches from the bad ones. Based on the PSD analysis result, the DoE batches were split into a training set of nine batches that provided a normal PSD (symbolized with dots in Figure 16) and three test set batches, which included the fine and course batches (symbolized with triangles in Figure 16). The test batches are named val_1, val_2 and val_3. After drying, the granules of DoE batch #2 (val_1) had a large proportion of fines and a low average particle size while DoE batch #3 (val_2) granules consisted of coarse particles. DoE batch #7 (val_3) was known for having a particle size distribution similar to the other nine DoE batches

i.e. good particle quality. The training set batches were used to develop control charts and the test batches were used to validate the control charts.

MSPC models

Two multivariate statistical process control (MSPC) models were developed using NIR_1 and NIR_2 measurements separately (Figure 15). The first step is to develop the control charts using the training set data; a *D* chart capturing the systematic variation in the data and a *SPE* chart capturing the non-systematic variation. The *D* and *SPE* statistics are then calculated for the test set data and plotted in the control charts in order to validate the control charts.

NIR_1 input

In each of the nine NOC batches, fourteen spectra were recorded after the dry mixing step (NIR_1). It was difficult to measure in the powder mixture because of a low density and some spectra were identified as clear spectral outliers and removed. The remaining spectra were collected in a 119×2281 matrix. These spectra were assumed to represent the normal spectral variation after the dry mixing was finalized.

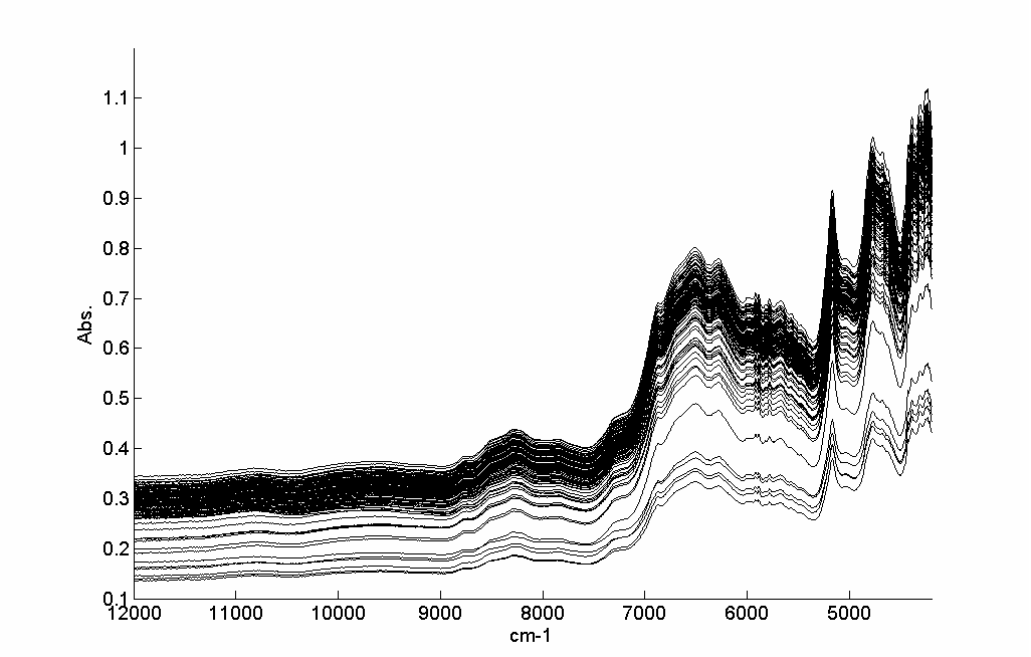

Figure 17. The NOC spectra without any pre-processing or wavelength selection.

The spectra were mean centred and a PCA model fitted to the spectra. The 95% confidence limit for the *D* statistic was calculated and used as warning limit in the *D* chart. For the residuals the 95% confidence limit was calculated and used as warning limit in the *SPE* chart.

Validation of NIR_1 model

The NIR_1 spectra from the test batches were mean centred and projected on the PCA model. Their *D* and *SPE* statistics were calculated and plotted in the control charts (Figure 18). The val_1 observations (stars) were almost all under the warning limits in both charts. Most of the val_2 observations (triangles) were flagged in the *SPE* chart, but also some of the val_3 observations (circles) were flagged in both the *D* and *SPE* chart. Different pre-processing and wavelength selection were tried out but the results did not improve. The conclusion was that a MSPC model using NIR_1 was not sufficient for identification of the batches with particle size quality problems.

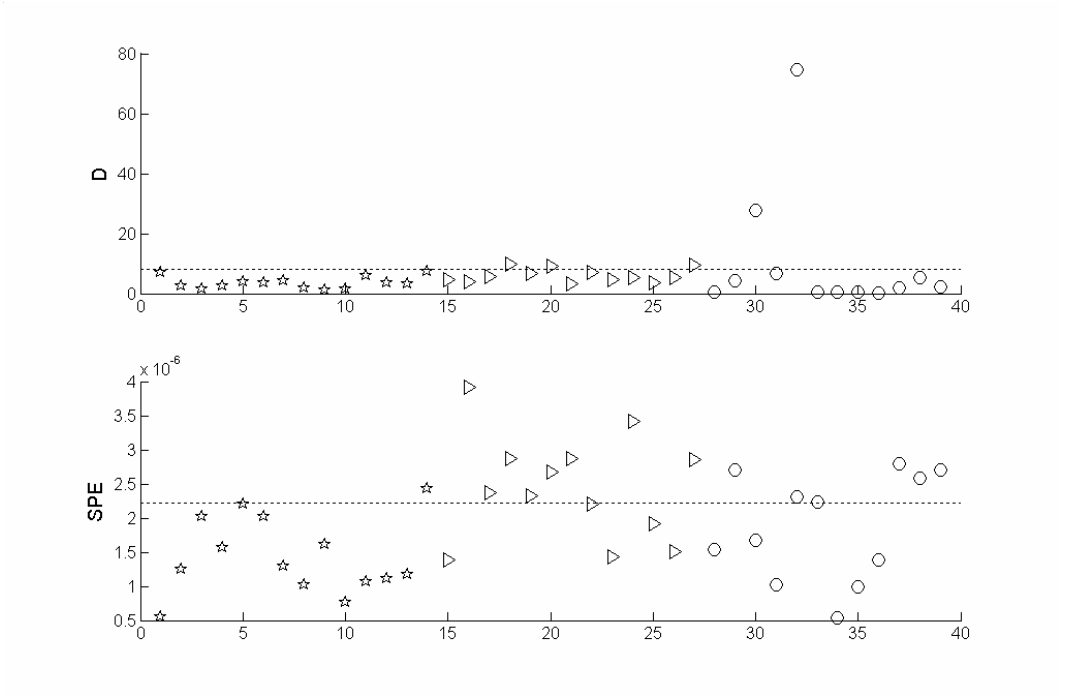

Figure 18. The NIR_1 data from the validation batches plotted in the *D* chart and the *SPE* chart. Val_1 is symbolized with stars, val_2 with triangles and val_3 with circles. The dotted lines in both charts are the 95% confidence limit.

NIR_2 input

Now a MSPC model and control charts were developed with NIR_2 as input. Various pre-processing methods and wavelength selection were tried out and by using 1st derivative and the wavelength region from 4700 to 5700 cm^{-1} a good discrimination of the test set spectra in the control charts were obtained (Figure 19). Except for spectra number 7, 8 and 19, all val_1 and val_2 spectra were flagged above the control limits in the *SPE* or *D* chart. The *SPE* chart was the most sensitive of the two control charts. All val_3 spectra were below the control limits in both charts as expected (circles in Figure 19).

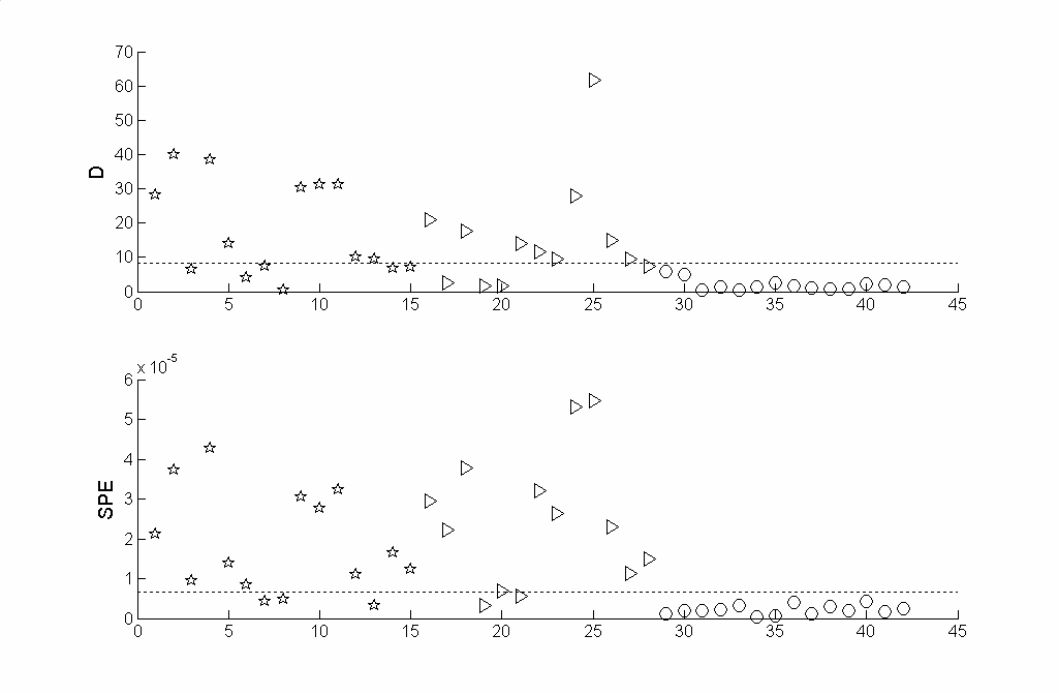

Figure 19. The NIR_2 data from the test batches plotted in the *D* chart and the *SPE* chart. Val_1 is symbolized with stars, val_2 with triangles and val_3 with circles. The dotted lines in both charts are the 95% confidence limit.

In order to identify a possible cause why the val_1 and val_2 batches showed quality problems the residual vectors were inspected (Figure 20). Distinct features at 5300 cm-1 and 4900 cm-1 were identified. The first band location can be assigned to water absorption indicating that there was increased moisture content in the problem batches. The latter band at 4900 cm^{-1} is more difficult to

assign. An explanation could be that the variation in raw material is causing the spectral deviation and the quality problems with particle size of the dried granules.

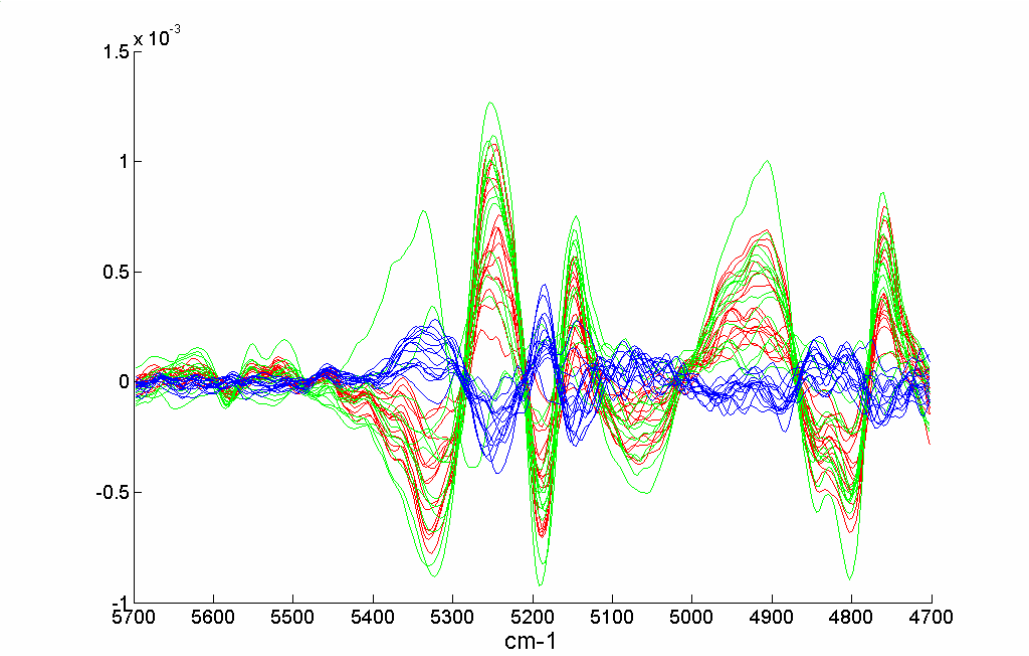

Figure 20. Residuals of test set spectra (NIR_2). Val_1 and val_2 (red and green) and val_3 (blue) residual vectors.

The result also demonstrated that particle size quality is partly being determined in the granulation process which also has been demonstrated by other authors[69;87;88]. The result showed that it is possible to use NIR spectra recorded after the granulation step in combination with a MSPC model to identify arising manufacturing problems. The natural extension of this application is to find a way to control the granulation process in order to achieve a consistent particle size quality and the MSPC model with NIR_2 spectra could support that.

Regression model B.1 (local prediction of quality)

The quality problem

The purpose of the drying process is to remove excess water in the granules and produce dried granules that are easily compressed into tablets. If the water

content is not within a certain range, compression problems might occur[89] and it might be necessary to discard the entire batch. Secondly, the drying rate influences, in some cases, also the tabletting properties of the dried granules[60;90]. Monitoring the water content during drying is an example of monitoring a local quality characteristic.

Measurements

During the drying of the granules in the fluid bed reactor NIR spectra were recorded continuously through a special constructed probe port (see page 30). The FT-NIR instrument was equipped with a three meter long fibre optical cable and a custom designed diffuse reflectance probe was used. A spectral resolution of 8 cm^{-1} was used and each spectrum was calculated as the average of 64 scans. Spectrum acquisition time was almost 25 seconds ensuring a good sample representation and a high S/N. A spectrum was automatically collected every half minute during drying. Samples were removed from the fluid bed reactor during the drying from a sample port located in close proximity to the NIR port (see page 33). The water amount in the samples was determined as % weight loss-on-drying (LOD), using a moisture analyzer (Mettler Toledo Halogen Moisture Analyzer HR73). It is important to remember that water is dominantly present as bound (crystallized water/monohydrate) and as water liquid (free water) in the granulated material. The LOD measurement is primarily determining the amount of free water while Karl-Fisher water titration is determining the total amount of water in the sample.

The spectrum that was recorded during the removal of the sample was assigned the corresponding LOD reference value. In some cases two spectra were recorded during the removal of a sample and then both spectra were assigned the same reference LOD value.

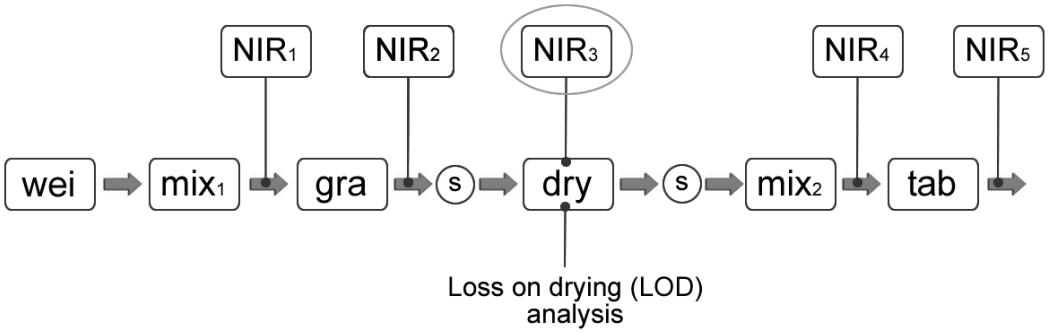

Figure 21. Process overview and overview of NIR measurements and LOD reference analysis.

During drying the spectra changed. The OH absorption peak decreased and a general drop in baseline indicating decreasing particle size was observed (Figure 22).

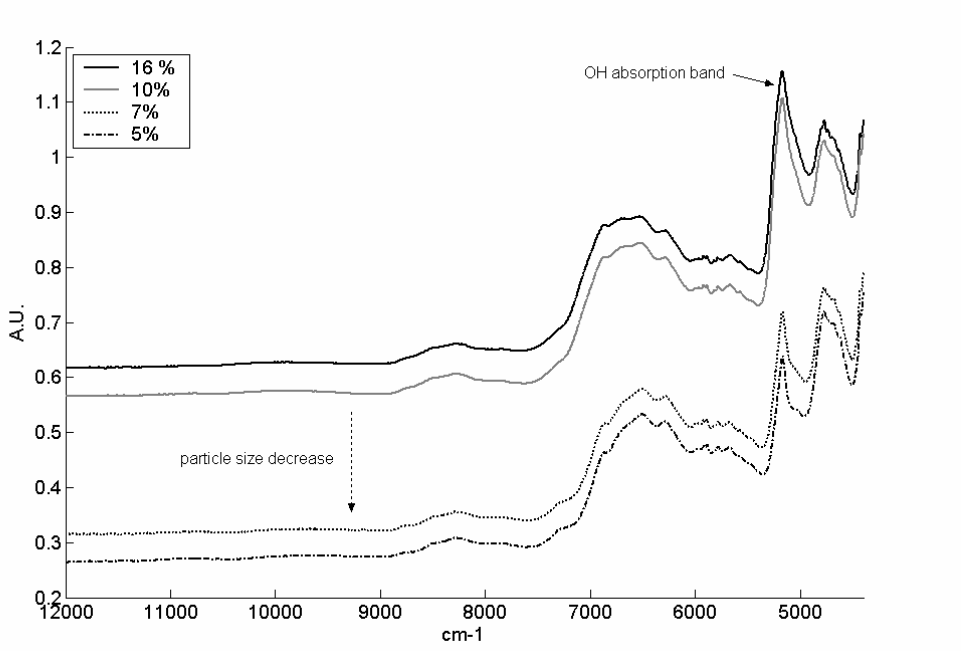

Figure 22. Four calibration spectra with different moisture content i.e. 16%, 10%, 7% and 5% water. The decreasing water content is identified as the OH absorption band at 5170 cm^{-1} is decreasing. During the drying process the particle size is decreasing which is clearly recognized as a baseline shift to lower absorption values.

Regression model

A PLS model with three latent variables was developed using 28 calibration spectra representing all DoE batches. Many different pre-processing methods were investigated and also wavelength selection routines were applied in order to minimize non-relevant spectral variation and improve model statistics. Savitzky-Golay 1st derivative with a second order polynomial fit using 17 spectral points was selected as the optimal pre-processing method. The combined wavelength regions 4597 to 5450 cm^{-1} and 7500 to 12500 cm^{-1} were used. These wavelength regions cover the water bands in the combinational and second overtone region in the NIR spectra. The first three latent variables explained 99.08 % of the variation in X and 98.70 % of Y variation. The cross validated predictions are presented in Figure 23. The cross validated prediction error was 0.53 which was similar other in-line NIR calibrations of LOD in fluid bed drying[91].

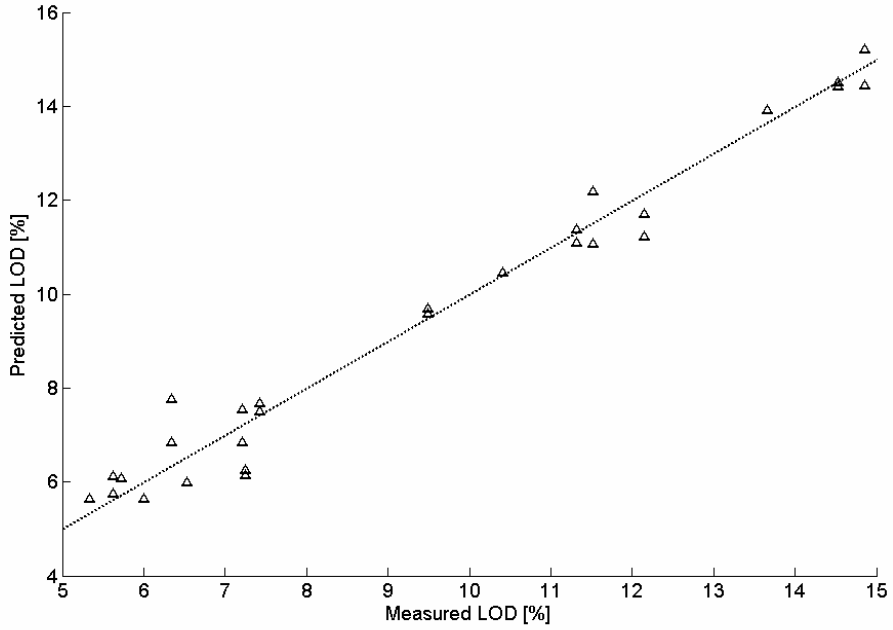

Figure 23. Calibration line for 3 LV PLS model. Measured LOD values vs. predicted values from cross validation. With three LV the RMSEC was 0.37 and the RMSECV was 0.53. The dotted line indicates perfect fit.

Applying the model to DoE batches

All drying processes were always performed with inlet airflow of 100 m^3/hour the first five minutes in order to get a good fluidization of the wet granules. After five minutes the airflow was decreased to 50 m^3/hour and kept during the remaining drying. The airflow should not be too low, otherwise the powder bed can start to collapse and a too high airflow can cause high shear stress and destroy the granules which might provide final granules with a large degree of fines and lack of tabletting properties. Fluid bed drying processes are normally controlled by fixed drying time or termination at a certain product temperature measured with a thermo probe inserted in the fluid bed reactor. All drying processes in this study were terminated when the product temperature reached 34 °C ± 1 °C.

In the DoE batches three process variables were adjusted according to a design i.e. dry mixing time, granulation liquid flow and drying inlet air temperature. It was discovered that granulation liquid flow and inlet air temperature had significant influence on the drying profiles which will be demonstrated in the following.

Influence of drying temperature

Figure 24 shows drying profiles of two batches. In both cases the granulation liquid flow was 90 ml/min. The batches were dried at 50°C and 70°C and terminated at the same product temperature. Not surprisingly, drying at 70°C was more rapid and finished after 23 min. while drying at 50°C continued to 38 min. Both batches showed a steep decrease of the drying curve the first five minutes when airflow was 100 m^3/h compared to 50 m^3/h, this was in accordance with literature results[92]. After the first five minutes, both drying curves went through the *constant drying-rate* and *falling drying-rate* periods until they reached a plateau after approximately 18.5 and 24 minutes for the seventy and fifty degree batch respectively. This is called the *equilibrium* period[93]. The transition between the *constant* and *falling* drying-rate period were difficult to identify. When the granules reach the *equilibrium* period, further drying does not decrease the final moisture content. The final moisture content is primarily determined by the

granule temperature and partial pressure of the water in the drying air. Especially the role of the humidity in the inlet air is significant[93]. According to Hlinak et al.[93] a lower drying temperature will result in higher equilibrium moisture content for the granules. This was also observed in Figure 24.

In a large number of the drying curves of the DoE batches, a small increase in the LOD was observed near the end of the drying. At this point in the equilibrium period the temperature of the granules starts to increase. When heat is transferred to the centre of the granules, the evaporation of liquid increases and a net mass transfer of water from the core to the surface will appear i.e. water is forced from a bound to a free state[92] and the LOD will increase.

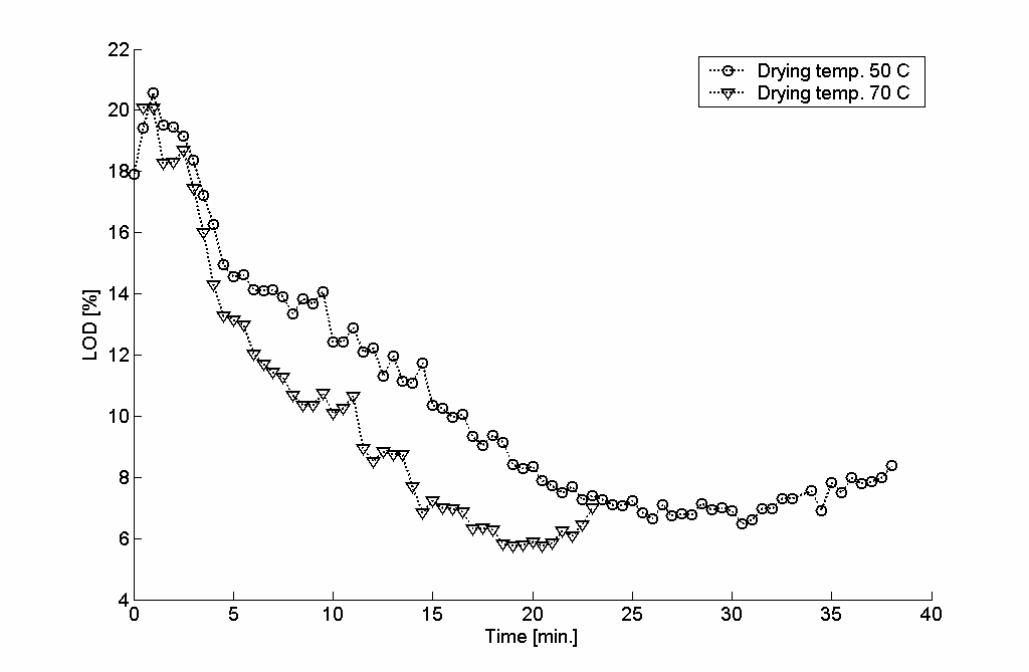

Figure 24. Drying curves for two DoE batches with drying temperatures 50 °C (-o-) and 70 °C (-∇-). Both batches were granulated using a granulation liquid flow of 90 ml/min.

Influence of granulation

The drying curves of two DoE batches are depicted in Figure 25. Both batches were dried at fifty degrees but were granulated different i.e. 30 ml/min and 90 ml/min granulation liquid flow. Their drying curves were very different. The drying curves of batches granulated with a low granulation flow were always below drying curves for batches granulated with a higher granulation flow, when dried at the same temperature. An explanation could be that in batches with a granulation liquid flow of 30 ml/min the binder liquid was better incorporated into the granules compared to batches with a high granulation liquid flow i.e. these batches possessed less free water. Also the starting value of LOD was always lower for the batches granulated with 30 ml/min compared to batches granulated at 90 ml/min. The theoretical water % in the starting wet granules is 18.8 % (Table 6), which was is agreement with the NIR predictions of the batches granulated at 90 ml/min. The drying times were 31.5 min. and 38 min. and when drying was terminated the LOD was approximately the same in both batches. Both batches also showed a slight increase in LOD towards the end of the drying.

An interesting observation was a U-shaped drying profile the first five minutes. This was observed in most of the batches with a low granulation liquid flow. The U-shape was not seen in batches granulated with a high granulation liquid flow. An explanation could be that there is less free water in the batches with a low granulation flow. During the first five minutes (high air flow rate of 100 m^3/h) the granules rapidly pass the constant and falling-rate period and enter a first equilibrium period (marked with vertical arrow after two minutes of drying). When the air flow is halved (50 m^3/h) after five minutes, the pressure and temperature difference between the granules and surrounding air stream changes and bound water is transferred to free water in the granules and the next drying sequence commence until the second equilibrium period is reached at approximately twenty-two minutes. For the batches granulated with 90 ml/min the free water is not completely removed during the first five minutes of drying and the U-shape does not appear.

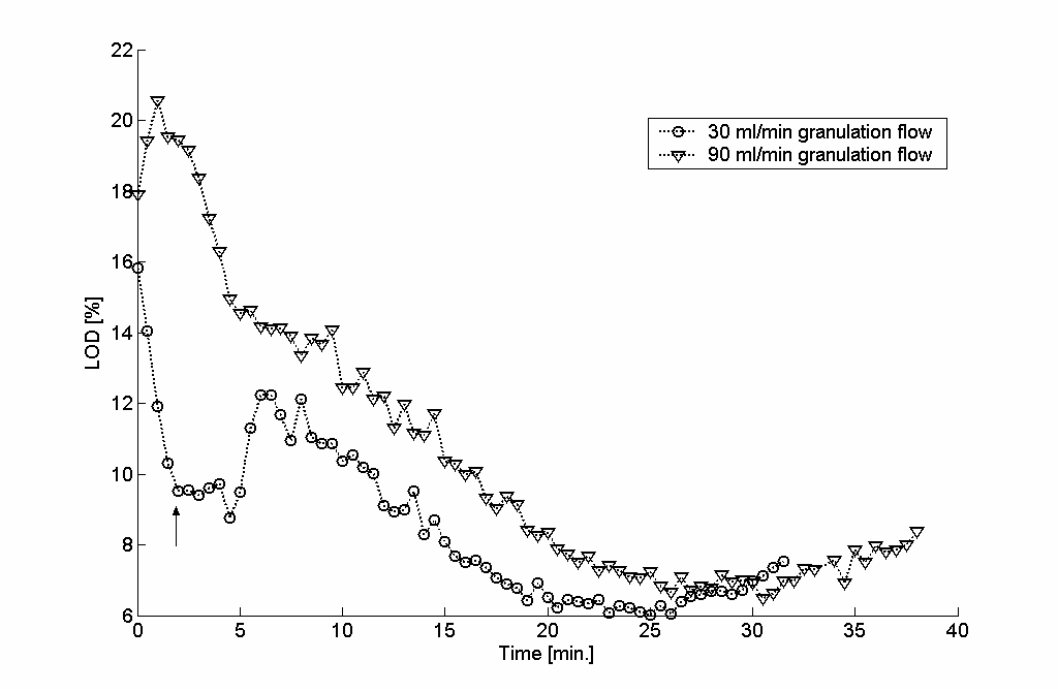

Figure 25. Drying profile of two batches dried at 50 °C. The two batches were granulated with a flow of 30 ml/min (-o-) and 90 ml/min (-∇-).

It was observed how the drying curves were influenced by granulation characteristics, air flow and drying temperature. The observed differences were supported by literature results. In-line NIR has previously been used for end-point control of drying processes[91]. But because the final moisture content is not controlled by the drying time but by the relative humidity and temperature of the drying air and the particle characteristics, this may not be an ultimate use of NIR. Instead the trajectory of the drying curve is more interesting to control as this is not possible with today's monitoring tools. The trajectory reveals distinct quality differences in the granules. By having a consistent drying trajectory the solidification rate of crystal bridges within the granules and the removal of water can be reproduced and this could likely standardize the quality properties of the dried granules.

Regression model B.2 (forecasting quality and process control)

The quality problem

The ability to forecast final quality characteristics, prior to the product is fully manufactured, is advantageous in a RTR system. If the operator upfront has a tool to predict the quality, possibilities exist for correcting the process in order to produce a high quality product. In this example it is tried out to build regression models between controlled process variables and quality measurements and final quality characteristics. It is also demonstrated how these regression models can be used to make feed forward control, to achieve a desired quality of the final product.

The disintegration and dissolution of a tablet when entering the patient, is of vital importance for the absorption of the API into the organism and hence the functionality of the drug product. In tablets that are based on an instant release principle, it might not be of equal importance as for tablets with controlled release, but for any tablet type the physical and chemical characteristics of the formulation compounds as well as the manufacturing process are impacting the disintegration time and dissolution profile. For this example disintegration time was selected as the final quality variable.

Data

The twelve DoE batches were used. Three process variables were controlled according to the design; the dry mixing time (mix), the granulation liquid flow (gran) and the inlet air temperature during drying (airT). The drying time (dryTime) was controlled according to the product temperature within the fluid bed dryer and the punch force (punF) in the tablet machine was controlled in a way so the tablets achieved certain hardness (75 kN). In each batch the disintegration time was determined for six tablets using an automated disintegration testing instrument (Tablet Disintegration System PTZ Auto 2EZ, Pharma-Test Germany). The average disintegration time (disT) of the six tablets was used as quality variable. The average disintegration time ranged from 120

seconds to 248 seconds. The standard deviation on the average disintegration time was approximately 30 seconds. After dry mixing, fourteen spectra were recorded directly in the high shear granulator, the average spectrum was calculated (NIR1*). After granulation the same procedure was repeated (NIR2*). During drying, in-line NIR spectra were recorded, the average spectrum of the last two spectra was used to represent the quality of drying (NIR3*). The dried granules were mixed with glidants and twenty-one spectra recorded directly in the mixer. The average spectrum was calculated (NIR4*).

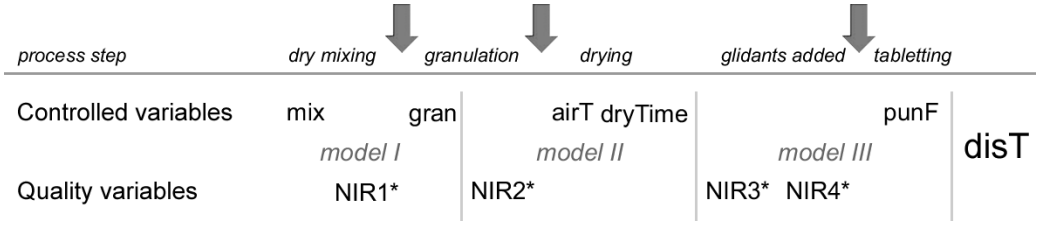

Figure 26. Overview of controlled and quality variables used for modelling. The controlled variables are; mixing time of the dry powders (mix), the granulation liquid flow (gran), the air temperature in the fluid bed (airT), the drying time in the fluid bed (dryTime) and the average upper punch force during tabletting (punF). The average NIR measurements after the process steps are denoted NIR* 1 to 4. The quality variable is the mean disintegration time of the final tablets (disT). The predictors used in each of the three models are symbolized with vertical grey lines e.g. model II uses; mix, NIR1*, gran, NIR2*, airT and dryTime.

Regression models

Three models were made with different predictors and mean disintegration time as final quality variable. With the models the operator could stop op during manufacturing, look on the model predictions of the final disintegration time and based on the result make a decision how to set the next process step in order to achieve a certain disintegration time i.e. feed forward control. The decisions points are symbolized with vertical grey arrows in Figure 26. The first decision point is after the dry mixing step, the second after the granulation and the last decision point is just before tabletting. The NIR spectra consisted of more than 2250 spectral variables and in order to perform data fusion between a few

process variables and thousands of spectral variables, the NIR spectra were first decomposed using PCA and the scores were then fused with the process variables.

Model I

In model I, the predictors; mix, NIR1* and gran were used. First the NIR1* spectra were mean centred (Figure 27). A PCA model with three principal components was fitted to the mean centred spectra. The three components explained 99.5 % of the variance of the NIR spectra. The scores and the mix and gran variables were collected in a 12 x 5 matrix, all variables were auto scaled and a PLS model was established.

The model was validated using leave-one-out cross validation. Using two PLS components a RMSECV of 50.4 was achieved and 66 % of y variance was explained (Table 9).

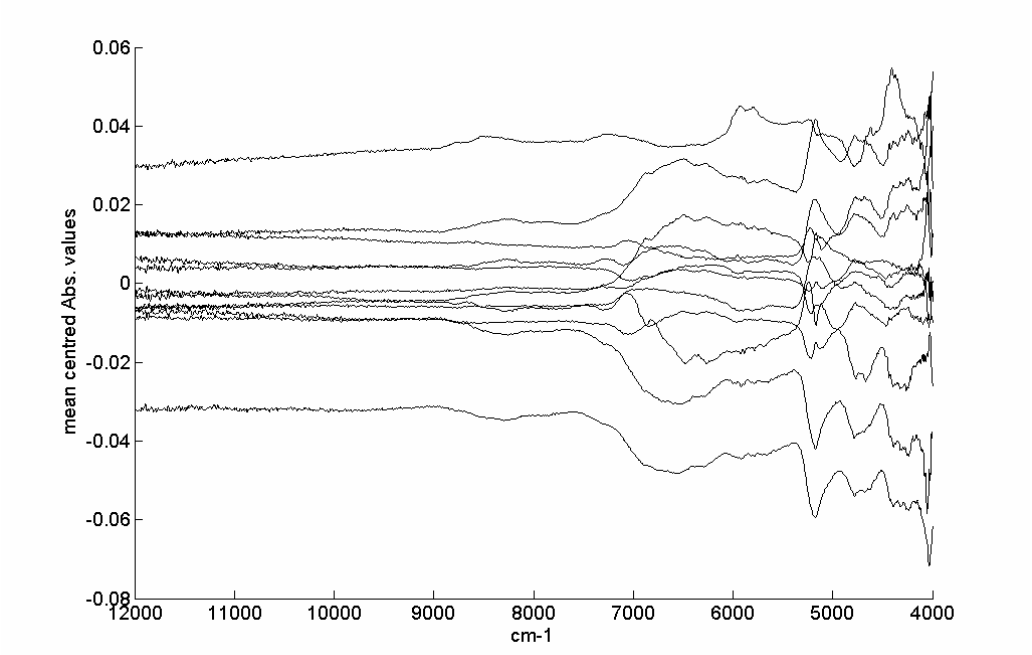

Figure 27. The mean centred NIR1* spectra.

Model II

In model II, the predictor block from model I was extended with; scores from a PCA model of NIR2*, airT and dryTime creating a 12x10 matrix. Again the variables were auto scaled before a 2 component PLS model was established. Statistics are shown in Table 9.

Model III

In model III was the predictor block from model II now extended with; scores from PCA models of NIR3* and NIR4* and punF and a matrix of 12x17 was made. The predictors were auto scaled and a two component PLS model build between the auto scaled predictors and y. The model explained 93% of y variation and a RMSECV of 36.3 were achieved.

The measured vs. predicted of model III is displayed (Figure 28).

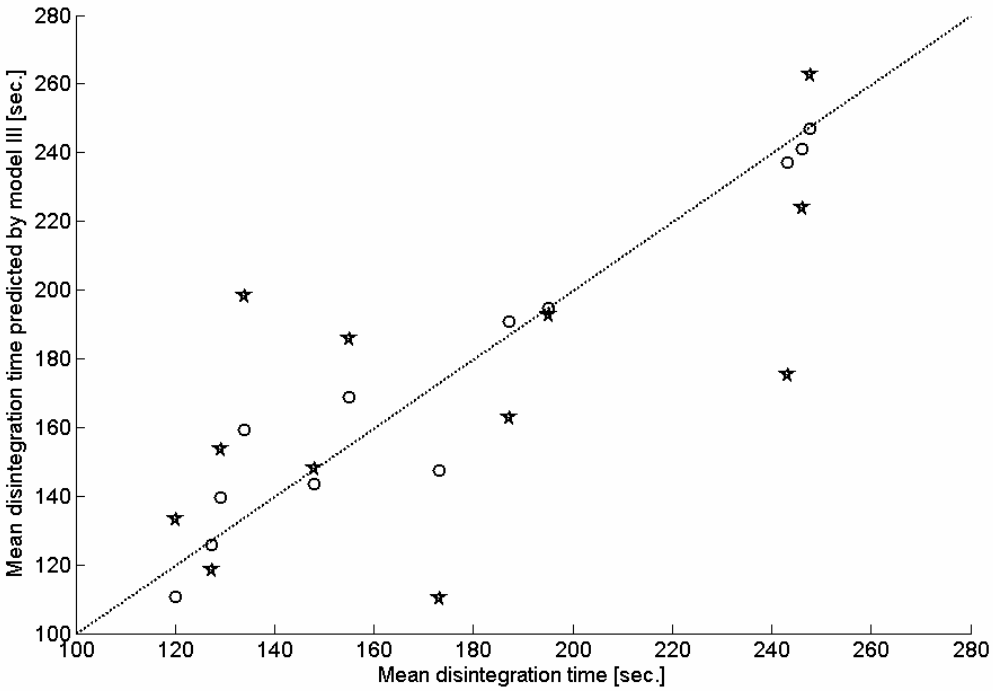

Figure 28. Measured vs. predicted mean disintegration time for PLS model III. The values from calibration are symbolized with circles and the values from LOO CV are symbolized with stars. The dotted line symbolizes perfect fit.

Table 9. Model statistics for the three PLS models I, II and III. The rank of the models is symbolized with bold numbers.

Model I				
LV #	Expl. X var.	Expl. y var.	RMSEC	RMSECV
1	26.9	61.5	28.7	46.4
2	**51.6**	**66.0**	**27.0**	**50.4**
3	73.3	67.2	26.5	55.8
4	81.6	67.3	26.5	59.8
5	100.0	67.3	26.5	60.6
6				
Model II				
LV #	Expl. X var.	Expl. y var.	RMSEC	RMSECV
1	20.6	62.5	28.4	53.0
2	**38.7**	**72.3**	**24.4**	**57.7**
3	54.5	80.7	20.3	64.4
4	67.4	85.1	17.9	65.2
5	81.6	87.4	16.5	72.5
6	92.1	89.2	15.2	74.3
Model III				
LV #	Expl. X var.	Expl. y var.	RMSEC	RMSECV
1	22.3	85.6	17.6	36.2
2	**34.4**	**93.0**	**12.2**	**36.3**
3	50.9	96.8	8.3	38.8
4	63.4	98.3	6.0	36.0
5	76.2	98.9	4.9	33.3
6	84.3	99.5	3.3	33.0

Process control

In each of three decision points (symbolized with grey vertical arrows in Figure 26), process control is shown. By interpretation of the regression coefficients of the PLS models information can be found on how to set process variable(s) for the following step (feed forward control) in order to achieve a certain disintegration time.

By inspection of the regression coefficients for model I (Figure 29) it was found that mixing time and granulation liquid flow were more influential then the NIR scores. Granulation liquid flow was inverse correlated to disintegration time, so increasing granulation liquid flow would decrease disintegration time. An explanation could be that low granulation liquid flow (=long granulation time) would mean that larger granules were built[61] which again would give tablets with a longer disintegration time.

This hypothesis is further supported when inspecting the regression coefficients for model II and III. It has also been demonstrated by other authors that the granulation step has a significant effect on tablet properties[94].

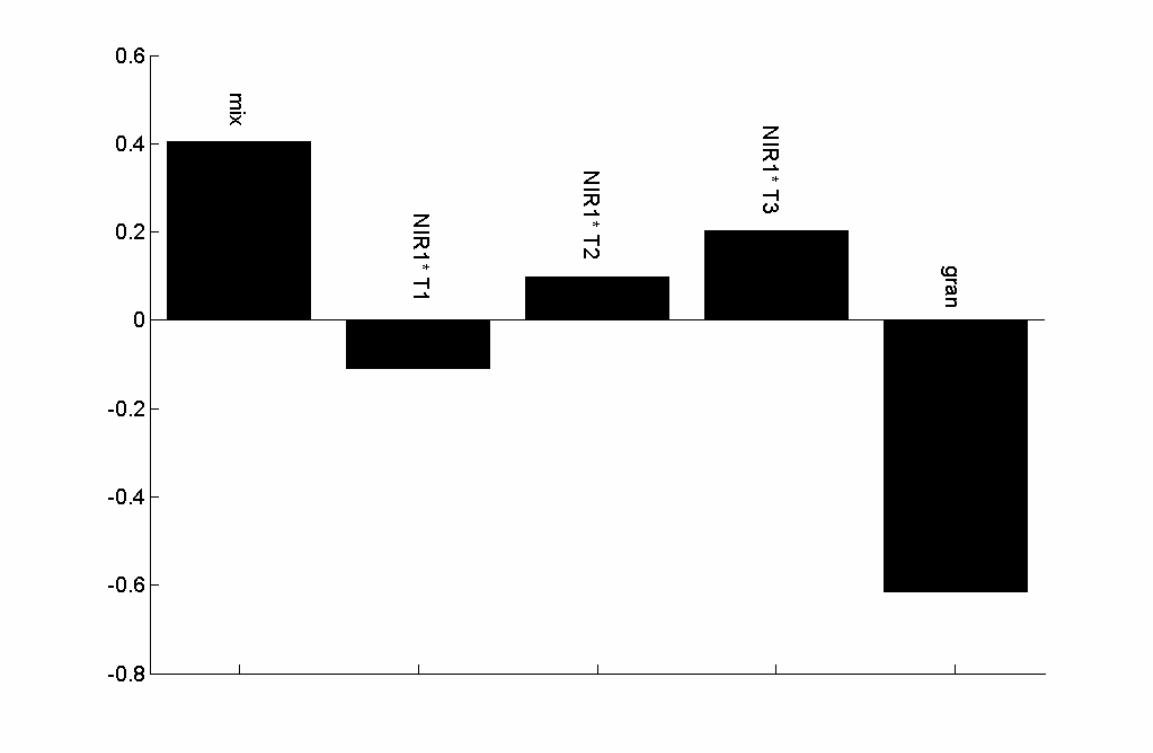

Figure 29. The regression coefficients for PLS model I.

The first decision point and ability for process control is after dry mixing is finalized and the operator would like to know how the granulation liquid flow should be set based on the available information at the point i.e. the mixing time and the recorded spectra after mixing (quality of mixing). First the mixing time is auto scaled with the scaling factors from model I, the new NIR1* spectrum is projected onto the PCA model for NIR1* and the score values calculated. Now different hypothetical values for the granulation liquid flow can be used with the measured mixing time and NIR score values and disintegration times predicted. Based on the results a granulation liquid flow value is selected and used in the subsequent granulation step. This approach was demonstrated using the twelve DoE batches. Using granulation flow values ranging from 30 to 90 ml/min the

mean disintegration time was predicted in each of the twelve DoE batches (Figure 30). The difference between the DoE batches at that point was mixing time i.e. 1, 2.5 or 4 minutes, and the difference as characterised by NIR. The predicted disintegration time was plotted against hypothetical granulation liquid flow. As expected the mean disintegration time decreases when the granulation liquid flow is increased. Also when the dry mixing time is increased the disintegration time is increased. The shift between the lines of the batches with the same dry mixing time indicates quality differences between the dry mixed powder mixture e.g. humidity differences and particle size differences (starting material differences).

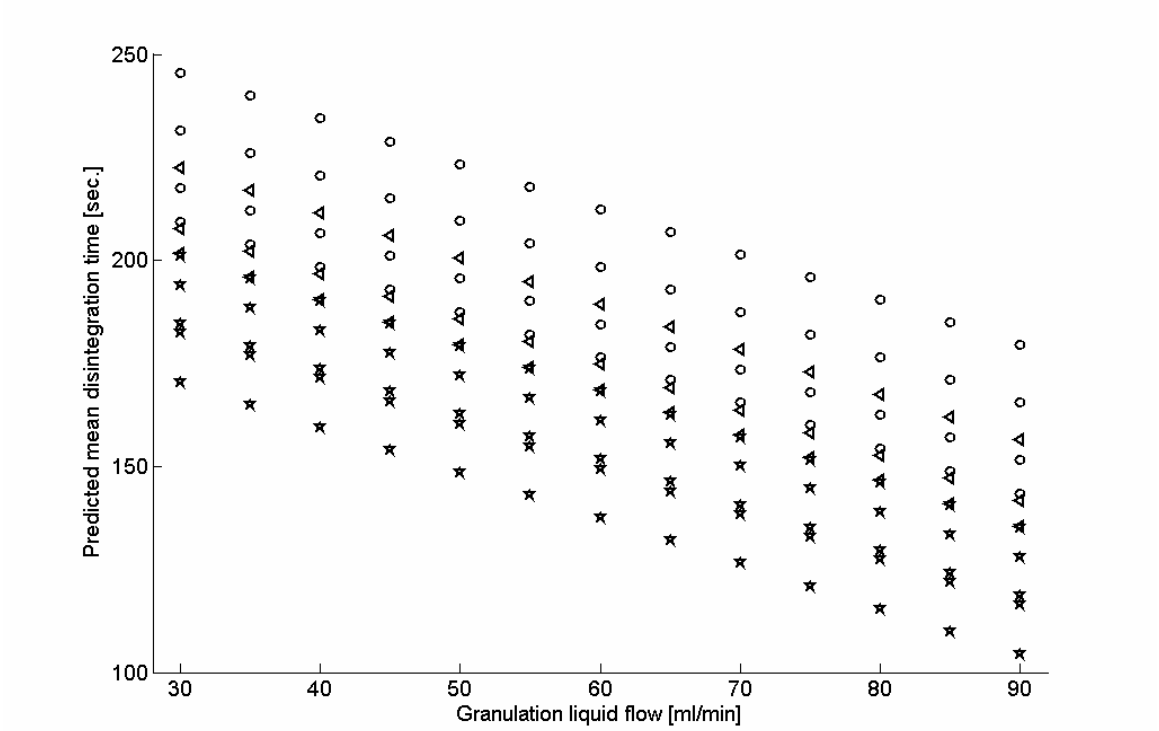

Figure 30. Process control chart for setting of granulation liquid flow using Model I. The DoE with mix time 1 minute is symbolized with stars, 2.5 minutes are symbolized with triangles and 4 minutes with circles.

Inspection of the regression coefficients for Model II (Figure 31) showed granulation and inlet air temperature to be influential of the disintegration time. The first score for the NIR2* was positively correlated and important to the

disintegration time. When inspecting the first loadings for the PCA model for NIR2* it was seen that it was explaining baseline shift between the spectra i.e. particle size differences. The bigger the granules, the longer the disintegration time.

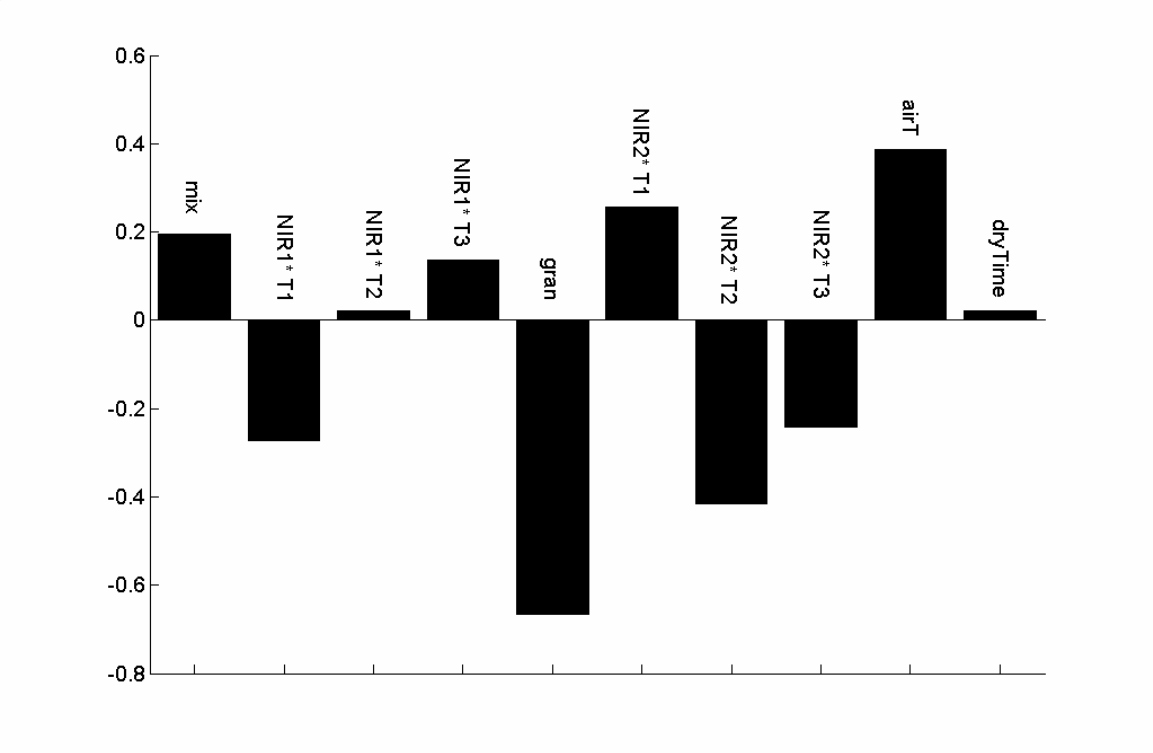

Figure 31. The b coefficients for PLS model II.

The regression coefficients for punch force in model III (Figure 32) was clearly positively correlated to the disintegration time. This result showed that the operator at the last decision point could increase the disintegration time by increasing the punch force during tabletting.

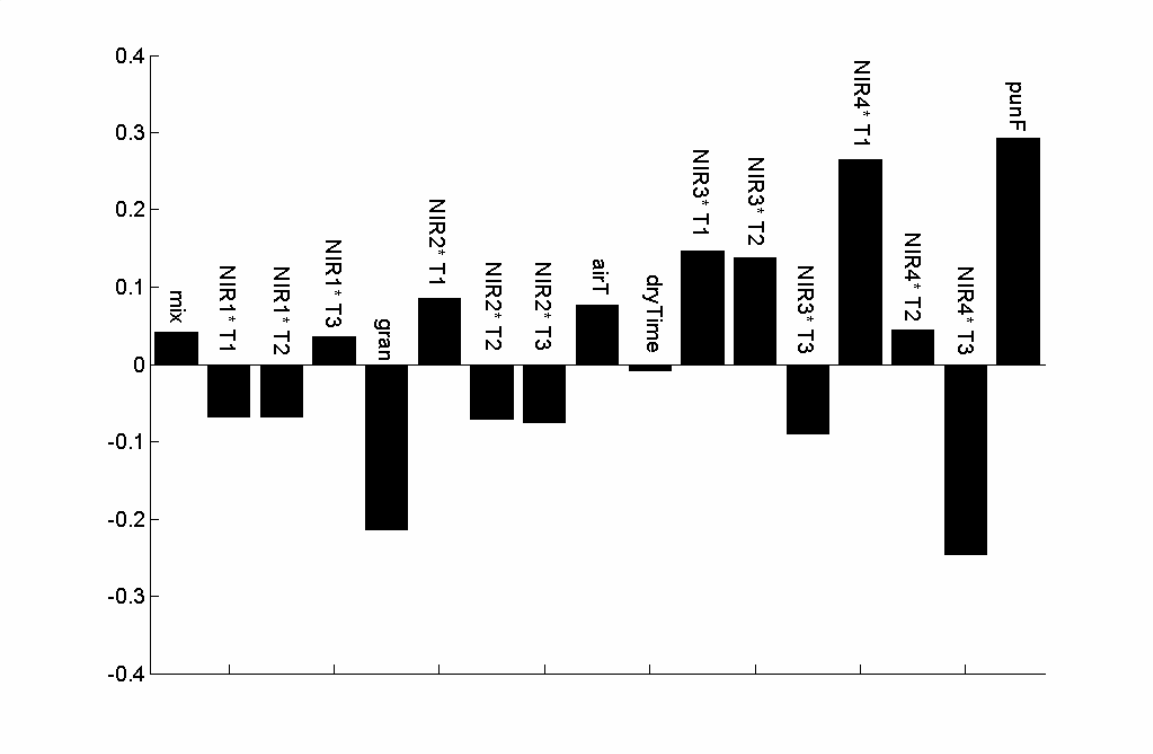

Figure 32. The b coefficients for PLS model III.

The effect of different settings of punch force was quantified by predicting disintegration time with Model III, inserting different values for punF ranging from 8 to 14 kN. It was seen that the disintegration time could be increased approximately 50 seconds when the punch force was increased from 8 to 14 kN. Secondly there was predicted a large range of disintegration times using the same punch force depending on the other process parameters. The predictions are symbolized with a star, triangle or circle depending on granulation liquid flow. Though a low granulation liquid flow would give a higher disintegration time compared to a high granulation liquid flow other factors also influences disintegration time as there is overlap between the predictions from batches with different granulation liquid flow.

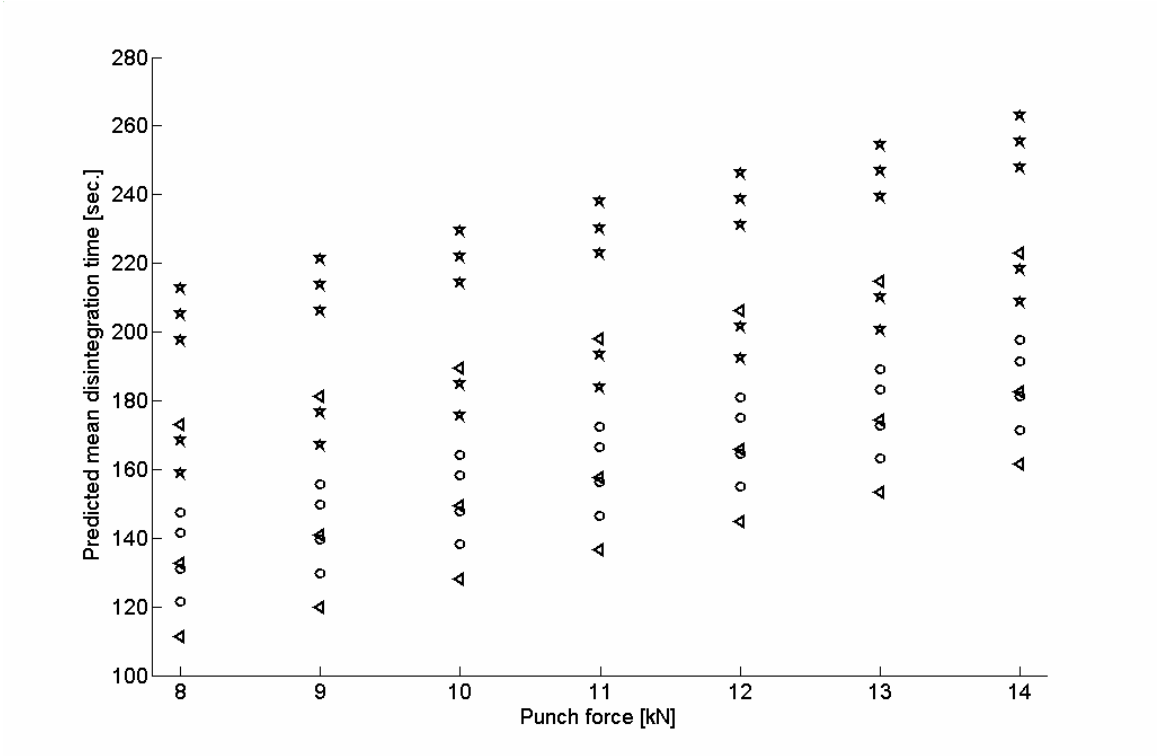

Figure 33. Predicted mean disintegration time as a function of various upper punch force values (punF) of the twelve DoE batches. The batches with gran = 30ml/min are symbolized with stars, 60 ml/min are symbolized with triangles and 90 ml/min symbolized with circles.

It has been demonstrated how final quality characteristics can be predicted using regression models between process variable settings and quality measurements obtained during manufacturing and final quality characteristics. As more data becomes available, a larger percentage of the variance of the final disintegration time can be modelled and the prediction improved. The uncertainty of the determination of mean disintegration time was approximately 30 seconds and this might account for the high prediction error of e.g. model III with a RMSECV of 36.3 seconds.

Based on the regression models, suggestions for feed forward process control were established. The challenge of data fusion between a few process variables and thousands of NIR variables was dealt with by decomposing the NIR spectra

using PCA and using the scores instead of using the original spectra together with the process variables.

The results were only indicative since more data should be available for a thorough treatment. Secondly was the range of disintegration time not wide and very little variation was observed. The manufactured tablet was not a sustained release product and was expected to be dissolved quickly. For a sustained release tablet the potential range of disintegration and dissolution time are much wider compared to instant release drugs. For such a tablet type, the use of regression models and NIR spectroscopy of granules could be of even greater value, and the tests for disintegration and dissolution could be omitted and a real time release of the tablets be implemented. The examples is meant as a general example of how to develop process control tool and feed-forward control.

Regression model B.3 (final quality predictions)

Quality problem

The content of active pharmaceutical ingredient (API) in the final tablets is a major quality parameter. Traditional quality control is performed on a small set of tablets i.e. ten to thirty tablets in distant laboratories using time consuming analysis methods e.g. HPLC. This means that the batch is quarantined for two to three weeks before the analysis result is ready and the batch can be released to market. Secondly by only analyzing a small number of samples there is an increased risk that quality defects are not detected.

With a real time release (RTR) system, quality is assured when the product leaves the final production step e.g. the tablet press. Real time or near real time quality control at the final production step would be an example of final quality predictions. There exists a commercial on-line NIR based system which is mounted directly on the tablet press and withdraws tablets from the press and analyzes several quality parameters during tabletting e.g. the API content (TANDEM, Bruker Optics, Ettlingen, Germany). In this example, the final quality

analysis of API content in tablets is made with an at-line based NIR system which can be placed next to the tablet press in order to perform the analysis of the tablets directly after the press.

Samples and measurements

For all the calibration and DoE batches, tablets of 180 mg were pressed using a laboratory scale rotary tablet pres with six stations (Fette GMBH, Schwarzenbek Germany). Each batch weighted 1.6 kg so a total of approximately 8900 tablets were produced per batch. From each of the calibration batches, hundred and twenty tablets were measured with NIR and from each of the DoE batches ninety tablets were measured with transmission NIR from 7500 cm^{-1} to 12500 cm^{-1}. The ninety tablets from each of the DoE batches were removed during tabletting in three steps i.e. thirty tablets withdrawn from the start, mid and end of the tabletting process respectively.

Before analysis the tablets were placed in customized tablet holders which were placed in a thirty sample capacity carousel, on top of the NIR instrument. After the carousel was placed, the analysis was initiated and the instrument automatically performed a transmission measurement of all tablets in the carousel in approximately ten minutes. It was found that a single transmission spectrum through one side of the tablet was representative of the entire tablet.

Regression model

For each of the six calibration batches one calibration spectrum was made by averaging all the hundred and twenty spectra from each batch. Then each calibration spectrum was assigned a reference value which was the average API content in the corresponding calibration batch and finally a regression model was built between the average calibration spectra and their reference values (which here was of course the weighing of the different compounds). This calibration method does not rely on reference analysis, and the assumption for using this method is that by measuring a large number of samples from a batch the

average content in all samples approaches the average content of the entire batch. The target API content of the tablet product was 19.7 mg API/tablet. One calibration batch was made as a placebo batch without API and the other five batches were manufactured as 14.8, 16.7, 19.7, 22.6 and 24.6 mg API/tablet batches, corresponding to 75%, 85%, 100%, 115% and 125% of target API content.

A PLS regression model was constructed. Several pre-processing methods were tried and evaluated based on the RMSECV from LOO CV and number of PLS components needed. It was found that Savitzky-Golay 1st derivative followed by MSC gave the best result. It was also found that the number of spectral points to use in the Savitzky-Golay algorithm was important to optimize, in order to get a low prediction error. The RMSECV was calculated using different numbers of spectral points (Figure 34). When using one PLS component the RMSECV was lowest (0.066) when using thirty-five spectral points in the Savitzky-Golay filter. Using more PLS components worsened the RMSECV significantly.

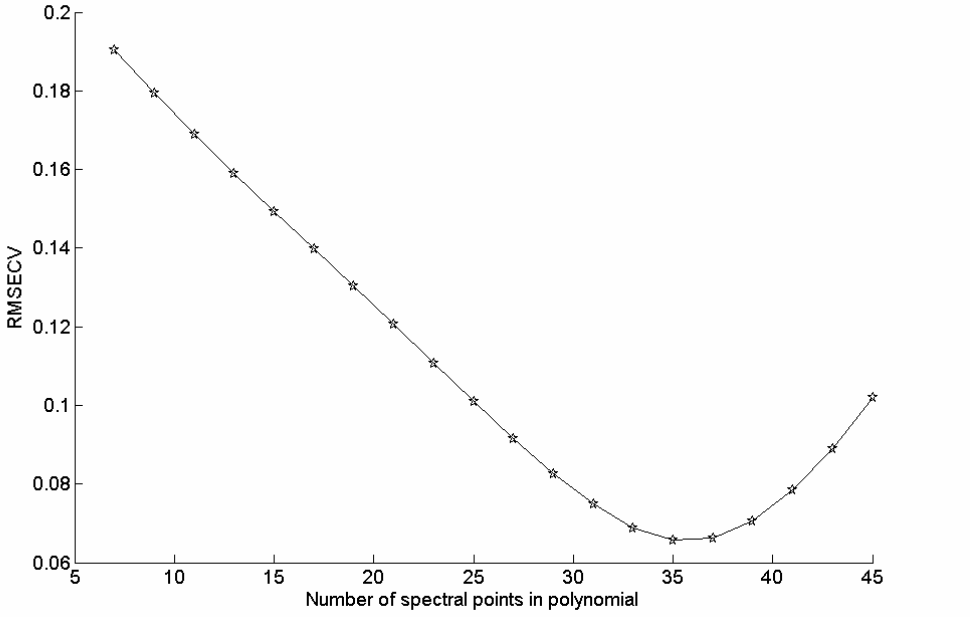

Figure 34. RMSECV as a function of number of spectral points used in the Savitzky-Golay algorithm. When using 35 spectral points a RMSECV of 0.066 was found using one PLS component.

The pre-processed calibration spectra and the regression vector for the final PLS model are depicted in Figure 35.

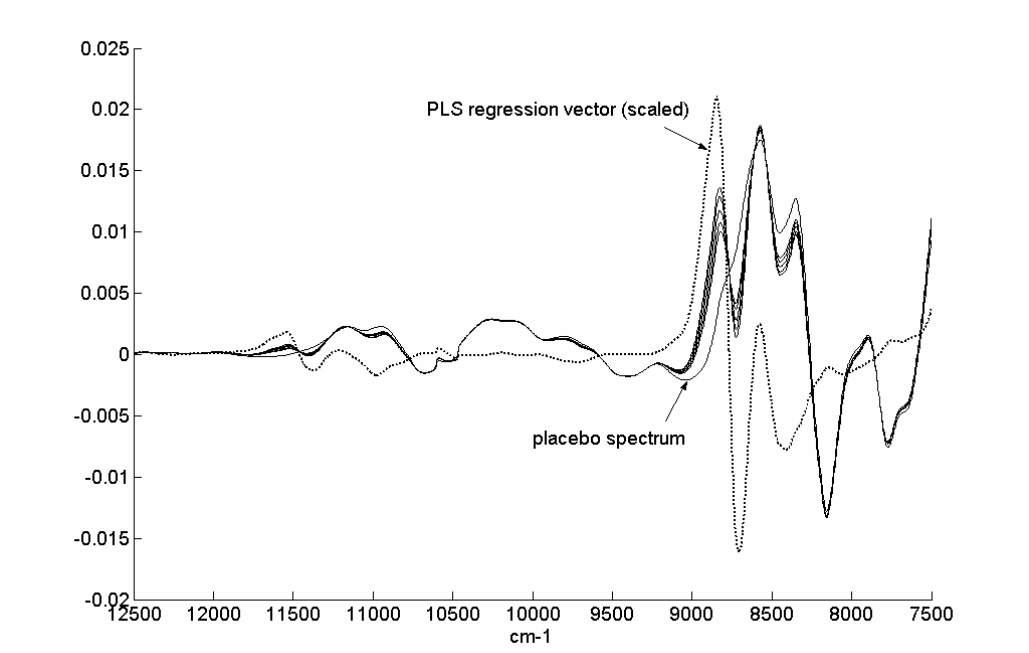

Figure 35. The average calibration spectra after pre-processing. Spectral features which were correlated to API absorbance peaks were present at 8700 cm^{-1} and 11500 cm^{-1}. The regression vector from the PLS model is scaled for the purpose of visualization (dotted line).

Using 1st derivative and MSC as pre-processing and the entire wavelength region a one component PLS model was built. The calibration model is depicted in Figure 36. A RMSECV of 0.066 which is corresponding to a prediction error of 0.3% was found and a correlation coefficient of 0.9999.

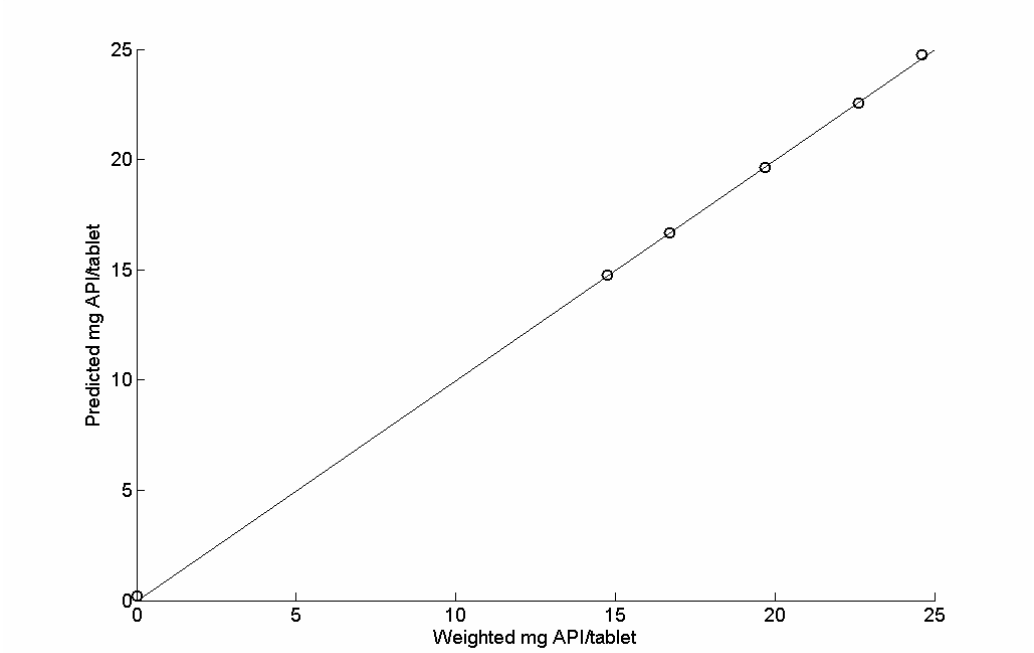

Figure 36. PLS model with one component using the wavelength region from 7500 cm^{-1} to 12500 cm^{-1}. The predicted values from cross validation, of the calibration spectra vs. their reference values. The R2 is 0.9999; the RMSECV is 0.066 which is 0.3%.

Predictions

The PLS model was applied to the ninety spectra from each of twelve DoE batches. From the batch records it was confirmed that all DoE batches were prepared with the same target API content of 19.7 mg API/tablet. The mean and variance were calculated for the assay predictions from the start, mid and end of each DoE batch (Table 10). The DoE batch no 1 showed the lowest API content in all tablets analyzed together with DoE batch no 2. The average tablet weight was 180 mg for both calibration and DoE batches so this cannot explain why some of the DoE batches show a lower API content. An explanation could be that if some of the API is caught in granule fines, then this material could be lost in the filters during the drying in the fluid bed reactor.

Table 10. Assay predictions for twelve DoE batches. The mean and variance are calculated for the start, mid and end of tabletting process.

	Mean			Variance		
DoE #	Start	Mid	End	Start	Mid	End
1	19.2	19.2	19.1	0.03	0.02	0.03
2	19.4	19.4	19.4	0.03	0.02	0.02
3	19.6	19.5	19.6	0.03	0.03	0.04
4	19.6	19.6	19.6	0.03	0.03	0.02
5	19.6	19.7	19.8	0.04	0.02	0.04
6	19.5	19.5	19.5	0.03	0.04	0.02
7	19.8	19.5	19.5	0.05	0.06	0.02
8	19.6	19.6	19.5	0.02	0.02	0.03
9	19.4	19.4	19.5	0.04	0.02	0.01
10	19.6	19.7	19.6	0.02	0.03	0.01
11	19.6	19.5	19.4	0.02	0.03	0.03
12	19.5	19.6	19.5	0.02	0.04	0.03

As an example are the assay values depicted for DoE batch #7. Generally there was generally more API in the tablets in the beginning of the tabletting process compared to the mid and end of the process. Also the variance was higher in the start of the process. This behaviour would be difficult to identify and control if only a few samples were analyzed using classical methods.

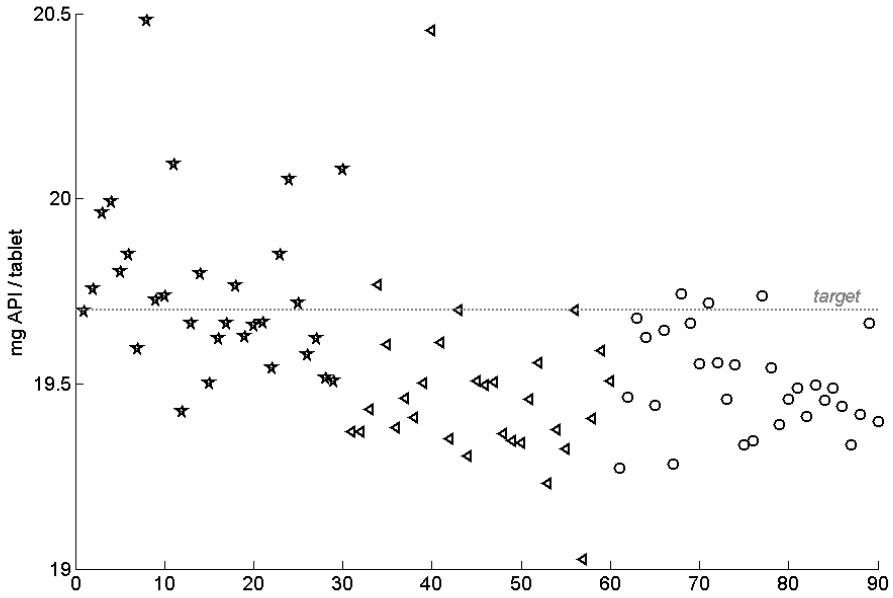

Figure 37. Ninety assay predictions from DoE batch no. 7, thirty from start (star), mid (triangle) and end (circle) respectively. The average API content was higher in the first part of the tabletting compared to the mid and end of the tabletting process.

It was demonstrated how an important final quality control of tablet assay could be applied at-line the tablet pres using transmission NIR spectroscopy. The analysis of thirty samples could be performed in less than fifteen minutes including sample placement in sample cups and sample carousel. A one component PLS regression model was developed. The regression model had a very low prediction error of 0.3 % and was simple to develop with a set of calibration batches.

Because of the speed, precision and simplicity of the analysis, the method is a viable candidate for a real time release analysis method which can be applied next to the tablet press and during the actual tabletting. Finally, the number of tablets analyzed can be greatly increased and quality defects as blend uniformity problems e.g. segregation is more likely to be detected and taken action upon. The last example showed how RTR capability of the tablets could be achieved.

CHAPTER 6. CONCLUSION AND FUTURE RESEARCH

This thesis documents four years of research with NIR, multivariate data analysis and tablet manufacturing processes. Given the widespread possibilities of applying NIR in almost any process control and quality decision task during tablet manufacturing, there is little doubt that this technology will dominate in the future. However, there are some obstacles for which research should be addressed. The NIR spectrum is influenced by many physical and chemical factors. In order to implement the technology successfully it is mandatory to understand these factors for a given application and sample type. In some cases it is necessary to suppress these influences by pre-processing and wavelength selection. One of the first research goals was to develop an alternative way of selecting the optimal pre-processing and wavelength regions. This was achieved with a novel indicator called signal-to-error (SE) indicator. Some of the existing methods to judge pre-processing and wavelength selection suffer in cases where the reference analysis is erroneous or not enough calibration samples are simply available. The SE indicator does not rely on reference analysis results and requires only a few samples. The method and two similar methods were demonstrated on two pharmaceutical NIR data sets. The SE indicator was superior in all examples.

Furthermore, NIR has often mistakenly been suggested as a technique which first can be used when a drug development program has reached a high degree of maturity. At the early stage in a drug development program a lot of different tablet formulations are usually tested out and the number of bathes is few. This circumstance makes traditional quantitative NIR calibration cumbersome and is therefore often avoided. In the thesis are several examples on how calculations based on net analyte signal can substitute the traditional calibration efforts with a much smaller number of calibration samples and achieving the same results. With the described techniques, NIR can be used successfully even at an early stage in the drug development program. Then when more batches become available, quantitative calibration models can be developed and finally transferred to the manufacturing.

One of the most critical operations, with respect to tablet quality is powder mixing. In the literature several examples of NIR applications for that operation have been demonstrated. Some of the benefits and drawbacks for these methods were evaluated. A new NIR method to evaluate powder mixing was developed. It differentiated from the existing methods in many ways. First, it was based on net analyte signal calculations which offered two approaches to evaluate the analyte concentration either qualitatively or quantitative. Both approaches provided similar results and the method can then be used both in the early and late stages of drug development. Secondly, the NIR predictions were evaluated in control charts using well known statistical tests. The hypothesis was that the mixing quality matched a ‘golden batch’ representing the desired mixing quality. Finally, the sampling procedure mimic existing industry practice for determining mixing quality and is capable of identifying ‘dead spots’ in the mixer which a large number of the previous NIR methods were not capable of.

In a real time release system quality monitoring is one of the pillars. Before the final drug is released to the market it has to meet several qualities. Because the NIR spectrum is influenced by all the components within the sample matrix, there exists opportunities to monitor several quality characteristics with one spectrum. In order to evaluate that, a new method called net analyte signal statistically quality control (NAS-SQC) was developed. With models based on net analyte signal calculations and principal component analysis, the measured spectrum was split into three independent parts. For each part a statistic was calculated and plotted in a separate control chart. With one control chart the content of active pharmaceutical ingredient was monitored. With another, the homogeneity of the other components in the drug product and with the final control chart the non-systematic or residual variation was monitored. The method was demonstrated with NIR spectra of a commercial drug product. It was shown how samples that were out-of-control with respect to different quality problems were

flagged in the different control charts and how good quality samples stayed within acceptance limits in the control charts.

The ability of releasing the product to the market when it exits the last manufacturing step needs support by measurements during manufacturing to ensure the final quality. A theoretical framework for a real time release system was developed. The objective of the framework was to show how the collected process measurements could be used to monitor and control the quality of both intermediate and final product quality. This is done by using models to correlate the observations with the quality characteristics. Four distinct models were identified and explained. With process and NIR data from a complete tablet manufacturing process the four models were demonstrated.

It is the intention and hope of the author that this thesis will provide both theoretical and practical solutions for the researcher that is going to develop and implement a real time release system, based on NIR and multivariate statistics.

Future research

In this section some of the experience and ideas that are obtained during the research will be dealt with. These have not been presented previously in the thesis. It should be noted that the examples are not validated and should merely work as inspiration for further research.

Net Analyte Signal based methods

One of the corner stones in the research has been the use of net analyte signal calculations. This method has some interesting properties, especially for the pharmaceutical industry. The basis of net analyte signal calculations is a model of the interference. For that blank samples are an optimal solutions and these are always available in pharmaceutical processes i.e. placebo samples. During the work with the NAS-SQC method, the method was also tested with simulated spectra. It was discovered that if a peak in the spectrum of one of the

components shifted slightly compared to the normal peak position it was picked up in the residual control chart. Reasons for peak shifts in the spectrum are; spectrometers malfunction or changes of the crystallinity of one compound. If the spectrometer is malfunctioning with respect to wavelength accuracy and a shift is present, all peaks in the spectrum will shift at the same time. This is of course a problem and will also be detected with the NAS-SQC method. The other possibility is if only one component and especially the active pharmaceutical ingredient demonstrate a peak shift which signals a potential quality problem. If e.g. the active pharmaceutical ingredient has several polymorph forms the different forms will affect the NIR spectrum especially as peak shifts. Polymorph control of the active pharmaceutical ingredient is a major quality issue. It would be very interesting to investigate the feasibility of NAS-SQC for quality control of drug products with polymorphism quality problems.

In-line use of NIR in fluid bed reactors

During the work with drying monitoring with in-line NIR, some ideas of process control were discussed. Because the final moisture content is not controlled by drying time in the last equilibrium period but by the inlet air properties, it was suggested that NIR should be used to control the drying trajectory instead of the drying end-point. The effect on product quality when a tight NIR based control of the drying trajectory is applied would be an interesting research topic.

Along side the PhD project some experiments with in-line NIR in fluid bed granulation and drying were also performed. In Figure 38 are some results depicted from a larger series of designed experiments. The NIR spectra were fitted to a PCA model. The first principal component was correlated to the water in the granules and by plotting the score value of PC1 vs. time the granulation and drying phases were identified. The score value of PC1 can be regarded as a pseudo water concentration. In batch D, 23% less water was used for the granulation process which is very clear in the figure. When the process profile of batch E is compared to batch A, B and C significant differences are also

recognized. Other results illustrated how process problems i.e. disfunctioning dust filters and missing spraying pressure were detected very early in the granulation process with NIR. The performance of unit operations involving fluid bed reactors are significantly influenced by many factors e.g. environmental humidity, process equipment and raw material variation and at Novo this will most likely be a key area for PAT research in the future.

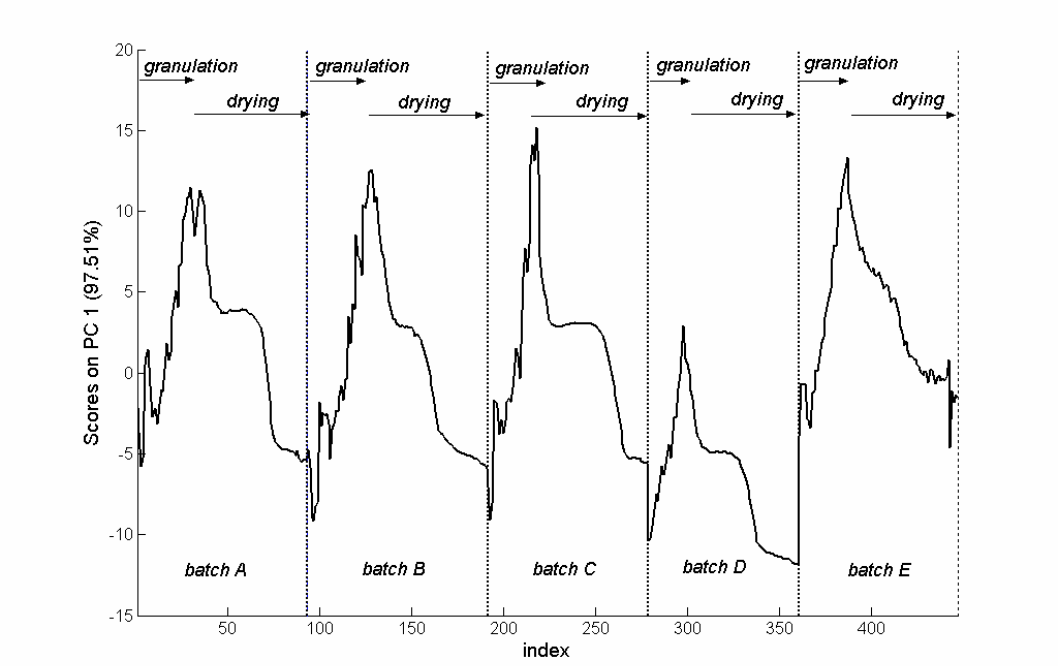

Figure 38. A score plot of fluid bed granulation and drying monitored with in-line NIR. In batch D, 23% less water was used for the granulation compared to the other batches.

Drying monitoring without regression models

This section is intended as an inspirational postscript to the use of regression models for predicting the LOD. Two phenomena will be dealt with i.e. the particle size changes during drying and the ratio between free and bound water during drying.

During the drying of the granules some drastic particle size changes appear. At a certain moment the granule surface is dried out and shear forces between the

granules and the granules and the reactor walls cause a rapid decrease of the particle size as the dry layers are pealed off.

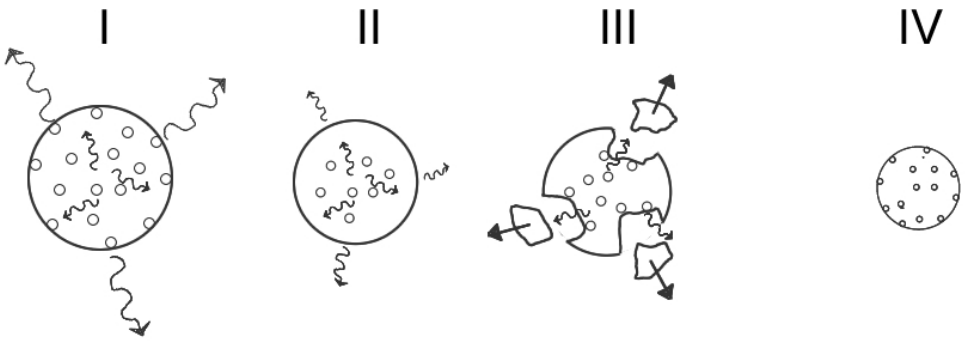

Figure 39. First there is constant evaporation from the surface called constant drying-rate period (I), During the constant drying-rate period the granules are also shrinking as water is replaced by crystal bridges. At a point the evaporation decreases from the surface, this is called falling drying-rate period (II), when the surface is completely dry fragile surface layer breaks off (III) and granules are now clearly reduced in size (IV). In the last part of drying the moisture content is constant in the granules, this is called equilibrium period. Waved arrows indicate evaporation and solid arrows indicates motion. Water molecules are symbolized with small spheres.

When the particle size of the granules is decreasing, the baseline of the NIR spectra shifts towards lower absorption values. A simple plot of the absorbance value of a single wavenumber, where water was not absorbing, was capable of showing the trends in the particle size (Figure 40). The rapid decrease of the particle size (point III in Figure 40) is known by the Novo operators and the trajectory of this absorption band was reproducible and characteristic in all drying batches monitored with NIR.

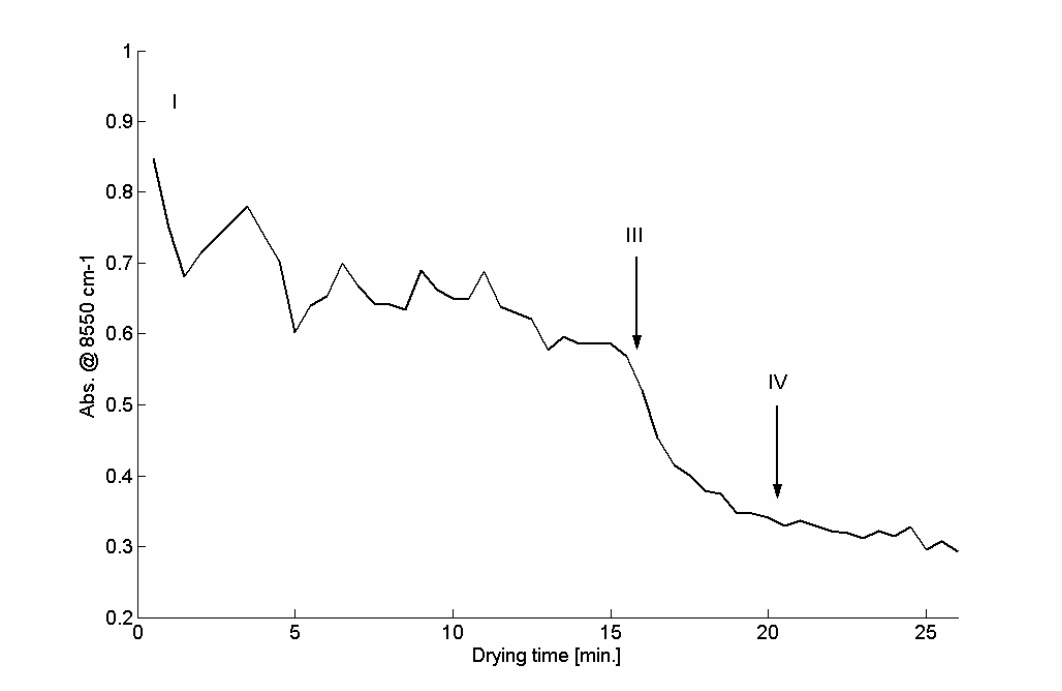

Figure 40. The absorbance @ 8550 cm^{-1} vs. drying time of DoE batch #10. The roman numbers indicates different distinct changes in the particle size (see Figure 39).

As mentioned previously, water is present as monohydrate and free water. When the 2nd order derivative spectrum is obtained, the water peak in the 1st overtone region is split into two peaks[70]. At 5172 cm^{-1} is the water present as monohydrate absorbing, while at 5253 cm^{-1} is the free water absorbing. In Figure 41 are the 2nd derivative of two spectra from the start and end of a drying process depicted. The free water peak is decreasing during drying while the monohydrate water peak increases. This is most likely because there is a large size reduction of the granules during the drying phase and the effective sample size represented in the NIR spectrum is increasing. When the regression vector for the quantitative PLS model was scrutinized it was discovered that it had a primary and sharp peak at 5253 cm^{-1}. Thus, the correlation between the spectra and offline LOD was dominated by the change in free water and not monohydrate water.

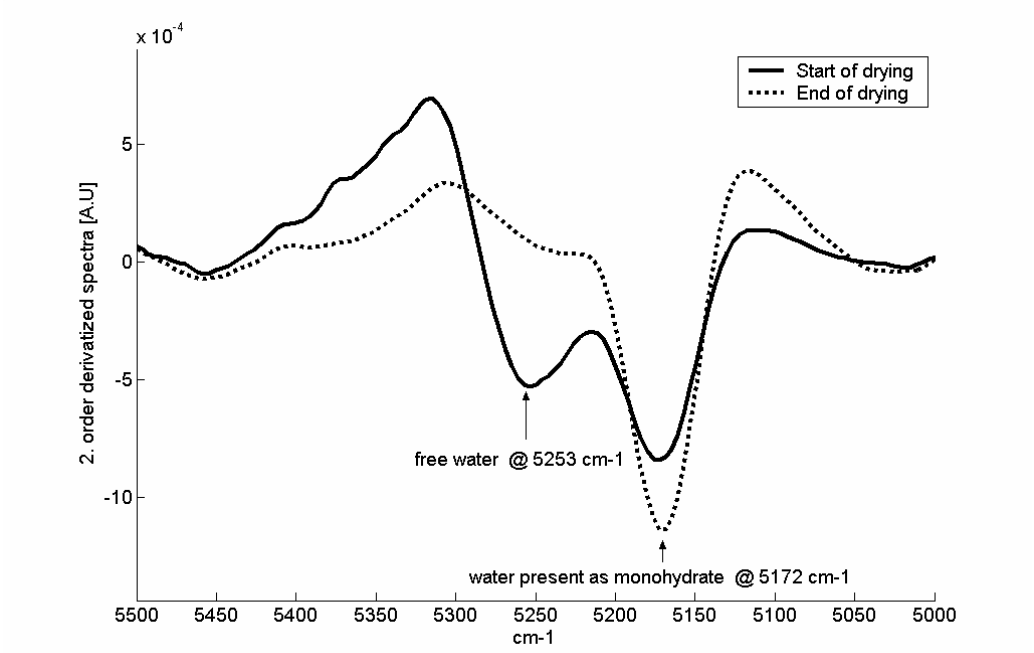

Figure 41. 2nd order derivative NIR spectrum of the water peak in first over tone region. The free water is absorbing at 5253 cm^{-1} and the bound water (monohydrate) is absorbing at 5172 cm^{-1}.

By plotting the ratio of the absorbance values at 5172 cm^{-1} and 5253 cm^{-1}, the different drying phases could be identified. This was illustrated for the same batch as depicted in Figure 40. The ratio and the LOD predicted by the regression model are plotted in the same figure. The ratio curves did always show that same trajectory. During the constant drying rate period, the ratio did not change much and the ratio curve was only increasing slightly. When the drying enters the falling drying rate period, the ratio curve starts to increase more and at a certain moment there is a rapid increase to a high positive value and then a large drop to a large negative value and then the ratio increases to a smaller negative value and flattens out again during the equilibrium period of the drying.

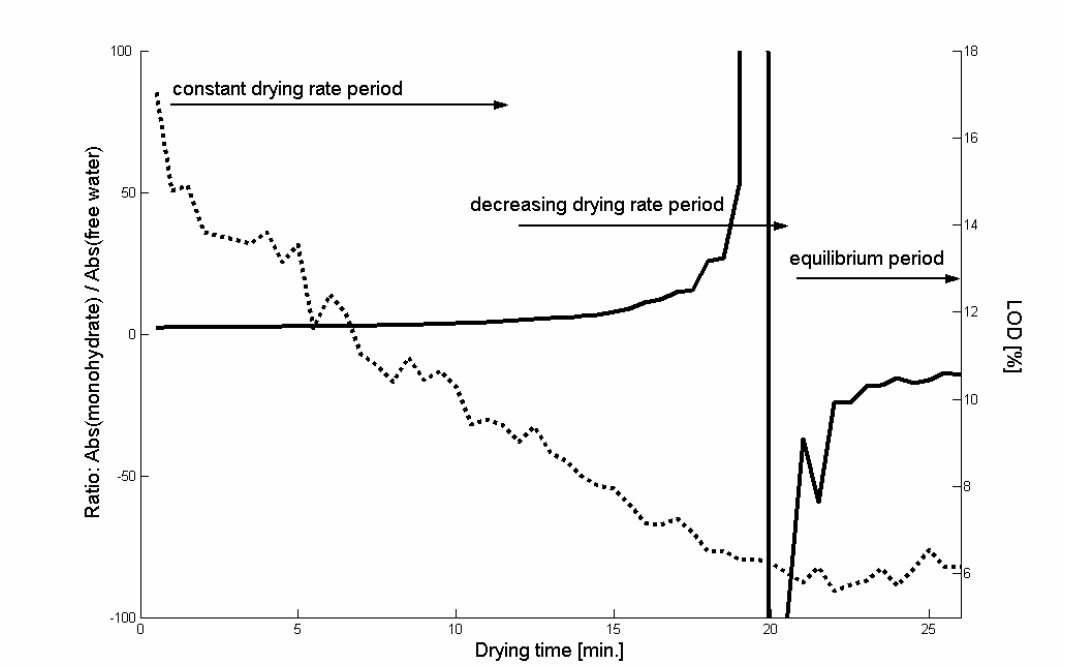

Figure 42. The ratio between absorbance @ 5172 cm^{-1} and absorbance @ 5253 cm^{-1} is plotted (solid line, left y-axis) vs. time for the same batch as depicted in Figure 40. The LOD predictions by the PLS model are also plotted vs. time (dotted line, right y-axis).

The two alternative examples of using the in-line NIR spectra recorded during drying ads to the possibilities of monitoring, understanding and controlling the drying process.

Use of NIR in high shear granulators

One of the processes that were used in the project was wet granulation in a high shear mixer. It was discovered how NIR in conjunction with a statistical model could be used to identify batches that would have future quality problems. It would also be of great interest to see if process control could be applied and these quality problems avoided. A mini experiment was conducted in the beginning of the project, to explore the possibilities with NIR measurements performed during high shear wet granulation. Three batches were made using the same formulation but with different process settings. From each batch, six to eight samples were removed during granulation and measured with reflectance

NIR. A PCA model with two principal components was fitted to the offset corrected spectra. In the scoreplot, it was clear that each process had its unique trajectory i.e. the process settings influenced the granules in a way that could be discriminated with NIR. When inspecting the offset corrected spectra the granule growth was also apparent in the spectra. Because the process settings were not done in a designed way it was not possible to clearly say what causes the differences, only that differences was observed with NIR.

Table 11. Experimental details for mini experiment with high shear granulation and NIR.

	Process setting	LOW	TARGET	HIGH
Dry blending step	Time	0.5 min	1 min	2 min
	Impellar speed	750 rpm	1000 rpm	1250 rpm
	Chopper speed			
Granulation step	Time	3 min	4 min	5 min
	Impellar speed	1000 rpm	2000 rpm	3000 rpm
	Chopper speed	1000 rpm	1500 rpm	1800 rpm
After granulation step	Time	0.5 min	1 min	2 min
	Impellar speed	3000 rpm	3000 rpm	3000 rpm
	Chopper speed	1500 rpm	1500 rpm	1500 rpm

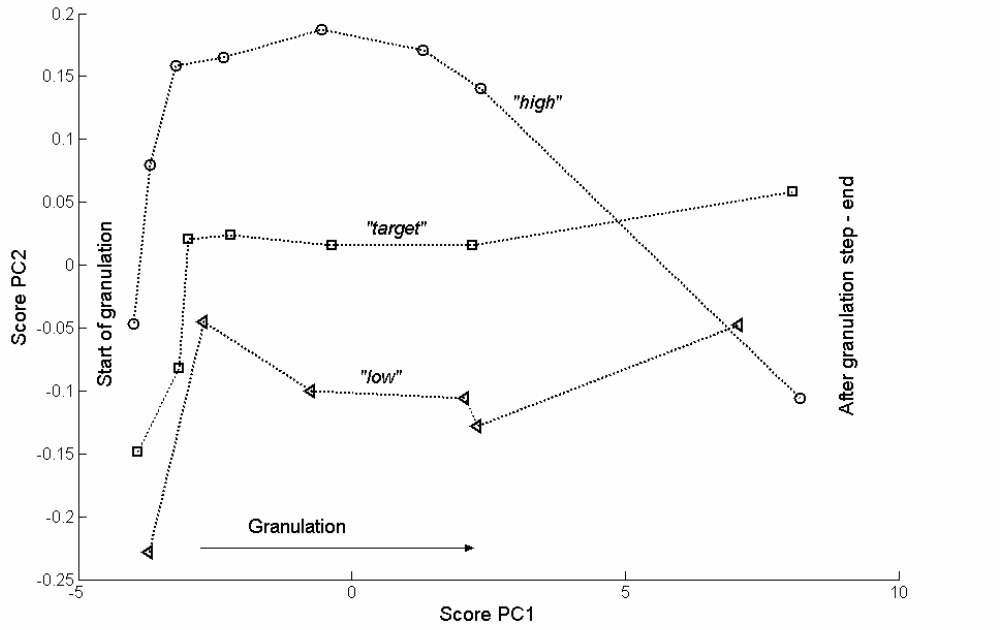

Figure 43. Scoreplot of PC1 vs. PC2 from PCA model of NIR spectra from samples obtained from three high shear granulation processes with different process settings. Each symbol indicates a measurement.

The spectra from the 'target' experiment were offset corrected at 12000 cm^{-1}. The corrected spectra are depicted in Figure 44. As the granulation is going on there is an increase in the water band absorption around 5200 and 7100 cm^{-1} which comes from the added granulation liquid. There is also a general increase in the absorption of the entire spectra which can be caused by the increasing particle size i.e. granule growth. This result was not validated and further research will be invested into how NIR can be used to monitor and control the high shear granulation process.

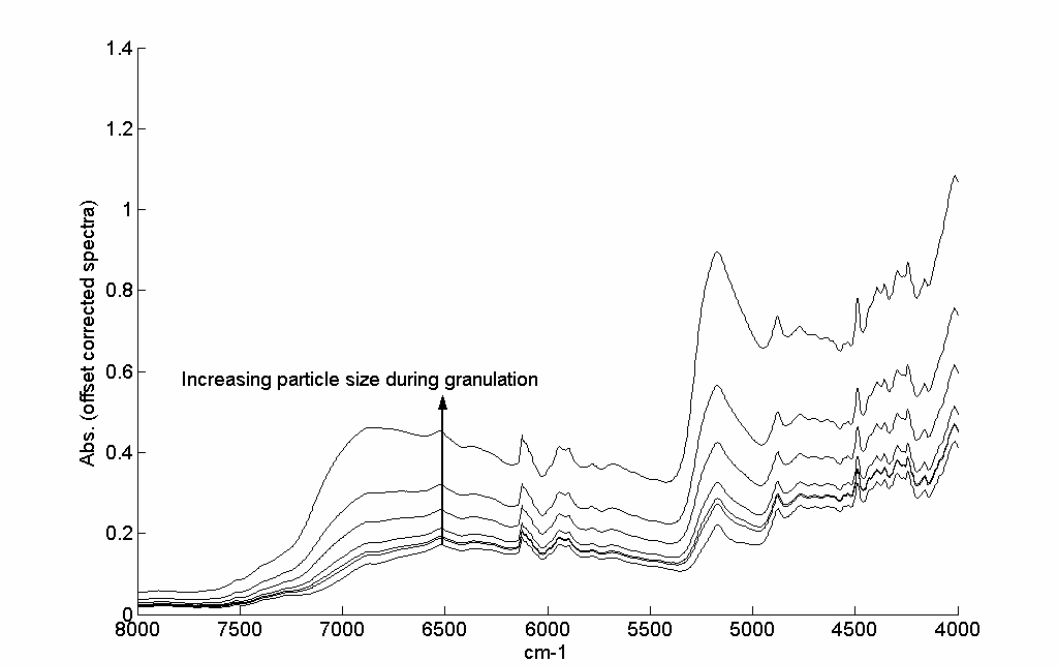

Figure 44. Offset corrected spectra from TARGET granulation process.

NIR imaging

An emerging PAT technique is NIR imaging[95]. In conventional NIR spectroscopy is the sample analyzed by one NIR spectrum e.g. a reflection spectrum from a surface scan of a tablet sample. In NIR imaging is the spectroscopy combined with imaging technology. There exists a wealth of different NIR imaging systems but the basic principle is the same. The sample is illuminated with a light source and after interaction with the sample transferred to an array of detectors instead of a single element detector. Each detector element in the array detector is

arranged adjacent to each other like pixels in a picture. In each 'pixel' is a spectrum measured and the resulting data file is often referred to as a hyper spectral data cube. In Figure 45 represents X and Y coordinates on the surface of the sample and λ a wavelength number; together they form a data cube. With different algorithms[96-99] can the data cube be transformed into chemical images where the spatial distribution of the various chemical components in e.g. a tablet surface can be exposed. Chemical imaging technology is a very powerful analysis tool to extract process-related information from the sample[100]. The technique can be used for both at-line quality control and more elaborate root-cause investigations when facing manufacturing problems. And recently has NIR imaging also been tested in-line with instruments mounted directly on powder blending equipment.

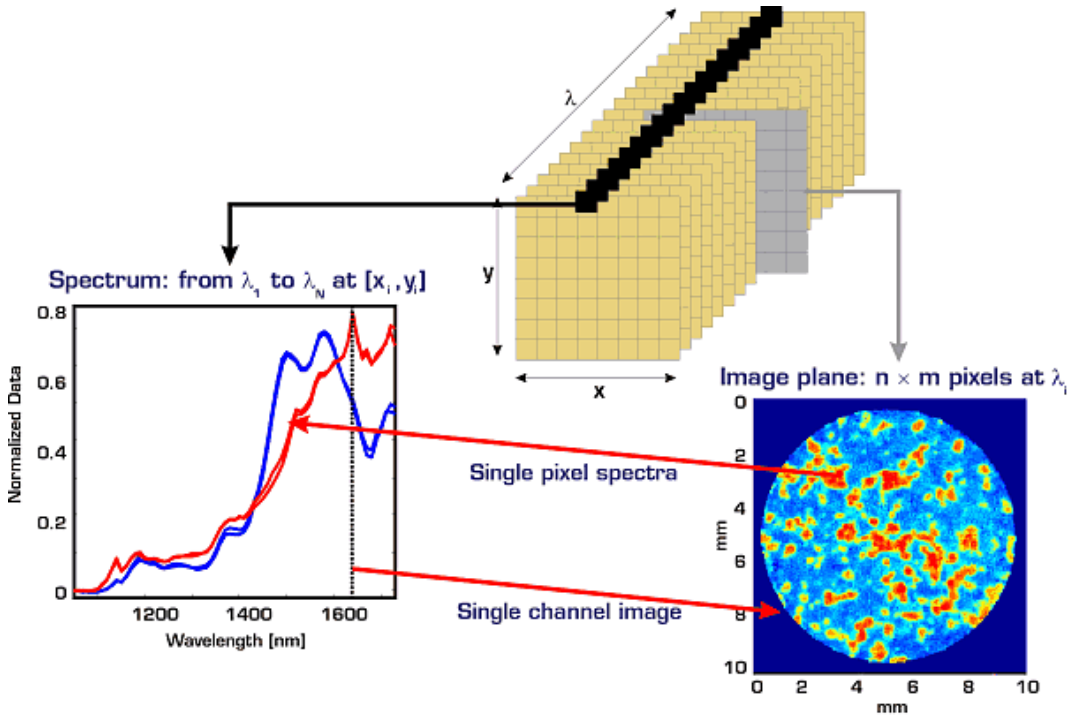

Figure 45. Schematic presentation of hyper spectral data cube (source: www.spectraldimensions.com).

One tablet from each of the three DoE batches #3, #7 and #8 (see Table 7 on page 44) were analyzed with reflectance NIR imaging by Spectral Dimensions. The images were recorded with a Sapphire NIR Chemical Imaging System from Spectral Dimensions. Spectral Dimensions also performed the data analysis. The spectral range was 1200 to 2400 nm. The instrument has a focal plane InSb, Stirling cooled detector with 320 x 256 pixels. A magnification level was used so each pixel represented a 28 x 28 µm square on the sample surface. This means that the field of view (area sampled on tablet surface) was 8960 x 7168 µm or each picture was approximately a 9 x 7.2 mm square of the tablet surface. A series of compressed tablets of the pure constituents in the tablet formulation were also analyzed with the imaging system. These where used to make a 'calibration' library.

First a picture called 'API Domains Binary Images' was made for each tablet image. At 1680 nm was a peak from the API dominating the NIR spectrum. By calculation of the intensity of the 1680 nm band at each image pixel, the pixel was assigned either the value 1 (classified as 'API pixel') or 0 (classified as 'something else pixel'). The resulting binary images represent API domains (clusters of pixels of high API concentration). By applying the domain clusters to different statistical analysis it was concluded;

- API domains are more evenly distributed in the tablet from the DoE #8 batch than in other tablets (seems more homogeneous).
- Variance in API domain size is less in the tablet from DoE #8 batch than in other tablets (less clumping).
- API domains are smaller in the tablet from DoE #8 than in other tablets.

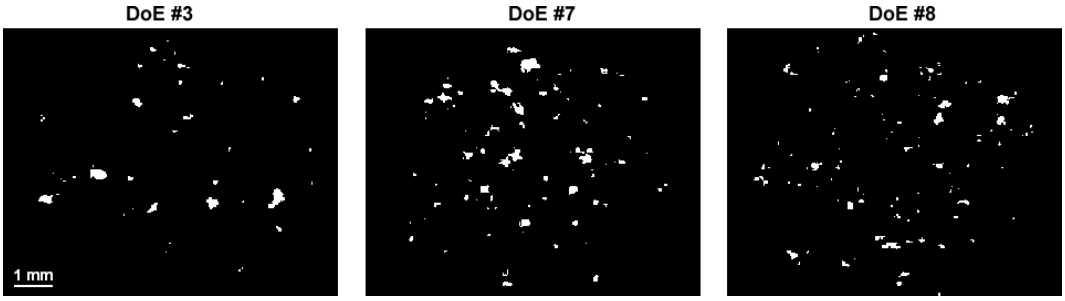

Figure 46. API domain binary images of tablet surfaces. API dominated pixels are white.

When comparing these results with the conventional NIR analysis of the API content of tablets, it was interesting to note that also the conventional NIR analysis find that the DoE #8 batch seems to be the most homogeneous (see Table 10 on page 74) of these three batches.

An interesting research topic would be to compare the API homogeneity on different scales tablet vs. entire batch.

Second a multi colour picture presenting the spatial distribution of the major tablet components was made for each tablet using PLS models with library spectra. The chemical image for the tablet from DoE #3 appeared very different to the tablets from the two other batches. The DoE #3 batch also had some distinct different batch quality characteristics compared to the two other batches. The dried granules from DoE #3 batch were significantly larger then the other DoE batches. This batch was the val_2 batch with quality problems in the example with MSPC monitoring (see example on page 45). Secondly was the average required punch force during tabletting 13 kN for the DoE #3 batch and 8.7 kN and 9 kN for the DoE #7 and DoE #8 batches respectively.

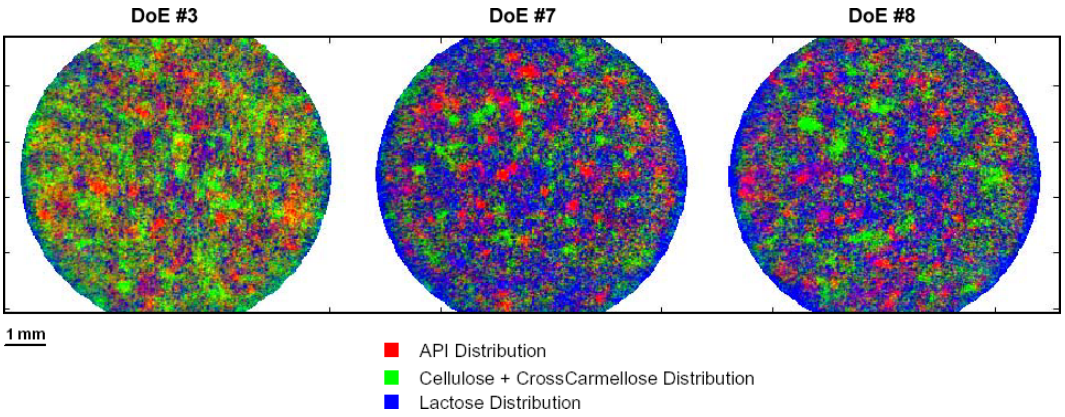

Figure 47. Multi colour images showing spatial distribution of major components in tablet surfaces. Red colour pixels represent API, green colour pixels represent cellulose+crosscarmellose and blue colour pixels represent lactose.

Novo will start research on how to extract process information from NIR images of tablet surfaces, which hopefully will facilitate better choices for formulation and processes. Secondly, the technology might be very helpful in up-scaling of processes and for trouble shooting of manufacturing problems.

REFERENCES

1. Schott, J. R., *Matrix Analysis for Statistics*, JOHN WILEY & SONS, INC 1997.

2. American Food and Drug Administration (FDA), Guidance for Industry PAT - A framework for innovative pharmaceutical development, manufacturing and quality assurance. 2004.

3. Leila Abboud and Scott Hensley. New prescription for drug makers: update the plants. *The Wall Street Journal* . 3-9-2003.

4. Skibsted, E. T. S., Westerhuis, J. A., Boelens, H. F., Smilde, A. K., and Witte, D. T.. A New Indicator for Optimal Preprocessing and Wavelengths Selection of Near-Infrared Spectra. *Applied Spectroscopy* 58[3], 264-271. 2004.

5. Skibsted, E. T. S., Boelens, H. F., Westerhuis, J. A., Witte, D. T., and Smilde, A. K.. Simple Assesment of Homogeneity in Pharmaceutical Mixing Processes Using a Near-Infrared Reflectance Probe and Control Charts. *Journal of Pharmaceutical and Biomedical Analysis* submitted. 2005.

6. Skibsted, E. T. S., Boelens, H. F., Westerhuis, J. A., Smilde, A. K., Broad, N. W., Rees, D. R., and Witte, D. T.. Net Analyte Signal Based Statistical Quality Control (NAS-SQC). *Analytical Chemistry* in press. 2005.

7. Skibsted, E. T. S., Westerhuis, J. A., and Smilde, A. K.. Examples of NIR based Real Time Release in Tablet Manufacturing. *Journal of Pharmaceutical and Biomedical Analysis* submitted. 2005.

8. Skibsted, E. T. S., Westerhuis, J. A., Smilde, A. K., and Witte, D. T.. A Theoretical Framework for Real Time Release of Pharmaceutical Products. *NIRNews* submitted. 2005.

9. International Conference on Harmonisation (ICH). Draft consensus guideline Quality Risk Management Q9. 2005.

10. Raju, G. K.. White paper: New Opportunities in Pharmaceutical Manufacturing. *http://www.pharmamanufacturing.com/whitepapers/2004/118.html* . 2001.

11. Borer, M. W., Zhou, X., Hays, D. M., Hofer, J. D., and White, K. C.. Evaluation of key sources of variability in the measurement of pharmaceutical drug products by near infrared reflectance spectroscopy. *Journal of Pharmaceutical and Biomedical Analysis* 17, 641-650. 1998.

12. Geladi, P., McDougall, D., and Martens, H.. Multiplicative Signal Correction. *Applied Spectroscopy* 39, 491-500. 1985.

13. Savitzky, A. and Golay, M. J. E.. *Analytical Chemistry* 36, 1627-1639. 1964.

14. Barnes, R. J., Dhanoa, M. S., and Lister, S. J.. Standard normale variate and de-trending of near-infrared diffuse reflectance spectra. *Applied Spectroscopy* 43[5], 772-777. 1989.

15. Martens, H., Nielsen, J. P., and Engelsen, S. B.. Light Scattering and Light Absorbance Separated by Extended Multiplicative Signal Correction. Application to Near-Infrared Transmission Analysis of Powder Mixtures. *Analytical Chemistry* **75**, 394-404. 2003.

16. Wold, S., Antti, H., Lindgren, F., and Öhman, J.. Orthogonal signal correction of near-infrared spectra. *Chemometrics and Intelligent Laboratory Systems* 44, 175-185. 1998.

17. Hansen, P. W.. Pre-processing method minimizing the need for reference analyses. *Journal of Chemometrics* 15, 123-131. 2001.

18. Nřrgaard, L., Saudland, A., Wagner, J., Nielsen, J. P., Munck, L., and Engelsen, S. B.. Interval partial least-squares regression (iPLS): A new comparative chemometric study with an example from near-infrared spectroscopy. *Applied Spectroscopy* 54[3], 413-419.

19. Smith, B. M. and Gemperline, P. J.. Wavelength selection and optimization of pattern recognition methods using the genetic algorithm. *Analytica Chimica Acta* 423, 167-177. 2000.

20. Abrahamsson, C., Johansson, J., Sparén, A., and Lindgren, F.. Comparison of different variable selection methods conducted on NIR transmission measurements on intact tablets. *Chemometrics and Intelligent Laboratory Systems* 69, 3-12. 2003.

21. Xu, L. and Schechter, I.. Wavelength Selection for Simultaneous Spectroscopic Analysis. Experimental and Theoretical Study. *Analytical Chemistry* 68, 2392-2400. 1996.

22. Lorber, A.. Error Propagation and Figures of Merit for Quantification by Solving Matrix Equations. *Analytical Chemistry* 58, 1167-1172. 1986.

23. Faber, N. M.. Multivariate Sensitivity for The Interpretation of The Effect of Spectral Pretreatment Methods on Near-Infrared Calibration Model Predictions. *Anal.Chem* 71, 557-565. 1999.

24. Xu, L. and Schechter, I.. Wavelength Selection for Simultaneous Spectroscopic Analysis. Experimental and Theoretical Study. *Analytical Chemistry* 68, 2392-2400. 1996.

25. Boelens, H. F., Kok, W. T., de Noord, O. E., and Smilde, A. K.. Performance Optimization of Spectroscopic Process Analyzers. *Analytical Chemistry* 76, 2656-2663. 2004.

26. Skibsted, E. T. S., Westerhuis, J. A., Boelens, H. F., Smilde, A. K., and Witte, D. T.. A New Indicator for Optimal Preprocessing and Wavelengths

Selection of Near-Infrared Spectra. *Applied Spectroscopy* 58[3], 264-271. 2004.

27. H.G.Kristensen, *Almen farmaci*, 3 ed., Department of Pharmacy, The Danish University of Pharmaceutical Sciences 2004.

28. Railkar, A. M. and Schwartz, J. B.. Evaluation and Comparison of a Moist Granulation Technique to Conventional Methods. *Drug Development and Industrial Pharmacy* 26[8], 885-889. 2000.

29. Faure, A., York, P., and Rowe, R. C.. Process control and scale-up of a pharmaceutical wet granulation processes: a review. *Euopean Journal of Pharmaceutics and Biopharmaceutics* 52, 269-277. 2001.

30. Christina Gustafsson. Solid State Characterisation and Compaction Behavious of Pharmaceutical Materials. 2000. Faculty of Pharmacy, Uppsala University.

31. Cooper, J. B.. Chemometric analysis of Raman spectroscopic data for process control applications. *Chemometrics and Intelligent Laboratory Systems* 46, 231-247. 1999.

32. Furusjö, E., Danielsson, L. G., Könberg, E., Rentsch-Jonas, M., and Skagerberg, B.. Evaluation techniques for two-way data from in situ Fourier transform mid-infrared reaction monitoring in aqueous solution. *Analytical Chemistry* 70, 1726-1734. 1998.

33. LeBlond, C., Wang, J., Larsen, R., Orella, C., and Sun, Y.-K.. A combined approach to characterization of catalytic reactions using in insitu kinetic probes. *Topics in Catalysis* 5, 149-158. 1998.

34. Stordrange, L., Libnau, F. O., Malthe-Sřrenssen, D., and Kvalheim, O. M.. Feasability study of NIR for surveillance of a pharmaceutical process, including a study of different preprocessing techniques. *Journal of Chemometrics* 16, 529-541. 2002.

35. Heath, A. R., Fawell, P. D., Bahri, P. A., and Swift, J. D.. Estimating average particle size by focused beam reflectance measurement (FBRM). *Particle and Particle System Characterization* 19, 84-95. 2002.

36. Furusjö, E., Danielsson, L. G., Könberg, E., Rentsch-Jonas, M., and Skagerberg, B.. Evaluation techniques for two-way data from in situ Fourier transform mid-infrared reaction monitoring in aqueous solution. *Analytical Chemistry* 70, 1726-1734. 1998.

37. Whitaker, M., Baker, G. R., Westrup, J., Goulding, P. A., Rudd, D. R., Belchamber, R. M., and Collins, M. P.. Application of acoustic emission to the monitoring and end point determination of a high shear granulation process. *International Journal of Pharmaceutics* 205, 79-91. 2000.

38. Weyer, L. G., Yee, D., Pearson, G. I., and Wade, J.. Installation of multiplexed Raman system in a chemical process. *Applied Spectroscopy* 58[12], 1500-1505. 2004.

39. Vaccari, G., Tamburini, E., Tosi, G., Sgualdino, G., and Bernadi, T.. In-line control and automatic management of industrial crystallizations using NIR technique. *Chemical Engineering and Technology* 26[3], 273-276. 2003.

40. Fujiwara, M., Chow, P. S., Ma, D. L., and Braatz, R. D.. Paracetamol crystallization using laser backscattering and ATR-FTIR spectroscopy: Metastability, agglomoration, and control. *Crystal Growth & Design* 2[5], 363-370. 2002.

41. Falcon, J. A. and Berglund, K. A.. In situ monitoring of antisolvent addition crystallization with principal component analysis of raman spectra. *Crystal Growth & Design* 4[3], 457-463. 2004.

42. Févotte, G., Calas, J., Puel, F., and Hoff, C.. Applications of NIR spectroscopy to monitoring and analyzing the solid state during industrial

crystallization processes. *International Journal of Pharmaceutics* 273, 159-169. 2004.

43. LeBlond, C., Wang, J., Larsen, R., Orella, C., and Sun, Y.-K.. A combined approach to characterization of catalytic reactions using in insitu kinetic probes. *Topics in Catalysis* 5, 149-158. 1998.

44. Lawrence X.Y., Lionberger, R. A., Raw, A. S., D'Costa, R., Wu, H., and Hussain, A. S.. Applications of Process Analytical Technology to Crystallization Processes. *www.fda.gov/cder/OPS/patcrystalSub.pdf* . 2003.

45. Popo, M., Romero-Torres, S., Conde, C., and Romańach, R. J.. Blend uniformity analysis using stream sampling and near infrared spectroscopy. *AAPS PharmSciTech* 2[3]. 2002.

46. Ufret, C. and Morris, K.. Modeling of powder blending using on-line near-infrared measurements. *Drug Development and Industrial Pharmacy* 27[7], 719-729. 2001.

47. Hailey, P. A., Doherty, P., Tapsell, P., Oliver, T., and Aldridge, P. K.. Automated systems for the on-line monitoring of powder blending processes using near-infrared spectroscopy: Part I. System development and control. *Journal of Pharmaceutical and Biomedical Analysis* 14, 551-559. 1996.

48. Sekulic, S. S., Ward, H. W., II, Brannegan, D. R., Stanley, E. D., Evans, C. L., Sciavolino, S. T., Hailey, P. A., and Aldridge, P. K.. On-line monitoring of powder blend homogeneity by near-infrared spectroscopy. *Analytical Chemistry* 68, 509-513. 1996.

49. El-Hagrasy, A. S., Morris, H. R., D'Amico, F., Lodder, R. A., and Drennen J.K.. Near-infrared spectroscopy and imaging for the monitoring of powder

blend homogeneity. *Journal of Pharmaceutical sciences* 90[9], 1298-1307. 2001.

50. Chen, Y., Thosar, S. S., Forbess, R. A., Kemper, M. A., Rubinovitz, R. L., and Shukla, A. J.. Prediction of drug content and hardness of intact tablets using artificial neural network and near-infrared spectroscopy. *Drug Development and Industrial Pharmacy* 27[7], 623-631. 2001.

51. Donoso, M., Kildsig, D. O., and Ghaly, E. S.. Prediction of tablet hardness and porosity using near-infrared diffuse reflectance spectroscopy as a nondestructive method. *Pharmaceutical Development and Technology* 8[4], 357-366. 2003.

52. Han, S. M. and Faulkner, P. G.. Determination of SB 216469-S during tablet production using near-infrared reflectance spectroscopy. *Journal of Pharmaceutical and Biomedical Analysis* 14, 1681-1689. 1996.

53. Eustaquio, A., Graham, P., Jee, R. D., Moffatt, A. C., and Trafford, A. D.. Quantification of paracetamol in intact tablets using near-infrared transmittance spectroscopy. *Analyst* 123, 2303-2306. 1998.

54. Griffiths, P. R., "Beer's law," *Handbook of Vibrational Spectroscopy Volume 3*, edited by J. M. Chalmers and P. R. Griffiths Wiley, 2002, pp. 2225-2234.

55. Andersson, M., Josefson, M., Langkilde, F. W., and Wahlund, K.-G.. Monitoring of film coating process for tablets using near-infrared reflectance spectrometry. *Journal of Pharmaceutical and Biomedical Analysis* 20, 27-37. 1999.

56. Andersson, M., Folestad, S., Gottfries, J., Johansson, M. O., Josefson, M., and Wahlund, K.-G.. Quantitative analysis of film coating in a fluidized bed process by in-line NIR spectrometry and multivariate batch calibration. *Analytical Chemistry* 72, 2099-2108. 2000.

57. Aldridge, P. K., Mushinsky, R. F., Andino, M. M., and Evans, C. L.. Identification of tablet formulations inside blister packages be near-infrared spectroscopy. *Applied Spectroscopy* 48[10], 1272-1276. 1994.

58. Barrett, P. and Glennon, B.. In-line FBRM monitoring of particle size in dilute agitated suspensions. *Particle and Particle System Characterization* 16, 207-211. 1999.

59. Dempster, M. A., MacDonald, B. F., Gemperline, P. J., and Boyer, N. R.. A near-infrared reflectance analysis method for the noninvasive identification of film-coated and non-film-coated, blister-packed tablets. *Analytica Chimica Acta* 310, 43-51. 1995.

60. Badawy, S. F., Menning, M. M., Gorko, M. A., and Gilbert, D. L.. Effect of process parameters on compressibility of granulation manufactured in a high-shear mixer. *International Journal of Pharmaceutics* 198, 51-61. 2000.

61. Bardin, M., Knight, P. C., and Seville, J. P. K.. On control of particle size distribution in granulation using high-shear mixers. *Powder Technology* 140, 169-175. 2004.

62. Blanco, M. and Serrano, D.. On-line monitoring and quantification of a process reaction by near-infrared spectroscopy. Catalysed esterification of butan-1-ol by acetic acid. *Analyst* 125, 2059-2064. 2000.

63. Faure, A., York, P., and Rowe, R. C.. Process control and scale-up of a pharmaceutical wet granulation processes: a review. *Euopean Journal of Pharmaceutics and Biopharmaceutics* 52, 269-277. 2001.

64. Corvari, V., Fry, W. C., Seibert, W. L., and Augsburger, L.. Instrumentation of a high-shear mixer: evaluation and comparison of a new capacitive sensor, a watt meter, and a strain-gage torque sensor for wet granulation monitoring. *Pharmaceutical Research* 9[12], 1525-1533. 1993.

65. Watano, S., Numa, T., Koizumi, I., and Osako, Y.. Feedback control in high shear granulation of pharmaceutical powders. *European Journal of Pharmaceutics and Biopharmaceutics* 52, 337-345. 2001.

66. Whitaker, M., Baker, G. R., Westrup, J., Goulding, P. A., Rudd, D. R., Belchamber, R. M., and Collins, M. P.. Application of acoustic emission to the monitoring and end point determination of a high shear granulation process. *International Journal of Pharmaceutics* 205, 79-91. 2000.

67. Otsuka, M., Mouri, Y., and Matsuda, Y.. Chemometric evaluation of pharmaceutical properties of Antipyrine granules by near-infrared spectroscopy. *AAPS PharmSciTech* 4[3], 1-7. 2003.

68. Rantanen, J., Antikainen, O., Mannermaa, J.-P., and Yliruusi, J.. Use of the near-infrared reflectance method for measurement of moisture content during granulation. *Pharmaceutical Development and Technology* 5[2], 209-217. 2000.

69. Rantanen, J., Wikström, H., Turner, R., and Taylor, L. S.. Use of in-line near-infrared spectroscopy in combination with chemometrics for improved understanding of pharmaceutical processes. *Analytical Chemistry* 77, 556-563. 2005.

70. Zhou, G. X., Gi, Z., Dorwart, J., Izzo, B., Kukura, J., Bicker, G., and Wyvratt, J.. Determination and differentiation of surface and bound water in drug substances by near infrared spectroscopy. *Journal of Pharmaceutical sciences* 92[5], 1058-1065. 2002.

71. Dziki, W., Bauer, J. F., Szpylman, J. J., Quick, J. E., and Nichols, B. C.. The use of near-infrared spectroscopy to monitor the mobility of water within the sarafloxacin crystal lattice. *Journal of Pharmaceutical and Biomedical Analysis* 22, 829-848. 2000.

72. Ufret, C. and Morris, K.. Modeling of powder blending using on-line near-infrared measurements. *Drug Development and Industrial Pharmacy* 27[7], 719-729. 2001.

73. Frake, P., Greenhalgh, D., Grierson, S. M., Hempenstall, J. M., and Rudd, D. R.. Process control and end-point determination of a fluid bed granulation by application of near infra-red spectroscopy. *International Journal of Pharmaceutics* 151, 75-80. 1997.

74. Committee for Proprietary Medicinal Products (CPMP), EMEA. Note for Guidance on Parametric Release. 2001.

75. *NIST/SEMATECH e-Handbook of Statistical Methods*. *NIST* . 2005.

76. Westerhuis, J. A., Gurden, S. P., and Smilde, A. K.. Generalized contribution plots in multivariate statistical process monitoring. *Chemometrics and Intelligent Laboratory Systems* 51, 95-114. 2000.

77. Jackson, J. E., *A User's Guide to Principal Components*, John Wiley & Sons, New York, 1991.

78. Nomikos, P. and MacGregor, J. F.. Multiway partial least squares in monitoring batch processes. *Chemometrics and Intelligent Laboratory Systems* 30, 97-108. 1995.

79. Box, G. E. P. and Kramer, T.. Statistical process monitoring and feedback adjustment-a discussion. *Technometrics* 34[3], 251-285. 1992.

80. Jřrgensen, K. and Nćs, T.. A design and analysis strategy for situations with uncontrolled raw material variation. *Journal of Chemometrics* 18, 45-52. 2004.

81. Gustafsson, C., Nyström, C., Lennholm, H., Bonferoni, M. C., and Caramella, C. M.. Characteristics of Hydroxypropyl Methylcellulose Influencing Compactibility and Prediction of Particle and Tablet Properties

by Infrared Spectroscopy. *Journal of Pharmaceutical sciences* 92[3], 460-470. 2003.

82. Westerhuis, J. A. and Coenegracht, P. M. J.. Multivariate modelling of the pharmaceutical two-step process of wet granulation and tableting with multiblock partial least-sqaures. *Journal of Chemometrics* 11, 379-392. 1997.

83. Wold, S., Sjöström, M., and Eriksson, L.. PLS-regression: a basic tool of chemometrics. *Chemometrics and Intelligent Laboratory Systems* 58, 109-130. 2001.

84. Smilde, A. K., Westerhuis, J. A., and Boqué, R.. Multiway multiblock component and covariates regression models. *Journal of Chemometrics* 14, 301-331. 2000.

85. Bro, R.. Multiway Calibration. Multilinear PLS. *Journal of Chemometrics* 10, 47-61. 1996.

86. Gustafsson, C., Lennholm, H., and Nyström, C.. Evaluation of Surface and Bulk Characteristics of Cellulose I Powders in Relation to Compaction Behavior and Tablet Properties. *Drug Development and Industrial Pharmacy* 29[10], 1095-1107. 2003.

87. Pottmann, M., Ogunnaike, B. A., Adetayo, A. A., and Ennis, B. J.. Model-based control of a granulation system. *Powder Technology* 108, 192-201. 2000.

88. Bardin, M., Knight, P. C., and Seville, J. P. K.. On control of particle size distribution in granulation using high-shear mixers. *Powder Technology* 140, 169-175. 2004.

89. Korhonen, O., Pohja, S., Peltonen, S., Suihko, E., Vidgren, M., Paronen, P., and Ketolainen, J.. Effects of Physical Properties for Starch Acetate Powders on Tableting. *AAPS PharmSciTech* **3**[**4**]. 2002.

90. Berggren, J. and Alderborn, G.. Effect of drying rate on porosity and tabletting behaviour of cellulose pellets. *International Journal of Pharmaceutics* 227, 81-96. 2001.

91. Vázquez, E. R.. Optimization of Drying-End-Points Measurements for the Automation of a Fluidized-Bed Dryer Using FT-NIR Spectroscopy. 2004. CHEMICAL ENGINEERING, UNIVERSITY OF PUERTO RICO, MAYAGÜEZ CAMPUS.

92. Wang, Z. H. and Chen, G.. Heat and mass transfer in batch fluidized-bed drying of porous particles. *Chemical Engineering Science* 55, 1857-1869. 2000.

93. Hlinak, A. J. and Saleki-Gerhardt, A.. An evaluation of fluid bed drying of aqueous granulations. *Pharmaceutical Development and Technology* 5[1], 11-17. 2000.

94. Badawy, S. F., Menning, M. M., Gorko, M. A., and Gilbert, D. L.. Effect of process parameters on compressibility of granulation manufactured in a high-shear mixer. *International Journal of Pharmaceutics* 198, 51-61. 2000.

95. Lewis, N. E., Schoppelrei, J., and Lee, E.. Near-Infrared Chemical Imaging and the PAT Initative. *Spectroscopy* 19[4]. 2004.

96. Geladi, P., Isakson, H., Lindquist, L., Wold, S., and Esbensen, K.. Principal Component Analysis of Multivariate Images. *Chemometrics and Intelligent Laboratory Systems* 5, 209-220. 1989.

97. Geladi, P. and Esbensen, K. H.. Regression on multivariate images: principal component regression for modeling, prediction and visual diagnostic tools. *Journal of Chemometrics* 5, 97-111. 1991.

98. Geladi, P. and Grahn, H., *Multivariate image analysis*, John Wiley & Sons, Chichester, 1996.

99. Geladi, P., Wold, S., and Esbensen, K. H.. Image analysis and chemical information in images. *Analytica Chimica Acta* 191, 473-480. 1986.

100. Clarke, F.. Extracting process-related information from pharmaceutical dosage forms using near infrared microscopy. *Vibrational Spectroscopy* 34, 25-35. 2004.

SUMMARY IN ENGLISH, DANISH AND DUTCH

The interest and investments in PAT in pharmaceutical companies worldwide are fast increasing. Some of the drives are: the regulatory bodies point at PAT as the future backbone of the quality systems for pharmaceutical manufacturing and secondly the industry has started to realize the benefits of process monitoring and control. In this project has PAT been studied in the context of solid dosage form manufacturing. The use of near-infrared (NIR) spectroscopy has dominated the research as this technique is potentially the main analytical technique in solid dosage form. One obstacle in the use of NIR is the choice of a proper pre-processing method and wavelength selection of the spectra. The thesis presents a novel method to identify optimal parameters for these. In the solid dosage form manufacturing plays the mixing process a pivotal role when it comes to the uniform distribution of active pharmaceutical ingredient (API) in the finalized products. A new method to monitor and control the optimal homogeneous distribution of API in a powder mixing process using NIR and statistical control charts were also presented in the thesis. The NIR spectrum contains variance components from many sources e.g. all the constituents in the sample matrix absorbing in NIR and physical attributes like particle size differences. A new methodology named net analyte signal based statistical quality control (NAS-SQC) was developed. With NIR spectra of tablets and NAS-SQC it was demonstrated how several quality parameters could be monitored by one spectrum only. One of the appealing aspects of PAT is the ability of real time release i.e. the quality of the final drug product is assured continuously during manufacturing and further quality control is therefore not necessary when manufacturing is finished. In lack of real time release examples in the industry an overview of the different models which can be used in a real time release system is provided in chapter four. The fifth chapter then shows practical examples of the different model types.

Interessen og investeringerne i PAT I den farmaceutiske industri er stærkt stigende. Nogle af de forskellige motivations faktorer er: myndighederne peger på PAT som rygraden i fremtidens kvalitetssikring af farmaceutisk produktion desuden har større farma virksomheder begyndt at realisere fordelene ved proces monitorering og kontrol. I dette projekt er der blevet arbejdet med PAT i solid dosage form produktion. Der er primært fokuseret på anvendelsen af nær-infrarød spektroskopi (NIR) idet denne teknik potentielt set vil være en af de dominerende analytiske teknikker i solid dosage form produktion. En af forhindringerne i anvendelsen af NIR er at finde en god forbehandlings metode og foretage bølgelængde udvælgelse på spektrene. Denne afhandling præsenterer en ny metode til at identificere de bedste parametre. Under solid dosage form produktion er blande processen central når det kommer til drejer sig om at opnå en homogen distribution af det aktive lægemiddel (API) i det færdige produkt. En ny metode til at måle og kontrollere den optimal homogene fordeling af lægemiddel i en pulver blandings proces med NIR og statistiske kontrol kort præsenteres også i denne afhandling. NIR spektret indeholder varians komponenter fra mange kilder f.eks. alle indholds stofferne i prøve matricen der absorberer i NIR området og fysiske parametre som partikel størrelsen. En ny metode der kaldes for net analyte signal based statistical quality control (NAS-SQC) blev udviklet. Med et data sæt bestående af NIR spektre af tabletter blev det demonstreret hvordan adskillige kvalitets parametre kunne monitoreres med kun et spektrum. En interessant mulighed med PAT er real time release dvs. kvaliteten af produktet kontrolleres løbende under selve fremstillings processen således at slut kontrol overflødiggøres. Idet der mangler praktiske eksempler i industrien på real time release er der samlet en oversigt over de mulige model typer og deres anvendelse i et real time release system, dette præsenteres i kapitel fire. I kapitel fem demonstreres så de fremlagte model typer med praktiske eksempler fra en serie batch produktioner af tabletter.

De interesse en investeringen in PAT nemen wereldwijd toe. Een van de drijvende krachten zijn de regelgevers die PAT hebben aangewezen als het fundament voor kwaliteitssystemen in de farmaceutische productie. Een tweede, zijn de economische voordelen die procesmonitoren en procescontrole met zich meebrengen. In dit project is gekeken naar PAT in combinatie met het doseren van vaste stoffen. Nabij infrarood (NIR) speelt een dominante rol in dit onderzoek omdat dit een van de meeste gebruikte technieken is voor gebruik in dit soort toepassingen. Een van de nadelen van NIR is het selecteren van golflengten en het voorbewerken van spectra. Dit proefschrift presenteert een nieuwe methode om de optimale parameters te vinden. In de productie van vaste stoffen speelt het mengen en mixen een centrale rol. Met name de uniforme distributie van de actieve ingrediënten (API) in het uiteindelijke product is belangrijk. Om de homogeniteit in een mengproces te optimaliseren en te monitoren, worden er nieuwe controlekaarten gepresenteerd. Een NIR spectrum is onderhevig aan diverse bronnen van variatie zoals de individuele absorptie van de componenten en/of verschillen in deeltjesgrootte. In dit proefschrift is een nieuwe methode gepresenteerd; Net Analyte Signal based statistical quality control (NAS-SQC). Er wordt aangetoond hoe diverse kwaliteitsparameters gevolgd worden met een spectrum. Een belangrijke eigenschap van PAT, is de mogelijkheid tot real-time vrijgeven van de producten. Dit betekent dat de kwaliteit van het uiteindelijke product wordt gewaarborgd gedurende de productie en niet achteraf. Om een idee te geven van de mogelijkheden zijn, is er in hoofstuk vier een overzicht gegeven van modellen die gebruikt kunnen worden voor real time release. In hoofdstuk vijf worden diverse praktische voorbeelden gegeven.

OTHER ACTIVITIES

Date	Conferences	Title
10-15 June, 2001	10th International Conference on Near Infrared Spectroscopy, NIR2001, Kyongju, Korea (participant)	
11th September, 2001	Q-Interline NIR User group meeting in Sweden (invited speaker)	*Quantitative NIR calibration of powder; diagnostics and calibration with net analyte signal*
10th October, 2001	PSM Meeting in Stockholm, Sweden (participant)	
November, 2001	Novo Seminar on PAT (organizer/speaker)	*NIR*
21st November, 2002	Meeting at The Royal Veterinary and Agricultural University, Denmark (speaker)	*Parametric Release in Pharmaceutical tablet Production*
6-11 April, 2003	11th International Conference on Near Infrared Spectroscopy, NIR2003, Cordoba, Spain (speaker)	*Optimal Preprocessing and Wavelength Selection Without the Need of Reference Measurements: Introduction of a New Error Indicator*
3-6 June, 2003	Process Analytical Technology (PAT), Hotel Hilton, Brussels, Belgium (participant)	
15th October, 2003	PAT Pharma Öresunds meeting, Helsingborg, Sweden (speaker)	*PAT at Novo Nordisk*
5th December, 2003	PAT meeting at Organon, OOS, The Netherlands (invited speaker)	*PAT at Novo Nordisk*
January, 2004	Meeting at Pfizer R&D site, Ann Arbor, Michigan, USA (invited speaker)	*SE Indicator*

January, 2004	University of Michigan, USA (invited speaker)	*PAT in A Pharmaceutical R&D Environment: A PhD Student Experience in the Application of Online NIR in A Fluid Bed Reactor*
April, 2004	Procesanalyse dag 2004, Delft, DSM-Giest, The Netherlands (invited speaker)	*Process Analytical Technology (PAT) in Pharmaceutical Industry*
24-25 June, 2004	Process Analytical Technologies for Biologics, Sheraton National Hotel, Washington, USA (participant)	
20-23 September, 2004	9th International Conference, Chemometrics in Analytical Chemistry, CAC-2004 Lisboa, Portugal (speaker)	*Net Analyte Signal based Statistical Quality Control (NAS-SQC)*
8th December, 2004	Meeting for Danish Diary Association members, Aarhus, Denmark (invited speaker)	*PAT and Multivariate Statistical Process Control*
14-16 February, 2005	9th NIR Nord Meeting, Vasa, Finland (invited speaker)	*NIR in The Pharmaceutical Industry*
9-10 June, 2005	NIR & Blend/Dose Uniformity Testing, Park Hyatt, Philadelphia, USA (invited speaker)	*Blend Uniformity Analysis Using NIR Probe and Control Charts: New Method Based on Net Analyte Signal Calculations*

Courses

January, 2002	Advanced Chemometric Methods Multi-way Analysis, 3 week PhD course at KVL, Copenhagen, Denmark
	Algebra Course, University of Amsterdam, The Netherlands
1st June, 2004	Advanced Patent Course, Novo Nordisk, Copenhagen

Supervisor assignments

June-October, 2002	Laboratory technician final project; Sladjana Ivanovic, CVU Øresund Laborantskolen, Copenhagen, Denmark	*Raw Material Identification Using Near-Infrared Spectroscopy*
January-July, 2004	Master Thesis Project; Anders Juul Lawaetz, The Royal Veterinary and Agricultural University, Denmark	*Potential Use of NIR and Chemometrics for Biomonitoring of Cell Cultivation*
August-December, 2004	Master Thesis Project; Peter Dalsgaard Mønsted, The Danish University of Pharmaceutical Sciences, Denmark	*Use of Near-Infrared Spectroscopy for Examination of Powder Homogeniety of Cohesive API*
On-going	Master Thesis Project; Jacon Aaman Jensen, University of Copenhagen, Denmark	*Control of Synthesis Based on Near-Infrared Spectroscopy*

Miscellaneous

Member of International Society of Pharmaceutical Engineering (ISPE)

Member of Nordic Special Interest Group in PAT

Member of PPAR Industry Roundtable for PAT

ACKNOWLEDGEMENTS

This has been a long journey and time has come to acknowledge some of the people who helped and supported me throughout the past years and gave me the opportunity to achieve such an important personal goal as this thesis is to me.

First I will thank my primary supervisor Johan Westerhuis. Before I even knew about the PhD position I read Johan's own thesis and funny enough a few years later I was his student, some kind of coincidence. I have spent a lot of time with meetings at Johan's office discussing ideas and results on the blackboard and I appreciate the time and guidance you have invested in the project. Big thanks go to the two persons who made it all possible Professor Age Smilde and Eric Witte. They formulated the PhD project proposal and throughout the years I have been privileged to learn from their experience. I have learned a lot from watching how Age breaks down complex problems into smaller meaningful parts and then stitching the solution together. Eric has been a big support and though he moved from Novo during the project he kept a genuine interest in the project and added valuable comments and real industry experience. I would also like to thank the committee members I hope you found the thesis interesting and novel and I appreciate your participation.

When I first came to the University of Amsterdam I was installed in the office of Henk-Jan and Eric Sprang. It was the most fantastic office with large towers made of soda cans, posters with half naked women and finally a huge fish tank with three large piranhas, what can I say, a truly academic environment. You and your families have become good friends and Johanna, our kids and I have enjoyed your hospitality many times and hope to keep our friendship in the future. At UvA I have also enjoyed help provided by Hans Boelens. You helped me to understand the net analyte signal theory, which has become the backbone in much of my research. A guy not to miss is Jeroen Jansen. You are a person who knows everything on the internet (and a little extra) and I mean it in a positive

way. You are a fun guy to be around and we have shared many nice moments which I appreciate. Also for the rest of my fellow students and the staff members at UvA who I know, thank you very much for making my stay at UvA a memorable time.

Two guys at KVL in Copenhagen have influenced my interest in multivariate data analysis, Professor Rasmus Bro and Associate Professor Lars Noergaard. Besides they are providing inspiration at courses and conferences Lars was the first to introduce me to chemometrics when he handed me a cd-rom with Unscrambler and got me started with doing PCA on fluorescence data. I can certainly recommend visiting the website of their group http://www.models.kvl.dk for some nice reading and download of the hottest new algorithms.

During the project I have meet a lot of very interesting and inspiring people at conferences and meetings throughout the world. There are two many to mention but I would like to thank Neville Broad from Pfizer for some nice talks and also for providing data for the NAS-SQC paper, also Steve Arrivo from Pfizer in Ann Arbor. We had a bang of a conference in Brussels and later I visited you at Pfizer in US which definitely were a highlight during my PhD project. Thank you very much and I certainly hope we can continue to meet and collaborate in the future.

At Novo Nordisk I would like to thank Cooperate Research Affairs (CORA) who has financed my project, especially Marianne Søndergaard who has been very helpful with practical arrangements. I have had the opportunity to receive help and guidance from numerous colleagues at Novo but I would most of all like to thank all technicians and chemists in Analytical Development where I have been working and my department manager Ole Nordfang who has caught interest in PAT and also kindly sponsored extra conference trips and thesis printing costs. It is a privilege to listen and learn from all of you and I truly appreciate your patience with my endless questions about GMP and when I forget to clean up my mess after been doing experiments.

To all my friends who I have been bored stiff with endless talks about the wonders of chemometrics and spectroscopy – sorry! I promise that from now on I will try to broaden my horisont so it exceeds the region from 12000 to 4000 cm^{-1}.

A big thanks to ThaSprout who has designed the front cover of the thesis. You can find more cool artwork from ThaSprout at http://thasprout.deviantart.com. He is a young artist and I predict him to make it big time somewhere showcasing his obvious talent.

Also thank you to my mom and dad. You have always been very supportive and have encouraged me. You are always ready to help and have been babysitting when needed.

And finally, the three most important people in my life, my girlfriend Johanna and our twins William and Maya. After only eight months into the project I became father of the most wonderful twins in the world and even though this was very exciting I must admit that it might happened once or twice that even the most electrifying article could not keep my eyes open and I might have closed them for a few seconds during work, owing one or two sleepless nights. But due to the support, love and dedication from Johanna, raising babies and doing a PhD have been a wonderful combination. You have been very patient with me and my project throughout the last couple of years and I truly appreciate that. You help me with everyday to set my priorities and I promise you to improve even further on that.

Erik, Valby 18th October 2005.

PAPER 1.

New Indicator for Optimal Preprocessing and Wavelength Selection of Near-Infrared Spectra

E. T. S. SKIBSTED, H. F. M. BOELENS, J. A. WESTERHUIS,* D. T. WITTE, and A. K. SMILDE

Published in Applied Spectroscopy, Volume 58, Number 3, 2004

A New Indicator for Optimal Preprocessing and Wavelengths Selection of Near-Infrared Spectra.

Authors: E. T. S. Skibsted [a,b], H. F. M. Boelens [a], J. A. Westerhuis [a,*], D. T. Witte [c], A. K. Smilde [a]

[a]Process Analysis and Chemometrics, University of Amsterdam, Nieuwe Achtergracht 166, 1018 WV Amsterdam, The Netherlands.

[b]Pharmaceutical Site Maaloev, Novo Nordisk A/S, Novo Nordisk Park, 2760 Maaloev, Denmark.

[c]QA/ALC-A, N.V. Organon, Molenstraat 10, P.O. Box 20, 5340 BH Oss, The Netherlands.

Abstract

Preprocessing of near infrared spectra to remove unwanted i.e. non-related spectral variation and selection of informative wavelengths is considered to be a crucial step prior to the construction of a quantitative calibration model. The standard methodology when comparing various preprocessing techniques and selecting different wavelengths is to compare prediction statistics computed with an independent set of data not used to make the actual calibration model. When the errors of reference value are large, no such values are available at all, or only a limited number of samples are available, other methods exist to evaluate the preprocessing method and wavelength selection. In this work we present a new

* Corresponding author: westerhuis@science.uva.nl

indicator (SE) that only requires blank sample spectra i.e. spectra of samples that are mixtures of the interfering constituents (everything except the analyte), a pure analyte spectrum or alternatively a sample spectrum where the analyte is present. The indicator is based on computing the net analyte signal of the analyte and the total error i.e. instrumental noise and bias. By comparing the indicator values when different preprocessing techniques and wavelength selections are applied to the spectra, the optimal preprocessing technique and the optimal wavelength selection can be determined without knowledge of reference values i.e. minimizes the non-related spectral variation. The SE indicator is compared to two other indicators also using net analyte signal computations. To demonstrate the feasibility of the SE indicator two near infrared spectral data sets from the pharmaceutical industry were used i.e. diffuse reflectance spectra of powder samples and transmission spectra of tablets. Especially in pharmaceutical spectroscopic applications it is expected on forehand that the non-related spectral variation is rather large and it is important to remove it. The indicator gave excellent results with respect to wavelength selection and optimal preprocessing. The SE indicator performs better than the two other indicators and it is also applicable to other applications where Beer-Lamberts law is valid.

Keywords

Spectral preprocessing, wavelength selection, near-infrared spectroscopy, error indicator, net analyte signal, signal-to-noise ratio, pharmaceutical powders and tablets.

Introduction

Near infrared spectroscopy is gaining popularity as a quantitative analytical method in the pharmaceutical industry[1-3]. Quality control of incoming raw materials and quantitative analysis of intermediate[4,5] and finalized products[3] are examples of that. Spectra can be recorded fast and non-invasive and combined with a multivariate calibration technique e.g. principal component regression[6]

(PCR) and partial least squares regression[7] (PLS), quantitative measures can easily be obtained. One known problem in near infrared spectroscopy is spectral variations that are not related to the property of interest[8]. Especially in pharmaceutical applications of NIR this non-related variation is important. In pharmaceutical industry spectra are often recorded in reflectance mode. Varying particle sizes and varying compression of e.g. powders cause non-related spectral variation. To correct for this variation various spectral preprocessing techniques are used prior to calibration e.g. multiplicative scatter correction[9] (MSC), offset correction or Savitzky-Golay[10] derivatives. Another problem is that if a large part of the recorded spectrum does not contain any information about the analyte wavelength selection becomes very important. Several methods have been proposed for wavelength selection[11,12]. Until recently, it was believed that full spectrum methods e.g. PLS would automatically overcome the problem of wavelength selection by setting the regression coefficients for non-informative wavelengths to zero or near zero. However this is not the case and PLS based calibrations can in many cases be improved by a proper selection of wavelengths[13].

The most common way of judging if a preprocessing method whether beneficial for the analytical performance is to compute the prediction uncertainty for an independent test set i.e. the root mean square error of prediction (RMSEP) or root mean square error of prediction cross-validated (RMSECV) if only a smaller dataset is available and then select the preprocessing method that gives the lowest RMSEP/RMSECV. Some pitfalls with this method are that it requires a fairly large number of samples i.e. both calibration and test set data. Secondly, if the uncertainty of the reference values is high then judgments are based on reference values with errors. Finally, when using PCR or PLS the RMSEP/RMSECV values are influenced by the model dimensionality. If the model dimensionality is not estimated correctly with some kind of validation technique the RMSEP/RMSECV values will be misleading and therefore also

judgments of preprocessing method selection or wavelength selection may be incorrect.

Other methods exist to help choosing the optimal preprocessing method i.e. methods using the net analyte signal (NAS) concept. Net analyte signal is defined as the part of a signal that is unique for the analyte of interest[14]. Lorber[14] demonstrated how figures of merit e.g. multivariate sensitivity, signal-to-noise ratio, selectivity and limit of detection could be computed from the net analyte signal of the analyte. These figures of merit can be used to judge whether a preprocessing method is beneficial for the analytical performance and they can also be used for wavelength selection. Faber[15] used the inverse multivariate sensitivity of the analyte to judge whether a certain preprocessing method e.g. derivative would improve the predictive ability of the calibration model or not. Xu and Schechter[16] developed an error indicator for wavelength selection. Boelens et al. have also demonstrated the usability of NAS for improving detection limit for a spectroscopic process analysis by tuning Savitzky-Golay filters[17]. All these methodologies use the net analyte signal of the analyte of interest.

In this work we introduce a new error indicator called the signal-to-error indicator (SE). A signal-to-error (SE) value is computed for the analyte when various preprocessing methods and wavelength selections are applied to the spectra. The highest SE value indicates the optimal preprocessing and wavelength interval.

We will demonstrate the performance of the inverse sensitivity indicator, the error indicator and the signal-to-error indicator with two NIR data sets from different stages in a pharmaceutical tablet production. The indicators are compared to the standard PLS methodology and the RMSECV. For the applications presented in this paper the PLS method is used as a standard to compare the other indicators to. This is possible since the reference method is known to be accurate. The first set contains spectra of powder samples after mixing the tablet constituents. In

the second data set finalized tablets using the powder composition from the first data set are measured. In both cases the analyte is the active pharmaceutical ingredient (API) and the optimal preprocessing and wavelength selection is sought for.

First some theory about net analyte signal and the way to compute figures of merit will be presented. Secondly the different error indicators will be described and compared. Then in the experimental section the instrumentation and different data sets used are described in detail and finally in the results and discussion chapter the different error indicators are compared and the results are commented.

Theory

Notation

Boldface capital characters denote matrices, boldface lower-case characters denote vectors and lower case italic characters denote scalars, $\|\mathbf{r}\|$ is the Euclidean norm of the vector $\mathbf{r}$, superscript T denotes the transposed matrix or vector and the superscript + denotes the Moore-Penrose generalized inverse of a matrix. The matrix $\mathbf{I}_J$ is the $J \times J$ identity matrix.

Net Analyte Signal

The net analyte signal is defined as the part of a spectrum that is orthogonal to a subspace spanned by the spectra of all constituents except the analyte i.e. all interfering constituents[14]. So the net analyte signal of analyte *k* can be found by the following orthogonal projection:

$$\mathbf{r}_k^* = \left(\mathbf{I}_J - \mathbf{S}_{-k}\mathbf{S}_{-k}^+\right)\mathbf{r}_k \qquad \textbf{Equation 1}$$

$$\mathbf{s}_k^* = \left(\mathbf{I}_J - \mathbf{S}_{-k}\mathbf{S}_{-k}^+\right)\mathbf{s}_k \qquad \textbf{Equation 2}$$

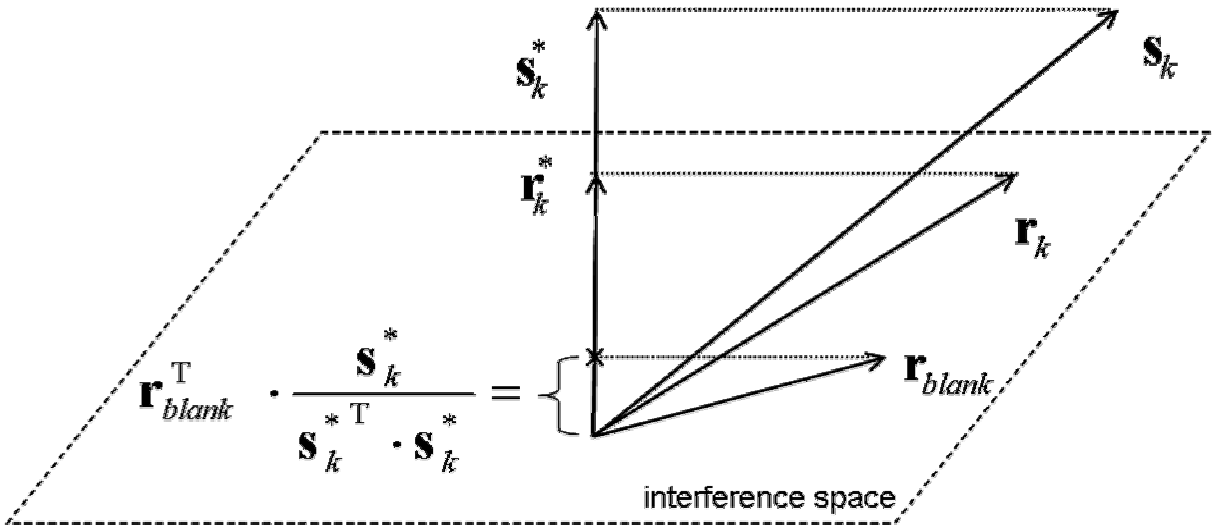

Figure 1: Geometrical display of the interference space and the net analyte signal vectors.

Where $\mathbf{r}_k$ is a *J×1* vector containing the spectral response for a sample including the analyte *k* measured at *J* wavenumbers. The pure analyte spectrum $\mathbf{s}_k$ is a *J×1* vector. $\mathbf{S}_{-k}$ is a *J×L* matrix with *L* spectra of blank samples. In some publications[14] pure spectra of the interfering constituents are used to construct the $\mathbf{S}_{-k}$ matrix. In our experience this is not best method e.g. pure spectra are not always available and the pure constituent spectrum might differ slightly in shape from the spectral contribution in a mixture of interfering constituents. Practically, the $\mathbf{S}_{-k}$ matrix is most easy constructed by measuring mixtures of the interfering constituents. $\mathbf{S}_{-k}^{+}$ is its Moore-Penrose inverse a *L×J* matrix. The $\mathbf{r}_k^*$ and $\mathbf{s}_k^*$ are *J×1* vectors called the net analyte signal vector of the *k'th* constituent. The net analyte signal for constituent *k* in any sample can now be computed with Equation 1.

2.1 Inverse sensitivity

Various figures of merit[14] can be computed using the net analyte signal concept e.g. analyte sensitivity. Faber[15] evaluated the effect of various preprocessing methods of near infrared spectra with an error indicator based on computation of the inverse of the analyte sensitivity (α^{-1}; from here we denote this as invSEN)

using the net analyte signal concept. Faber used the assumption that the length of the net analyte signal vector is proportional to the concentration of the analyte. Faber converted the net analyte signal vector into a scalar value by taking the Euclidean norm[15] of the net analyte signal vector and plotted the value against the analyte concentration of the sample thereby constructing a univariate calibration plot. The analyte sensitivity can then be computed with:

$$\alpha = \frac{\left\| \mathbf{r}_{k,c}^{*} \right\|}{c_{k,c}} \qquad \textbf{Equation 3}$$

$$\text{invSEN} = \alpha^{-1} = \frac{c_{k,c}}{\left\| \mathbf{r}_{k,c}^{*} \right\|} \qquad \textbf{Equation 4}$$

Where $\left\| \mathbf{r}_{k,c}^{*} \right\|$ is the norm of the net analyte signal of a calibration sample with concentration $c_{k,c}$ and the slope of the calibration line α is the sensitivity of analyte *k*. Faber concluded that a preprocessing method is beneficial for the final predictive ability if the inverse sensitivity is decreasing with that particular pretreatment. The effect on the inverse sensitivity when doing first and second derivatives compared to multiplicative scatter corrected (MSC) spectra was evaluated. This indicator needs a collection of spectra to span the interference space and spectra containing the analyte and their respective reference concentrations of the analyte to compute analyte sensitivity.

2.2 Error Indicator

Xu and Schechter[16] developed an error indicator (EI) for wavelength selection. The assumption for their EI is that the prediction error in multivariate analysis is determined by the quality of the corresponding net analyte signal. By minimizing the relative error in the norm of the NAS, the analytical conditions are optimized and lower prediction errors are achieved. The EI was defined as follows:

$$EI = \frac{\mathrm{var}\left(\left\|\mathbf{r}_k^*\right\| - \left\|\mathbf{r}_{k,true}^*\right\|\right)^{1/2}}{\left\|\mathbf{r}_{k,true}^*\right\|} \qquad \textbf{Equation 5}$$

Due to non-related variations (interferents or baseline offsets) the norm of the NAS may be affected. The numerator of the EI describes the variance in the norm of the NAS caused by noise in the spectra due to non-related variations. Xu and Schechter assume that the noise in the spectra due to non-related variations is homoscedastic, i.e. each wavenumber has the same variance, and that the noise is not correlated for neighboring wavenumbers. In that case the variance in the norm of the NAS due to non-related variation can be written as follows[18]:

$$\mathrm{var}\left(\left\|\mathbf{r}_k^*\right\| - \left\|\mathbf{r}_{k,true}^*\right\|\right) = \frac{\left[\left(2\left\|\mathbf{r}_{k,true}^*\right\|s\right)^2 + \left(Js^2\right)^2\right]}{\left(\left\|\mathbf{r}_k^*\right\| + \left\|\mathbf{r}_{k,true}^*\right\|\right)^2} \qquad \textbf{Equation 6}$$

Here *J* is the number of wavenumbers in the spectra used. The standard deviation of the spectral noise described above is represented by *s*. Since $\left\|\mathbf{r}_{k,true}^*\right\|$ cannot be known, Xu and Schechter propose to replace it with $\left\|\mathbf{r}_k^*\right\|$, which leads, according to Ferre and Rius[18] to the following expression for the error indicator:

$$EI = \frac{\left[s^2\left(1 + \frac{J^2 s^2}{4\left\|\mathbf{r}_k^*\right\|^2}\right)\right]^{1/2}}{\left\|\mathbf{r}_k^*\right\|} \qquad \textbf{Equation 7}$$

The standard deviation of the spectral noise, *s*, is found from the net analyte signal regression plot (NASRP). First take the NAS vector of the pure analyte spectrum $\mathbf{s}_k^*$ and the NAS vector of a sample spectrum containing the analyte $\mathbf{r}_k^*$. Then the absorbance at each wavelength *j* in $\mathbf{s}_k^*$ is plotted against the

absorbance in $\mathbf{r}_k^*$ at the same wavelength, for all *j*=1,..,*J* wavelengths in the vectors this results the NASRP plot. In the ideal case with no non-related variation both NAS vectors will point in the same direction and the points in the NASRP plot will form a perfectly straight line passing (0,0). The assumption made by Xu and Schechter[16] is that at each wavelength the error is normally distributed with the same standard deviation i.e. white noise. A straight line is fitted through the points in the NASRP plot in a least square sense and by computing the residual vector i.e. deviation of each of the points from the line *s* can be computed[18].

$$s = \sqrt{\frac{\mathbf{e}_{k,\mathrm{res}}^{\mathrm{T}} \cdot \mathbf{e}_{k,\mathrm{res}}}{J-1}} \qquad \textbf{Equation 8}$$

Where $\mathbf{e}_{k,res}$ is a $J \times 1$ vector containing the residuals. The residuals are computed in the following manner:

$$\mathbf{e}_{k,\mathrm{res}} = \mathbf{r}_k^* - \mathbf{s}_k^* c_k \qquad \textbf{Equation 9}$$

$$c_k = \mathbf{r}_k^{*\mathrm{T}} \cdot \mathbf{s}_k^* / \left\| \mathbf{s}_k^* \right\|^2 \qquad \textbf{Equation 10}$$

The error indicator needs a collection of blank spectra to span the interference space, the pure analyte spectrum and a sample spectrum containing the analyte.

2.3 Signal to Error indicator

In this work we present a new indicator based on the computations of the signal-to-error (SE). We assume that the error in the spectra is made of two contributions i.e. noise and bias. If a certain preprocessing method or wavelength selection is not removing unwanted interference, then extra blank samples may have a small contribution orthogonal to $\mathbf{S}_{\_k}$ when they are projected onto the interference space. We compute this contribution as the projection ($PROJ_{blank}$) of

some extra blank spectra ($\mathbf{r}_{blank}$) on the normed $\mathbf{s}_k^*$ vector i.e. normed to unit length. We call the normed $\mathbf{s}_k^*$ vector for the net analyte signal regression vector ($\mathbf{nas}_{reg}$).

$$PROJ_{blank} = \mathbf{r}_{blank}^{\mathrm{T}} \frac{\mathbf{s}_k^*}{\mathbf{s}_k^{*\mathrm{T}} \mathbf{s}_k^*} \qquad \textbf{Equation 11}$$

$$PROJ_{blank} = \mathbf{r}_{blank}^{\mathrm{T}} \mathbf{nas}_{reg} \qquad \textbf{Equation 12}$$

The error taken into account both bias and noise is computed by:

$$error = \sqrt{\frac{\sum_{i=1}^{I} \left(PROJ_{blank,i} - 0\right)^2}{I}} = \sqrt{\frac{\sum_{i=1}^{I} \left(PROJ_{blank,i}\right)^2}{I}} \qquad \textbf{Equation 13}$$

In the nominator we use *I* and not *I-1* because no mean is subtracted so the degrees of freedom are preserved.

The signal is then computed by projecting the analyte spectrum on the NAS regression vector and the SE can be computed as the ratio between the signal and the error:

$$Signal = \mathbf{s}_k^{\mathrm{T}} \mathbf{nas}_{reg} \qquad \textbf{Equation 14}$$

$$SE = \frac{Signal}{error} \qquad \textbf{Equation 15}$$

This error indicator needs a collection of blank spectra to span the interference space and to quantify the error part plus the pure analyte spectrum. If the pure

analyte spectrum is not available a sample spectrum containing the analyte can be used alternatively.

Although the Error Indicator and the Signal to Error indictor seem to be comparable, there are some important differences. The EI minimize the difference between the length of two vectors, $\mathbf{r}_{k,true}^{*}$ and $\mathbf{r}_{k}^{*}$. However these vectors will not necessarily point in the same direction. Therefore, the difference in lengths is not directly related to errors in concentration. The SE indicator focuses on errors in the direction of the NAS regression vector i.e. the same direction. The projections on the NAS regression vector are used (can also be negative) and not only the lengths of the projected vector. These projections are directly related to the concentrations.

Toolboxes for net analyte signal calibrations are available for free download at http://www.bdagroup.nl/index.html.

Experimental section

The powder samples were measured with a BOMEM MB 160 FT-NIR spectrometer equipped with a SpinningVial™ accessory for measuring powder samples, the samples were measured with diffuse reflectance and an InGa detector was used. The SpinningVial™ accessory measured through the sample vials through the side of glass vials (were the glass walls are assumed to be most homogeneous). The wave number range from 3800 cm^{-1} to 12000 cm^{-1} was recorded and the spectral resolution was set to 8 cm^{-1}. For each spectrum a total of 32 scans were averaged (the scanning time for 32 scans measured with a spectral resolution of 8 cm^{-1} is the same time as the SpinningVial™ accessory uses to spin the sample vial one revolution). The tablet samples were measured with a BOMEM MB 160 FT-NIR spectrometer equipped with a TabletSamplIR™ accessory. The tablets were measured with a transmission measurement and an InGaAs detector was used. The wave number range from 4000 cm^{-1} to 12000

cm^{-1} was recorded and the spectral resolution was set to 16 cm^{-1}. When measuring transmission spectra of tablets normally only broad peaks in the first and second overtone region are useful for quantification and 16 cm^{-1} is a reasonably resolution. For each spectrum a total of 32 scans were averaged. In both cases the data were collected with GRAMS32 (ThermoGalactic.com. GRAMS/32. 1998) software and imported into Matlab (MathWorks Inc. Matlab ver. 12.1., 2001) with in-house written software. Computations were performed in Matlab with in-house written routines plus the PLS_toolbox (Eigenvector Research, Inc. PLS_Toolbox. Version 2.1., 1998).

Dataset 1: Powder samples

The samples were made according to a triangular mixture design. The samples contained five constituents i.e. the active pharmaceutical ingredient (API), two filler binders (A and B) and two glidants (C and D). Three doses are normally produced i.e. 0.64, 1.27 and 2.57 API w/w % (low, medium and high strength). To have samples that resemble the heterogeneous nature of powder mixtures, samples with over- and under dose of API, filler binder A and filler binder B were produced according to a triangular mixture design (Figure 2). Samples with +/- 10 % of target dose of API, +/- 10 and +/- 20 w/w % of target dose of filler binder A and filler binder B were made while the added amount of glidant C and glidant D were kept constant. Initial experiments (not shown here) indicated that homogeneity of filler binder A and filler binder B could be difficult to obtain in a large scale mixing process. It was therefore assumed that the span i.e. +/- 20% from target concentration of those constituents would resemble the heterogeneity that could be expected in the interference matrix, while glidant C and glidant D are assumed to be less important and for practical reasons the added amount was kept constant. Blank samples without API were also prepared (marked with squares in Figure 2). The samples were prepared in 25 ml glass vials that fitted into the SpinningVial™ accessory. The total sample size was 8.0 gram and the samples were prepared in the following manner. First the filler binder A was weighed with an electronic precision weight and transferred into the vial. Then

API was weighed and transferred into the vial the constituents were mixed manually with a metal spatula. Then filler binder B, glidant C and finally the glidant D each time manually mixing with a metal spatula were performed. Each sample was measured eight times in the SpinningVial™ accessory and between each measurement the sample was removed and shaken viciously. The mean of the eight spectra was then used to represent the sample. The powder samples are generally problematic to measure because of the heterogeneous distribution of the sample constituents, but other studies (not shown) have shown that the SpinningVial™ accessory and the use of the mean spectrum is a valid methodology and the methodology has also been reported elsewere[19]. As a reference method, the weighed amount was used (gravimetric) and the uncertainty on this value were believed to be low i.e. +/- 10^{-4} g.

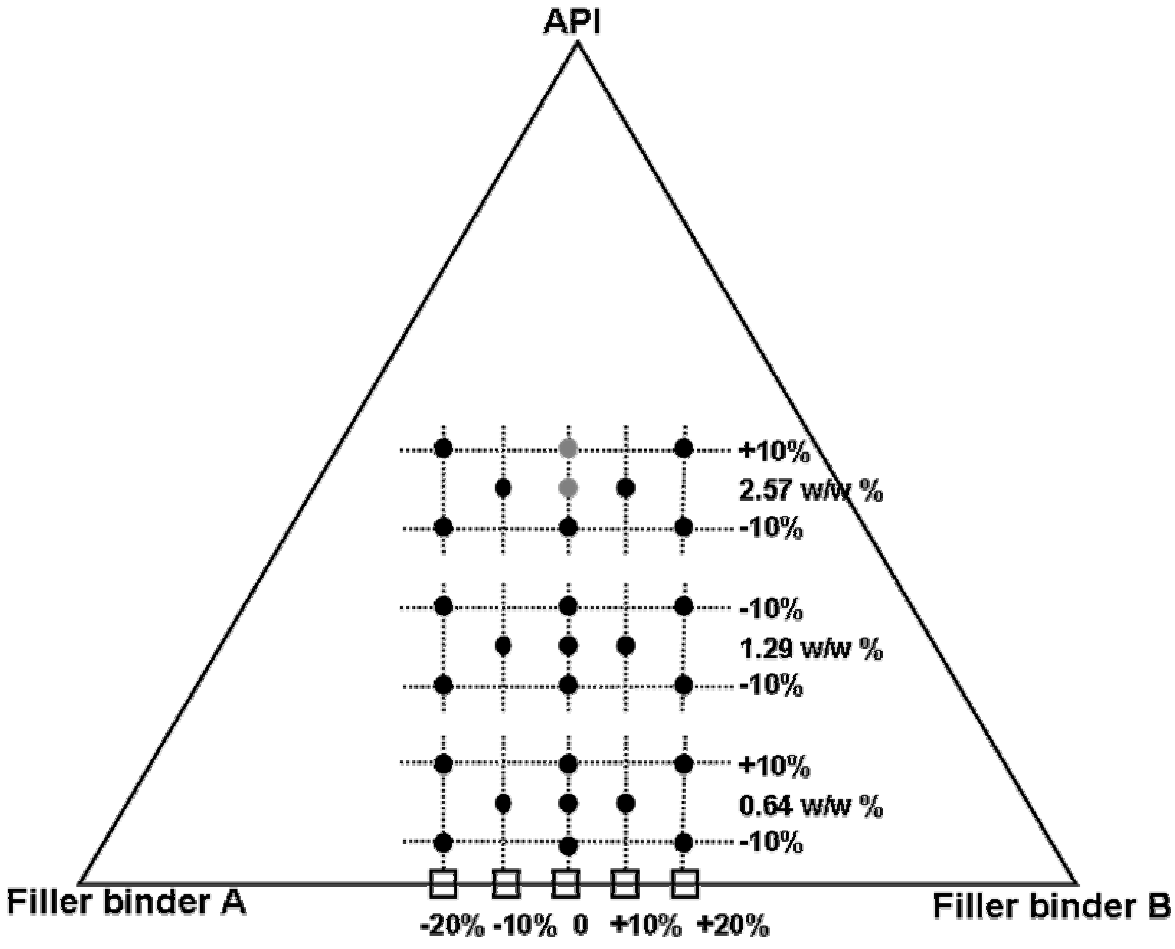

Figure 2: Triangular mixture design for powder samples.

Dataset 2: Tablet samples

No specific experimental design was used for the tablet samples, but a small data set based on a stratified sampling scheme was used. Tablets were taken from nine different production batches (pilot scale batches). Three batches with placebo tablets i.e. blank samples without API and six batches with API in three different levels. From each batch two tablets were used in total 18 tablets. Because it is not possible to measure a transmission spectrum of the pure API ($\mathbf{s}_k$) we used a spectrum of a tablet from a batch with high concentration of API as replacement for the pure analyte spectrum. One tablet spectrum from each of the placebo batches i.e. three spectra were used to span the interference space and the three remaining spectra were used as blank samples to quantify the error.

Results and discussion

A selection of different preprocessing methods (Table 1) that are normally[20,21] applied when doing preprocessing of NIR spectra obtained from diffuse reflectance measurements of powders and transmission spectra of tablets were compared. For both data sets we compared the same preprocessing methods. The wavelength selection can be conducted in many different ways. In this article we used the prior knowledge we have about the analyte i.e. location of main analyte peaks. The search for the optimal wavelength interval was conducted by choosing a starting point i.e. a wavenumber where an analyte peak is present and then compute the various indicator values and RMSECV for a wavelength interval defined around this starting point. Then the interval was extended in both directions and new indicator values and RMSECV were computed. This was done a proper number of times using an increasing interval width until a large part of the wavelength axis was examined. The selection of wavelength intervals to examine can be done in numerous ways either using prior knowledge about major peak locations or more automatic routines e.g. moving windows. In any case the indicator values can be computed and therefore applied to existing wavelength selection methods.

For the powder samples the starting point was 6000 cm^{-1} i.e. an analyte peak is found there (Figure 3) with an interval width of 160 cm^{-1} i.e. from 5920-6080 cm^{-1}. Then the interval was extended 160 cm^{-1} to 5840-6160 cm^{-1}, this was repeated until 20 intervals were examined, the last covering 4400-7600 cm^{-1}. For the tablet samples the starting point was 8800 cm^{-1} i.e. an analyte peak is found there with an interval width of 120 cm^{-1} i.e. from 8740 - 8860 cm^{-1}. Then the interval was extended 120 cm^{-1} to 8680-8920 cm^{-1}, this was repeated until 15 intervals were examined, the last covering 7900-9700 cm^{-1}.

Table 1: Preprocessing methods.

No.	Method	Note
1	No preprocessing	
2	MSC	
3	Offset	Using the 9990-10000 cm^{-1} as offset point
4	1. Derivative	Using 11 spectral points
5	1. Derivative	Using 25 spectral points
6	2. Derivative	Using 11 spectral points
7	2. Derivative	Using 25 spectral points

Comparing the indicator values and RMSECV using GAIN values

To compare the indicator values and the RMSECV we compute the GAIN for each value. The GAIN is computed as the ratio between an indicator or RMSECV value to a reference value. The reference value for the indicators or RMSECV is the value when using spectra without any preprocessing applied and the whole wavelength range.

$$SE_{gain} = \frac{SE_{pre}}{SE_{ref}} \qquad \textbf{Equation 16}$$

$$invSEN_{gain} = \frac{invSEN_{ref}}{invSEN_{pre}}$$ **Equation 17**

$$EI_{gain} = \frac{EI_{ref}}{EI_{pre}}$$ **Equation 18**

$$RMSECV_{gain} = \frac{RMSECV_{ref}}{RMSECV_{pre}}$$ **Equation 19**

Where the index *ref* means that the indicator and RMSECV value are computed using non-preprocessed spectra and the whole wavelength range i.e. 4000 to 10000 cm^{-1} for the powder samples and 7300 to 10000 cm^{-1} for the tablet samples. The index *pre* means that a preprocessing method or preprocessing method and wavelength interval selection have been applied to the spectra. Note that the SE_{ref} is the denominator in equation 17, this is because the optimal preprocessing and wavelength selection is equal to the highest SE value opposite the other indicators and RMSECV where the lowest value equals the optimal preprocessing and wavelength selection. If the gain value is bigger then one then the preprocessing or preprocessing and wavelength selection will improve the final calibration model, if the gain value is equal to or lower then one then the preprocessing or preprocessing and wavelength selection are not improving or worsen the final calibration model.

Results powder samples

In Figure 3 the pure analyte spectrum, a spectrum of a blank sample and a spectrum of a sample containing 2.57 w/w % API are depicted. The difference between the blank spectrum and the spectrum containing 2.57 w/w % API is mainly caused by scattering phenomena seen as offset differences from 7000 to 12000 cm^{-1}. In the API spectrum main peaks are identified in the combinational bands region i.e. 4650 cm^{-1} and 4940 cm^{-1}, in the first overtone region we find a

peak at 6000 cm^{-1} and in the second overtone region a peak at 8800 cm^{-1} is apparent.

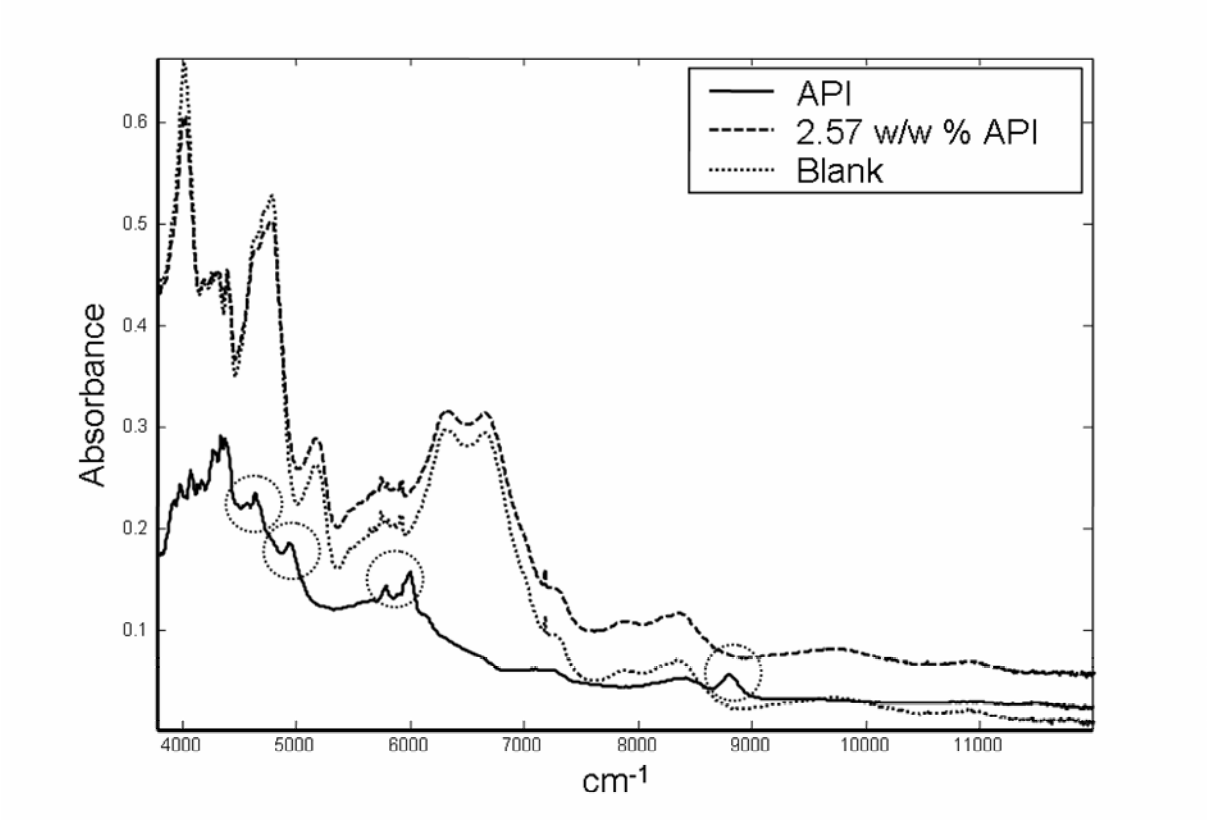

Figure 3: NIR spectra of i) blank powder sample, ii) powder sample with 2.57 w/w% API and iii) analyte spectrum.

Choosing the optimal preprocessing method for the powder samples

To span the interference space for the invSEN, SE and EI indicator we used five blank sample spectra, symbolized with open squares in Figure 2. To compute the invSEN we used two sample spectra containing the analyte i.e. samples marked with grey circles in Figure 2. To compute the SE we used two analyte spectra to compute the signal and additional twenty-five blank sample spectra to compute the error. To compute the EI two sample spectra i.e. samples marked with grey color in Figure 2 and two analyte spectra were used. The RMSECV values were calculated using the 32 samples depicted in Figure 2. When computing the RMSECV values the 32 samples were divided into 11 blocks i.e. 10 blocks with 3 samples each and one block with two samples, then cross validation was

performed leaving out one block at the time. Based on the cross validation results 5 PLS components were selected for the PLS model of the whole wavelength range. The indicator values and the RMSECV were calculated using the 4000-10000 cm^{-1} wavelength region and applying the preprocessing methods listed in Table 1. In Figure 4 the gain values are depicted for the indicators and RMSECV. The RMSECV shows that best preprocessing method is 1. derivatives using 25 spectral points with a gain value of 2.9. The SE indicator has the highest gain for 1. derivatives, while the EI indicator has the highest gain for 2. derivatives. The invSEN indicator has the highest gain for MSC, which is clearly wrong compared to the PLS results.

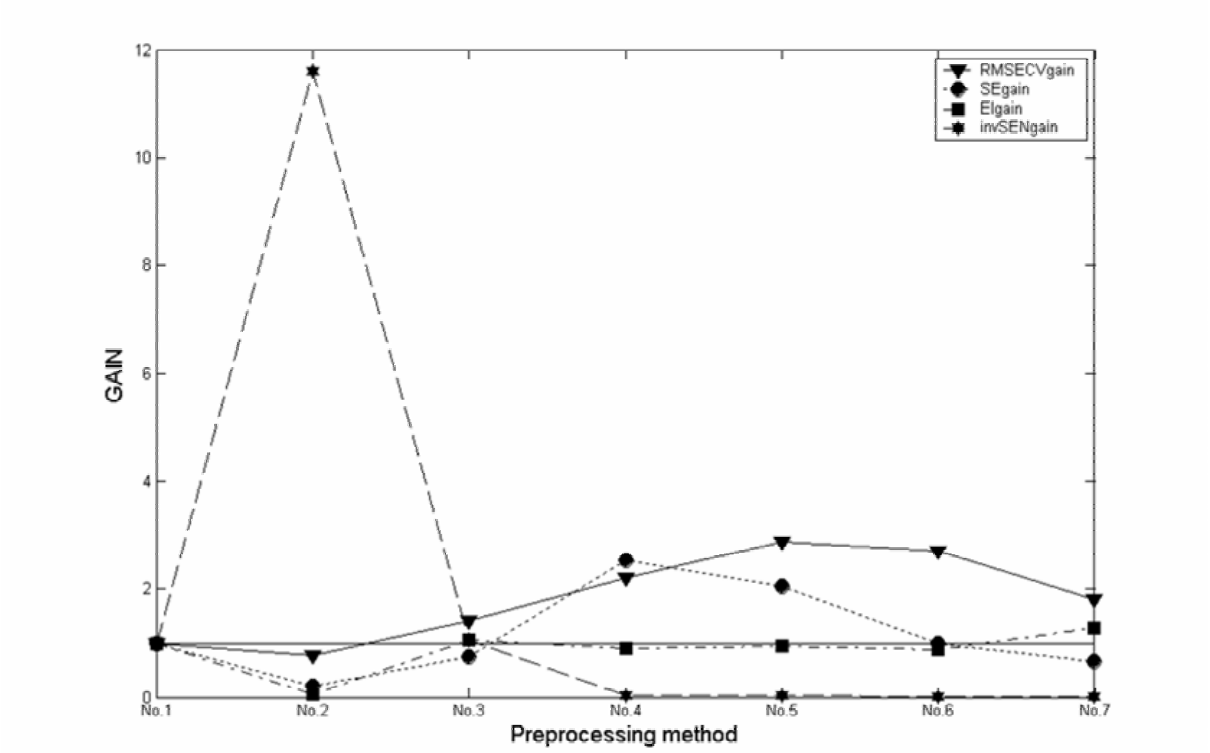

Figure 4: Optimal preprocessing method. Gain values for indicators and RMSECV for powder samples.

Wavelength selection for the powder samples

Indicator and RMSECV values were computed for twenty wavelength intervals around 6000 cm^{-1}. For all intervals 4 PLS components were used to calculate the RMSECV values. Again the number of PLS components is based on cross

validation results. This was done for all seven preprocessing methods and the highest gain values for the RMSECV was then found to be 5.95 when preprocessing method 5 was used with the wavelength interval from 5840-6160 cm^{-1} (Figure 5). This matched perfectly the SE indicator that had the highest gain value for the same preprocessing method and wavelength interval as the PLS method. Also the EI indicator had the highest gain value for preprocessing method 5 but the wavelength interval from 5760-6240 cm^{-1}. The shape of the RMSECV gain curve corresponded well with the shape of the SE gain curve and also the gain values were all above one for the RMSECV and the SE. The gain values for the EI when applying preprocessing method 5 were only above one for three intervals i.e. I-2, I-3 and I-4 while for the remaining intervals were less then one indicating that no preprocessing and using the whole wavelength region was better for those intervals (Figure 5). The invSEN indicator was not useful for wavelength selection using any of the preprocessing methods. The highest gain value for the invSEN was 11.8 using MSC as preprocessing and the wavelength interval from 4000 - 10000 cm^{-1}, when using all other preprocessing methods the gain for the invSEN was always below one with the lowest value for the smallest wavelength interval i.e. I-1 and increasing with increasing interval width e.g. inserted figure in Figure 5.

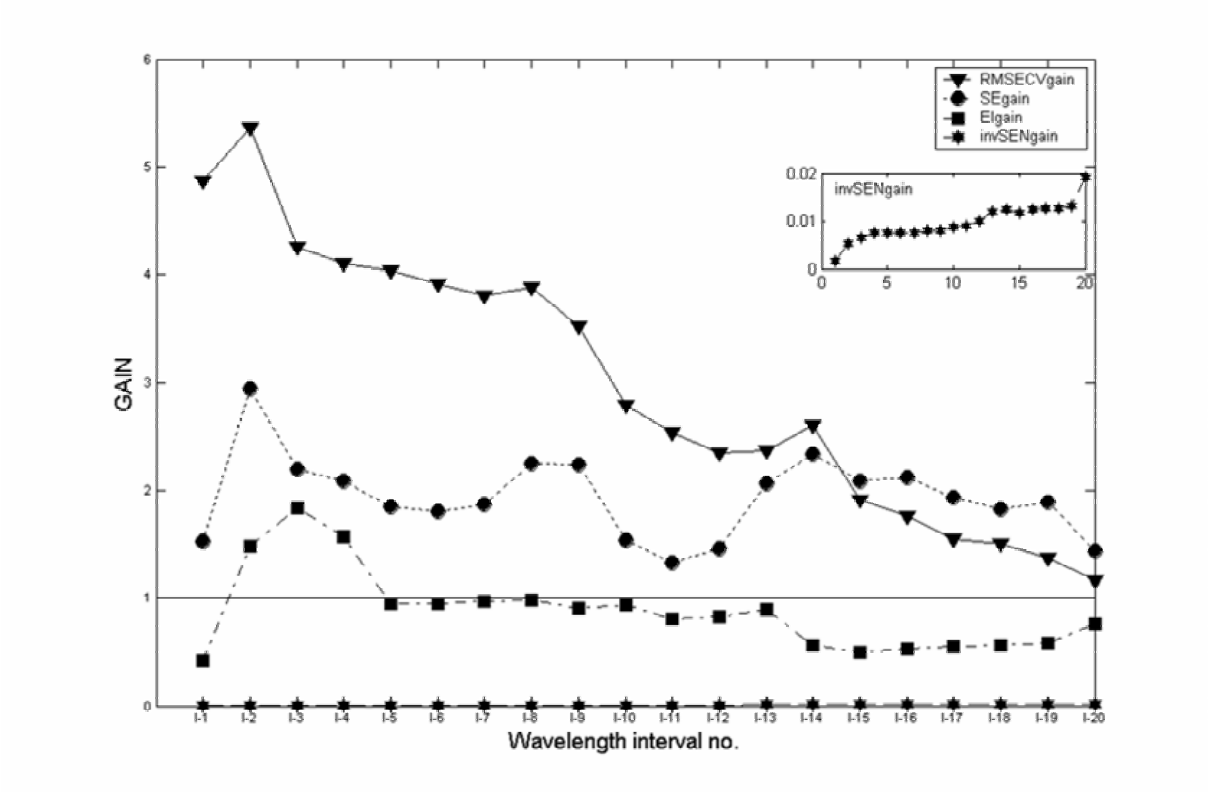

Figure 5: Optimal preprocessing/wavelength selection. Gain values for indicators and RMSECV for powder samples.

It is important to notice that the selection of preprocessing method using the whole wavenumber range is not representative for the results when only a small wavelength region is used. So therefore, combining preprocessing and wavelength selection, as is done here, seems to be necessary.

Results Tablet samples

To span the interference space for the invSEN, SE and EI indicator we used three blank sample spectra. To compute the invSEN we used two samples with a high concentration of API. To compute the SE we used two sample spectra i.e. using two samples with a high concentration of API as substitution for pure analyte tablet spectra which were not available to compute the signal and additional three blank sample spectra to compute the error. To compute the EI four sample spectra with a high API concentration were used. Two of the sample

spectra were used to compute the average $\mathbf{r}_k^*$ and the two other sample spectra were used to compute the average $\mathbf{s}_k^*$ (Equation 2 and 3) because no pure analyte tablet samples are available. The RMSECV values were calculated using all 18 samples. When the RMSECV value was computed the leave-one-out principle was used because of the limited size of the dataset.

Choosing the optimal preprocessing method for the tablet samples

Also for the tablet samples, comparison of the preprocessing methods using a broad spectral range were not a feasible method i.e. preprocessing combined with wavelength selection were necessary.

Wavelength selection for the tablet samples

Indicator and RMSECV values were computed for fifteen wavelength intervals around 8800 cm^{-1} with all the preprocessing methods described in Table 1. All PLS models were calculated using 4 PLS components. The highest gain value for the RMSECV was 3.6 when using preprocessing method no. 5 i.e. 1. derivatives with 25 spectral points and the wavelength interval 8620-8980 cm^{-1} (Figure 6). Also the SE had the maximum gain value of 3.8 using preprocessing method no. 5 and the interval 8620-8980 cm^{-1} (Figure 6). The shape of the RMSECV and the SE gain curves were fairly similar. As for the powder samples the invSEN was not useful for wavelength selection and the gain values were less then one except for the MSC method. The EI had a maximum gain at 1.29 when MSC was used for preprocessing and the wavelength interval was 8320-9280 cm^{-1} (not depicted) and was in general not useful for wavelength selection of the tablet samples.

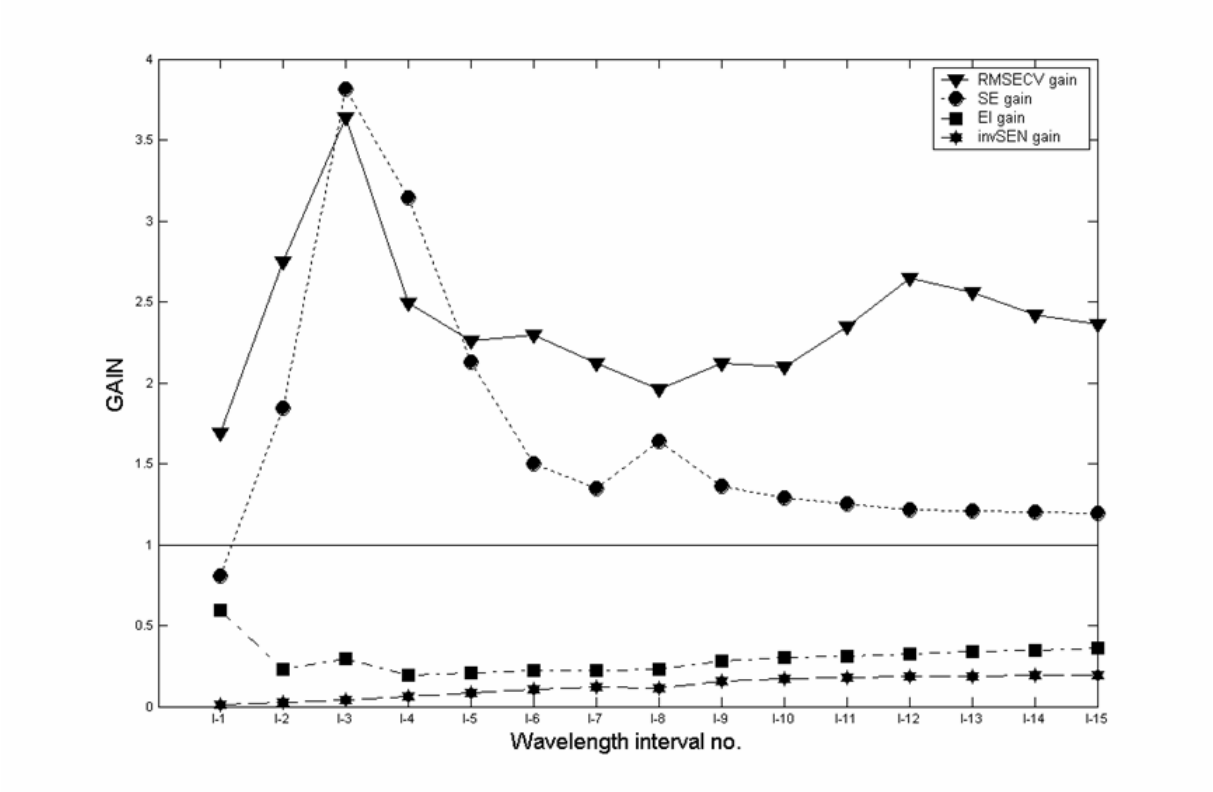

Figure 6: Optimal preprocessing/wavelength selection. Gain values for indicators and RMSECV for tablet samples.

The problem with the invSEN indicator is that when the spectra are preprocessed using 1. and 2. derivatives the Euclidean length of the spectra and subsequently the net analyte signal vectors are lowered. This decreases the analyte sensitivity as computed in equation 4 without regards to the analytical performance of a calibration model using derivative spectra. In the original publication Faber assumed only white noise is present, which is a huge simplification of real spectroscopic systems in pharmaceutical applications. This might also explain why the method fails with our examples.

The EI indicator performed reasonably well but with failures. Wavelength selection of the tablet samples was not possible. The reason for the failure with the tablet samples might be that no “pure analyte tablet” was available. In the EI the net analyte signal vector of a sample and analyte spectra are compared. But

as pure analyte spectra are not always available and generally not for tablet samples the EI is not usable for this sample type.

During the work we discovered that a good selection of blank samples is the “key” to this indicator. For the powder samples we had measured each of the five blank samples eight times giving forty blank spectra. Among these spectra we picked a few spectra to span the interference space and a larger portion to quantify the error. We recommend that as many blank samples as possible are measured using repeated measurements in that manner instrumental noise and baseline drift are included. This is easy to do in most industrial applications, but might be more difficult for environmental products. Also reposition samples and for powder samples shake samples in that manner heterogeneous samples are best measured.

Conclusion

We have demonstrated a new indicator for choosing the optimal preprocessing method and conducting wavelength selection of NIR spectra. The indicator was compared to existing indicators also using net analyte signal computations and the standard methodology using cross validation results from a PLS regression model. The indicator performed better then the two reference methods using net analyte signal methodology. The invSEN failed generally to find the optimal preprocessing method and was not useful for wavelength selection either. The EI indicator was developed for wavelength selection but we tried to use it for selection of optimal preprocessing method without success for both the powder and tablet samples. For wavelength selection the EI indicator performed reasonably for the powder samples and identified a few wavelength intervals that were improving the calibration model, but not the optimal selection (Figure 5). The indicator was not able to be used for wavelength selection of the tablet samples. The SE indicator identified the right preprocessing method and also the optimal wavelength selection both for the powder and the tablet samples. For the tablet samples the right preprocessing method was not imminent identified only

after subsequent wavelength selection was performed (Figure 6). So in cases where only a few samples are available, reference values are determined with a high error or not available we recommend this new indicator. A problematic issue for all NAS methods is that it is unclear how interactions between the analyte and the interferents are dealt with. This is a general problem of the NAS approach, but even for more commonly used inverse calibration methods as PLS or PCR this is not clear. The validation of the SE method is only performed on the zero concentration level. Therefore it can be expected that the method will work better for low concentrations. Also the proposed method is only demonstrated for reflectance spectra of powder samples and transmittance spectra of whole tablets and we have no data available to demonstrate it with other sample types and spectroscopic setup. In this study only two experiments have been used for the investigation and in other cases it might be that the proposed indicator is not the best choice compared to the other NAS based methods or other methods for selection of the optimal preprocessing and wavelength points.

Acknowledgements

Novo Nordisk, Corporate Research Affairs (CORA) sponsored this work as a part of E.T.S. Skibsted's Ph.D. project.

References

1. M. Blanco, H. Iturriaga, S. Maspoch and C. Pezuela, Analyst **123,** 135 (1998).

2. M. Blanco, J. Coello, A. Eustaquio, H. Iturriaga, and S. Maspoch, Analytica Chimica Acta **392,** 237 (1999).

3. M. Blanco, J. Coello, H. Iturriaga, S. Maspoch and D. Serrano, Analyst **123,** 2307 (1998).

4. R. D. Maesschalck, F. C. Sánchz, D. L. Massart and P. Doherty, Appl. Spectrosc. **52[5]**, (1998).

5. F. C. Sánchz, J. Toft, B. Bogaert, S. S. Dive and P. Hailey, Fresenius J. Anal. Chem. **352,** 771 (1995).

6. H. Martens and T. Næs, Trends in Anal. Chem. **3,** 204 (1984).

7. H. Martens and T. Næs, Multivariate calibration (John Wiley & Sons, 1989).

8. H. Swierenga, A. P. de Weijer, R. J. van Wijk and L. M. C. Buydens, Chemom. Intell. Lab. Syst. **49,** 1 (1999).

9. P. Geladi, D. McDougall and H. Martens, Appl. Spectrosc. **39,** 491 (1985).

10. A. Savitzky and M. J. E. Golay, Anal. Chem. **36,** 1627 (1964).

11. Q. Ding and G. W. Small, Anal. Chem. **70,** 4472 (1998).

12. L. Nørgaard, A. Saudland, J. Wagner, J. P. Nielsen, L. Munck and S. B. Engelsen, Appl. Spectrosc. **54[3],** 413 (2000).

13. C. H. Spiegelman, M. J. McShane, M. J. Goetz, M. Motamedi, Q. L. Yue, and G. L. Coté, Anal. Chem. **70,** 35 (1998).

14. A. Lorber, Anal. Chem. **58,** 1167 (1986).

15. N. M. Faber, Anal. Chem. **71,** 557 (1999).

16. L. Xu and I. Schechter, Anal. Chem. **68,** 1842 (1996).

17. H. F. Boelens, W. T. Kok, O. E. de Noord and A. K. Smilde, Anal. Chem. **76**, 2656-2663, 2004.

18. J. Ferré and F. X. Rius, Anal. Chem. **70,** 1999 (1998).

19. O. Berntsson, L. G. Danielsson, M. O. Johansson and S. Folestad, Anal. Chimica Acta **419,** 45 (2000).

20. O. Berntsson, Characterization and Application of Near Infrared Reflection Spectroscopy for Quantitative Process Analysis of Powder Mixtures (Ph.D. thesis, Kungliga Tekniska Högskolan (KTH), Stockholm, Sweden, 2001).

21. H. Swierenga, Robust Multivariate Calibration Models in Vibrational Spectroscopic Applications (Ph.D.thesis, Katholieke Universiteit Nijmegen, The Netherlands, 2000).

PAPER 2.

Simple Assessment of Homogeneity in Pharmaceutical Mixing Processes Using a Near-Infrared Reflectance Probe and control charts

E. T. S. SKIBSTED, H. F. M. BOELENS, J. A. WESTERHUIS,* D. T. WITTE, and A. K. SMILDE

Accepted (Oktober 2005) in Journal of Pharmaceutical and Biomedical Analysis.

Simple Assessment of Homogeneity in Pharmaceutical Mixing Processes Using a Near-Infrared Reflectance Probe and control charts

Authors: E. T. S. Skibsted [a,b], H. F. M. Boelens [a], J. A. Westerhuis [a,*], D. T. Witte[c], A. K. Smilde [a]

[a] Biosystems Data Analysis , University of Amsterdam, Nieuwe Achtergracht 166, 1018 WV Amsterdam, The Netherlands.

[b]Pharmaceutical Site Maaloev, Novo Nordisk A/S, Novo Nordisk Park, 2760 Maaloev, Denmark.

[c]QA/ALC-A, N.V. Organon, Molenstraat 10, P.O. Box 20, 5340 BH Oss, The Netherlands.

Abstract

Determination of homogeneous mixing of the Active Pharmaceutical Ingredient (API) is an important in-process control within the manufacturing of solid dosage forms. In this paper two new near-infrared (NIR) based methods were presented; a qualitative and a quantitative method. Both methods are based on the calculation of Net Analyte Signal (NAS) models which were very easy to develop, specific with respect to the API and required no additional reference analysis. Using a well mixed batch as a 'golden standard' batch, control charts were developed and used for monitoring the homogeneity of other batches with NIR. The methods were fast, easy to use, non-destructive and provided statistical tests of homogeneity. A mixing study was characterized with the two methods and the methods were validated by comparison with traditional HPLC analysis.

Keywords

Net analyte signal, process analytical technology, powder homogeneity, near-infrared spectroscopy, process control charts

---

* Corresponding author: westerhuis@science.uva.nl

Introduction

An important unit operation in the production of a pharmaceutical solid dosage form is the mixing of the powder constituents. One of the primary objectives of the mixing process is to obtain a homogeneous mixing of the active pharmaceutical ingredient (API) in the formulation. The homogeneity is normally determined by removing a small number of powder samples from the powder mixer with a probe thief and sending the samples to a quality control laboratory distant from the process line for e.g. high pressure liquid chromatography (HPLC) analysis. The API content in the samples and the relative standard deviation (RSD) of the API content between the samples is then obtained and compared to specified values in order to decide wherever the batch is sufficiently homogeneous[1]. This procedure is slow and is not suited for process control of the mixing process to obtain the highest possible homogeneity. Also a limited number of samples are used which makes a full characterization of homogeneity difficult.

Therefore, near-infrared (NIR) based spectroscopic methods which are non-destructive, fast and require little resources have been proposed[2-10]. NIR has been applied in many different manners. Samples were removed from the system and measured with NIR (off line)[2;4]. This method faces some of the classical powder sampling problems where large variance is introduced when inserting a sample thief into the powder bed and removing a sample. In other papers, diffuse reflectance probes have been inserted directly into the powder bed at a fixed position (in-line)[5;6] or the mixer was fitted with quartz windows through which monitoring could be applied from outside the mixer (semi♣ non-invasive)[7]. These types of methods only monitor the powder bed at one or a few points and only provide information about the homogeneity in these particular positions

♣ The application was not truly *in-line* because the mixer had to be stopped to perform monitoring with a diffuse reflectance probe that was moved around from window to window.

assuming that the point or points are representative for the entire powder bed. In cases with ‘dead spots’ or de-mixing phenomena this assumption would not hold. Many different data analysis methods have been applied to the spectral data in order to derive the optimal mixing time. The span of methodologies are from simple qualitative methods looking for absence of changes in the spectra i.e. moving block[5], dissimilarity indexing[2], principal component analysis (PCA)[4], soft independent model class analogy (SIMCA)[7] and bootstrapping techniques (BEST) to quantitative calibration models using partial least squares (PLS). The qualitative approaches evaluate only spectral homogeneity i.e. variation between spectra in time or position but are not specific for the analyte. The PLS method on the other hand, directly evaluates the concentration homogeneity of the analyte of interest. Some of the qualitative methods compare the measured spectra with a set of “target” spectra of a homogeneous mixture.

In the present paper we introduce a new method for monitoring homogeneity of powder mixtures by testing the variation and the level of the API content over the mixer. The API content is based on the net analyte signal (NAS) value of NIR spectra. The NIR spectra are recorded directly in the mixer using a fibre based handheld diffuse reflectance probe. Thus, by just sticking the probe in the mixer a number of times, a measure of homogeneity is obtained that is statistically validated.

A qualitative approach of the method is suited for early development studies when only a few batches are available and further on in the development stage, calibration can be used to make the method quantitative. In both methods a ‘golden batch’ is chosen and two control charts are developed based on measurements of the ‘golden batch’. In the two control charts the variance and the mean are observed. With the proposed method, a mixing process is examined. In order to validate the proposed NIR methods control charts are also developed using values obtained from traditional HPLC analysis of powder samples. Results from four independent batches are then plotted in the control

charts and the results are compared to NIR. Variance components in the measured signal are described and finally we show how many spectra need to be recorded in order to not make false conclusions about homogeneity.

Theory

In this theory section we will first discuss the mixing of pharmaceutical powders and the idea of a random and homogeneous mixture. Then the different sources of variation in analytical measurements of homogeneity are discussed. The net analyte signal approach used to relate a multivariate NIR measurement to the API content is discussed shortly. Afterwards we first introduce the qualitative approach for monitoring homogeneity. Finally we will also show how a quantitative model can be developed in which actual concentrations of the API are monitored.

Mixing and determination of a random mixture

Definition of mixing[11].

"*Mixing is the treatment of two or more components in such a way, that the individual particles of the different components in the mixture are evenly distributed and lie adjacent to each other within the highest possible probability.*"

A perfect mixture between two or more components would be one in which each sample contains exactly the proper amount of each of the components. If e.g. two components were mixed (A and B) in a 1:1 relationship a perfect mixture would be when every second particle would be A. Such a perfect mixture is not achievable but a random mixture is[11] and the aim of a pharmaceutical mixing process is to achieve a random mixture which then would stand for a homogeneous mixture. An example of a random mixture was presented by Muzzio et al.[12]. A random mixture can be considered as a mixture where all samples removed from the mixture would be normally distributed with same

mean (μ) and standard deviation (σ) regardless from where in the mixture the sample was removed.

Variance component model

In order to understand the total variance the following variance component model is proposed for a NIR based method.

$$\sigma^2_{\text{total}} = \sigma^2_{\text{analysis}} + \sigma^2_{\text{sampling}} + \sigma^2_{\text{random mixture}} + \sigma^2_{\text{heterogeneity}} \qquad \textbf{Equation 1}$$

The variance due to the analysis, $\sigma^2_{\text{analysis}}$ e.g. repeatability, is low for modern Fourier-transform FT-NIR instruments with cooled detectors.

The sampling procedure is recognized as a major contributor of error in the final result when samples are withdrawn with a sample thief[12]. When using a NIR probe, the sampling variance component, $\sigma^2_{\text{sampling}}$ is believed to be affected by some of the same phenomena as sample thieves e.g. transportation of powder from higher placed layers when penetrating the mixture. Some studies recommend sample thieves with front sampling instead of side port sampling. A NIR probe can be compared to a front sampling thieve. When the NIR probe is inserted into the powder mixture at a given position, the probe can be tilted slightly prior to the measurement in order to measure an undisturbed sample. This method has been tested in our laboratory and it appears to be an efficient way to avoid sampling material which has been transported with the probe during insertion.

Another advance of NIR is that no sample preparation is required which in return minimize sampling error. Finally, using a proper preprocessing and wavelength selection of the NIR spectra would minimize the influence of artefacts in the spectra from varying particle sizes or other physical parameters.

The variance component due to the random mixture, $\sigma^2_{\text{random mixture}}$, is the inherent variance one observes in a random mixture. This is the variation in API concentration between several measurements inside the random mixture. This variation greatly depends on the sample size[11]. An increase in sample size will show a decrease in this variance component. The last variance component $\sigma^2_{\text{heterogeneity}}$ (the mixing component) represents the degree of heterogeneity. In a random mixture the variance due to heterogeneity will be zero. Thus in monitoring homogeneity, the actual test is whether the $\sigma^2_{\text{heterogeneity}} = 0$.

Net Analyte Signal (NAS)

When the analyte of interest is absorbing in the near-infrared (NIR) wavelength region and the shape of the analyte spectrum and interfering constituents spectra is different, a net analyte signal (NAS) vector, which is unique for the analyte, can be derived. The NAS vector is defined as the part of the sample spectral vector that is orthogonal to a subspace called the interferent space. The NAS vector is unique for the analyte of interest in the given mixture of interferents. The interferent space is spanned by spectral vectors of the interfering constituents in the sample matrix i.e. all other components except for the analyte of interest. In order to construct a robust NAS vector sufficient variation should be present in the NIR measurements of interferents mixtures. This can be assured by manufacturing batches of interferents mixtures after designed experiments.

Notation

The following notation is used during the presentation of equations. Boldface capital characters denote matrices, boldface lower-case characters denote vectors and lower case italic characters denote scalars, superscript T denotes the transposed matrix or vector and the superscript + denotes the Moore-Penrose generalised inverse of a matrix. The matrix $\mathbf{I}_J$ is the *J*×*J* identity matrix.

Calculation of the NAS value of a spectrum

Using a set of NAS vectors, a NAS regression vector can be calculated. With the NAS regression vector the net analyte signal value or simply the net analyte signal of a sample spectrum can be computed. The NAS is directly proportional to the analyte concentration[13] which makes this value a potential candidate to be used to evaluate the distribution of analyte in a set of samples.

To compute the NAS regression vector, first the interference space needs to be defined. Pure component spectra of the interferents can be used to span the interferent space. In our experience[14-16] it is better to use spectra of blank samples i.e. mixture samples of the interfering constituents only.

First the anti-projector ($\mathbf{A}_{\mathbf{R}}$) is constructed using a set of blank spectra ($\mathbf{R}_{-k}$).

$$\mathbf{A}_{\mathbf{R}} = \left(\mathbf{I}_J - \mathbf{R}_{-k}\mathbf{R}_{-k}^{+}\right) \qquad \textbf{Equation 2}$$

$\mathbf{R}_{-k}$ is a $J \times I_b$ matrix with I_b blank spectra measured at J channels. The subscript $-k$ indicates that the spectra does not contain NIR response from the analyte k. $\mathbf{R}_{-k}^{+}$ is the pseudo-inverse matrix of the blank samples, an $I_b \times J$ matrix.

Next the NAS regression vector is computed with a set of model spectra ($\mathbf{R}_{\text{mod}}$). Pure analyte spectra or spectra of samples with the interfering constituents and the analyte can be used. The latter is preferred because the spectral response of the analyte in presence of other constituents might be different than the spectrum of the pure analyte alone. With the anti-projection matrix and the model spectra the orthogonal part to the interferent space can now be computed.

$$\mathbf{B} = \mathbf{A}_{\mathbf{R}} \cdot \mathbf{R}_{\text{mod}} \qquad \textbf{Equation 3}$$

The $\mathbf{B}$ is a $J \times I_{\text{mod}}$ matrix with I_{mod} vectors which all are orthogonal to the interference space and point more or less in the same direction. The average vector $\mathbf{b}$ is used to define the unique NAS direction and is called the NAS regression vector.

$$\mathbf{b} = \frac{\sum_{i=1}^{I_{\text{mod}}} \mathbf{B}_i}{I_{\text{mod}}} \qquad \textbf{Equation 4}$$

With the NAS regression vector, the NAS value of a sample spectrum ($\mathbf{r}$, a $J \times 1$ vector) can be computed simply as the score of the projected spectral vector onto the NAS regression vector.

$$nas = \mathbf{r}^{\mathrm{T}}\mathbf{b} \qquad \textbf{Equation 5}$$

Development of a qualitative model based on NAS values

In the early stages of a drug development program different formulations are assessed. Development of quantitative NIR models using several calibration batches for each formulation would require many resources. A qualitative method that requires a minimum of resources is therefore beneficial. The proposed method requires two batches; (1) a placebo batch and (2) a batch with API that is homogeneous mixed i.e. a 'golden batch' where the $\sigma^2_{\text{heterogeneity}} = 0$. In the following a stepwise procedure is described how to develop the qualitative method and control charts. Pre-processing method and wavelength selection of the NIR spectra are chosen based on the SE indicator[14].

Step 1: A placebo batch is measured with the NIR probe. The spectra are used to calculate the anti-projector (Equation 2).

Step 2: A batch with 100 % of the concentration in the final drug product is prepared and mixed until homogeneity and then measured extensively with the NIR probe. This batch is named ‘golden batch’ in the text.

Step 3: A few spectra from the ‘golden batch’ are used as model spectra ($\mathbf{R}_{\text{mod}}$) and the NAS regression vector is calculated (Equation 3 and 4).

Step 4: The NAS values of the remaining spectra from the ‘golden batch’ are calculated with equation 5.

Step 5: The mean NAS value $\overline{nas}_{\text{gb}}$ and variance $s^2_{\text{total nas, gb}}$ of the NAS values are determined.

Step 6: Finally two control charts are constructed; a variance and mean chart.

Development of control charts for qualitative NAS model

In this section are the assumptions and equations presented for limits in the control charts. Note that since it is a qualitative approach, it is not possible to test whether a new batch is on target with respect to concentration of API; it is only possible to test whether the batch is equal to a ‘golden batch’. Two charts are developed; a variance chart and a mean chart.

Variance chart

In the variance chart the variance for a new batch is compared statistically to the variance of the ‘golden batch’. Comparison is done using the ratio between the variance of the new batch and the variance of the ‘golden batch’. The ratio of variances follows an F-statistic;

$$\frac{\mathbf{s}^2_{\mathbf{total\,nas,new}}}{\mathbf{s}^2_{\mathbf{total\,nas,gb}}} \propto \mathbf{F}_{(\alpha,\mathbf{N_{new}}-1,\mathbf{N_{gb}}-1)}$$

where N_{gb} is the number of spectra used to calculate the ‘golden batch’ variance. A one-sided *F* test is used because it is assumed that in monitoring homogeneity, the actual test is whether $\sigma^2_{\text{heterogeneity}} = 0$. The assumption is that the ‘golden batch’ has zero heterogeneity and if the new observation would deviate from the ‘golden

batch' then $\sigma^2_{\text{heterogeneity, new}} > 0$. The upper control limit is then calculated using the following equation:

$$\text{upper control limit} = s^2_{\text{total nas, gb}} \times F_{(\alpha, N_{\text{new}}-1, N_{\text{gb}}-1)}$$ **Equation 6**

Where the critical value can be found in an *F* table.

Although the variance of a new batch is expected to be equal to or higher than that of the 'golden batch', in some cases, a lower variance could be found. A lower variance does not signal for heterogeneity, but for model incompetence or probe fouling. Therefore, do we also calculate a lower limit which is called the warning limit;

$$\text{warning limit} = s^2_{\text{total nas, gb}} \times F_{(1-\alpha, N_{\text{new}}-1, N_{\text{gb}}-1)}$$ **Equation 7**

Mean chart

If the two variance of the new batch is equal to the 'golden batch', the mean of the new batch can be compared to the mean of the 'golden batch'. This is done by computing the t-value for the new batch and then plot the t-value in the mean chart and compare to the critical value obtained from a table of critical values of *t*;

$$t - value = \frac{\overline{nas}_{\text{new}} - \overline{nas}_{\text{gb}}}{s \cdot \sqrt{\frac{1}{N_{\text{new}}} + \frac{1}{N_{\text{gb}}}}}$$

where s is calculated from : **Equation 8**

$$s^2 = \frac{(N_{\text{new}} - 1) \cdot s^2_{\text{total nas, new}} + (N_{\text{gb}} - 1) \cdot s^2_{\text{total nas, gb}}}{N_{\text{new}} + N_{\text{gb}} - 2}$$

The critical t-values can be found for a α confidence level and (N_{new}+N_{gb}-2) degrees of freedom. A two-sided test will be used for the t test to detect whether the operator put too much or too little API in the mixer (compared to the 'golden batch'). The control limits for the mean chart are then;

$$\text{control limits} = 0 \pm t(\alpha / 2, N_{\text{new}} + N_{\text{gb}} - 2) \quad \textbf{Equation 9}$$

The critical step in this method is in step 2. It is stated that a batch is mixed to homogeneity ('golden batch') and then measured extensively with NIR. One approach to identify the point of homogeneity could be to make a temporary NAS model. First the anti-projector is calculated from the placebo batch spectra. Carry out a few minutes of mixing of the calibration batch and measure a few NIR spectra. These spectra are used to calculate a temporary NAS regression vector. Then continue mixing of the calibration batch. At different time points the mixer is stopped and high number (e.g. fifty) NIR spectra are recorded. The NAS values of the spectra are calculated with the temporary NAS regression vector. By simply plotting the variance over time the point of homogeneity can be identified as time point with lowest variance.

Development of a quantitative model based on NAS values

When a final formulation has been chosen during the R&D development phase more calibration work can be added and a quantitative model between the NIR spectra and the API concentration developed. A major benefit of a quantitative model is that numbers are now expressed in concentration of the API which is comparable to the standard regulatory methodologies. Also now the mean can be compared to the target content of API instead of mean of 'golden batch'.

The development of the quantitative method is described by the following steps:

Step 1: First a placebo batch is prepared and measured with the NIR probe. The spectra are used to calculate the anti-projector (Equation 2).

Step 2: A set of calibration batches spanning a fair API concentration range are prepared e.g. 70, 85, 100, 115 and 130% of the concentration in the final drug product. The batches are mixed until they are homogeneous and measured extensively with the NIR probe. The spectra are split into a calibration set and a test set.

Step 3: The calibration spectra from each batch are averaged to one calibration spectrum for each calibration batch. Each calibration spectrum is assigned a reference value which is the average API concentration in the particular calibration batch. This value is known from the preparation of the calibration batch[8].

Step 4: A few spectra from one of the calibration batches are used as model spectra ($\mathbf{R}_{\mathrm{mod}}$) and the NAS regression vector is calculated (Equation 3 and 4).

Step 5: Now the NAS value of the average calibration spectra and some extra placebo spectra is calculated (Equation 5). These extra placebo spectra should not have been used to construct the anti-projector in step 1.

Step 6: The NAS values of the average calibration spectra are plotted against their reference value in a NAS value vs. concentration plot. A straight line is fitted to the points in a least square sense. With the equation for the line (calibration model) the API concentration can now be calculated for a given spectrum [17].

Step 7: With the calibration model the API concentration c is predicted in all test set spectra.

Step 8: The variance $\mathbf{s}^2_{total\ \mathbf{c},\,gb}$ is determined of all concentration predictions as the pooled variance from all test set data.

Because all calibration batches are assumed to be homogeneous all concentration predictions from the test set can be used to calculated a pooled variance which provides more degrees of freedom;

$$s^2_{\text{total}\,c,\,\text{gb}} = s^2_{\text{pooled}} = \frac{\sum_{i=!}^{N_1}\left(c_{1,i} - \bar{c}_1\right)^2 + \sum_{i=!}^{N_2}\left(c_{2,i} - \bar{c}_2\right)^2 + \ldots}{\left(N_1 - 1\right) + \left(N_2 - 1\right) + \ldots}$$ **Equation 10**

Where $\bar{c}_1$ is the average concentration of N_1 predictions from calibration batch 1.

Step 9: A variance and a mean chart is developed and used for monitoring of future batches.

Development of control charts for quantitative NAS model

Variance chart

For the quantitative NAS model, also the spread in the measurements is compared to the spread found for the 'golden batches' in the same way as was presented for the qualitative NAS model. The limits are calculated in the same way substituting variance of NAS values with the pooled variance of the concentration predictions.

$$\frac{s^2_{\text{total}\,c,\,\text{new}}}{s^2_{\text{total}\,c,\,\text{gb}}} \sim F(\alpha, N_{new} - 1, N_{gb} - 1)$$

Mean chart

With the quantitative model the mean of a new batch can be compared to the target concentration of the product (instead of comparing to the mean a 'golden batch' of which the exact API concentration is unknown). This implies that the mean chart now compares whether the average concentration is within target limits.

The mean chart is constructed like a Shewart chart[18] and the control limits are then;

$$\text{control limits} = \text{target} \pm t_{(\alpha/2, N_{\text{gb}}\text{-1})} \cdot \frac{s_{\text{total c, gb}}}{\sqrt{N_{new}}} \qquad \textbf{Equation 9}$$

Experimental section

NIR measuring techniques

All NIR measurements were measured with the same Bruker FT-NIR spectrometer, MPA (Multi Purpose Analyzer) [19]. An extended length fibre optic sampling probe with pistol grip was used. The probe was fitted to the MPA with a 1.5 m optical fibre. The probe head diameter is 14 mm and the optical window has a diameter of 4 mm. The length of the probe is 325 mm. A resolution of 8 cm^{-1} was used. The spectral range from 4000 cm^{-1} to 12794 cm^{-1} was scanned. As background, a Spectralon disc was used with 32 coadded scans per spectrum. For sample spectra 16 co-added scans per spectrum were used. The acquisition time per sample spectrum was approximately 8 seconds which is a practical time for a steady handheld measurement. The reflectance signal from the sample in front of the probe was detected with an InGaAs detector.

Reference analysis

Powder samples that were removed from the batches were of approximately 300 mg of size. The samples were analyzed with a HPLC method. First the samples were dissolved followed by injection into the HPLC system which used UV-detection at 275 nm, a C18 column and a mobile phase consisting of a salt buffer and acetonitril.

Composition of pharmaceutical mixture

The analyte of interest was the active pharmaceutical ingredient (API). For reasons of secrecy the chemical identify of the API can not be revealed. All batch sizes were 1000 grams and the composition is listed in Table 1. All mixing was performed in a drum mixer.

Table 1. Mixture composition.

Component	Gram	w/w %
API	100	10
Microcrystalline cellulose	200	20
Tablettose	677.5	67.75
Magnesium stearate	7.5	0.75
Talc	15	1.50
Sum	1000	100

Experiments

In Table 2 is a list of the batches that were used. In the calibration batches the API was interchanged with microcrystalline cellulose and tablettose while maintaining the weight ratio between the microcrystalline cellulose and tablettose.

Table 2. Batch overview.

Name	Description and sampling	Use
Placebo batch	No API is added	Calculating of the anti-projector
70%, 85%, 100%, 115% and 130% calibration batches	Varying amount of API from 7 to 13 w/w %. Fifty NIR spectra/batch Thirty samples for HPLC analysis/batch	Calibration and calculating control limits
Mixing batch	A batch with 10 w/w % API. Fifty spectra/time point. Several time points measured during mixing.	Demonstrate how the methods could be used to monitor a mixing process
Validation batches (4 batches)	Each was with 10 w/w % API concentration. The batch differences were mixing time and mixing order Thirty NIR spectra/batch Twelve samples for HPLC analysis/batch	Used to validate the NIR methods

NIR measurements and samples analyzed with reference method

Ninety spectra were recorded in the placebo batch. From each of the calibration batches, fifty spectra were recorded. In the mixing experiment the mixer was stopped at various time points, the lid was removed and fifty spectra were recorded at each time point. In all experiments an evenly spatial placement of the probe in the powder mixture was attempted. Samples were also removed for HPLC analysis in the calibration batches and in the validation batches.

Data acquisition and analysis

All spectra were collected using the OPUS 4.2 software for the NIR instrument[20]. The spectra were converted from the OPUS format to Jcamp and imported into

MatLab 6.5[21] using in-house written routines. All data analysis was performed in MatLab using in-house developed algorithms.

Results and discussion

In this section first a qualitative model and control charts are developed. The mixing data are applied to the qualitative model. Then a quantitative model is developed and the mixing data assessed. The NIR models are validated by comparison with HPLC. Finally, the influence of number of spectra on the method is evaluated.

Qualitative model.

Model and control charts.

Twenty three placebo spectra were used to develop the anti-projector $\mathbf{A}_R$ (see eq 2). A calibration batch with 10 w/w % API was prepared. After mixing, fifty spectra were recorded with the probe in the mixer. Five spectra were used as model spectra to calculate the NAS regression vector. Using the NAS regression vector the NAS values were calculated for the remaining forty five spectra. The limits for the variance and mean charts were calculated.

Mixing data.

A batch with a composition of 10 w/w % API was prepared. During the mixing of the batch the mixer was stopped at time points 16, 20, 25, 30, 35 and 40 minutes. At each time point fifty spectra were recorded in the mixer. The variances and means were calculated and plotted in the control charts (Figure 1). The results showed that at time points 16, 20, 25 and 30 minutes the variance was comparable to the ‘golden batch’. At time points 35 and 40 the variance was higher then in the ‘golden batch’ showing that demixing took place. The means from time point 16, 20, 25 and 30 were compared to the ‘golden batch’ in the mean chart. They were all within the limits and therefore not different from the mean of the ‘golden batch’. The means of time point 35 and 40 minutes are

indicated with (x) since the equal variance requirement for the t-test was not fulfilled anymore and thus the results cannot be trusted.

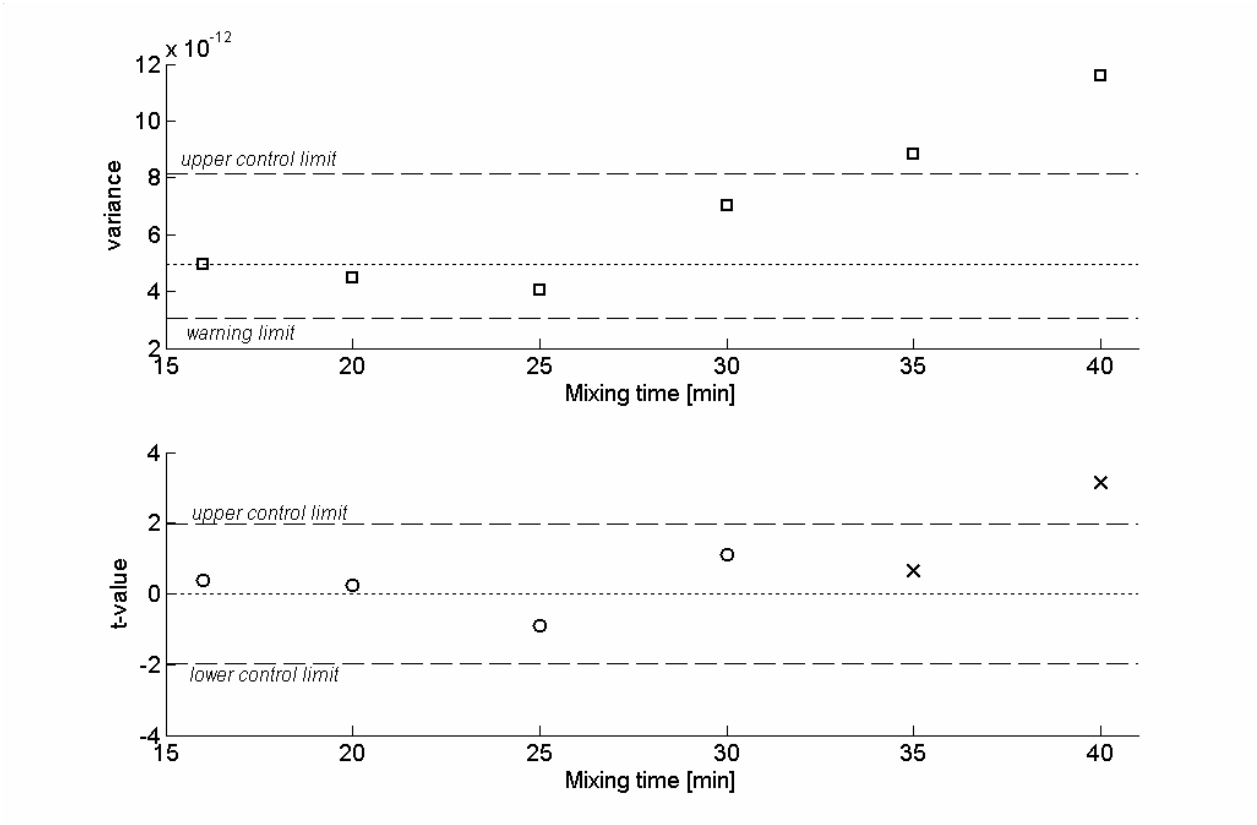

Figure 1. Mixing experiment data plotted in variance and mean chart using qualitative method. The mean values symbolized with × indicate that the assumption for the t-test is not fulfilled because the variance is different from the 'golden batch'.

Quantitative model.

Model and control charts

To develop the quantitative model another four calibration batches were prepared i.e. with 7, 8.5, 11.5 and 13 w/w % API. In all five calibration batches (including the 10 w/w % batch used in the qualitative model) fifty spectra were recorded when they were homogeneously mixed. The spectra from each batch were split into twenty spectra that were used to construct an average calibration spectrum for each calibration batch and thirty spectra called test set spectra. Also after recording of the spectra, thirty powder samples (each approximately 300 mg)

were removed from every calibration batch and subject to HPLC analysis. Now the anti-projector was developed. Five spectra from the 130% batch were used to calculate the NAS regression vector. The average calibration spectra from each of the 5 calibration batches and the NAS regression vector are depicted in Figure 2. The methodology of using average spectra of powder samples and assigning the nominal batch concentration was first demonstrated by Berntsson et al [8]. In this study it showed to be a very easy, fast and precise method for making the quantitative calibration models.

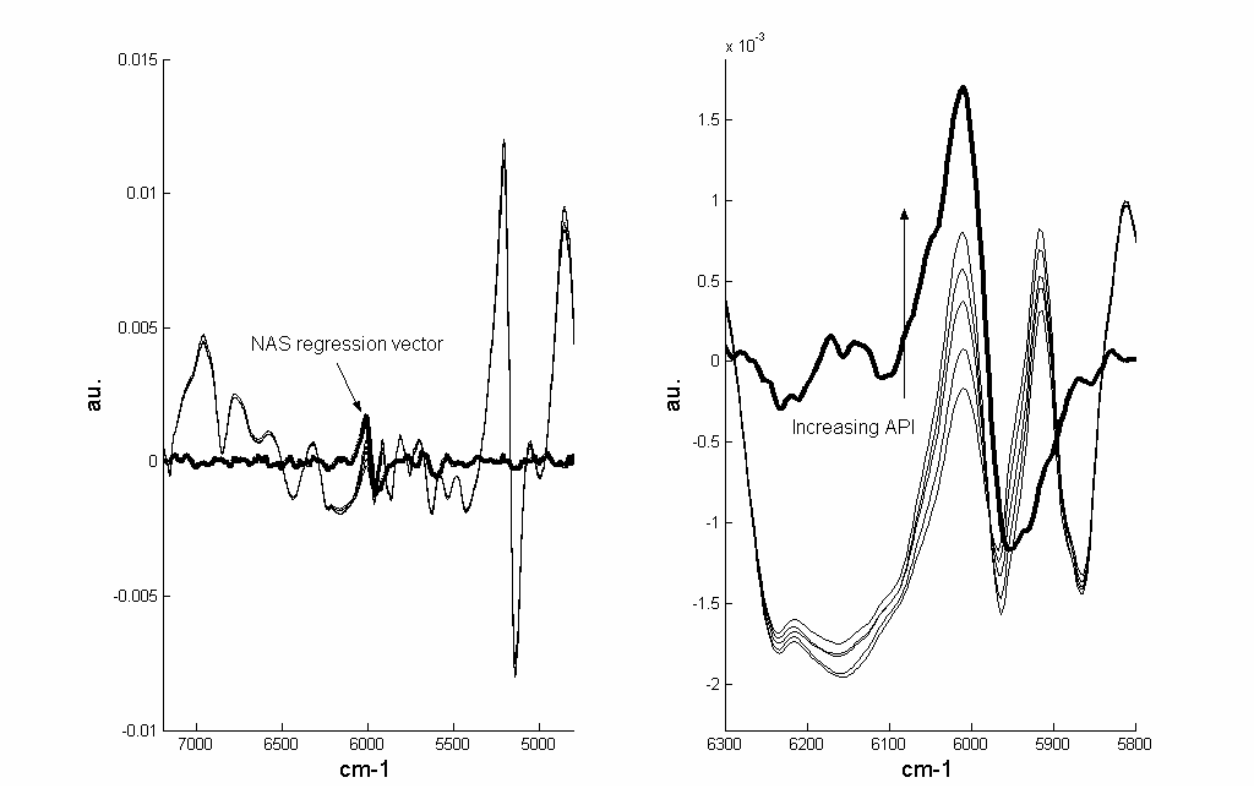

Figure 2. The five average calibration spectra and the NAS regression vector (bolded line) (left). The API had a characteristic peak near 6000 cm-1. This feature was easily recognized in the calibration spectra and the NAS regression vector (right).

The NAS values of the average calibration spectra and twenty extra placebo spectra were plotted against their reference values (symbolized with circles in Figure 3) and a straight line was fitted to the points in a least square sense (line in Figure 3). The correlation coefficient was 0.9998. The NAS values of test set

spectra were also plotted in order to demonstrate the variance of the API within each batch (symbolized with dots in Figure 3).

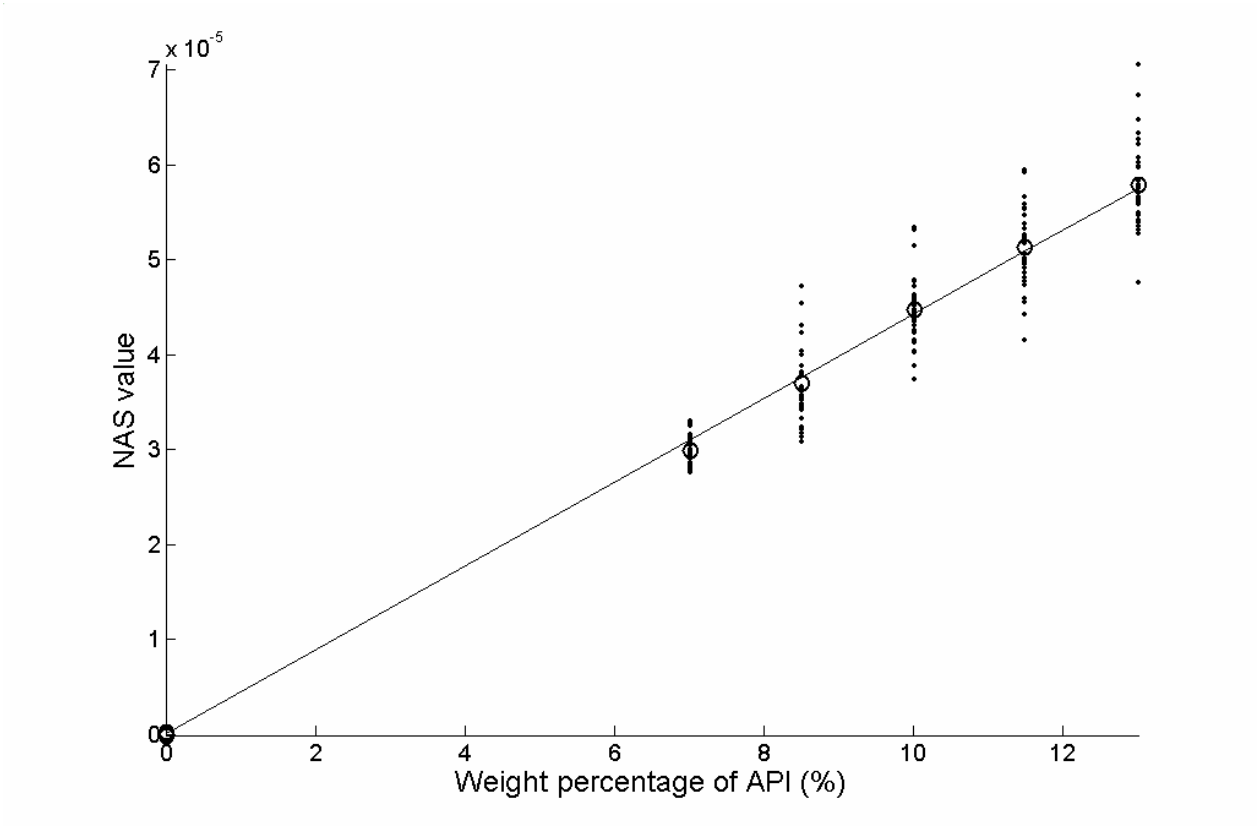

Figure 3. NAS values vs. concentration plot. The ○ symbolizes the average calibration spectra and the dots symbolize the test set spectra.

Using the calibration model concentration predictions were obtained from the test set spectra. The pooled variance was calculated and control charts made.

Mixing data.

The concentration predictions of the mixing data were calculated. Variances and means were plotted in the variance chart and mean chart (Figure 4).

The variances at time point 16, 20 and 25 minutes were all within the limits and at 25 minutes the variance was lowest. The variances at 30, 35 and 40 minutes were higher then the ‘golden batches’. This behaviour of the variances clearly

shows a de-mixing behaviour i.e. optimal mixing time existed around 20-25 minutes and further mixing worsened homogeneity.

The means at 16, 20 and 25 minutes were also within the target limits. At 25 minutes the batch was on target with a variance comparable to the 'golden batch'. This optimal mixing time was also identified using the qualitative model.

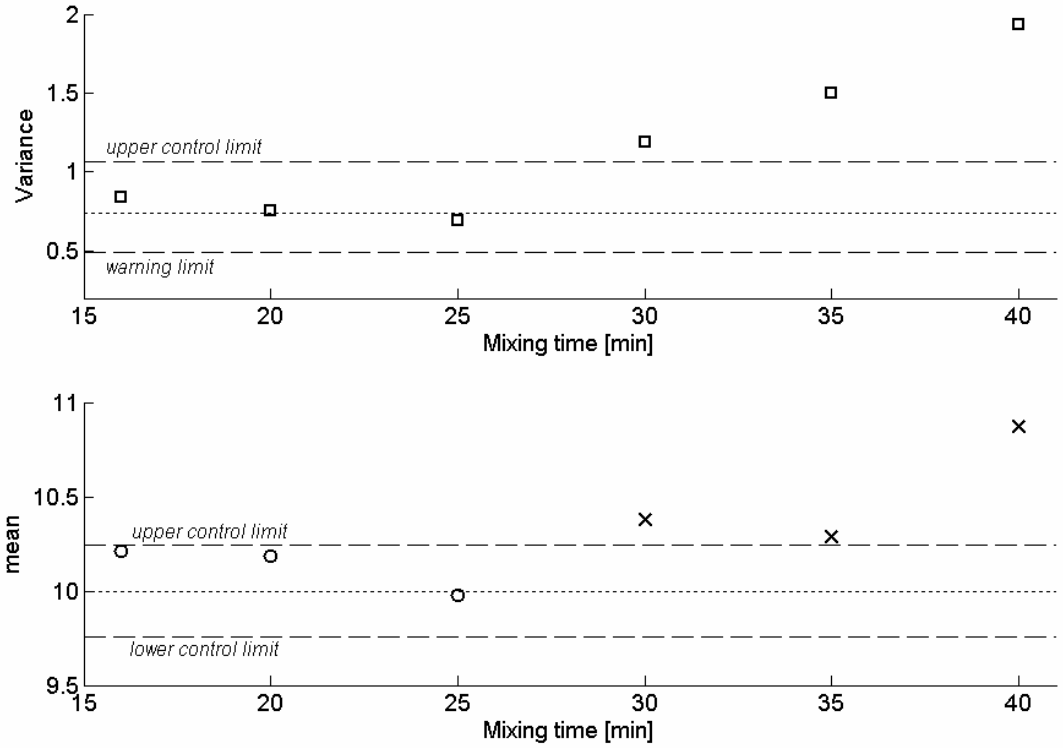

Figure 4. Mixing experiment data in variance chart and mean chart using quantitative model. The mean values symbolized with × indicate that the assumption for the t-test is not fulfilled because the variance is different from the 'golden batches'.

The results showed that with the qualitative NAS method it was possible to monitor API homogeneity though no calibration model with reference values was developed. The qualitative method required fewer batches and is therefore a strong candidate as method in the early development stages. The advantage of the quantitative model over the qualitative approach was that tighter limits were obtained due to the more degrees of freedom and calculations were in

concentration values. Also the mean could be compared to the declared target content of the pharmaceutical product. These differences make adaptation into a highly regulated manufacturing environment easier and the interpretation is straightforward.

Secondly, by making a quantitative calibration line, non-linear behaviour can be detected and more confidence can be put into the pre-processing method and wavelength selection, this is not possible in the qualitative model. With the current formulation no such problems were observed but this is not always the case.

Validation of proposed methods

To validate the NIR methods comparisons were made between traditional HPLC and NIR using four different validation batches. All four validation batches were prepared with 10 w/w % API. The differences between the batches were the order of mixing the constituents and the mixing time. When mixing was finalized, thirty NIR spectra were recorded and twelve powder samples were removed for HPLC analysis from each batch. First results from HPLC will be demonstrated and then compared to NIR results.

Validation batch evaluation using HPLC

From the 100% calibration batch ('golden batch') thirty powder samples of three hundred mg were removed and subject to HPLC analysis. A variance chart was developed. The limits were calculated using equation 6 and 7, substituting $s^2_{\text{total nas, gb}}$ with $s^2_{\text{total HPLC, gb}}$ and a mean chart was developed using 10 w/w % as target and equation 9 to calculate the upper and lower control limits, substituting $s_{\text{total } c\text{, gb}}$ with $s_{\text{total HPLC, gb}}$.

Now for each of the four validation batches the following was done; the variance and mean of the twelve HPLC values were calculated and plotted in the variance

and the mean chart. (Figure 5). Outliers were identified using a Grubbs test (α=0.05) and removed prior to the calculation of the variance and mean.

The variances of Batch 2 and 4 were within the limits and thereby equal to the 'golden batch'. The variance of Batch 1 and 3 was below the warning limit signalling model incompetence. The means of the validation batches were all lower then the target value. The means of batch 1 and 3 (symbolized with ×) could not be compared with the 'golden batch' using the t-statistic because their variances were different from the 'golden batch'.

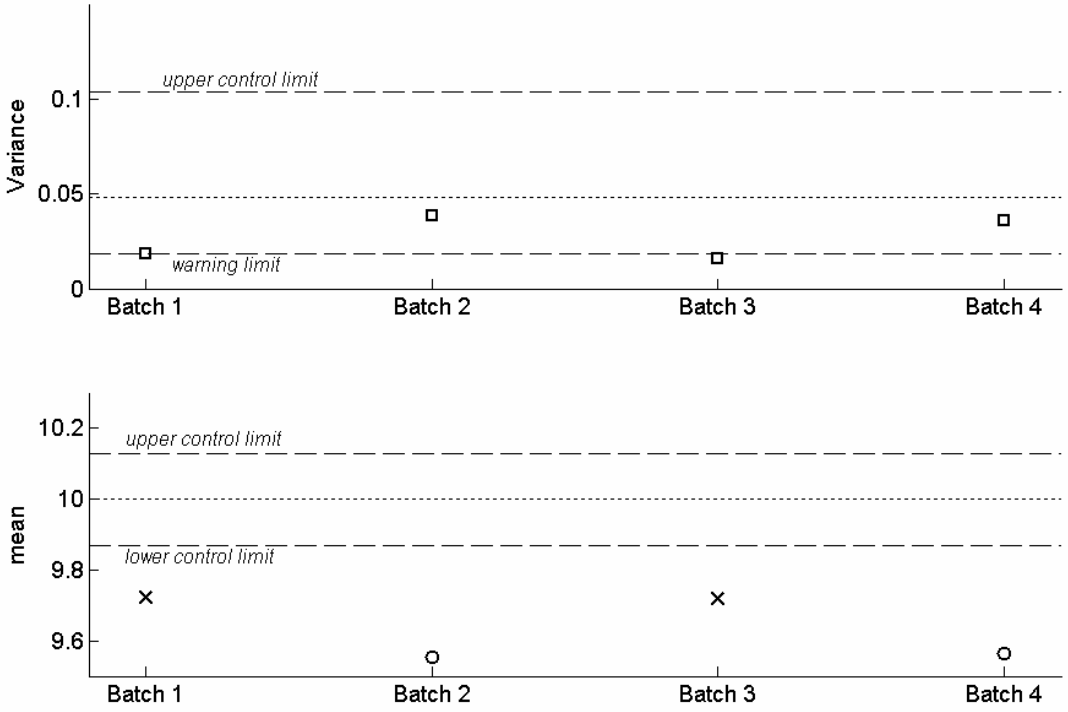

Figure 5. Variances and means of HPLC values from validation batches in variance and mean charts.

Validation batch evaluation using NIR

Concentration predictions of the NIR spectra from the four validation batches were calculated. Variances and means were calculated and plotted in the control charts (Figure 6). The variances for batch 2 and 4 were within the upper control

limit and the warning limit. The variances of batch 1 and 3 were below the warning limit signalling model incompetence as in the HPLC variance chart.
The mean of batch 1 was on target but due to the fact that the variance of batch 1 was different from the 'golden batch' the mean could not be compared to the 'golden batch' using t-statistics. The means of batch 2, 3 and 4 were below the lower control limit and smaller then target. This was also observed using HPLC.

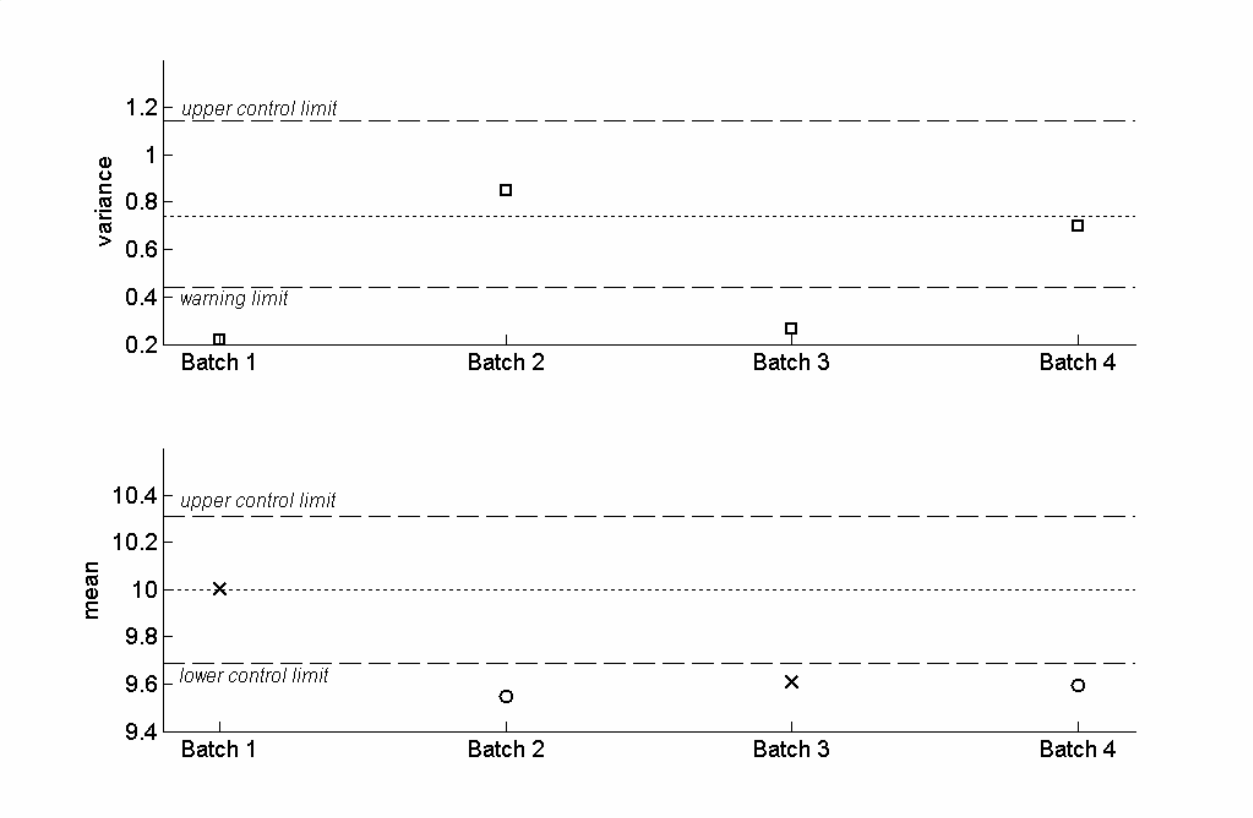

Figure 6. Variances (upper figure) and means (lower figure) of concentration NIR predictions for the validation batches.

The conclusions when using NIR or HPLC were comparable i.e. the variances of batch 2 and 4 were similar to the 'golden batch' and their means below the target value. Also the variances of batch 1 and 3 were below the warning limit signalling model incompetence.

When the control limits for the HPLC values were compared to the control limits for the quantitative NIR method it was clear that there were big differences. The reason was the effective sample size in the two methods which was very different. In the HPLC method the average sample weight was approximately 300 mg. The effective sample size in a NIR measurement is defined as the amount of sample that contributes to the spectrum. It is difficult to quantify the effective sample size for a NIR spectrum but some methods have been proposed[22]. Effective sample size ranged from 34 to 492 mg/cm^2 illuminated spot area in some typical pharmaceutical powders. The NIR probe used in this study had a spot area of 0.13 cm^2 which would correspond to effective sample sizes from of 5 to 64 mg.

Control limits dependency on number of samples

The ultimate method to characterize blend homogeneity would be a technique where the entire batch would be sampled. In practice this is not possible and one has to consider how many times it is needed to stick the probe into the powder bed in order to make a good characterization of the homogeneity.

When the 'golden batch' is measured with NIR, many spectra e.g. fifty to hundred should be used. If new batches are evaluated at many time points and in a manufacturing environment these numbers of spectra are maybe not practical. Therefore the influence of number of spectra was examined. In order to show how the number of spectra would influence the control limits and the conclusions one derives from the results, spectra from the mixing experiment were used. In the mixing experiment de-mixing was clearly identified at 40 minutes. Because of the clear indication of a heterogeneous mixture at time point 40 minutes, the fifty concentration predictions from time point 40 minutes were used for demonstration because they were excellent to demonstrate the danger of using too few measurements to detect de-mixing.

First control limits for the variance and the mean chart were calculated using different values for N_{new} from three to fifty. The control limits were plotted against N_{new} (Figure 7). As expected the control limits were wide for small N_{new} and narrowed when N_{new} increased. Then the fifty concentration predictions and variances and means were calculated using different number of concentration predictions (N_{new}). Example wise for $N_{new} = 10$ the calculations were made in the following manner;

Ten values were picked randomly from the original fifty concentration predictions. After a value was picked it was "returned" meaning that each value had the same probability of being picked every time a value was selected i.e. bootstrap re sampling[23]. The mean $\bar{c}$ and variance $s^2_{total,c}$ were calculated from the ten values. Step 1-2 was repeated hundred times. The hundred mean and variance calculations were plotted in the control charts. Step 1-4 were performed using 5, 10, 15, 20, 25, 30, 35, 40, 45 and 50 values using the power calculation method described above. The results are displayed in Figure 7.

It was observed that when using a small number of samples e.g. ten a large proportion of the variances and means were within the control limits (Figure 7) though they supposed to be above the upper control limits in both charts. When the number of samples was increased to twenty, only a few results were below the upper warning limits.

The results showed how the risk of committing a Type II error (false positive) increased if N_{new} was low. One has to balance the risk of committing Type II errors with a practical number of spectra in order to choose N_{new} . In the present case twenty spectra seemed sufficient to identify de-mixing.

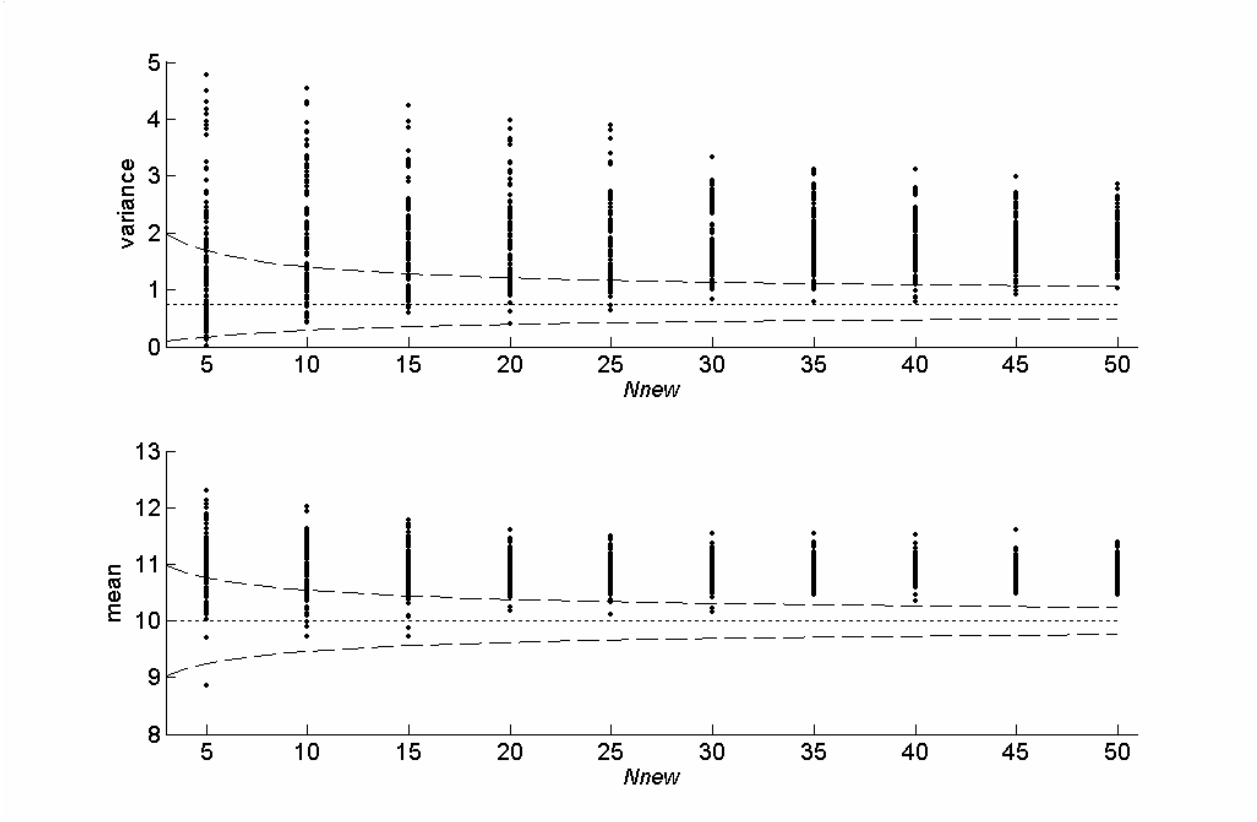

Figure 7. Control limits as a function of number of samples used to calculate limits.

Conclusions

Two NIR models were developed for monitoring blend homogeneity using a NIR probe. First a qualitative model using NAS values from a well mixed batch were used to generate control charts for future observations. Second a quantitative regression model between NAS values and reference concentration was developed for a set of calibration batches. With the regression model and well mixed batches, control charts were developed for the quantitative model. The qualitative method required less batches to develop and the performance was similar to the quantitative model but some other advantages of the quantitative method were presented. The qualitative model is suitable for initial R&D studies when developing a new solid dosage form drug product. When further development activities have been conducted or prior to implementation in manufacturing supplementary calibration batches can be measured and a

quantitative model developed. Generally the models are easily developed and the method and control charts mimics to some degree the current methodologies for determination of blend uniformity which makes implementation or replacement of current methods easier.

In our opinion the proposed methods are better to compare mixing processes and formulation performance then current methods[1]. In current methods two statistics are usually calculated and used for homogeneity evaluation and batch to batch comparison i.e. the mean value ($\bar{c}$) and the relative standard deviation (RSD%). The RSD% is calculated by dividing standard deviation with the mean value ($\mathrm{RSD\%} = 100\% \cdot s/\bar{c}$). The RSD% is then dependent on two numbers and therefore not a good statistic to do batch-to-batch comparison of homogeneity i.e. different information is mixed up in the statistic. With our proposed NIR methods the comparison is performed with two statistics i.e. mean concentration and variance which are independent and both can be directly compared to the target concentration of the drug product and the variance of a well mixed batch. Another aspect of the methods is that the control limits are based on actual process measurements and is therefore related to the process capability. In the standard regulatory approaches limits are generic limits and do not relate to the specific formulation or process.

The proposed methods were validated by comparing results obtained with NIR and with traditional HPLC analysis. The comparisons showed that both the qualitative and quantitative NIR models showed similar results as HPLC.
It was shown how the width of the control limits decreased when more samples were used and how the risk of committing a type II observation error also dropped when the number of measurements were increased. The result was used to provide guidance of picking a practical number of measurements.
The influence of the effective sample size on the variance was demonstrated by comparing NIR variance with HPLC variance. The NIR variance was

approximately ten times higher then the HPLC variance because of the small sample size in NIR.

The NIR models and control charts were used for monitoring of a mixing study and evidence was found of de-mixing after certain duration of mixing. The result showed the necessity and importance of monitoring tools like the proposed NIR methods.

Acknowledgements

Novo Nordisk, Corporate Research Affairs (CORA) who sponsored this work as a part of E.T.S. Skibsted's Ph.D. project. Technician Inga Fuchs who performed most of the mixing experiments and the staff at Analytical Development, CMC Development, Novo Nordisk A/S who performed the HPLC analysis.

References

[1] Chapter <905> Uniformity of dosage units, in: U.S. Pharmacopeia (USP), 2003, pp. 2227-2229.

[2] F.C. Sánchz, J. Toft, B. Bogaert, D.L. Massart, S.S. Dive, P. Hailey, Fresenius J.Anal Chem 352 (1995) 771-778.

[3] S.S. Sekulic, H.W. Ward, D.R. Brannegan, E.D. Stanley, C.L. Evans, S.T. Sciavolino, P.A. Hailey, P.K. Aldridge, Analytical Chemistry. 68 (1996) 509-513.

[4] D.J. Wargo, J.K. Drennen, Journal of Pharmaceutical and Biomedical Analysis. 14 (1996) 1415-1423.

[5] P.A. Hailey, P. Doherty, P. Tapsell, T. Oliver, P.K. Aldridge, Journal of Pharmaceutical and Biomedical Analysis. 14 (1996) 551-559.

[6] S.S. Sekulic, J. Wakeman, P. Doherty, P. Hailey, Journal of Pharmaceutical and Biomedical Analysis. 17 (1998) 1285-1309.

[7] R.D. Maesschalck, F.C. Sánchz, D.L. Massart, P. Doherty, Applied Spectroscopy. 52(5) (1998) 725-731.

[8] O. Berntsson, L.-G. Danielsson, M.O. Johansson, S. Folestad, Analytica Chimica Acta. 419 (2000) 45-54.

[9] O. Berntsson. Characterization and Application of Near Infrared Spectroscopy for Quantitative Process Analysis of Powder Mixtures. Doctoral Thesis (2001) Kungl Tekniska Högskolan, Department of Chemistry, Stockholm.

[10] A.S. El-Hagrasy, H.R. Morris, F.D. Amico, R.A. Lodder, J.K. Drennen, Journal of Pharmaceutical sciences. 90(9) (2001) 1298-1307.

[11] O.Vaizoglu, Tr.J.of Physics. 23 (1999) 97-104.

[12] F.J. Muzzio, P. Robinson, C. Wightman, D. Brone, International Journal of Pharmaceutics 155(2) (1997), 153-178.

[13] A. Lorber, Analytical Chemistry. 58 (1986) 1167-1172.

[14] E.T.S. Skibsted, J.A. Westerhuis, H.F. Boelens, A.K. Smilde, D.T. Witte, Applied Spectroscopy. 58 no. 3 (2004) 264-271.

[15] P.W.Hansen, Journal of Chemometrics. 15(2) (2001) 123-131.

[16] H.F. Boelens, W.T. Kok, O.E. de Noord, A.K. Smilde, Analytical Chemistry. 76 (2004) 2656-2663.

[17] N.M. Faber, Chemometrics and Intelligent Laboratory Systems. 50 (2000) 107-114.

[18] J.N. Miller, J.C. Miller, Statistics and Chemometrics for Analytical Chemistry, fourth ed., Pearson Prentice Hall, Harlow, 2000.

[19] http://www.brukeroptics.com.

[20] Brukeroptics. OPUS ver. 4.2

[21] MathWorks Inc. MatLab ver. 6.5 R13.

[22] O. Berntsson, L.G. Danielsson, S. Folestad, Analytica Chimica Acta. 364 (1998) 243-251.

[23] B. Efron, R.J. Tibshiran,. An introduction to the bootstrap, Chapman & Hall, New York, 1993.

PAPER 3.

Net Analyte Signal Based Statistical Quality Control (NAS-SQC)

E. T. S. SKIBSTED, H. F. M. BOELENS, J. A. WESTERHUIS,* D. T. WITTE, A. K. SMILDE, N. W. Broad and D. R. Rees.

Published in Analytical Chemistry ASAP papers 8. October 2005

Net Analyte Signal Based Statistical Quality Control (NAS-SQC)

Authors: E. T. S. Skibsted[a,b], H. F. M. Boelens[a], J. A. Westerhuis[a *], A. K. Smilde[a, e], Neville W. Broad[c,d], David R. Rees[d,] and Eric Witte[f]

[a]Biosystems Data Analysis, Swammerdam Institute for Life Sciences, University of Amsterdam, Nieuwe Achtergracht 166, 1018 WV Amsterdam, The Netherlands.

[b]Pharmaceutical Site Maaloev, Novo Nordisk A/S, Novo Nordisk Park, 2760 Maaloev, Denmark.

[c]Process Analytical Support Group, Global Manufacturing Services, Pfizer UK Ltd, Ramsgate Road, Sandwich, Kent, UK. CT13 9NJ.

[d]Cardinal Health Oral Technologies (Zydis), Frankland Road, Blagrove, Swindon, Wiltshire, UK. SN5 8RU.

[e]TNO Nutrition and Food Research, Utrechtseweg 48, P.O.Box 360, 3700 AJ Zeist, The Netherlands.

[f]N.V. Organon, Molenstraat 10, P.O. Box 20, 5340 BH Oss, The Netherlands.

Abstract

Net Analyte Signal Statistical Quality Control (NAS-SQC) is a new methodology to perform multivariate product quality monitoring based on the net analyte signal approach. The main advantage of NAS-SQC is that the systematic variation in the product due to the analyte (or property) of interest is separated from the remaining systematic variation due to all other compounds in the matrix. This enhances the ability to flag products out of statistical control. Using control charts the analyte content, variation of other compounds, and the residual variation can be monitored.

---

* Corresponding author: westerhuis@science.uva.nl

As an example, NAS-SQC is used to appreciate the control content uniformity of a commercially available pharmaceutical tablet product measured with near-infrared spectroscopy (NIR). Using the NAS chart, the active pharmaceutical ingredient (API) content is easily monitored for new tablets. However, since quality is a multivariate property, also other quality parameters of the tablets are monitored simultaneously. It will be demonstrated that besides the API content also the water content of the tablets as well as the homogeneity of the other compounds are monitored.

Keywords

Near-infrared Spectroscopy, Net Analyte Signal, Statistical Quality Control, Principal Component Analysis, Control Charts, Pharmaceutical, Tablet Transmission Measurements.

Introduction

Fast, non-destructive spectroscopic measurements have gained a wide spread popularity as analytical methods in the pharmaceutical industry. Most notably, the use of near-infrared (NIR) spectroscopy to measure quality variables of raw materials[1,2], intermediates[3,4,5], and final products[6,7]. Since NIR is a rapid method, non-destructive and with almost no sample preparation required, the number of samples can be increased dramatically compared to conventional laboratory analysis, such as high performance liquid chromatography (HPLC). The analysis of the API content in individual tablets can be performed by NIR in reflectance or transmittance[6] mode. To quantify the amount of API, a quantitative NIR calibration model needs to be developed prior to the future predictive measurement. In most cases, a quantitative model is developed by producing and analysing sets of samples with various levels of API concentration. The measured spectra are then split into calibration and validation sets, which are used to calibrate and validate the quantitative model.

When applying tablet samples to spectroscopic analysis, the API content is usually the primary property of interest. However, since the entire sample is measured instantaneously using transmittance NIR, the spectrum also contains information on other compounds (called excipients) as well as physical properties of the tablets. Therefore e.g. the homogeneity of the excipients as well as water content can be obtained. Especially, when the API is the minor part in the product, i.e. low dose tablets, the excipients could be controlling important quality properties like e.g. dissolution and hardness.

In this paper, we present a new method to separate a measured spectrum into three independent contributions; the net analyte signal (NAS) contribution unique for the analyte of interest in the sample, a contribution representing the other compounds in the sample, and finally, residuals with the non-systematic variation. For each of the three parts, statistical limits are developed using a set of samples, which represent samples with a good quality and from manufacturing processes which are known to be in control. This results in three control charts, which can be used for classifying future samples. If necessary, the statistical limits in the analyte chart can be substituted for real concentration limits derived from an optional calibration step. This makes it possible to determine whether the analyte content in a sample is within a specified interval.

In the experimental section, NAS-SQC is demonstrated on a pharmaceutical tablet product. One key quality parameter is to determine how much API is present in the individual tablets and the variation of the amount of API between the tablets. In this paper, we will demonstrate how NAS-SQC can be used to demonstrate that the analyte content is within a specified concentration range and also that inhomogeneity of the excipients and elevated moisture content can be detected. The methodology is applicable to any spectroscopic system that follows the Beer-Lambert law.

Theory

The main idea of the NAS-SQC method is represented in Figure 1. Spectra **r** (a red and a blue example is given) are split into three contributions, the squares on the nas ($\mathbf{b}_k$) vector representing the amount of API in the sample, the dots on the Interference space (within the ellipse) representing the composition of the excipients of the sample and the residuals ($\mathbf{r}_{res}$) represented by the dashed arrows orthogonal to $\mathbf{b}_k$. The latter represents spectral variation not accounted for by API or excipients, and in normal operating conditions only contains instrumental noise. Each of the three contributions is quantified and control charts are developed for each part. In the following, the splitting of the spectral vector, the statistics and the development of control charts will be explained.

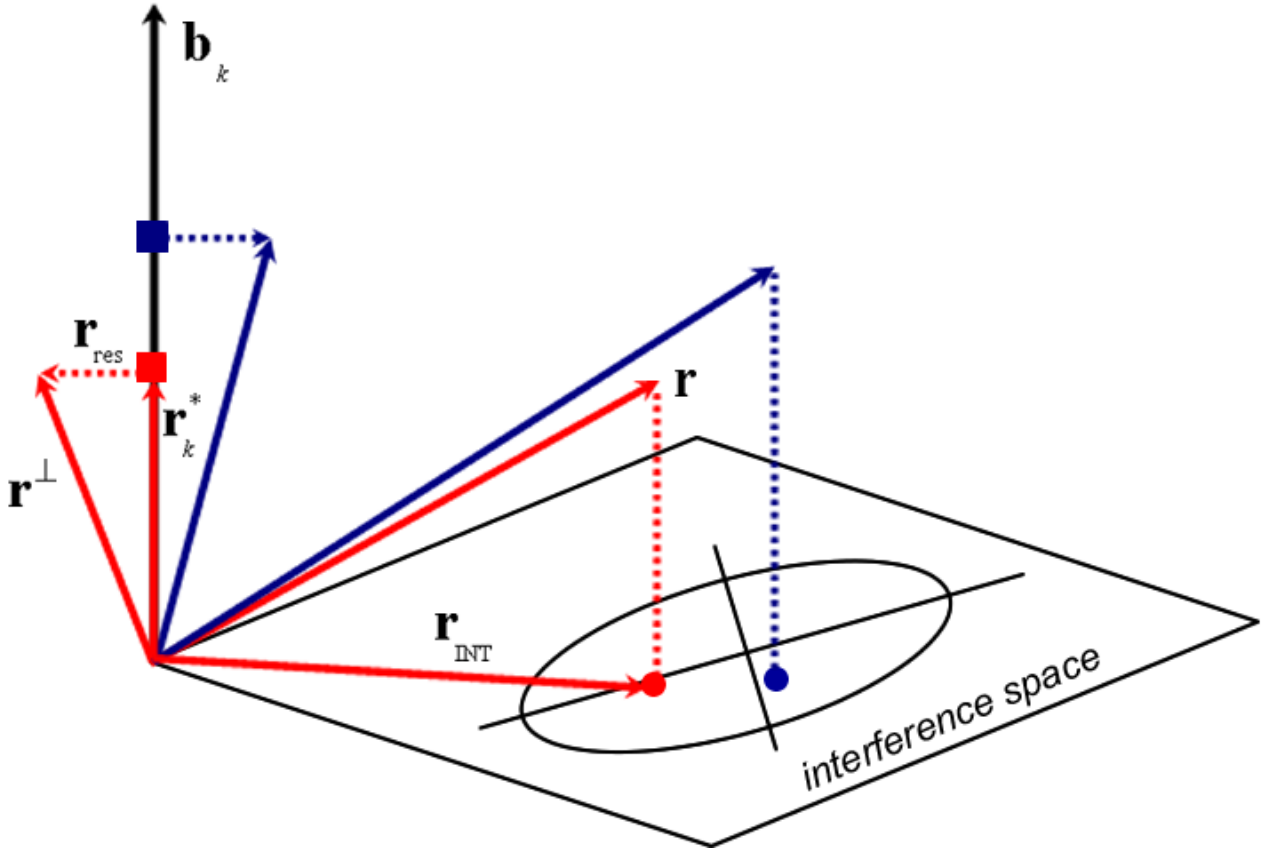

Figure 1: Schematic overview of the separation of the spectrum r into three different contributions, the NAS values indicated by the coloured squares, the composition of the excipients indicated by the coloured dots in the interferent space and the residuals indicated by the dashed arrows perpendicular of the NAS vector b_k.

Notation

Boldface capital characters denote matrices, boldface lower-case characters denote vectors and lower case italic characters denote scalars, superscript T denotes the transposed matrix or vector and the superscript + denotes the Moore-Penrose generalised inverse of a matrix. The matrix $\mathbf{I}_J$ is the $J \times J$ identity matrix. A list of symbols used in the theory section is given in Table 1.

Table 1: List of symbols used.

Symbol	Size	Explanation
IJ	JxJ	Identity Matrix
r	Jx1	spectrum
rk*	Jx1	NAS vector for analyte *k*
rINT	Jx1	Interference vector. Part of spectrum **r** described by all interferences
rRES	Jx1	Residual vector. Residual part not described by analyte or interferences
R-k	JxIb	Matrix of blank spectra with respect to analyte k
P	JxA	Loadings from PCA of **R**-*k*, A pc's are maintained
T	IbxA	Scores from PCA of **R**-*k*, A pc's are maintained
E	JxIb	Residuals from PCA of **R**-*k*
Rmod	*J*x*I*mod	Set of *Imod* model spectra used to define NAS direction
Bk	*J*x*I*mod	The orthogonal part of **R**mod on interference space
bk	Jx1	NAS regression vector. Mean vector of **B**k
RNOC	*J*x*I*NOC	Set of NOC spectra used to set control limits of NAS, INT and RES chart
nasNOC	*1*x*I*NOC	Vector with nas values of NOC spectra
nasNOC	1x1	Mean of nas values from NOC spectra
sNOC	1x1	Standard deviation of nas values from NOC spectra
RINT	*J*x*I*NOC	Part of NOC spectra described by interferent space
TNOC	IxA	Scores of **R**INT
S	AxA	Covariance matrix of **T**NOC scores used to calculate D-statistic
*d*NOC,I	1x1	D-statistic of i'th NOC sample calculated from **T**NOC, *i*
tNOC	1xA	Mean score vector of all NOC scores
TNOC	*I*NOCx*A*	Centered NOC scores
R*NOC	*J*x*I*NOC	NAS vectors of NOC spectra
RRES	*J*x*I*NOC	Residual vectors of NOC spectra
QNOC	*I*NOCx*I*NOC	Square matrix with *Q*-statistic of NOC spectra in the diagonal
Rcal	*J*x*I*cal	Set of calibration samples to relate the NAS to the actual concentration

Outline of method

NAS-SQC will be introduced in two stages with a third optional stage:

Stage 1: Model building
Stage 2: Calculation of statistical limits
Stage 3 (optional): Calibration

The three stages will be presented separately. The third optional stage is introduced in order to facilitate applications where statistical limits cannot be used for monitoring the analyte, which is the case in the application example used in the paper. Finally, a step-wise, practical description of how to apply new samples to the NAS-SQC model is introduced. The different stages are summarized in Table 2. The data needed for the stages (input), what action is performed in the stage and finally what the result of the stage is (output).

Table 2. Overview of stages.

Stage	Input	Action	Output
Stage 1: Model building	Blank spectra ($\mathbf{R}_{-k}$) Model spectra ($\mathbf{R}_{\text{mod}}$)	- PCA of blank spectra to define model for interference space - Projection of model spectra on interference space to define NAS regression vector	- Model for interference space - Projection matrix to project each vector on the interference space - NAS regression vector
Stage 2: Calculation of statistical limits	NOC spectra ($\mathbf{R}_{\text{NOC}}$)	Calculation of statistical limits	Statistical limits for NAS, INT and RES chart
Stage 3 (optional): Calibration	Calibration spectra ($\mathbf{R}_{\text{cal}}$)	Development of calibration model between NAS and reference values.	Quantitative limits for the NAS chart

Stage 1: Model building

In the first stage of NAS-SQC, a model of the system will be developed. This model consists of two parts, an interference space, describing all variation due to the other compounds (interfering constituents) and a NAS regression vector, which is unique for the analyte. For this, two data sets are needed; blank samples of the other compounds and samples including the analyte. The composition of the blank sample should reflect a real sample without the analyte. The outcome of stage 1 is a projection matrix (**PP**+) used to project any spectral vector on the interference space and a NAS regression vector to compute the analyte content. Using these, any spectrum (**r**, *J*×1) can be split into three independent parts (Figure 1):

The Net Analyte Signal vector (NAS) which is a vector unique for the analyte *k* of interest ($\mathbf{r}_k^*$). The Interference vector (INT) which is a vector unique for the interfering constituents ($\mathbf{r}_{\mathrm{INT}}$). A Residual vector (RES) which accounts for the part of spectrum which is not described by the NAS and INT vector ($\mathbf{r}_{\mathrm{RES}}$).

$$\mathbf{r} = \mathbf{r}_{\mathrm{INT}} + \mathbf{r}_k^* + \mathbf{r}_{\mathrm{RES}} \qquad \textbf{Eq. 1}$$

The net analyte signal is defined as the part of a spectrum, which is orthogonal to a subspace spanned by the spectra of the interfering constituents[8]. The subspace is called the interference space. The first step in splitting the spectral vector is to define the interference space. Spectra of blank samples $\mathbf{R}_{-k}$ are used to span the interference space. It is in our experience that using blank sample spectra is a better approach than using pure spectra of interfering constituents[9], as pure spectra are not always available. Also the pure constituent spectrum may differ slightly in shape from the spectral contribution of that constituent in a mixture.

The blank samples used to span the interference space are assumed to be made of a systematic part and a non-systematic part. By doing a principal component analysis (PCA), the systematic variation is split from the non-systematic variation. First, the blank spectra are mean centred followed by a PCA using *A* principal components.

$$\mathbf{R}_{-k} = \mathbf{P}\mathbf{T}^{\mathrm{T}} + \mathbf{E} \qquad \textbf{Eq. 2}$$

where $\mathbf{R}_{-k}$ is a $J\times I_b$ matrix with I_b mean centred blank spectra measured at J wavelength points, the loadings **P** ($J\times A$) and scores **T** ($I_b\times A$) capture the systematic variation, and the non-systematic part is contained in **E** ($J\times I_b$). The loadings define a model for the interference space. To select the right number of principal components cross-validation techniques can be used[10, 11] also the A+1 loading should not show systematic variation, which can be checked by visual inspection. Furthermore, in pharmaceutical application, the number of excipients is often a good choice for the number of components necessary. and knowledge of system rank is useful for determination of *A*. The size of *A* illustrates the number of independent phenomena in the blank spectra e.g. varying composition of the interfering constituents, varying levels of water content etc. It should be noted that it is not possible to perform a complete separation of systematic and non-systematic variation by doing a PCA i.e. some non-systematic spectral white noise will be embedded in the PC space. Secondly, systematic variation can be both relevant variation e.g. chemical variation and non-relevant variation e.g. spectrometer drift, which also will be embedded in the PC space.

The first split of the spectrum is to find the part which lies within the interference space, i.e. the interference vector. This vector is determined by projection of the spectrum into the interference space.

$$\mathbf{r}_{\mathrm{INT}} = \mathbf{P}\ \mathbf{P}^{+}\mathbf{r} \qquad \textbf{Eq. 3}$$

Where $\mathbf{P}^+$ is the Moore Penrose inverse of the matrix of loading vectors.

As stated earlier, the net analyte signal is defined as that part of a spectrum orthogonal to the interference space. However, many directions exist orthogonally to the interference space, so the direction of the analyte has to be defined specifically. This direction can be defined by I_{mod} model samples, which contain both analyte and other compounds, are representative for new samples and are known to be good samples (e.g. by reference measurements). The part of $\mathbf{R}_{mod}$ (JxI_{mod}) orthogonal to the interference space P is obtained by using the orthogonal anti-projector ($\mathbf{I}_J$-$\mathbf{PP}^+$)

$$\mathbf{B}_k = \left(\mathbf{I}_J - \mathbf{P}\mathbf{P}^+\right) \cdot \mathbf{R}_{mod} \qquad \textbf{Eq. 4}$$

$\mathbf{B}_k$ contains I_{mod} spectra which are all orthogonalised to the interference space and point more or less into the same NAS direction. In Figure 1 is the vector $\mathbf{r}^\perp$ the orthogonal projection of a spectrum **r** on the interference space. To reduce the noise, the average $\mathbf{b}_k$ of all these orthogonal vectors is taken as the actual NAS direction, (Figure 1):

$$\mathbf{b}_k = \frac{\sum_{i=1}^{I_{mod}} \mathbf{B}_{k,i}}{I_{mod}} \qquad \textbf{Eq. 5}$$

This vector $\mathbf{b}_k$ is called the NAS regression vector. The reasoning for using the average as NAS regression vector is that we want to find one common direction in the multivariate space, the NAS direction.

Now the NAS vector of the spectrum can be computed by a projection of the spectrum onto the NAS regression vector.

$$\mathbf{r}_k^* = \mathbf{b}_k \left(\mathbf{b}_k^{\mathrm{T}} \mathbf{b}_k \right)^{-1} \mathbf{b}_k^{\mathrm{T}} \mathbf{r} \qquad \textbf{Eq. 6}$$

It is important to notice that there is a slight difference between the $\mathbf{r}^{\perp}$ and $\mathbf{r}_k^*$ and this is the residual vector. This is simply computed as the part of the spectrum not described by the NAS and interference vectors. This is merely performed by a simple vector subtraction.

$$\mathbf{r}_{\mathrm{RES}} = \mathbf{r} - \mathbf{r}_{\mathrm{INT}} - \mathbf{r}_k^* \qquad \textbf{Eq. 7}$$

For samples, which are considered good e.g. the calibration samples, $\mathbf{r}_{\mathrm{RES}}$ will be small, since nearly all variations in the spectrum are described by analyte and interfering constituents.

Summarizing, the spectrum vector is split into a part that lies within the interference space and an orthogonal component to the interference space. The orthogonal component is then split into a part that points in the NAS regression vector direction and a residual part.

Stage 2: Calculation of statistical limits

In the second stage statistical limits are calculated (Table 2). To do this, a set of spectra that are statistical 'in-control' are used. $\mathbf{R}_{\mathrm{NOC}}$ is independent of the model parameters estimated, and is therefore representative for future data. All $\mathbf{R}_{\mathrm{NOC}}$ spectra are separated into the NAS, INT and RES contribution and for each a test statistic is defined. The test statistic values of the NOC data form the 'in control' distribution of which the statistical control limits are calculated and against which future measurements are compared.

The set of I_{NOC} NOC spectra ($\mathbf{R}_{\mathrm{NOC}}$) that are used, are independent of the blank samples and the model samples i.e. they have not been used to construct the interference space or define the NAS regression vector. They should represent the common-cause variation in spectra of the samples, when all of the three parts are within certain ranges i.e. the analyte concentration is acceptable, the homogeneity of the interfering constituents is acceptable, and the residuals are only non-systematic variation on the level of instrumental noise. The I_{NOC} spectra are named normal operating condition spectra or NOC spectra with the terminology from statistical process control[12]. If a future sample falls outside any of the limits in a chart, it is considered out of control.

NAS chart

The projection of the sample spectrum on the NAS regression vector is proportional to the concentration of the analyte in the sample[13]. The projection value is a scalar called the NAS value. To derive statistical limits for the NAS chart the NAS value for each of the NOC spectra is computed.

$$\mathbf{nas}_{\mathrm{NOC}} = \mathbf{R}_{\mathrm{NOC}}{}^{\mathrm{T}}\mathbf{b}_k \qquad \textbf{Eq. 8}$$

Where $\mathbf{nas}_{\mathrm{NOC}}$ is a vector with the NAS values of the individual NOC spectra. In Figure 1 are the NAS values of the two spectra symbolized as coloured squares on the NAS regression vector. The mean ($\overline{\mathbf{nas}}_{NOC}$) and standard deviation ($\mathbf{s}_{NOC}$) of the I_{NOC} NAS values are computed. With these values the statistical limits can be computed and plotted in the NAS chart.

$$\begin{aligned} 95\%\ \text{confidence limits} &= \overline{nas}_{\mathrm{NOC}} \pm 2 \cdot s_{\mathrm{NOC}} \\ 99.7\%\ \text{confidence limits} &= \overline{nas}_{\mathrm{NOC}} \pm 3 \cdot s_{\mathrm{NOC}} \end{aligned} \qquad \textbf{Eq. 9}$$

The 95 % confidence limits are also called the upper and lower warning line and 99.7 % confidence limits are called the upper and lower action line[14]. The NAS values are assumed to follow a normal distribution, which can easily be verified by any statistical normality test.

INT Chart

All NOC spectra project on a certain part of the interference space. Future 'in control' spectra should also project in this area, while spectra, which project out of this area are considered out of control. Remember that the interference space was modelled using a PCA model (Equation 2). Thus the 'in control' area can be represented by its corresponding score values of the PCA model of the interference space. The structure within these scores can be modelled using their covariance matrix. The INT chart is based on the distance of the projection of a new spectrum from the centre of the 'in control' area. The 'in control' area is symbolized with the ellipse in Figure 1 and the cross in the ellipse symbolizes the two first principal components.

First, the NOC spectra are projected on the interference space,

$$\mathbf{R}_{\mathrm{INT}} = \mathbf{P}\mathbf{P}^{+}\mathbf{R}_{\mathrm{NOC}} \qquad \textbf{Eq. 10}$$

then, the projected spectra $R_{INT,-k}$ are projected on the PCA model of the interference space to obtain the corresponding 'NOC' score values.

$$\mathbf{T}_{\mathrm{NOC}} = \mathbf{R}_{\mathrm{INT}}^{\mathrm{T}}\mathbf{P}\left(\mathbf{P}^{\mathrm{T}}\mathbf{P}\right)^{-1} \qquad \textbf{Eq. 11}$$

Now, the *d*-statistic of NOC spectrum $\mathbf{r}_{\mathrm{noc,i}}$ is defined as:

$$d_{\mathrm{NOC},i} = \left(\mathbf{t}_{\mathrm{NOC},i} - \bar{\mathbf{t}}_{\mathrm{NOC}}\right)^{\mathrm{T}}\mathbf{S}^{-1}\left(\mathbf{t}_{\mathrm{NOC},i} - \bar{\mathbf{t}}_{\mathrm{NOC}}\right) \qquad \textbf{Eq. 12}$$

where $\bar{\mathbf{t}}_{\mathbf{NOC}}$ is the mean score vector of all NOC scores T_{NOC}. **S** denotes the covariance matrix of the centred NOC scores. ($\overline{\mathbf{T}}_{\mathbf{NOC}}$)

$$\mathbf{S} = \frac{\overline{\mathbf{T}}_{\mathbf{NOC}}^{\mathbf{T}} \overline{\mathbf{T}}_{\mathbf{NOC}}}{I_{NOC} - 1} \qquad \textbf{Eq. 13}$$

The *d*-statistic of new samples multiplied by a constant follows an *F*-distribution with *A* and I_{noc}-*A* degrees of freedom. So, the 95% limit for the INT chart can then be computed:

$$D_{\mathrm{lim},0.95} = F_{0.95}\left(A, I_{\mathrm{NOC}} - A\right) \cdot \left(\frac{A \cdot \left({I_{\mathrm{NOC}}}^{2} - I_{\mathrm{NOC}} \right)}{I_{\mathrm{NOC}} \cdot \left(I_{\mathrm{NOC}} - A \right)} \right) \qquad \textbf{Eq. 14}$$

The *d*-statistic in the INT chart check, whether spectra of new samples follow the same covariance as the spectra of the NOC samples. If new samples show a different correlation, or when the variances are outside the variances in the NOC set, this chart will flag.

RES Chart

The NOC spectra are also used in order to derive the statistical limits for the RES chart, which is based on the *Q*-statistic[15]. The residual vectors of the NOC spectra are computed. It is assumed that the interference vectors of the NOC spectra are already available. First compute the NAS vectors,

$$\mathbf{R}_{\mathrm{NOC}}^{*} = \mathbf{b}_k \left(\mathbf{b}_k^{\mathrm{T}} \mathbf{b}_k \right)^{-1} \mathbf{b}_k^{\mathrm{T}} \mathbf{R}_{\mathrm{NOC}} \qquad \textbf{Eq. 15}$$

then the residual vectors.

$$\mathbf{R}_{\mathrm{RES}} = \mathbf{R}_{\mathrm{NOC}} - \mathbf{R}_{\mathrm{INT}} - \mathbf{R}^{*}_{\mathrm{NOC}} \qquad \textbf{Eq. 16}$$

It is assumed that the residuals vector only contains normally distributed random noise. The squared length of a residual vector is referred to as the *Q*-statistic, which is the inner product of the residual vector, i.e. sum of squared residuals.

$$\mathbf{Q}_{\mathrm{NOC}} = \mathbf{R}^{\mathrm{T}}_{\mathrm{RES}} \cdot \mathbf{R}_{\mathrm{RES}} \qquad \textbf{Eq. 17}$$

Where $\mathbf{Q}_{\mathrm{NOC}}$ contains the *Q*-statistic of the NOC spectra on its diagonal. The *Q*-statistic for new samples follows a chi-squared distribution[15].

$\mathbf{Q}_{\mathrm{NOC}} \sim g\chi^2_h$

The control limits for *Q* are obtained by fitting a χ^2 distribution to the reference distribution obtained from NOC data. Parameter h represents the degrees of freedom and g denotes the weight to account for the magnitude. These two parameters were estimated[15]. If the residual vector of a new observation is not only random noise this observation will have a large *Q*-statistic and flag in the RES chart.

Stage 3 (optional): Calibration

The third stage is an optional stage which is only needed in case the scope of the NAS chart is to monitor if the analyte content is within a certain concentration range. A calibration dataset is used and the outcome is limits for the NAS chart, which corresponds to specific analyte concentrations, i.e. not statistical limits that correspond to a specific distribution (Table 2).

In order to relate the analyte concentration to the NAS value, the calibration model is developed using a set of I_{cal} calibration samples $\mathbf{R}_{\mathrm{cal}}$, of which the analyte concentration is known from a reference measurement. The NAS values of the calibration samples are computed. The NAS values are then plotted against the corresponding reference analysis value in a NAS calibration plot[13]

and a polynomial is fitted to the points in a least squares sense to generate a calibration model,

$$nas = a_0 + a_1[analyte] + e \qquad \textbf{Eq. 18}$$

where a_0 and a_1 are the offset and slope of the NAS calibration line, and e is the error in concentration. The analyte concentration in the samples has to span the desired concentration range, then, the lower and upper limits for the NAS chart are related to the maximum and minimum allowed concentrations. It is important to remember that uncertainty in the reference space will propagate into the NAS space, and the estimation of concentration limits for the NAS chart is not straight forward.[16, 17] However, the topic of uncertainty propagation will not be dealt with within this publication.

How to Apply Future Samples to the NAS-SQC

In this section, a step-wise description is presented on how to apply a future sample to the NAS-SQC control charts.

NAS Chart

The NAS value of the new spectrum $\mathbf{r}_{new}$ is calculated and plotted in the NAS chart.

$$nas_{new} = \mathbf{r}_{new}^{T} \cdot \mathbf{b}_k \qquad \textbf{Eq. 19}$$

INT chart.

The *D*-statistic of the new spectrum is calculated and plotted in the INT chart.

$$\mathbf{r}_{INT,new} = \mathbf{P}\ \mathbf{P}^{+}\mathbf{r}_{new} \qquad \textbf{Eq. 20}$$

The scores of the new sample on the PCA model of the interference space are obtained as follows

$$\mathbf{t}_{\text{new}} = \mathbf{r}_{\text{new}}^{\text{T}}\mathbf{P}\left(\mathbf{P}^{\text{T}}\mathbf{P}\right)^{-1} \qquad \textbf{Eq. 21}$$

For the d-statistic of the new sample, the new score is related to the mean NOC score and the covariance matrix of the NOC data.

$$d_{new} = \left(\mathbf{t}_{\mathbf{new}} - \bar{\mathbf{t}}_{\mathbf{NOC}}\right)^{\mathbf{T}}\mathbf{S}^{-1}\left(\mathbf{t}_{\mathbf{new}} - \bar{\mathbf{t}}_{\mathbf{NOC}}\right) \qquad \textbf{Eq. 22}$$

RES Chart

The *Q*-statistic of the new spectrum is calculated and plotted in the RES chart.

$$\mathbf{r}_{new,k}^{*} = \mathbf{b}_{\mathbf{k}}\left(\mathbf{b}_{\mathbf{k}}^{T}\mathbf{b}_{\mathbf{k}}\right)^{-1}\mathbf{b}_{\mathbf{k}}^{T}\mathbf{r}_{new} \qquad \textbf{Eq. 23}$$

$$\mathbf{r}_{\text{RES},new} = \mathbf{r}_{\text{new}} - \mathbf{r}_{\text{INT},new} - \mathbf{r}_{\text{new},k}^{*} \qquad \textbf{Eq. 24}$$

$$q_{\mathbf{new}} = \mathbf{r}_{\mathbf{RES},\mathbf{new}}^{\mathbf{T}} \cdot \mathbf{r}_{\mathbf{RES},\mathbf{new}} \qquad \textbf{Eq. 25}$$

Experimental Section

Tablet Samples

Feldene Zydis 20mg production units were obtained from Cardinal Health Oral Technologies Ltd Zydis, Swindon, UK with nominal content of 20mg (approximately 37.5% m/m) of the active ingredient piroxicam per freeze-dried unit. Production lots were collected over a period of time to cover possible changes in sample constituent concentration, supplier, process changes, or variations in storage conditions up to 2 years of shelf life. These lots were also selected ensuring that the API concentration was varied within specification (i.e. from batch history/ manufacturing records). Units are manufactured by use of

freeze drying from a suspension mix of piroxicam (4.000% m/m), gelatine (3.590% m/m), mannitol (2.872% m/m), aspartame (0.050% m/m), and citric acid (0.220% m/m) in 89.268% m/m purified water. The suspensions are dosed as aliquots of 500mg into blisters of 16mm diameter and freeze-dried. Development scale samples were manufactured to form a suitable active range for United States Pharmacopeoia (USP) uniformity of content specification;[3] i.e. at 15, 17, 20, 23, and 25 mg/unit (75%, 85%, 100%, 115%, and 125% Label Claim (%L.C.)) of the active, piroxicam. Extra development samples were also available just outside the 85% to 115 % interval. Additional samples were made by varying the excipients mannitol and gelatine at 70% m/m and 130% m/m of nominal content, respectively. Individual excipients were available for specificity assessment as were blank (blank) samples, devoid of the active piroxicam. All freeze-dried units are highly porous, white, circular solids with no embossment or markings. The units are flat on one side with a lidded appearance to the reverse side as a result of the freeze drying/foiling/blister-sealing process.

NIR Instrument and Data Treatment

NIR transmission spectra were measured using a NIRSystems 6500-II near-infrared spectrophotometer (NR-6500-HI) (FOSS NIRSystems, Warrington, UK) fitted with an InTact^{TM} analyser (NR-1650) with an Indium-Gallium-Arsenide (InGaAs) detector. Units were analysed using a custom engineered sample holder to eliminate light leakage around the side of the sample. The instrument was controlled by Vision 2.51 software (NR-2094) (FOSS NIRSystems, Silver Spring, USA). Data were collected by Vision software and exported to MatLab as MatLab datafiles. Data treatment and analysis were performed in MatLab version 6.5 Release 13 (The MathWorks Inc., USA) using PLS Toolbox 2.1 (Eigenvector Research Inc., USA) and in-house written routines. Some of the MatLab M-files are available for download at http://www-its.chem.uva.nl/research/pac/index.html.

NIR Analytical Procedure

NIR spectra were measured for individual tablets over the wavelength range of 600 to 1900 nm at 2 nm intervals. Each recorded spectrum was an average of 32 scans (a total of 35 seconds scan time per unit) and recorded with respect to air as a reference using a blank tablet holder, (NR-1651-B) (FOSS NIRSystems, Silver Spring, USA). All measurements were made in normal laboratory conditions (20-23^{o}C, 35-55% Relative Humidity).

Reference analysis

After NIR analysis were the tablets subject to reference analysis using HPLC.

Results and Discussion

In the Results section, we will demonstrate the strong diagnostic properties of NAS-SQC. Following the steps earlier defined in the Theory section, the charts will be developed and validated using the tablet data described above.

Spectral pre-processing

Near-infrared spectra suffer from external variation e.g. varying particle size and shape, temperature, and density of the samples. To find a good initial pre-processing method and wavelength region to start with, the SE indicator[9] was utilised, which uses blank samples not relying on reference analysis. Different pre-processing methods (Standard Normale Variate (SNV), first order Savitsky-Golay filtering, second order Savitsky-Golay filtering, multiplicative Scatter Correction (MSC), offset correction and combinations of the above were tested in combination with wavelengths selection. Multiplicative scatter correction[18] followed by a 1st order derivative Savitsky-Golay[19] filtering using a 2nd order polynomial with 11 spectral points was used as the pre-processing method. For wavelength selection, the region from 800 nm to 1400 nm was used. Outside of these wavelengths noise due to detector saturation etc. affected spectral quality

Example of Split of Spectrum

In Figure 2, a production sample spectrum (named NOC sample spectrum) is depicted after pre-processing and wavelength selection. The NOC sample spectrum was split into the three independent vectors, which are also depicted together with the NOC sample spectrum. The RES vector appears like a flat line, but by close inspection, small non-systematic variation was observed. The NAS vector had increased positive amplitude at wavelengths, which corresponded very well with major absorbance peaks in the pure piroxicam spectrum, most notably at 1124 nm (second overtone aromatic C-H bond).

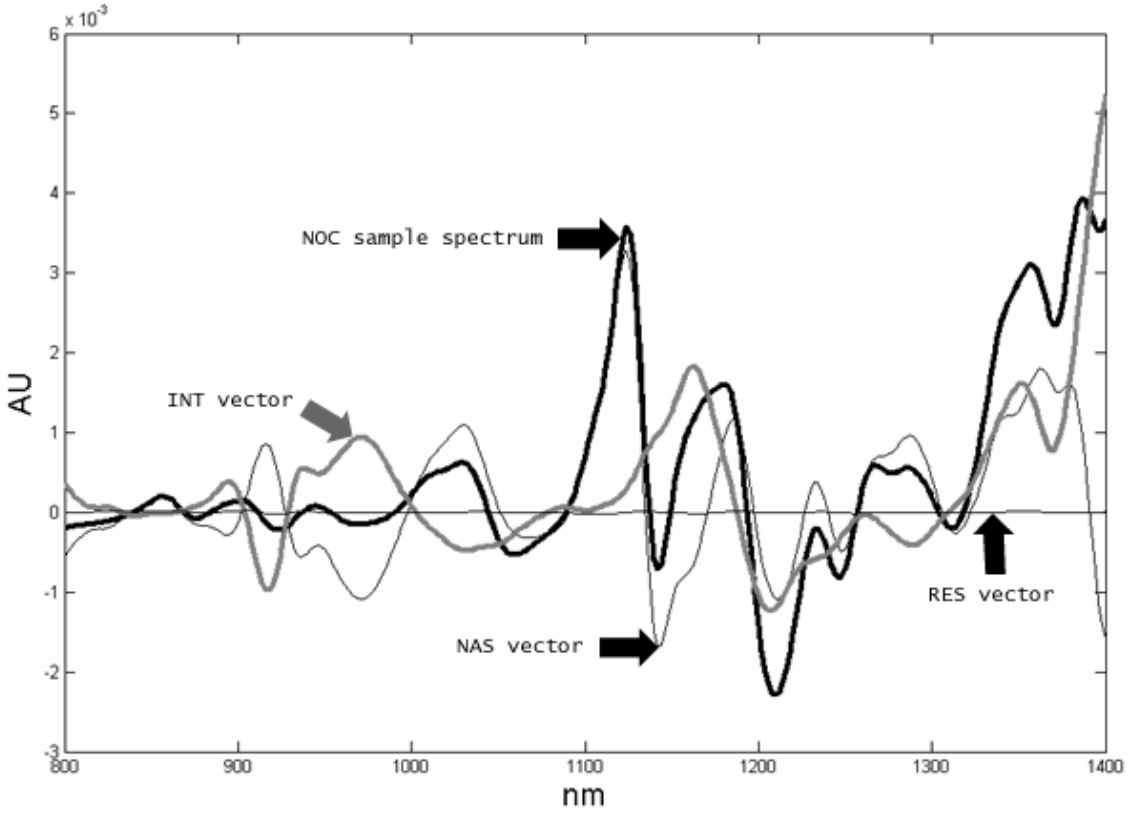

Figure 2: NOC sample spectrum and corresponding NAS, INT and RES vectors.

Samples

In Table 3 is an overview of the samples that were used to construct and validate the control charts.

Table 3: Overview of all samples used in figures 4 and 6.

	Description	*Used for*
	59 blank samples	create interference space
	5 production samples	create NAS regression vector
	124 calibration samples	create NAS chart concentration limits
Samples # in Figure 4		
# 1-100	10 samples times 10 production batches	create INT and RES chart limits
# 101-110	Lab samples with API close-to, but < 115 % label claim	create INT and RES chart limits
Samples # in Figure 6		
# 1-10	Lab. samples with API < 85% label claim	validate NAS limits
# 11-20	Lab. samples with API > 115% label claim	validate NAS limits
# 21-22	Two production samples with elevated moisture content	validate RES limits
# 23-34	Lab. samples with altered composition mannitol and gelatine (excipients)	validate INT chart
# 35-44	10 samples from an in-control production batch	validate all charts
# 45-54	Lab. samples with slightly elevated API but < 115% label claim	validate all charts

Development of Model for Interference Space

A total of fifty-nine blank (placebo) samples were collected from various development batches and analysed by NIR. Some of the blank samples had elevated moisture content. After pre-processing, the spectra were mean centred and subjected to PCA. A five component PCA model was fitted to the spectra. The five component model explained 99.7 % of the total variance. At a first glance, five components appeared a high number, but using a smaller number of components worsened the discriminative power of the INT chart of the validation samples. Furthermore, it represents the 5 compounds in a placebo sample (Gelatin, Mannitol, Aspartame, Citric Acid and Purified water).

Computation of NAS Regression Vector

A set of five NOC production sample spectra was used for calibration of the NAS regression vector. It was tried with more samples but that did not influence the results. Their orthogonal part on the interference space was found, and visual

inspection of the orthogonal vectors showed that they were very similar. The average vector of the orthogonal vectors was used as the NAS regression vector.

Computation of the Confidence Limits for the INT Chart

100 samples from 10 different production batches i.e. 10 units from each batch plus 10 special samples manufactured in the laboratory with close-to the 85% and 115% limit were used as NOC samples ($\mathbf{R}_{\mathrm{NOC}}$). The limits for the INT chart were calculated with a F-test table and Equation 14 with A=5 and I_{NOC} -A=105 degrees of freedom. The 95% and 99% confidence limit for the INT chart were 12.1 and 16.7, respectively. The d-statistics of the NOC sample spectra were calculated and plotted in an INT chart together with the confidence limits.

Computation of the Confidence Limits for the RES Chart

From the NOC sample spectra, the RES vectors were calculated. The RES vectors were then used to compute the statistical limits for the RES chart using the Jackson and Mudholkar approximation[15]. The 95% and 99% confidence limits were calculated to 1.0452×10^{-6} and 1.8603×10^{-6}, respectively.

Computation of the NAS concentration limits

To develop the limits for the NAS chart, a set of 124 calibration samples were used. The NAS values of the samples were computed and plotted against the piroxicam content (Figure 3). A first order polynomial was fitted to the points using least squares (solid diagonal line in Figure 3). The target concentration in the final product is 20 mg piroxicam per unit, so the lower 85% limit is 17 mg piroxicam per unit, and the upper 115% limit is 23 mg piroxicam per unit. Using the polynomial, the corresponding NAS values were computed. The lower NAS limit was computed to 2.1964×10^{-4} A.U., and the upper NAS limit was computed to 2.5984×10^{-4} A.U. (Figure 3). The limits are depicted as vertical and horizontal dotted lines in Figure 3.

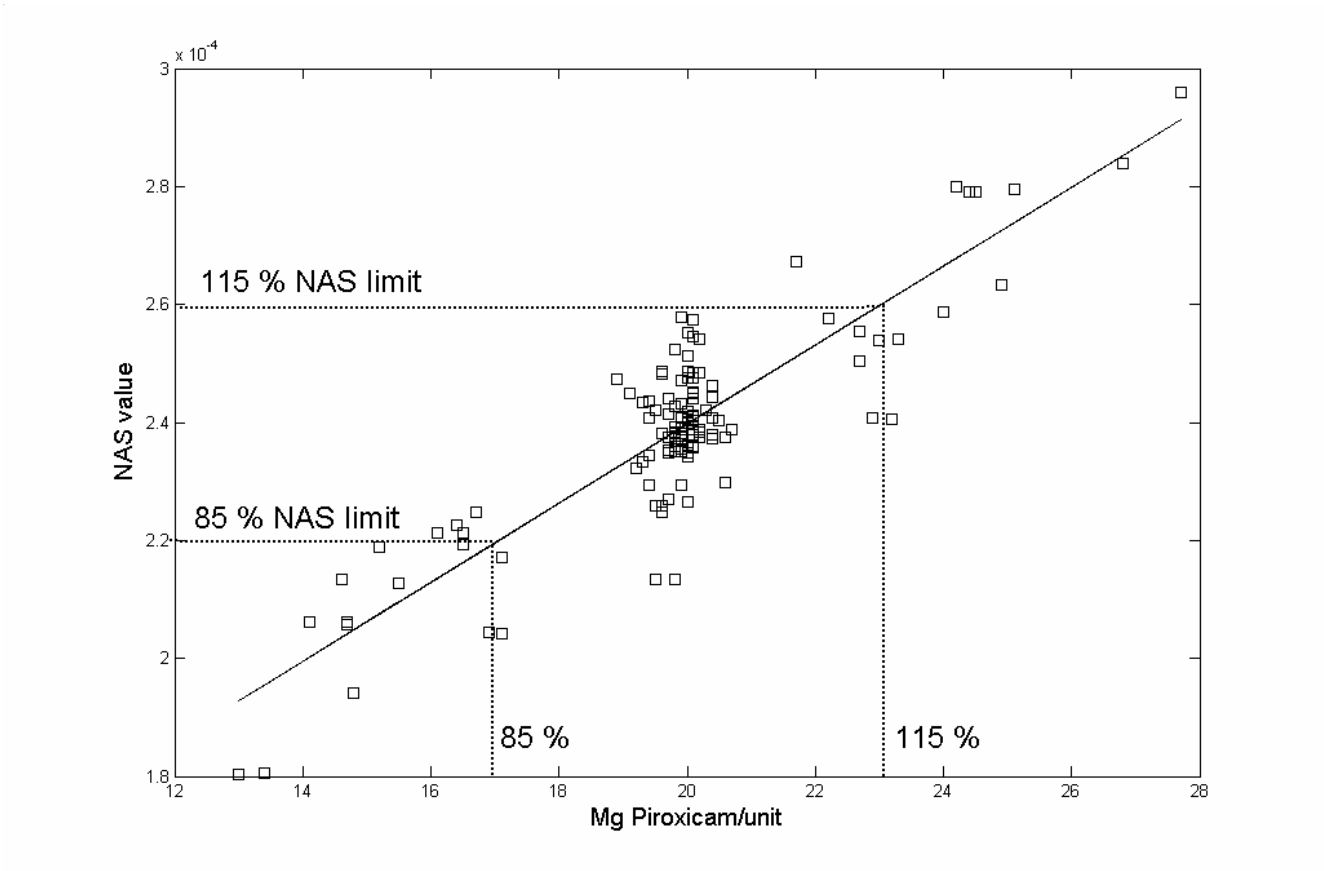

Figure 3: NAS value vs piroxicam/unit.

Plotting the NOC Samples in the Control Charts and Diagnostics

The NAS values, *D*-statistics and *Q*-statistics were calculated for the NOC samples and plotted in the control charts (Figure 4). Batch to batch differences in the mean API content were easily detected by inspecting the NAS values (Figure 4). Samples no. 61 to 70 (maybe use circles not squares for these samples) (ten samples from the same batch) were clearly lower than the other production samples (no. 1 to 60 and no. 71 to 100). This was confirmed by HPLC reference analysis. The ten laboratory samples (no. 101-110), which were made to be close to the NAS control limits, can easily be detected. Only two samples were available, which were close to the lower 85% limit (no. 109 and 110), and eight samples were available, which were close to the upper 115% limit (no. 101 to 108).

When inspecting the INT chart (Figure 4, middle), it appeared, as if all samples were more or less similar with respect to the composition of the interfering constituents except for samples 71-74.

In the RES chart, samples no. 41 to 50 and no. 101 to 110 deviated from the other samples, i.e. the sample spectra have higher Q-statistics. A closer examination of the RES vectors (Figure 5) showed that most of the RES vectors look similar (light grey vectors in Figure 5), but the RES vectors of sample no. 41 to 50 showed some unusual spectral features, i.e. peaks at approximately 1025 nm and 1300 nm (marked with arrows in Figure 5). The samples no. 41 to 50 were ten samples from the same production batch, which differed from the other NOC batches in a way that caused distinct peaks in the RES vector. Increased non-systematic variation in the spectra will cause higher Q-statistics, but then, the RES vector would not look systematic with distinct peaks like the RES vectors from sample no. 41 to 50 but more like the other RES vectors with increased amplitude. The RES vectors of samples no. 101 to 110 did not exhibit any distinct peaks but had increased amplitude. These samples were also special laboratory samples with an average weight difference from the production samples of 3 mg, which was approximately 6% weight difference. This weight difference could also potentially affect the thickness of the freeze-dried unit and again the effective path length of the NIR light beam.

When a new peak is present in the RES vector, it can be e.g. an absorbance feature from a compound not modelled by the interference space, or part of the NAS vector, or a peak shift in the spectrum indicating spectrometer malfunction, a new substance or polymorphism, which in many cases is featured as peak changes in the infra-red region[20]. It was not investigated, what caused these peaks, but the result shows the improved diagnostics using NAS-SQC.

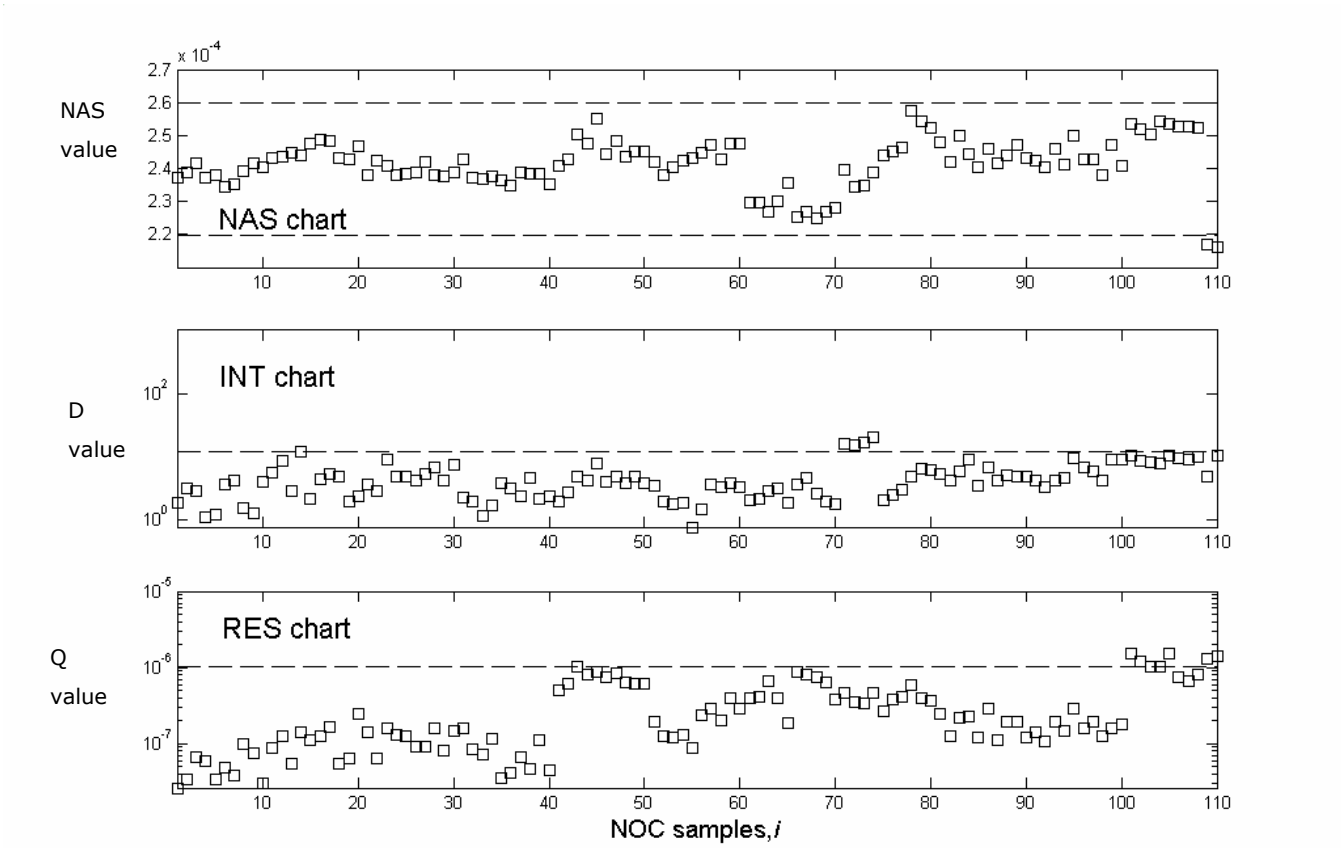

Figure 4: NOC samples in control charts.

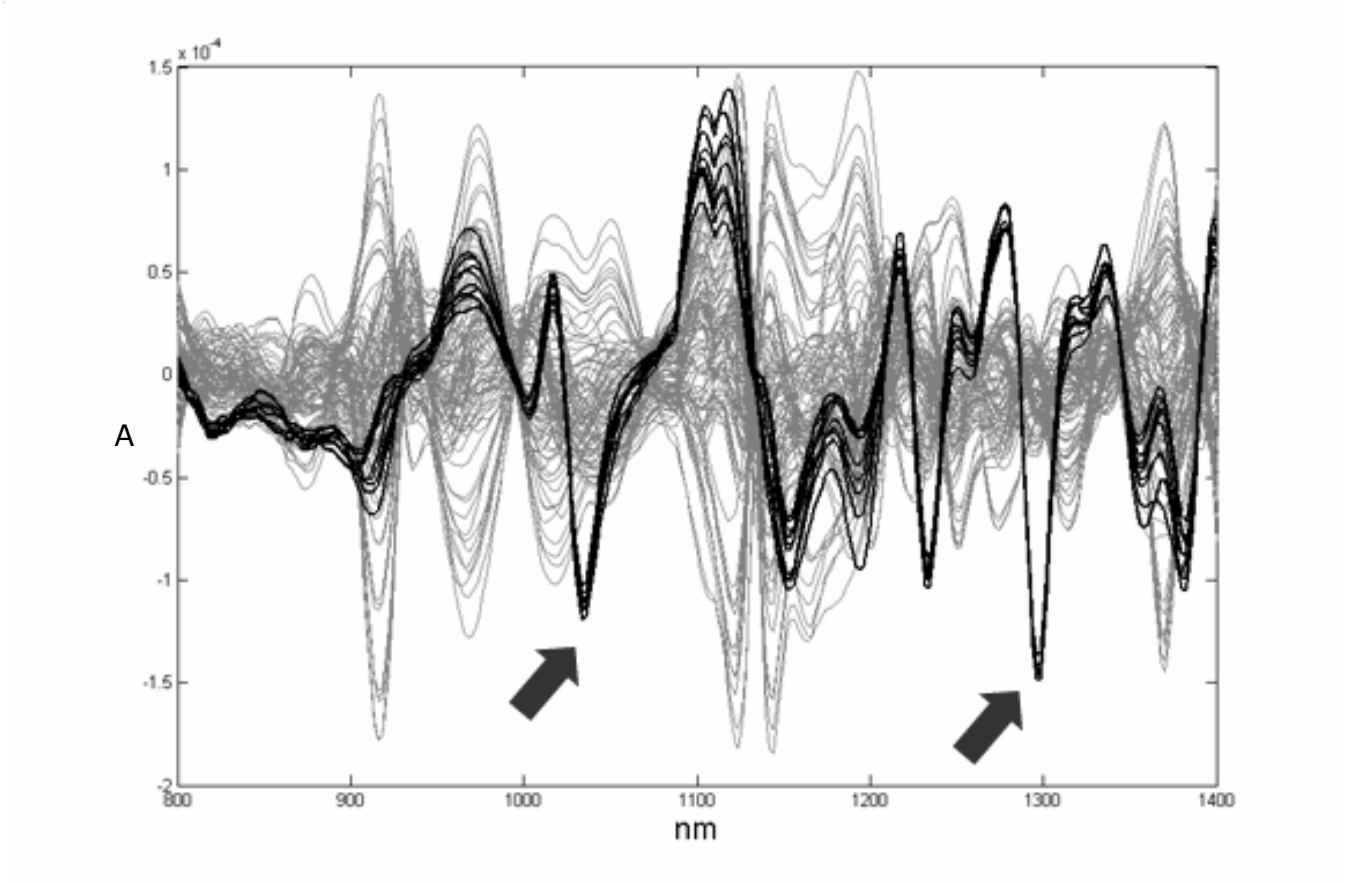

Figure 5: Diagnostics of NOC RES vectors.

Validation of Control Charts

In order to validate the control charts, a selection of out of control samples and NOC samples were applied to the NAS-SQC model and plotted in the control charts. Thirty-four out of control samples and twenty NOC samples were used. After pre-processing and wavelength selection, the out of control samples and NOC validation sample spectra were split into the three different vectors, statistics calculated, and plotted in the control charts (Figure 6). An out of control sample is symbolised with a cross and a NOC sample with a square. The y-axis in the INT and RES chart is on a logarithmic scale to amplify the statistic value differences.

Samples no. 1-10 were outside specifications with respect to API, except sample no. 5. According to reference analysis, they were all below the 85% API limit.

Most of them were also outside the 95% limit in the INT and RES chart, this can be explained by the fact that sample 1-10 were special laboratory samples, in which the piroxicam content was lowered. To compensate for the decrease in piroxicam content other excipients were added, which means that the interference composition is different from the model samples.

Samples 11-20 were all above the 115% API limit according to the reference analysis, and they were also above the upper limit in the NAS chart, as expected. Apart from sample no. 16, all fall within the limits in the INT chart. However, they all flag in the RES chart as not part of the 95% confidence interval for their *q*-statistics. These samples also originate from a special laboratory batch and the tablet units are slightly thicker than the tablets used in the NOC dataset. This might account for the higher values in the RES chart.

Sample 21-22 were two production samples, which were NOC with respect to the API content, but the units were exposed to elevated moisture conditions prior to the NIR and reference analysis. The samples were within the NAS limits as expected and flagged in the INT chart as expected and within the limits in the RES chart. When the INT vectors were investigated (Figure 7), the two samples showed a clear increased amplitude around 1400 nm, near to where water absorbs in the first overtone region of the NIR spectrum. This was a result that demonstrated how spectral features could be separated into each of the three vectors. When the interference space was constructed some of the blank spectra used were from samples that were exposed to elevated moisture conditions i.e. water variation in the spectra was modelled into the interference space. The ability to discriminate samples with excessive moisture content is a very valuable parameter, especially for the freeze-dried tablets used in this study. Variation in the *D*-statistics of the samples can be used to monitor the efficiency of the freeze drying process as well as the homogeneity of the excipients. Also, the stability and dissolution of a tablet product can be influenced by the moisture present[21]. These parameters are normally considered to be critical for a tablet manufacture

and the result enlightens the potential of the diagnostics provided with the method.

Samples 23-34 were all NOC with respect to the API content, but with decreased or elevated content of either mannitol or gelatine, (which were the two major excipients). The samples were from special laboratory batches and were manufactured so that they would fall inside the limits in the NAS chart and outside the limits in the INT chart.

Samples 23-25 with decreased mannitol content (70%), were above the limits in the NAS chart as well as the INT and RES chart. A potential explanation why the elevated mannitol samples were above the NAS limit, is partly explained by the way the samples were composed. When the mannitol content was decreased, the other components were not varied, so the API concentration was increased compared to NOC production samples. This may be only a partial explanation, because the API concentration in the decreased mannitol samples was approximately 109% of labelled content, which is inside the 85-115% range. A second explanation could be that the decreased mannitol content gave some structural changes e.g. tablet thickness or light scatter effects, which affected the spectra.

Samples 26-28 with increased mannitol (130%), samples 29-31 with decreased gelatine (70%) and samples 32-34 with extra gelatine (130%) were all within the NAS limits and clearly outside the limits in the INT and RES charts as expected.

Samples 35-44 are production samples from the same batch. They are all within the 85-115% API interval according to reference analysis and were also within the NAS limits as well as the limits in the INT and RES charts.

Samples 45-54 were laboratory samples with an increased API content but below the upper 115% limit. They also fell inside the limits of the NAS and INT chart. In

the RES chart, some of these samples did flag. This was previously detected when the NOC samples were plotted in the control charts. Another fifty production samples, i.e. ten units from five different batches were investigated, and all fell inside the NOC limits in all three charts as expected (not depicted). This illustrated the NAS-SQC method robustness.

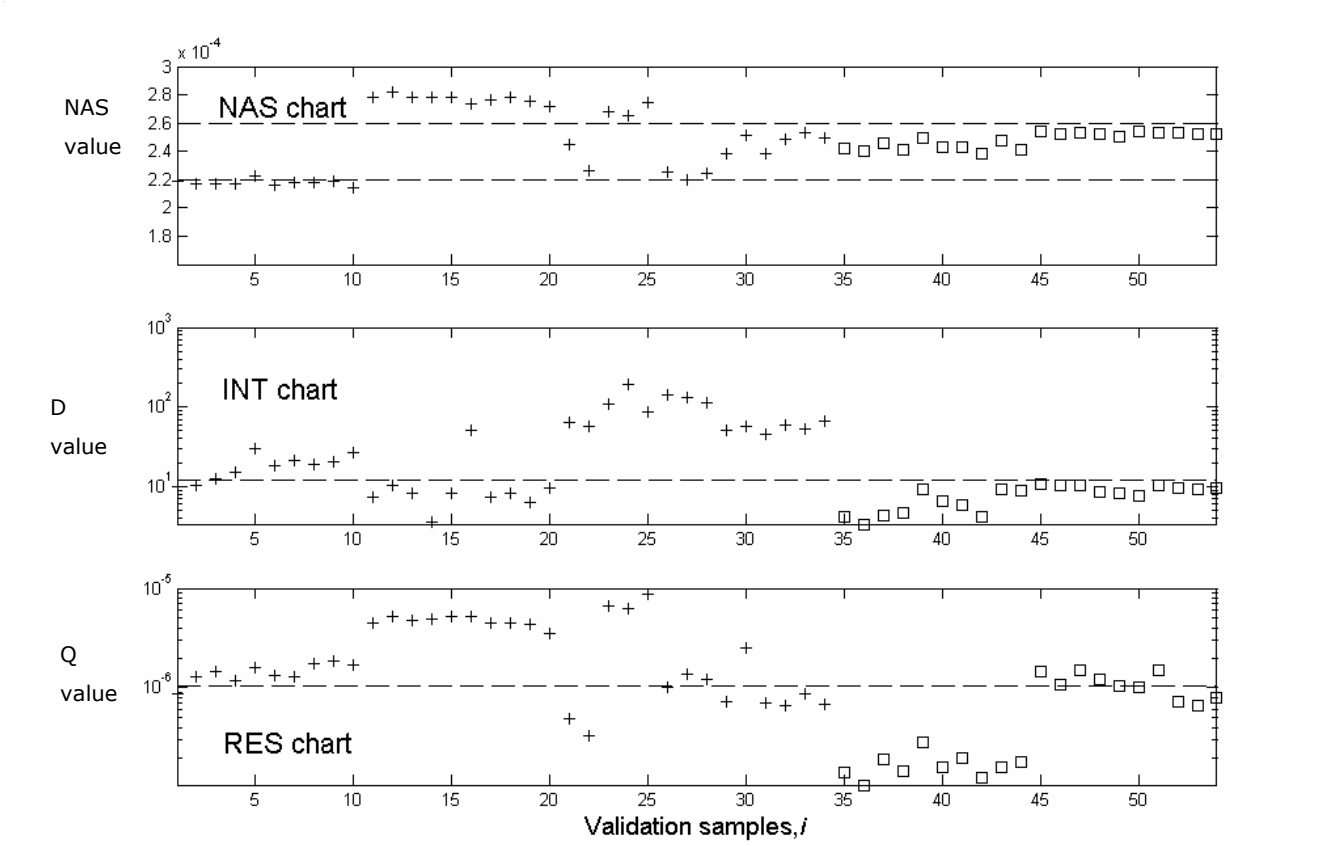

Figure 6: Validation samples in control charts.

The improved diagnostics is illustrated in Figure 7, at which the mean centred INT vectors of the validation sample spectra are depicted. The INT vectors from "wet" samples no. 21 and 22 have characteristic increased amplitude at 1400 nm, where water is absorbing in the second overtone region. Samples no. 29 to 31 were manufactured with a decreased amount of gelatine, and there are distinct "negative peaks" in their INT vectors observed at 905 nm and 1185 nm. For the samples nos. 32 – 34, an inverse spectral shape is observed. This result corresponded very well with fact that pure gelatine has two characteristic

absorption peaks at 905 and 1185 nm, i.e. the INT vectors from samples with increased gelatine will exhibit increased amplitude at these wavelengths and vice versa.

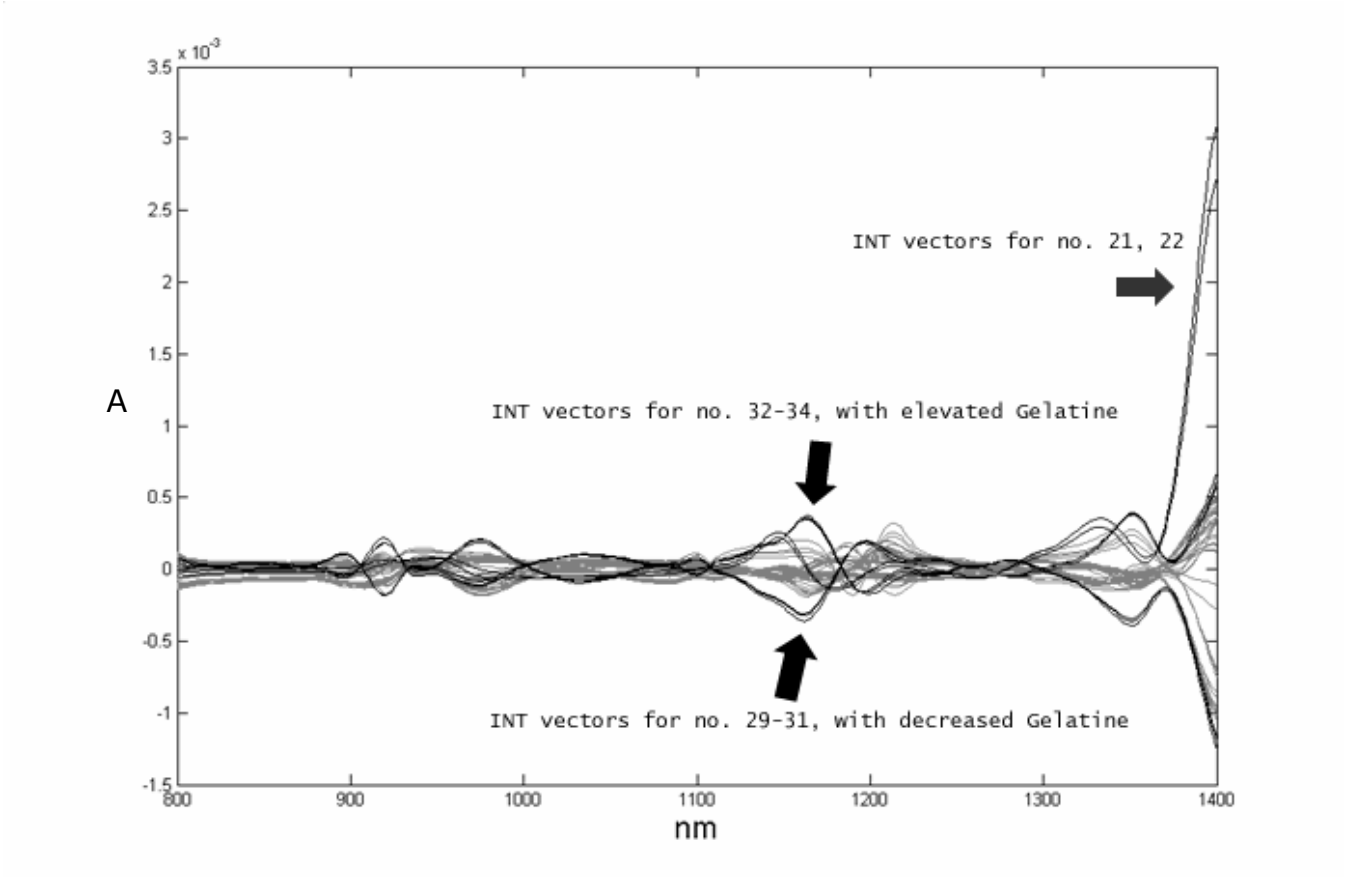

Figure 7: Diagnostics of validation of INT vectors.

NAS-SQC is theoretically applicable for any spectroscopic system that follows the Beer-Lambert law. An important factor when using NIR spectra is awareness that NIR spectra are subject to physical properties of the sample e.g. particle size differences, thickness, density etc. By applying a proper pre-processing method to the spectra the influence of these factors can be minimized.

The NAS method as described here is developed using blank samples. In pharmaceutical industry blank samples are in most cases available. In chemical industry and industries with well defined sample composition is blank samples also available. For more difficult applications, such as natural products or food

products, it might not be possible to obtain blank samples. In those cases other methods have been suggested to obtain the interference space[22]. Then, when the interferent space is developed, a NAS-SQC system can be developed also for these more difficult cases. It has been demonstrated, how the CU analysis can be performed with NAS-SQC. Other key quality parameters, e.g. water in the tablets were monitored. In some cases, water can affect the dissolution rate of the analyte, i.e. when the tablet is dissolved. This can be critical for the efficacy of the drug product. In this particular case, the piroxicam units were freeze-dried, thus the method can support control of the freeze drying process.

The homogeneity of the interfering constituents was also investigated. In some tablet products, the API concentration (m/m) is very low and the physical properties of the final tablet are mostly controlled by the other components in the tablet matrix. If the excipients are not mixed properly or the particle size is not well controlled, large variations in the physical properties of the tablets can be expected. Also, polymorph transformations which can affect bioavailability of the API can be detected using near-infrared spectroscopy and NAS-SQC. Many other parameters exist which are valuable to control or at least detect, if samples are out of control. We believe that a spectroscopic measurement combined with this novel method is a very valuable tool for quality control and determination of products with quality defects.

Crucial for the method is the selection of NOC and out of control samples. A suggested strategy is to investigate a large set of different samples with NAS-SQC. Samples that show increased statistics in either of the charts can be submitted for further reference analysis e.g. water content, breaking strength, dissolution etc. to determine the exact cause of deviation and classify the samples as either NOC or out of control for the final control charts.

Conclusion

NAS-SQC, a novel multivariate method for statistical quality control and diagnosis is introduced. The method uses spectral measurements of the product. With net analyte signal computations, principal component analysis and multivariate statistical process control theory, the spectra are split into three independent contributions. Control limits and statistics are derived and implemented into three control charts to monitor several quality parameters simultaneously. The main advantage of the method is that by splitting different parts the interpretability is enhanced.

The method was successfully demonstrated on a commercially available tablet product measured with near-infrared transmission spectroscopy. The method is easy to implement and allows the user to specify statistical or actual concentration limits for the analyte of interest. It gives the user control of the multivariate quality of the product as well as extensive diagnostic tools for troubleshooting and process optimisation based on the spectroscopic measurement. By using samples from many different batches which are all in control, the common cause variation is implemented in the model, which increases the robustness of the method.

Acknowledgements

The authors' thank Pfizer Ltd for funding this project and Cardinal Health Oral Technologies for providing samples. Also Novo Nordisk, Corporate Research Affairs (CORA) who sponsored this work as a part of E.T.S. Skibsted's Ph.D. project.

References

1. Plugge, W. and Vlies, van der C. *Journal of Pharmaceutical and Biomedical Analysis* **1996,** *14,* 891-898.

2. Langkilde, F. W. and Svantesson, A. *Journal of Pharmaceutical and Biomedical Analysis* **1995,** *13*, 409-414.

3. Han, S. M. and Faulkner, P. G. *Journal of Pharmaceutical and Biomedical Analysis* **1996,** *14*, 1681-1689.

4. Frake, P.; Greenhalgh, D.; Grierson, S. M.; Hempenstall, J. M.; Rudd, D. R. *International Journal of Pharmaceutics* **1997,** *151*, 75-80.

5. Duong, N-H., Arratia, P., Muzzio, F. J., Lange, A., Timmermans, J., and Reynolds, S. *Drug Development and Industrial Pharmacy* **2003,** *29[6]*, 679-687.

6. Gottfries, J., Depui, H., Fransson, M., Jongeneelen, M., Josefson, M., Langkilde, F. W., and Witte, D. T. *Journal of Pharmaceutical and Biomedical Analysis* **1996,** *14*, 1495-1503.

7. Plugge, W. and Vlies, van der C. *Journal of Pharmaceutical and Biomedical Analysis* **1993,** *11*, 435-442.

8. Lorber, A. *Analytical Chemistry* **1986,** *58*, 1167-72.

9. Skibsted, E. T. S., Westerhuis, J. A., Boelens, H. F., Smilde, A. K., and Witte, D. T. *Applied Spectroscopy* **2004,** *58(3)*, 264-271.

10. Martens, H.; Næs, T. *Multivariate calibration,* John Wiley & Sons: Chichester, 1989.

11. Wold, S.; Esbensen, K. H.; Geladi, P. *Chemometrics Intell.Lab.Syst.* **1987,** *2*, 37-52.

12. Ramaker, H.-J.; van Sprang, N. M. *Statistical Batch Process Monitoring,* PhD Thesis, University of Amsterdam, Process Analysis & Chemometrics Group, 2004.

13. Lorber, A., Faber, N. M., and Kowalski, B. R. *Analytical Chemistry* **1997,** *69*, 1620-1626.

14. Miller, J. N. and Miller, J. C. Statistics and Chemometrics for Analytical Chemistry. 4. 2000. Pearson Prentice Hall.

15. Jackson, J. E.; Mudholkar, G. S. *Technometrics* **1979,** *21*, 341-49.

16. Faber, N. M. *Analytical Chemistry* **1999,** *71*, 557-565.

17. Faber, N. M. *Chemometrics and Intelligent Laboratory Systems* **2000,** *50*, 107-114.

18. Geladi, P., McDougall, D., and Martens, H. *Applied Spectroscopy* **1985,** *39*, 491-500.

19. Savitzky, A. and Golay, M. J. E. *Analytical Chemistry* **1964,** *36*, 1627-1639.

20. Aldridge, P. K., Evans, C. L., Ward, H. W., II, and Colgan, S. T. *Analytical Chemistry* **1996,** *68*, 997-1002.

21. Zannikos, P. N., Li, W-I, Drennen, J. K., and Lodder, R. A. *Pharmaceutical Research* **1991,** *8[8]*, 974-978.

22. Berger, A. J.; Koo, T.-W.; Itzkan, I.; Feld, M. S. *Analytical Chemistry* **1998,** *70*, 623-27.

PAPER 4.

A Theoretical Framework for Real Time Release with NIR and Chemometrics.

Erik Skibsted, Johan Westerhuis, Age Smilde and D. T. Witte

This paper is being published in Validation Column in NIRNews. The paper is shown in full length (Chapter 4) in this thesis.

PAPER 5.

Examples of NIR based Real Time Release in Tablet Manufacturing

E. T. S. SKIBSTED, J. A. WESTERHUIS, A. K. SMILDE and D. T. WITTE.

Submitted (October 2005) to Journal of Pharmaceutical and Biomedical Analysis.

Examples of NIR based Real Time Release in Tablet Manufacturing

Authors: E. T. S. Skibsted [a,b], J. A. Westerhuis [a,*], A. K. Smilde [a], D.T. Witte[c]

[a] Biosystems Data Analysis, Swammerdam Institute for Life Sciences, University of Amsterdam, Nieuwe Achtergracht 166,

1018 WV Amsterdam, The Netherlands.

[b]Pharmaceutical Site Maaloev, Novo Nordisk A/S, Novo Nordisk Park, 2760 Maaloev, Denmark.

[c]N.V. Organon, Molenstraat 10, P.O. Box 20, 5340 BH Oss, The Netherlands

Abstract

Real time release (RTR) of products is a new paradigm in the pharmaceutical industry. With models using in-process data RTR can be realized. This paper presents some practical examples using near-infrared and process data obtained from a tablet manufacturing process.

Keywords

Real time release, near-infrared, process models, chemometrics, process analytical technology, multivariate statistical process control, regression models, tablet manufacturing.

[*] Corresponding author: westerhuis@science.uva.nl

Introduction

The publication of the Food and Drug Administration (FDA) process analytical technology (PAT) initiative[1] has increased the interest for PAT in the pharmaceutical industry. One of the principles that are described in the guidance document is real time release (RTR). Real time release is the ability to evaluate and ensure the quality of in-process and/or final product based on process data[1]. In a recent paper[2] we presented a theoretical framework for RTR, in which four theoretical and distinct different models were suggested for a RTR system. In the present paper will we demonstrate (practical) examples of these four model types, using near-infrared and process data from a tablet manufacturing process.

Theory of Real Time Release

An RTR system ensures that when the last manufacturing step is passed all the final release criteria are met. Three basic questions have to be addressed for such a system:

- Do we have a (preferably early) warning system if something is going wrong during manufacturing? – monitoring capability
- Do we have an idea how to adjust the process, and whether it is possible? – control capability
- If we monitor and control our processes, will the final product meet its quality criteria? - RTR capability

Different approaches can be used in order to address these three questions. In this paper the combination of near-infrared and process data is demonstrated as an example of the theoretical considerations discussed earlier. Four distinct different models can be used to evaluate the data (Table 1) i.e. one multivariate statistical process control (MSPC) model and three different regression models.

A: Statistical model

In a statistical model, new measurements are compared statistically to historical data from normal operating conditions (NOC) batches that provided good quality products. A classical method which can be used for the statistical monitoring strategy is multivariate statistical process control (MSPC) based on developing a Principal Component Analysis (PCA) model[3] on NOC batch data and two control charts for the operator based on *D* and *SPE* statistics[4]. In case that a future measurement exceeds the limits in the control charts the operator can switch to the contribution plot[5] and identify the cause of the process disturbance.

B: Regression models

In the occasions where a quality parameter (being it an intermediate property or the final product) is available, a regression model can be developed. The regression models all relate some process measurements to a quality measurement at the end (final product quality) or halfway (intermediate quality parameter) of the process. The regression models all need a calibration model to be developed between predictors and a response e.g. quality parameter. Three different regression models can be made. These are explained in Table 1. Multivariate regression methods e.g. PLS[6], multi-block PLS[7], N-way PLS[8] and other regression techniques can be used to develop models for predicting intermediate and final product quality parameters.

Table 1. Overview of the four different model types.

Class	Model symbol	Description
A. Statistical model	A	Statistical model comparing current process observations with historical process observations e.g. multivariate statistical process control (MSPC) models.
B. Regression models	B.1	Intermediate quality predictions. A regression model between predictors and intermediate quality parameters. For example, used for feedback control.
	B.2	Final quality predictions. A regression model between predictors and final quality parameters at a point where the entire manufacturing process has not been completed. For example, used for feed forward control.
	B.3	Final quality predictions. A regression model between predictors and final quality parameters when the entire manufacturing process has been completed. Used for RTR.

In the results section examples of these models will be presented.

Experimental section

Tablet manufacturing process

The manufacturing process consisted of several unit operations which are symbolized in Figure 1. In the brackets are the symbols which are used in Figure 1. First all compounds (see Table 2) were weighed (wei). Then the active pharmaceutical ingredient (API), lactose, microcrystalline cellulose, polyvinylpyrrolidone and crosscarmellose were mixed (mix_1) in a high shear mixer. A prepared mixture of polyvinylpyrrolidone and water was added to the high shear mixer and granulation was performed (gra). The wet granules were removed and put through a sieve (s) before added into a fluid bed reactor where the granules were dried (dry). The dried granules were removed and again put through a sieve (s) and placed in a drum mixer. Gliding compounds were added and mixed with the granules (mix_2). The finalized granules were compressed into tablets (tab) with a weight of 180 mg.

Analysis

During drying, samples were removed from the fluid bed reactor and loss on drying analysis was performed. After drying samples were subjected to particle size analysis. The tablet disintegration time was also determined for each batch. Finally, NIR analysis was performed extensively throughout the entire process which will be described later in this chapter.

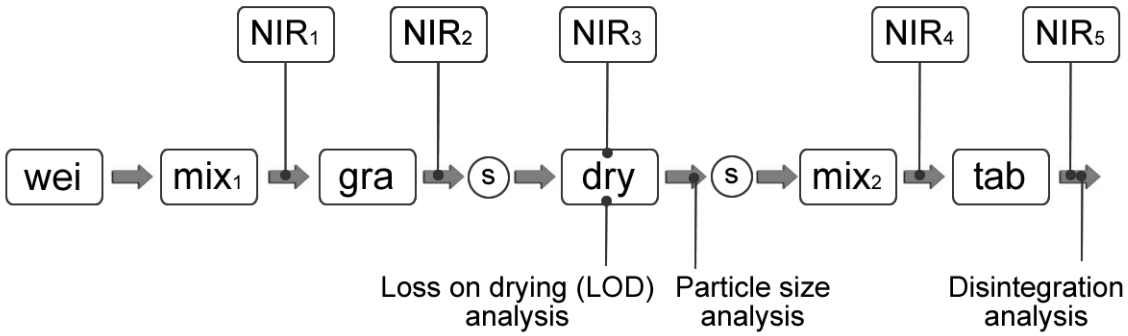

Figure 1. Overview of unit operations, NIR measurements (symbolized with NIR boxes) and reference analysis points.

Table 2. Batch formulation of main tablet, granulation liquid and glitter compounds.

	Compound	g
Main compounds	API	175
	Lactose	966
	Microcrystalline cellulose	221
	Polyvinylpyrrolidone	84
	Crosscarmellose	97
Granulation liquid	Polyvinylpyrrolidone	37
	Purified water	372
Glitter compounds	Magnesium stearate	8
	Talc	16

Batch overview

Six calibration batches with varying amount of API i.e. 0% (placebo), 75%, 85%, 100%, 115% and 125% of API label claim. In the calibration batches with API amount different from 100% label claim the API was interchanged with lactose and microcrystalline cellulose keeping the ratio between those two components

constant. Also a set of designed batches (DoE batches, all with 100% API label claim) were manufactured (Table 3). The tablets of all the calibration and DoE batches were weighing 180 mg. In the DoE batches three process variables; dry mixing time, granulation liquid flow and drying temperature were varied according to a full factorial design in total eleven batches plus an extra training batch (#1), and three centre points (#10-12). All calibration batches and the placebo batch were having a mixing time of 2 minutes, granulation liquid flow of 90 ml/min. and they were dried at 60 °C.

Table 3. Batch overview.

Batch	*Description*		
Placebo batch	a batch without API (also used for calibration)		
Calibration batches	Five batches with 75%, 85%, 100%, 115% and 125% of API label claim		
DoE batches	Mixing time [min.]	Gran. liquid flow [ml/min.]	Drying temp. [C]
# 1	1	30	60
# 2	1	30	50
# 3	4	30	50
# 4	1	90	50
# 5	4	90	50
# 6	1	30	70
# 7	4	90	70
# 8	1	90	70
# 9	4	30	70
# 10	2.5	60	60
# 11	2.5	60	60
# 12	2.5	60	60

NIR analyzer and measurement details

All NIR measurements were performed with a new versatile FT-NIR Bruker Multi Purpose Analyzer (MPA) (Bruker Optics, Ettlingen, Germany). With this NIR analyzer the manufacturing process was investigated at several points (Figure 14). In Figure 1, the NIR measurement points are symbolized with boxes with NIR_i inside. NIR_3 is an online measurement of the drying step, while the other NIR measurements are obtained after the process step was finished. Table 4 contains details for the NIR measurements displayed.

Table 4. NIR measurement details.

NIR_1, NIR_2 and NIR_4	Reflectance measurement with handheld probe. 16 scan pr spectrum. The region from 4000-12500 cm-1 was scanned. Resolution 8cm-1.
NIR_3	Reflectance measurement with process probe. 64 scan pr spectrum. The region from 4400-12500 cm-1 was scanned. Resolution 8 cm-1.
NIR_5	Transmission measurement. 32 scan pr spectrum. The region from 5800-12500 cm-1 was scanned. Resolution 8 cm-1.

Data analysis

All data analysis was done using MatLab[9], PLS toolbox[10] and in-house written m-files. The NIR spectra were imported into the MatLab environment after acquisition with the NIR instrument software.

Examples and discussion

In this section, four examples of applications in a RTR system are discussed. Please note that, while the examples were investigated thoroughly, here we only discuss them briefly, since the main goal is to show how all these examples fit in a RTR scheme.

Example 1: Statistical model

With this example it is demonstrated how two MSPC models based on NIR_1 or NIR_2 measurements could provide an early warning of manufacturing problems and separate good batches from the bad ones. Two DoE batches (# 2 and #3) experienced particle size problems after the drying step and this is referred to as the manufacturing problem. The DoE batches #1, #4-6 and #8-12 had no manufacturing problems; these are referred to as normal operating condition (NOC) batches. NIR spectra from the NOC batches were used to develop the MSPC control charts. The DoE batches #2 and #3 with manufacturing problems and #7 without manufacturing problems were then used to validate the MSPC control charts. After drying DoE batch #2 granules had a large proportion of fines and a low average particle size while DoE batch #3 granules consisted of coarse

particles. DoE batch #7 was known for having a particle size distribution similar to the other nine DoE batches i.e. good particle quality. These batches were called validation batches. Validation of MSPC models is done by showing that observations from batches with manufacturing problems are flagged above the control limits in the MSPC charts while observations from batches without manufacturing problems are below the control limits. It is an essential necessity for development and validation of a MSPC model that data exist for both NOC batches and batches with quality defects.

The first MSPC model used the raw NIR_1 spectra as input. The NIR_1 spectra from the NOC batches (on average fourteen spectra from each batch) were used. The spectra were collected in a 119×2281 matrix. The spectra were mean centred and a PCA model was fitted to the spectra. The 95% confidence limit for the *D* statistic was calculated and used as warning limit in the *D* chart[4]. For the residuals the 95% confidence limit was calculated and used as warning limit in the *SPE* chart[11]. Now the NIR_1 spectra from the validation batches were mean centred and projected on the PCA model; their *D* statistics were plotted in the *D* chart. The squared residuals were also calculated and plotted in the *SPE* chart (Figure 2). Fifteen spectra from DoE #2 (symbolized with stars), thirteen spectra from DoE #3 (symbolized with triangles) and fourteen spectra from DoE #7 (symbolized with circles) are depicted in Figure 2. These spectra are from independent measurement from different position in the powder mixture after the mixing step. Thus one should consider all the spectra of one batch as a whole. According to the control charts in Figure 2, batches DoE#3 and DoE#7 have problems while batch DoE#2 seems to be ok (except for the sample 14 that just exceeds the SPE limit. Various pre-processing and wavelength selection were tried out in order to see if a better result was obtained but without success. The conclusion was that a MSPC model with NIR_1 was not good for identification of the two batches with quality defects.

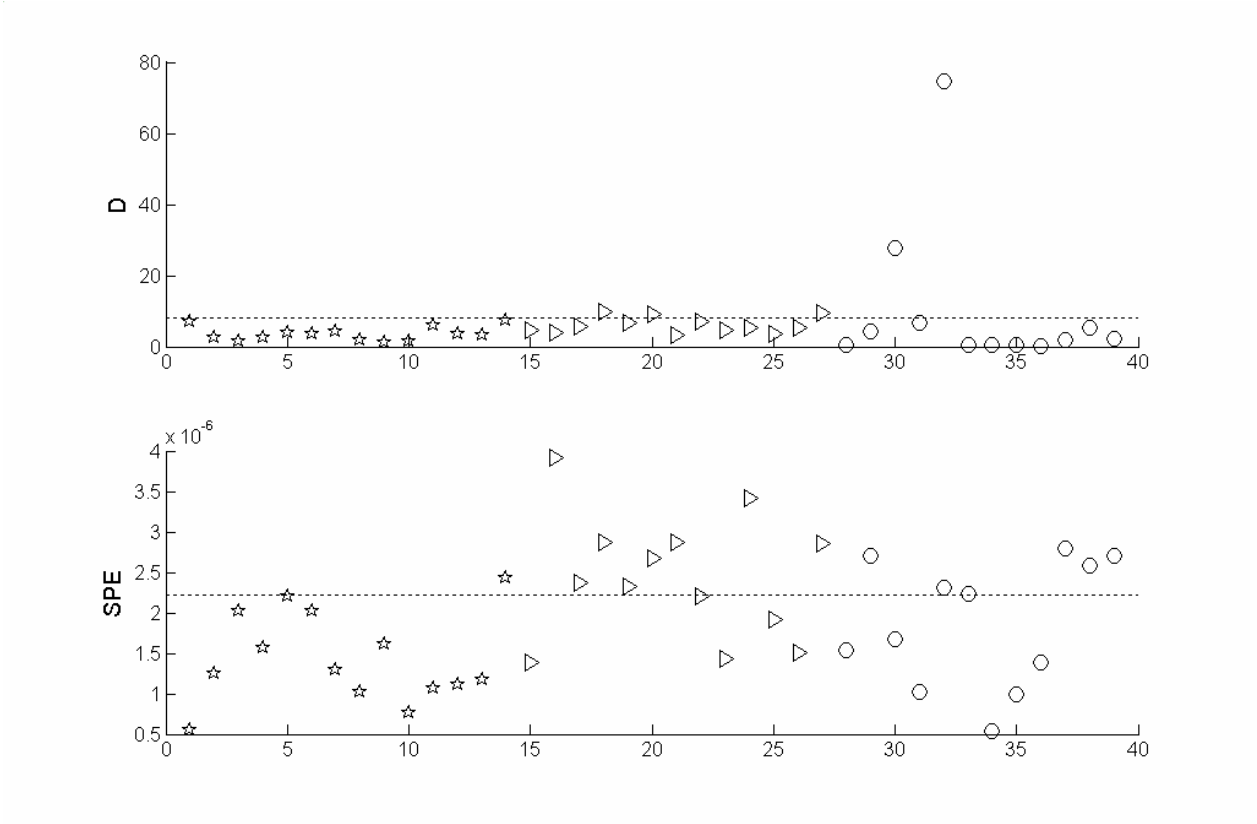

Figure 2. The NIR_1 data from the validation batches plotted in the *D*-chart and the *SPE*-chart. DoE #2 observations are symbolized with stars, DoE #3 with triangles and DoE #7 with circles. The dotted lines in both charts are the 95% confidence limit.

Therefore an MSPC model and control charts were developed with NIR_2 as input. Again various pre-processing methods and wavelength selection were tried out and the best results obtained with 1st derivative and the wavelength region from 4700 to 5700 cm^{-1}. With the spectra from the NOC batches the control limits were developed for the charts. Then the *D* and *SPE* statistics of the validation spectra were calculated and plotted in the control charts (Figure 3). Almost all data points from DoE #2 and DoE #3 spectra were flagged out in either the *D* or the *SPE* charts. All DoE #7 data points were below the control limits as expected (circles in Figure 3).

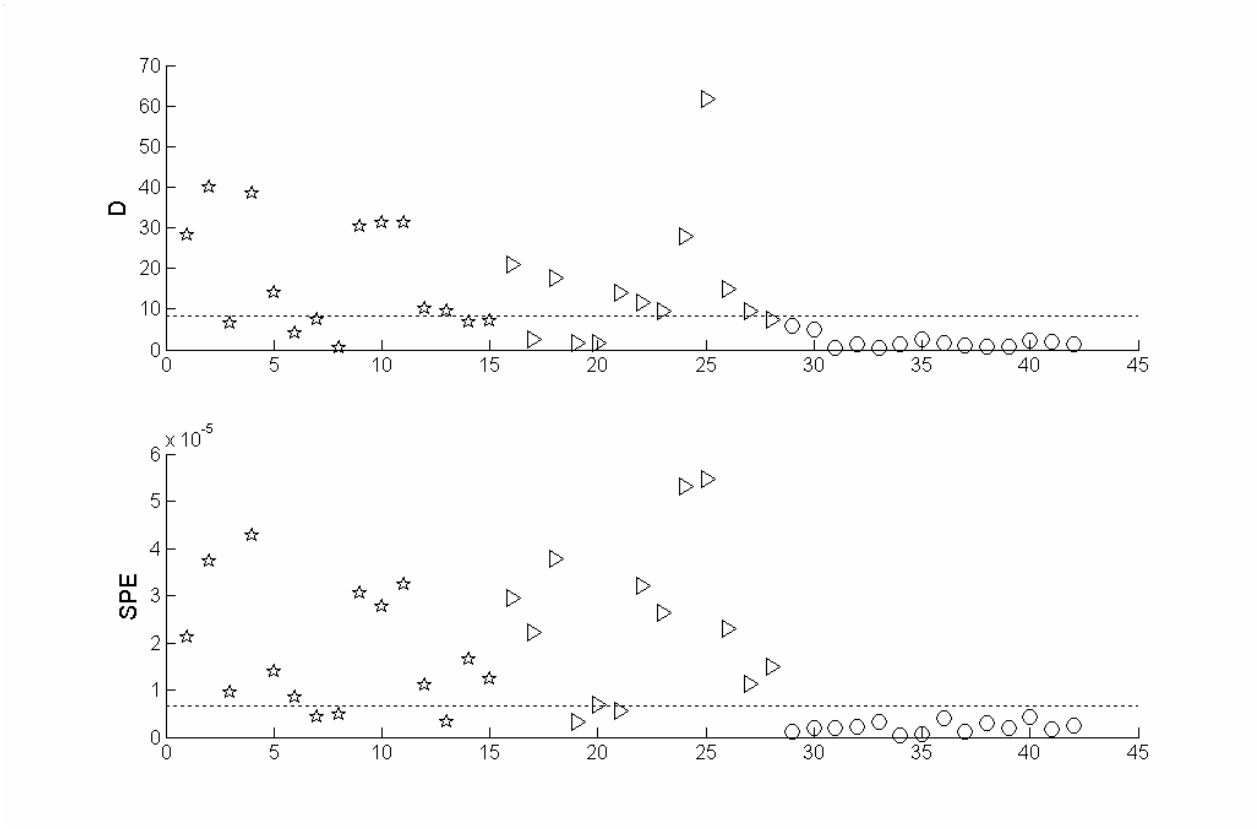

Figure 3. The NIR_2 data from the validation batches plotted in the *D*-chart and the *SPE*-chart. DoE #2 observations are symbolized with stars, DoE #3 with triangles and DoE #7 with circles. The dotted lines in both charts are the 95% confidence limit.

This demonstrated how early warning and monitoring capability of manufacturing problems was achieved with a statistical model using NIR_2 data. Secondly, it was found that the granulation step is important when it comes to particle size quality. The next step would be to investigate whether the granulation process could be controlled to get consistent particle size quality.

Example 2: Regression model B.1 (local prediction of quality)

Along the manufacturing chain several intermediate quality characteristics can be monitored. In some cases is it of vital importance that the intermediate quality is good in order to continue to the next process step and ultimately this will benefit a RTR system. Monitoring the water content during drying is an example of monitoring a local quality characteristic. The purpose of the drying process is to

remove excess water in the granules and produce dried granules that are easily compressed into tablets. If the water content is not within a certain range, compression problems will occur and it might be necessary to discard the entire batch.

During drying in the fluid bed reactor NIR spectra were automatically collected every half minute, with a process reflectance probe inserted in the reactor. Powder samples were removed from the fluid bed reactor during the drying from a sample port located in close proximity to the NIR probe port. The water amount in the samples was determined as % weight loss-on-drying (LOD), using a moisture analyzer (Mettler Toledo Halogen Moisture Analyzer HR73). The spectrum that was recorded during the removal of the sample was assigned to the corresponding LOD reference value. A PLS model with three latent variables was developed using 28 calibration spectra representing all DoE batches. Many different pre-processing methods were investigated and also wavelength selection routines were applied in order to minimize non-relevant spectral variation and improve model statistics. As pre-processing method Savitzky-Golay 1^{st} derivative with a second order polynomial fit using 17 spectral points was selected. The combined wavelength regions 4597 to 5450 cm^{-1} and 7500 to 12500 cm^{-1} were used. These wavelength regions cover the water bands in the combinational and second overtone region in the NIR spectra. The first three latent variables explained 99.08 % of the variation in X and 98.70 % of Y variation. The cross validated predictions are presented in Figure 4.

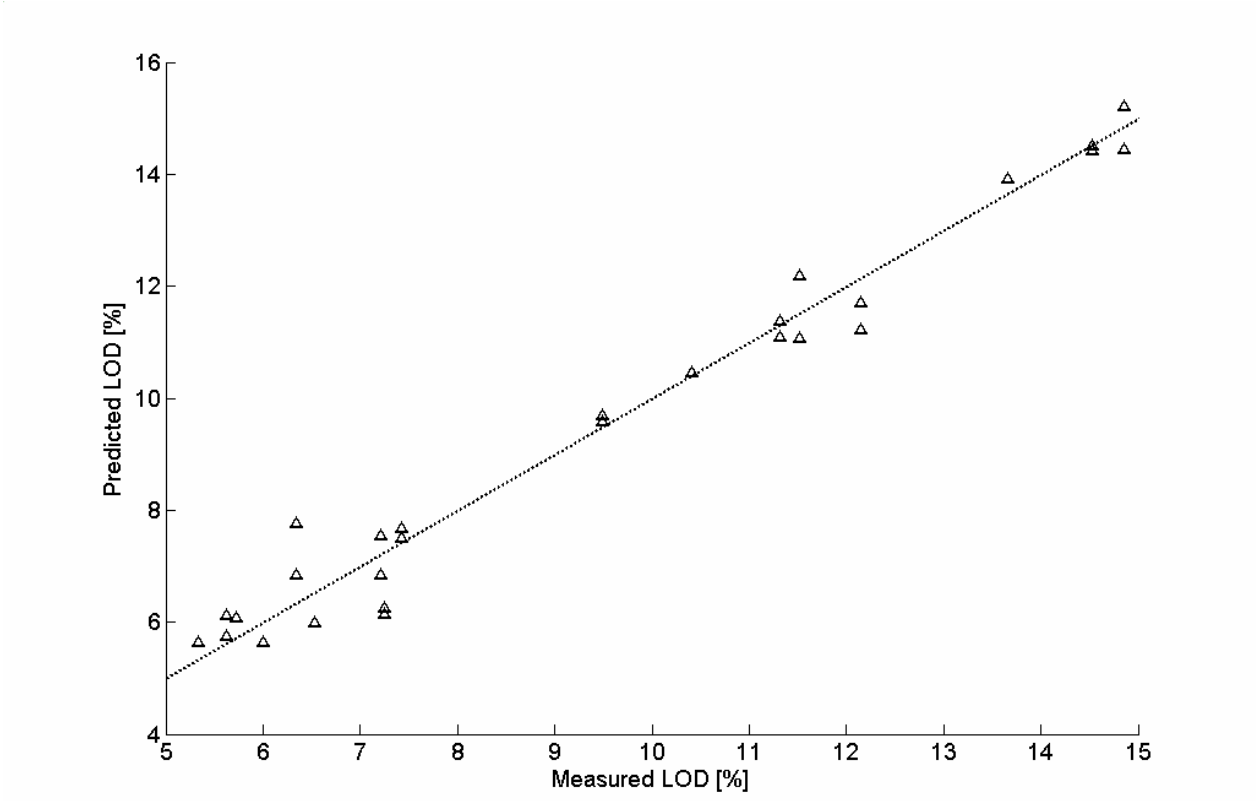

Figure 4. Calibration line for 3 LV PLS model. Measured LOD values vs. predicted values from cross validation. The dotted line indicates perfect fit. With three LV the RMSEC was 0.37 and the RMSECV was 0.53.

The NIR_3 spectra from the DoE batches were applied to the PLS model and drying (LOD) curves were predicted. Examples of the drying curves from two DoE batches dried at 50 °C and 70 °C respectively are shown in Figure 5. Both batches showed a steep decline in LOD the first five minutes because of high water evaporation caused by the airflow which always was 100 m^3/h the first five minutes and thereafter lowered to 50 m^3/h for the remaining drying. The drying of both batches was terminated when the product temperature reached 34 °C but due to the different drying temperature, the drying times differed from 23 to 38 minutes. Both drying curves showed a slight increase of the LOD near the end of the drying period. The increase can be explained with an increased diffusion of water from the core to the surface of the granules during what is known as the *equilibrium* period[12] where the granule temperature is increasing. The

phenomenon is a process signature and can be utilized into end-point control of the drying process, which is the natural extension of this example of in-line local quality predictions.

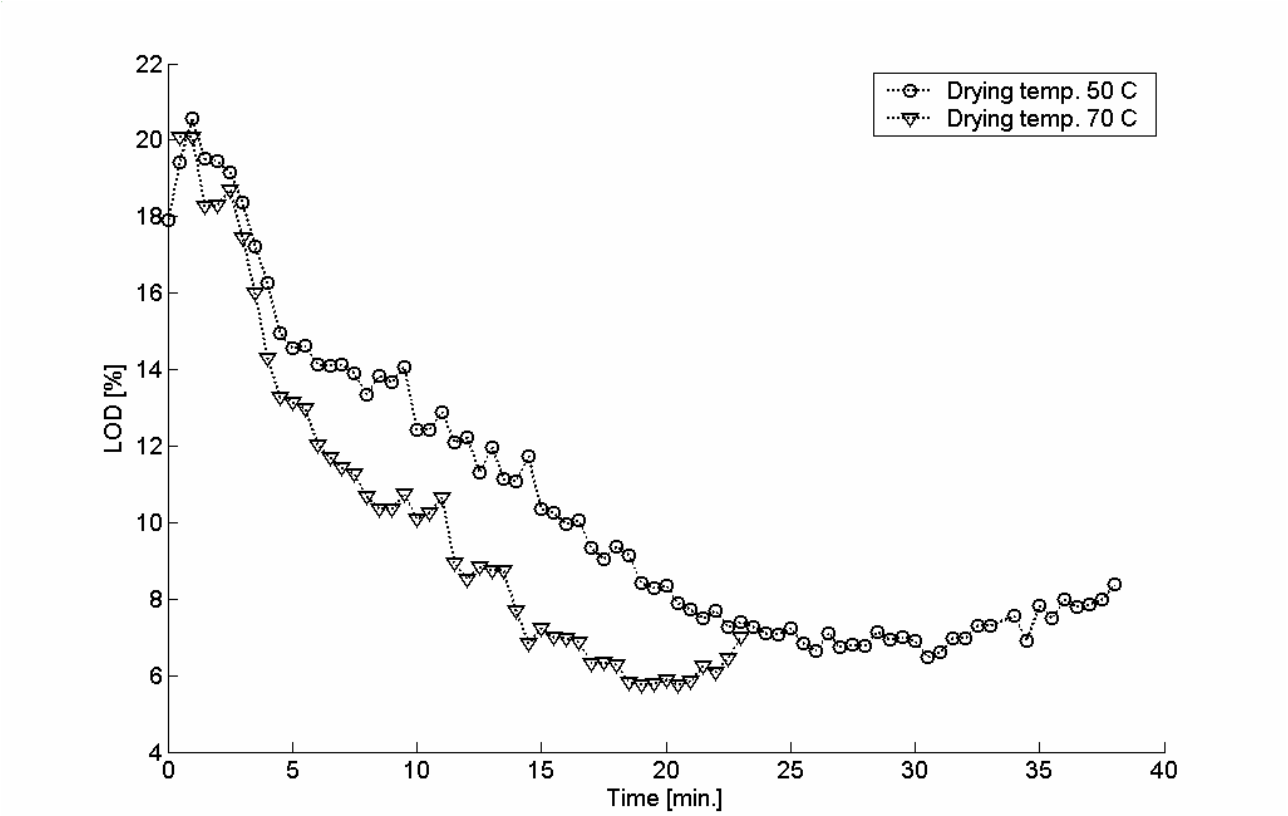

Figure 5. Drying curves for two DoE batches with drying temperatures 50 °C (-o-) and 70 °C (-∇-). Both batches were granulated with a granulation liquid flow of 90 ml/min.

With the example it was demonstrated how a regression model between in-line NIR spectra and LOD provided monitoring capability. Secondly, it is also be possible to implement the regression model for real-time control of the drying time, which can provide control capability of the process.

Example 3: Regression model B.2 (forecasting final quality and process control)

In any manufacturing system there will be variation in the process input e.g. raw material variation, environmental factors etc. which all affect the final quality,

unless the manufacturing process can comprehend these variations or process control exists to minimize the influence of input variation. In the following it will be demonstrated how to develop a feed forward process control tool with regression models between process variables, process measurements and a final quality characteristic i.e. the mean disintegration time for the tablets. In each batch the disintegration time was determined for six tablets using an automated disintegration testing instrument (Tablet Disintegration System PTZ Auto 2EZ, Pharma-Test Germany). The average disintegration time (disT) of six tablets was used as final quality variable. The average disintegration time ranged from 120 seconds to 248 seconds. The standard deviation on the average disintegration time was approximately 30 seconds. Two PLS models were developed (model I and II) using process variables and NIR spectra as predictors.

The NIR spectra consisted of more then 2250 spectral variables and in order to perform data fusion between a few process variables and thousands of spectral variables, the NIR spectra were first decomposed using PCA and the mean centred scores were then fused with the process variables. Then the scores and process variables were auto scaled and a PLS model established between the predictors and the mean disintegration time.

The predictors for model I were; mixing time (mix), the average NIR spectrum from the mixing (NIR1*) and the granulation liquid flow (gra). For model II, the predictors also included the average NIR spectrum of the granulation (NIR2*), drying temperature (airT), drying time (dryTime), the last spectrum from the drying process (NIR3*), the average NIR spectrum from glidants mixing (NIR4*) and upper punch force during tabletting (punF). The predictors and models are depicted in Figure 6.

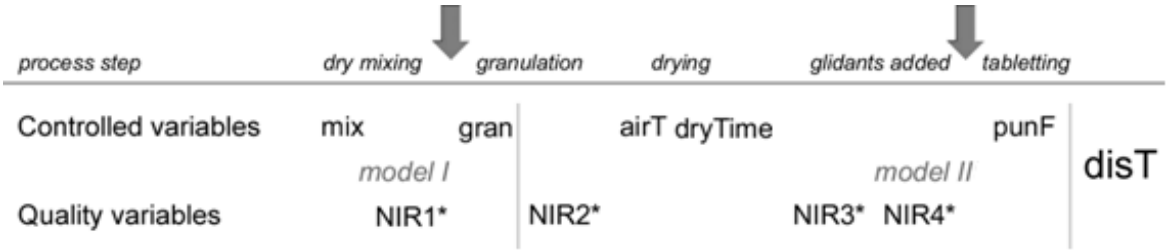

Figure 6. Overview of controlled and quality variables used for modelling. The controlled variables are; mixing time of the dry powders (mix), the granulation liquid flow (gran), the air temperature in the fluid bed (airT), the drying time in the fluid bed (dryTime) and the average upper punch force during tabletting (punF). The average NIR measurements after various process steps are denoted NIR* 1 to 4. The quality variable is the mean disintegration time of the final tablets (disT).

Using the data from the twelve DoE batches two PLS models were developed. The models statistics are listed in Table 5. Leave one out cross validation (LOO CV) was used given the limited number of data points. The root mean squared error obtained from cross-validation (RMSECV) of model II was 36.3 using two latent variables (LV) and 93 % of the Y variation explained compared to 66 % for model I. By adding more process information the prediction error decreased.

Table 5. Model statistics for PLS models I and II.

	Model I				**Model II**			
LV #	Expl. X var.	Expl. y var.	RMSEC	RMSECV	Expl. X var.	Expl. y var.	RMSEC	RMSECV
1	26.9	61.5	28.7	46.4	22.3	85.6	17.6	36.2
2	**51.6**	**66.0**	**27.0**	**50.4**	**34.4**	**93.0**	**12.2**	**36.3**
3	73.3	67.2	26.5	55.8	50.9	96.8	8.3	38.8
4	81.6	67.3	26.5	59.8	63.4	98.3	6.0	36.0
5	100.0	67.3	26.5	60.6	76.2	98.9	4.9	33.3
6					84.3	99.5	3.3	33.0

The measured vs predicted mean disintegration time for model II is depicted in Figure 7. The prediction error was in some cases high which might be owed to the relative high standard deviation of the mean disintegration time. Secondly is the reference analysis performed on only a fraction of the total number of tablets produced in each batch. Generally, a larger number of batches and tablets pr

batch should be used and secondly the experimental design space extended further in order to find a larger range of disintegration times.

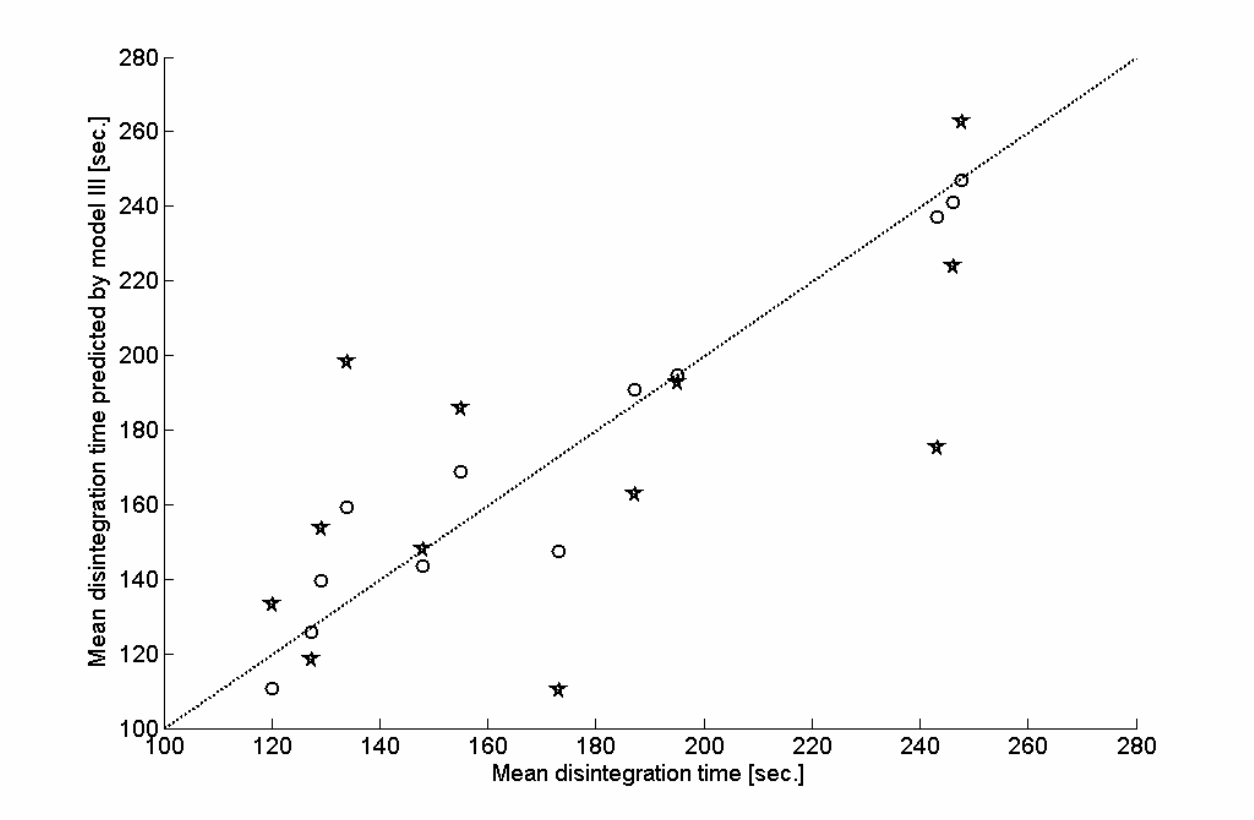

Figure 7. Measured vs. predicted mean disintegration time for PLS model III. The values from calibration are symbolized with circles and the values from LOO CV are symbolized with stars. The dotted line symbolizes perfect fit.

With the models, suggestions for feed forward process control can now be derived.

In Figure 8 this is demonstrated with model I. Model I can be used by the operator just before the granulation is started and the operator wants to know how to set the granulation liquid flow. By using the mixing times and NIR measurements from the DoE batches and then inserting hypothetical values for granulation liquid flow from 30 to 90 ml/min, hypothetical mean disintegration times were then predicted with model I. The results showed that by increasing the granulation liquid flow the disintegration time would decrease. This could of

course have been directly obtained from the negative b coefficient for granulation liquid flow and with model I the effect can be quantified.

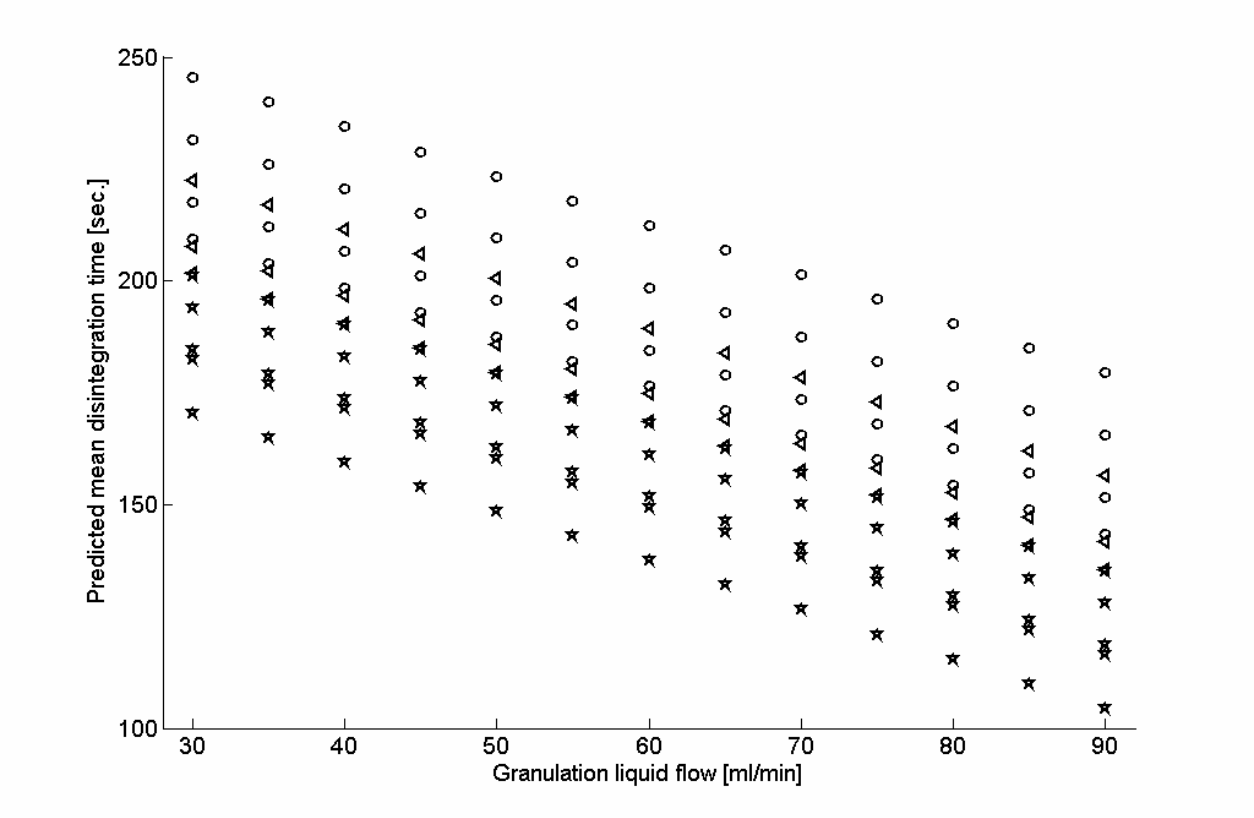

Figure 8. Process control chart for setting of granulation liquid flow using model I at the first decision point. The DoE batches with mix time 1 minute are symbolized with stars, 2.5 minutes are symbolized with triangles and 4 minutes with circles.

With the model, the operator now has a process control tool to set the granulation liquid flow after the mixing step in order to control disintegration time.

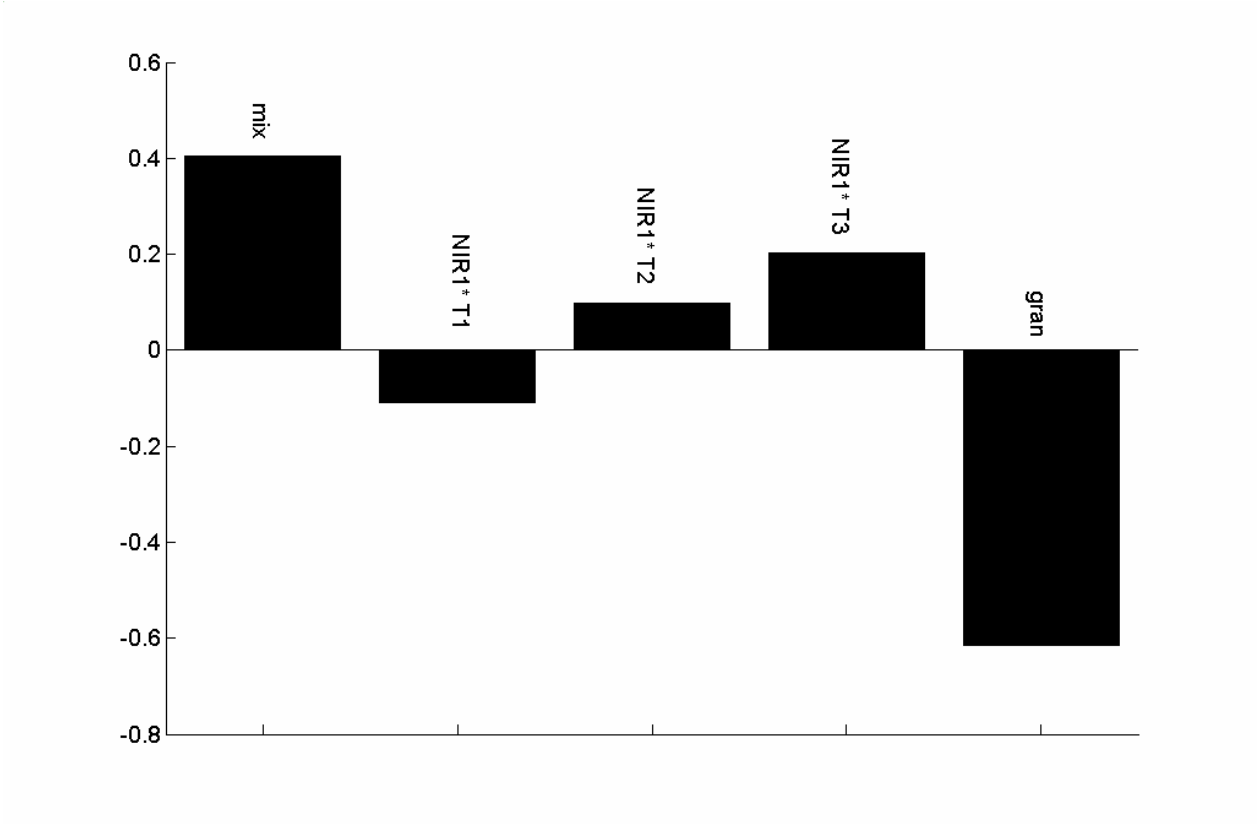

Figure 9. The b coefficients for PLS model I.

Before the operator starts the tabletting model II can be used to set the required upper punch force, in order to achieve a certain mean disintegration time of the final tablets. This was demonstrated by inserting different values for punch force in model II. The resulting predicted disintegration times are depicted in Figure 10.

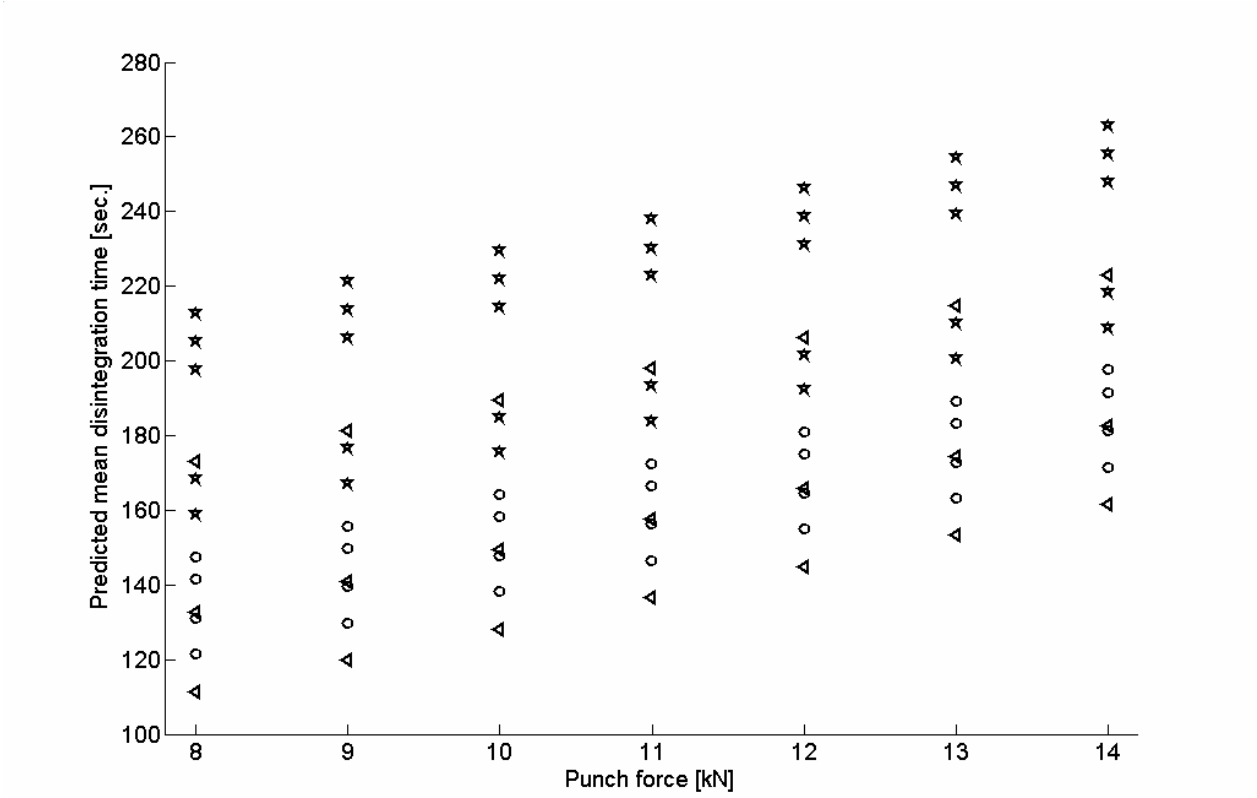

Figure 10. Predicted mean disintegration time as a function of various hypothetical upper punch force values (punF) for the twelve DoE batches. The batches with gran = 30ml/min are symbolized with stars, 60 ml/min are symbolized with triangles and 90 ml/min symbolized with circles.

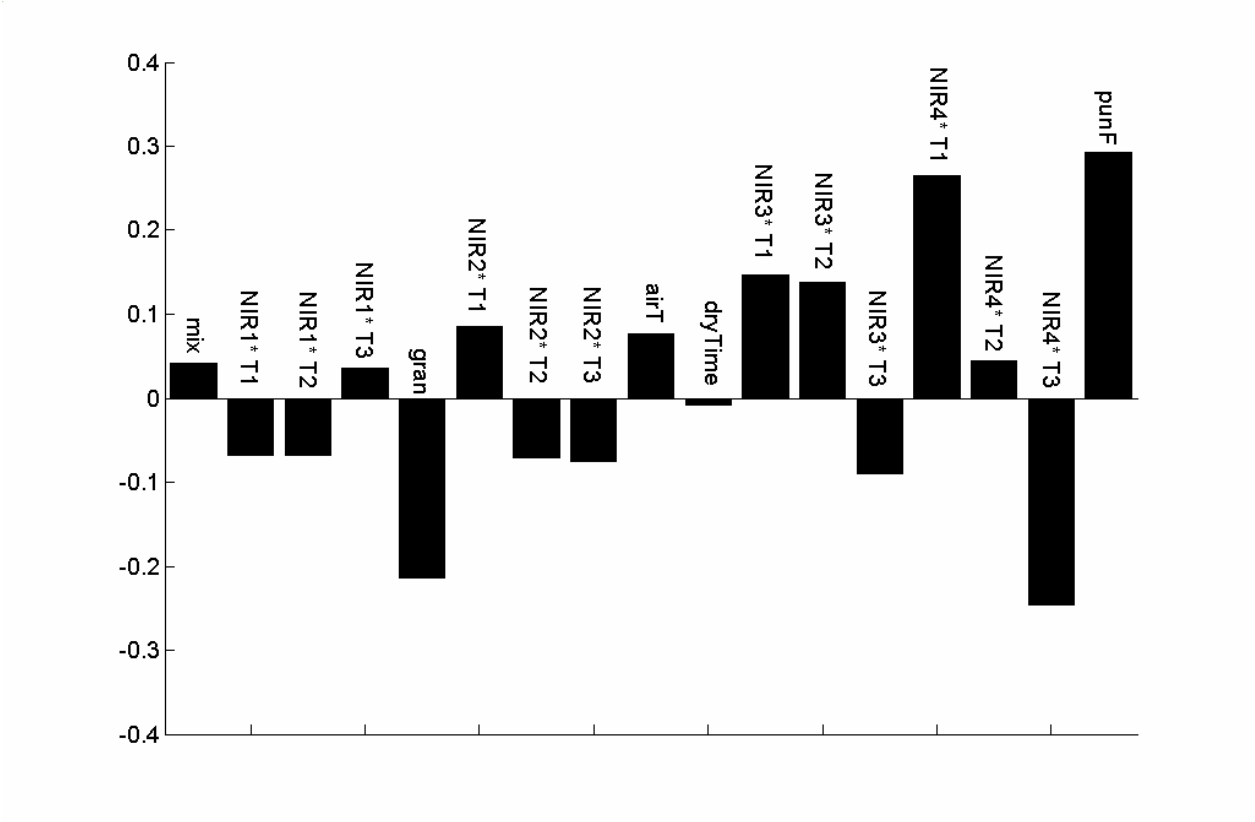

Figure 11. The b coefficients for PLS model II.

The results from this example are only indicative since more data should be available for a thorough treatment. Nevertheless does the example serve to demonstrate how to develop feed forward process control tools with regression models. The correlation between process variables and the final quality characteristic was illustrated by the b coefficients which showed 'in which way to turn the knob' in order to force the direction of the quality parameter. The regression models could then be used to quantify the effect of 'the turn'. The results demonstrated how to get control capability.

Example 4: Regression model B.3 (final quality predictions)

The most important quality characteristics for the customer are these of the final drug product. Measurements of final quality characteristics when the drug product leaves the manufacturing line in real-time or near real time would be an example of RTR.

The content of active pharmaceutical ingredient (API) in the final tablets is a major quality parameter. Traditional quality control is performed on a small set of tablets i.e. ten to thirty tablets in distant laboratories using time consuming analysis methods e.g. HPLC. This means that the batch is quarantined for two to three weeks before the analysis result is ready and the batch can be released to market. Secondly by only analyzing a small number of samples there is an increased risk that quality defects are not detected.

As an example of near real time quality control of the API content in individual tablets, a regression model was developed between NIR transmission spectra of the final tablets (NIR_5) and the API content. For each of the six calibration batches one calibration spectrum was made by averaging of 120 measured tablet spectra from each calibration batch. Then each calibration spectrum was assigned a reference value which was the average API content in the corresponding calibration batch and finally a regression model was build between the average calibration spectra and their reference values (which here was of course the weighing of the different compounds). This calibration method does not rely on reference analysis and the assumption for using this method is that by measuring a large number of samples from a batch the average content in all samples approach the average content of the entire batch.

A PLS regression model with one PLS component was constructed. A very low RMSECV of 0.066 and a correlation coefficient of 0.9999 were obtained. Fig 12 shows the cross-validated predictions of mg API/tablets. By visual inspection of the regression vector, the pre-processed calibration spectra and the pure API spectrum it was evident that it was the variation of the API that was modelled.

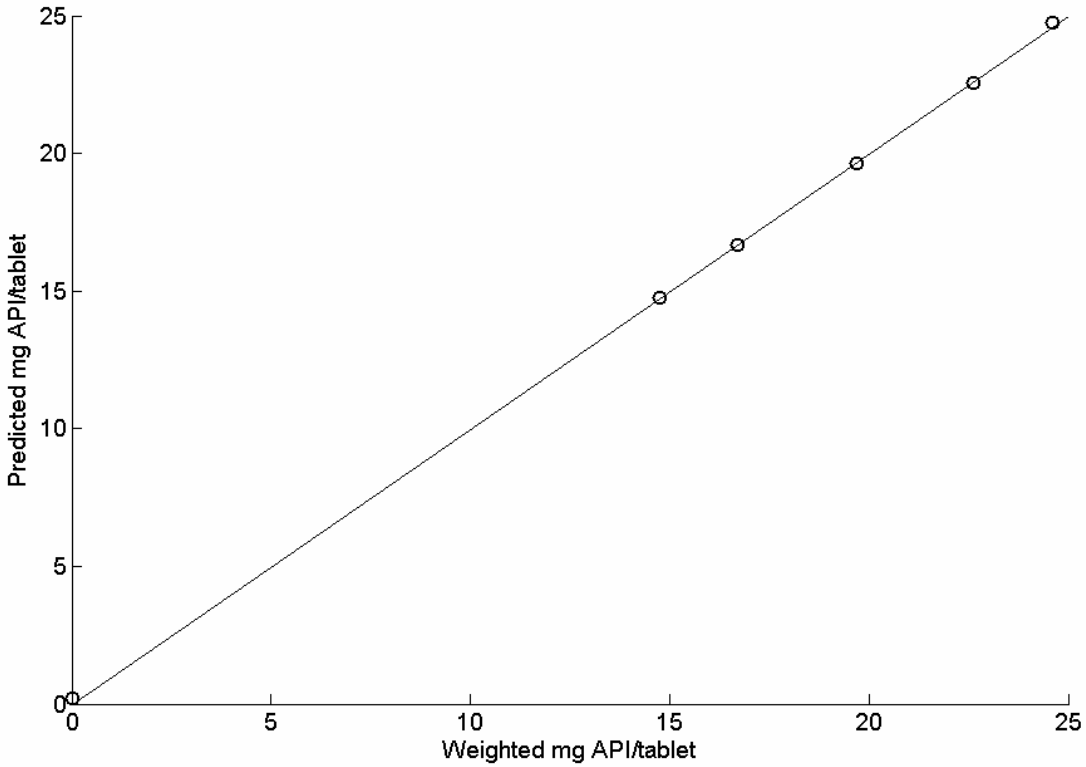

Figure 12. PLS model with one component using the wavelength region from 7500 cm^{-1} to 12500 cm^{-1}. The predicted values from cross validation, of the calibration spectra vs. their reference values. The R2 is 0.9999; the RMSECV is 0.066 which is 0.3%.

From each of the DoE batches ninety tablets were measured with transmission NIR. The ninety tablets were removed from the tabletting process in the following way; thirty tablets from the start, thirty tablets from the mid and thirty tablets from the end of the tabletting process. With the PLS model the assay (mg/tablet) was predicted in all tablet samples. The average and variance of the thirty assay predictions from the start, mid and end are listed for all DoE batches. It was discovered that there was very little variation in the API content.

Table 6. Assay predictions (mg API/tablet) for twelve DoE batches. The mean and variance are calculated for thirty tablets from the start, mid and end of tabletting process. The target content is 19.7 mg API/tablet.

	Mean			Variance		
DoE #	Start	Mid	End	Start	Mid	End
1	19.2	19.2	19.1	0.03	0.02	0.03
2	19.4	19.4	19.4	0.03	0.02	0.02
3	19.6	19.5	19.6	0.03	0.03	0.04
4	19.6	19.6	19.6	0.03	0.03	0.02
5	19.6	19.7	19.8	0.04	0.02	0.04
6	19.5	19.5	19.5	0.03	0.04	0.02
7	19.8	19.5	19.5	0.05	0.06	0.02
8	19.6	19.6	19.5	0.02	0.02	0.03
9	19.4	19.4	19.5	0.04	0.02	0.01
10	19.6	19.7	19.6	0.02	0.03	0.01
11	19.6	19.5	19.4	0.02	0.03	0.03
12	19.5	19.6	19.5	0.02	0.04	0.03

Though the API content was not varying much, few batches showed some variation in the API content. As an example the assay content of the ninety tablets from DoE batch # 7 is depicted in Figure 13. It was discovered that there was generally more API in the tablets in the beginning of the tabletting process compared to the mid and end of the process. Also the variance was higher in the start of the process. This behaviour would be difficult to identify and control if only a few samples were analyzed using classical methods.

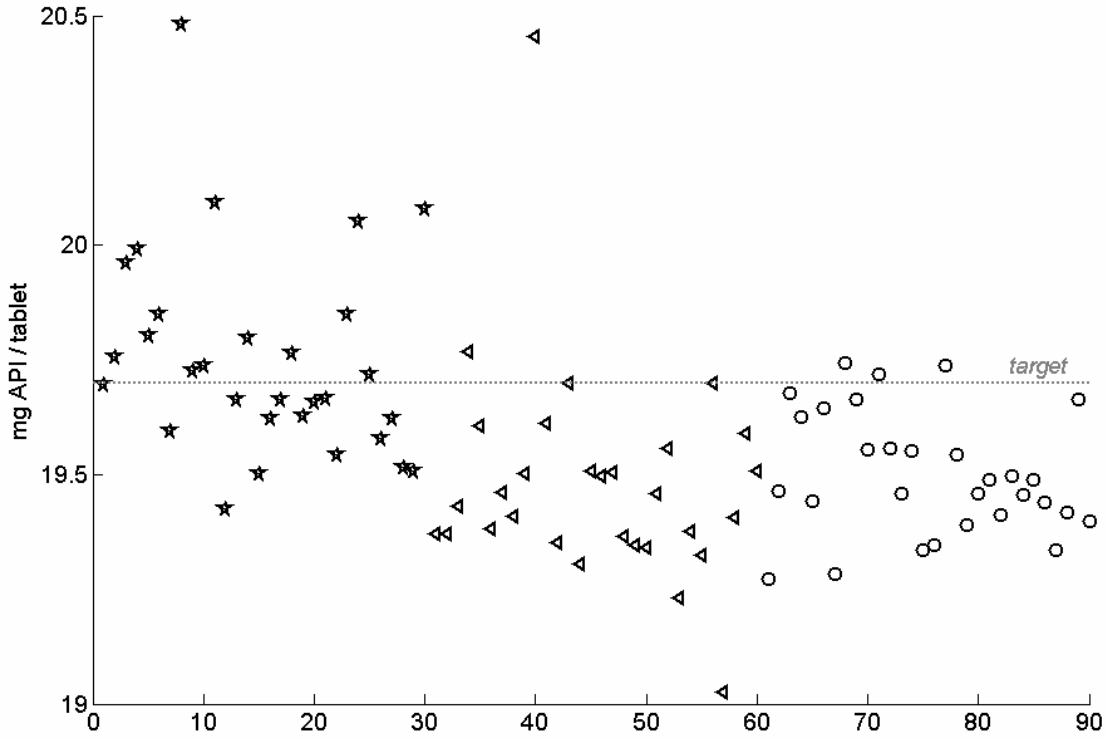

Figure 13. Ninety assay predictions from DoE batch no. 7, thirty from start (star), mid (triangle) and end (circle) respectively. The average API content was higher in the first part of the tabletting compared to the mid and end of the tabletting process.

The last example showed how RTR capability of the tablets could be achieved. Secondly, by analyzing a large number of samples trends in the process were discovered. This would be difficult using classical sampling schemes were only a few samples are analyzed.

Conclusions

An approach to RTR has been shows in this paper. Starting with the three levels of capability, each process step can be evaluated for its appropriateness in the RTR system. For a pharmaceutical tabletting process, examples for monitoring capability, control capability and RTR capability are provided. Different types of models are used to provide early warnings of future manufacturing problems.

Four different models were demonstrated using NIR and process data. First a MSPC model of NIR spectra from the granulation step, demonstrated how an early warning of future manufacturing problems could be given. In the first regression example (*local quality predictions*) a quantitative NIR model for in-line prediction of loss-on-drying in the drying process was demonstrated. The example showed monitoring capability and suggestion for process control was discussed.

For an RTR system it is important that the manufacturing process and process control can minimize the effect of input variation to the process that affects the final quality. In the second regression example (*forecasting final quality and process control*) it was tried out to establish process control models and forecast the disintegration time of the final tablets.

The last regression example (*final quality predictions*) demonstrated how the API content in individual tablets can be determined with transmission NIR which can be applied at-line the tabletting process.

Acknowledgements

Novo Nordisk, Corporate Research Affairs (CORA) who sponsored this work as a part of E.T.S. Skibsted's Ph.D. project. Technician Inga Fuchs who performed most of the mixing experiments and the staff at Analytical Development, CMC Development, Novo Nordisk A/S who performed the HPLC analysis.

References

1. American Food and Drug Administration (FDA), Guidance for Industry PAT - A framework for innovative pharmaceutical development, manufacturing and quality assurance. **2004**.

2. Skibsted, E. T. S., Westerhuis, J. A., Smilde, A. K., and Witte, D. T.. A Theoretical Framework for Real Time Release of Pharmaceutical Products. *NIRNews* submitted. **2005**.

3. Jackson, J. E., *A User's Guide to Principal Components*, John Wiley & Sons, New York, **1991**.

4. Tracy, N. D., Young, J. C., and Mason, R. L.. Multivariate control charts for individual observations. *Journal of Quality Technology* 24[2], 88-95. **1992**.

5. Westerhuis, J. A., Gurden, S. P., and Smilde, A. K.. Generalized contribution plots in multivariate statistical process monitoring. *Chemometrics and Intelligent Laboratory Systems* 51, 95-114. **2000**.

6. Wold, S., Eriksson, L., and Sjostrom, M., "PLS in chemistry," *Encyclopedia of Computational Chemistry* John Wiley & Sons, New York, **1998**.

7. Smilde, A. K., Westerhuis, J. A., and Boqué, R.. Multiway multiblock component and covariates regression models. *Journal of Chemometrics* 14, 301-331. **2000**.

8. Bro, R.. Multiway calibration. Multi- linear PLS. *Journal of Chemometrics* 10, 47-61. **1996**.

9. MathWorks Inc.. Matlab ver. 12.1. **2001**.

10. Eigenvector Research, I.. PLS_Toolbox. Version 2.1. **1998**.

11. Jackson, J. E. and Mudholkar, G. S.. Control procedures for residuals associated with principal component analysis. *Technometrics* 21[3], 341-349. **1979**.

12. Hlinak, A. J. and Saleki-Gerhardt, A.. An evaluation of fluid bed drying of aqueous granulations. *Pharmaceutical Development and Technology* 5[1], 11-17. **2000**.

ABOUT THE AUTHOR

Erik Türon Smidstrup Skibsted
Born 29.th April 1971 in Bogense, Denmark
Living in Copenhagen with Johanna and their twins William and Maya

I got my Master degree as civil engineer in chemistry from the Technical University of Denmark. At that time I worked with multi-wavelength fluorescence monitoring of biological processes and chemometric modelling. I continued that work for some years in a small engineering company called BioBalance until I started the PhD project. During my PhD project I have been working at Novo Nordisk performing all the experimental work and at the University of Amsterdam for writing papers. I was enrolled in the group BioSystems Data analysis group headed by Professor Age Smilde. The group was formerly known as Process Analysis and Chemometrics.

My main expertise is in fluorescence, vibrational spectroscopy, multivariate regression modelling and process analysis.

Contact details:
telephone: +45 4443 2778
fax: +45 4443 4073
mail: ersk@novonordisk.com